GEOLOGICAL SURVEY OF WESTERN AUSTRALIA

REPORT 26

PROFESSIONAL PAPERS

GEOLOGICAL SURVEY OF WESTERN AUSTRALIA

REPORT 26

PROFESSIONAL PAPERS

MINISTER FOR MINES
THE HONOURABLE JEFF CARR M.L.A.

DIRECTOR GENERAL OF MINES
D. R. KELLY

DIRECTOR, GEOLOGICAL SURVEY OF WESTERN AUSTRALIA
PHILLIP E. PLAYFORD

CONTENTS

GEOCHEMICAL STUDY OF INORGANIC COMPONENTS OF THE COLLIE COAL MEASURES

by R. Davy and A.C. Wilson

ABSTRACT

Three hundred and thirty-four samples of coal and shaly coal, together with a number of related inter-seam sediments, from the Collie Basin in Western Australia, have been analysed for their ash content and for up to 34 inorganic components. Samples were taken from 26 major seams and a number of minor seams. Ninety samples have been examined mineralogically.

In general, Collie coals are low in ash content (below 10%), and, in consequence, silicate components are also at low levels. Most of the coals have a low trace-element content; however, individual seams and occasional other samples have substantially higher values. In particular, Pb levels in the upper seams of the Cardiff Member are high, up to 480 ppm in the coal or 1% in the coal ash, and the maximum individual value of Pb in other samples reaches 595 ppm. The Al_2O_3:SiO_2 ratio of many coals is high, exceeding unity, and there is more Al_2O_3 present than can be absorbed in kaolinite, the only common clay mineral. The excess Al_2O_3 is present either as amorphous oxide and/or hydroxide, or as crystalline gibbsite, and may represent incipient bauxitization. Contents of rare-earth elements (Ce, La, and Y) in some coals are much higher than in coals reported from other parts of the world.

No seam has a chemical signature sufficiently distinctive for positive identification of a sample of unknown origin, or for correlation of seams across the three sub-basins. Nevertheless there are secular compositional trends, particularly in the Cardiff Sub-basin where rare earth elements (Ce, La, and Y) increase and alkaline earth elements (especially Ba and Sr) and P decrease in successively younger seams. On the basis of these trends the seam previously thought to be Ben is probably part of either Cardiff No. 1 or Cardiff No. 2 seams.

The minerals present indicate mixed origins, being variously related to detrital input, chemical precipitation, and authigenic growth. Detrital source material is dominantly felsic in origin and includes minerals derived from metasediments. Elements which seem to relate principally to detrital fractions include Al, Si, K, Cr, Cu, Li, Nb, Th, V, and Zr, and, to a lesser extent, Ce, La, Pb, and Y. Other elements, B in particular, can be related to the organic fraction of coal. Some elements (e.g. Mg, Na) appear to be partitioned between minerals of different origins and Ba and Sr, present as barytocelestite, have a mixed chemical–detrital origin.

High U levels occur locally in a shale below the Diana seam; the distribution of this element, and of Pb in other parts of the coalfield, may have potential economic significance in that they point to the possibility of mineralized source rocks in an area to the south and east of the coalfield.

KEYWORDS: Collie Basin; coal; geochemistry; sedimentary rocks.

INTRODUCTION

Western Australia's only producing coalfield occurs within the Collie Basin, some 160 km south-southeast of Perth (Fig. 1). The geology of the coalfield was first described in detail by Lord (1952), and most recently by Kristensen and Wilson (1986). Since 1952 there has been intensive company activity and further development of mines. In view of the wealth of new information, in 1982 the Geological Survey of Western Australia commenced a major review of the geology, hydrogeology and coal reserves of the basin. The present geochemical and mineralogical study of the non-combustible components of some of the coals and associated inter-seam sediments, forms part of that review.

The purpose of the study was to characterize the composition of as many seams as possible. It was hoped that distinctive geochemical characteristics would be recognized for specific seams so that the seams would be readily identified in drill material. Further, such seam recognition could be used to facilitate stratigraphic correlations across the basin and to help elucidate the structure of the basin (the impersistence of coal seams and the lack of coordination of company exploration has led to the proliferation of seam names in different parts of the basin).

These ideas are not new. Coals from other coalfields are known to display quite different trace element signatures (e.g. Brown and Swaine, 1964; Gluskoter and others, 1977; USGS, 1982). Other workers have suggested that some individual seams, within a single basin, could be distinguished from other seams in the same basin on the basis of different major or trace element patterns (e.g. Hawley, 1955; Clark and Swaine, 1962; Chatterjee and Pooley, 1977; Doolan and others, 1984). Patterns of compositional variation within seams have been studied by, for example, Harris and others (1981), and Hart and Leahy (1983). An orientation study of Collie Coals (Davy and Wilson, 1984), using a very limited number of analyses, suggested that there might be sufficient variation between the seams in the Collie coalfield to allow the identification of at least some individual seams.

GEOLOGICAL SETTING

The Collie Basin has an area of 225 km² and lies near the southwestern corner of the Archaean Yilgarn Craton (Fig. 1). The town of Collie lies close to the northwestern margin of the basin.

The geology has been described by Lord (1952), Low (1958), Lowry (1976), Wilde and Walker (1982), and Park (1982). The most recent summaries are those of Kristensen and Wilson (1986), and Wilson (in press). Figure 1 provides a generalized geological map of the basin.

The rocks of the basin are Permian, Cretaceous, and Holocene in age, and they lie unconformably on a basement of Precambrian crystalline rocks. The oldest Permian rocks comprise the Stockton Formation, a glacigene sedimentary unit (Lowry, 1976), which is overlain by the Collie Coal Measures. Above these is a 5–10 m thick cover of sand, minor clay, lag gravel, and laterite, of Cretaceous and Holocene age. This cover obscures the present boundaries of the Permian basin. Nowadays there are no natural exposures of Permian rocks, although coal was first identified in the banks of the deeply incised Collie River, west of the town of Collie.

The Collie Coal Measures comprise a fining-upwards, cyclic sequence of sandstone, siltstone, claystone or shale, and coal, with an erosional unconformity at the base of each cycle. Coal is not present in every cycle, but is clearly autochthonous, the seams having an underlying seat earth which contains remnants of short rootlets.
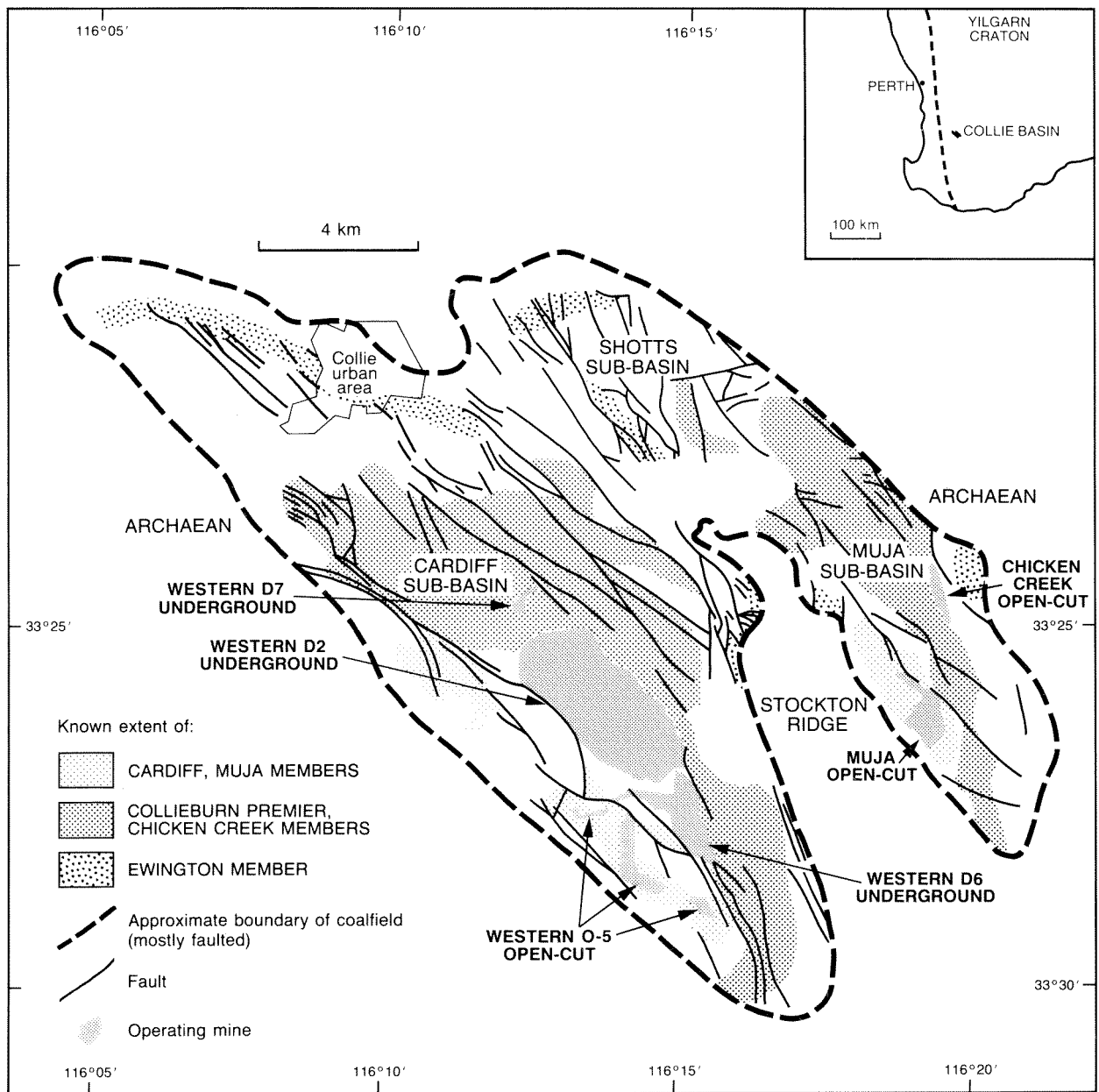

GSWA 23741

Figure 1. Location and geology of the Collie Basin.

2

The basin has a bilobate form and drilling has outlined the three sub-basins indicated on Figure 1. Current thinking, however, suggests that the two eastern sub-basins can be considered as one (Wilson, 1989). The concept of three sub-basins is retained for this report, because coal seams in the two eastern sub-basins have been named separately. The Cardiff Sub-basin is partly separated from the eastern sub-basin by a faulted basement ridge — the Stockton Ridge.

There are three coal-bearing members in the Cardiff and Muja Sub-basins and two in the Shotts Sub-basin (Table 1, Fig. 2). The basal member, the Ewington Member, occurs in all three sub-basins. Its seams, though persistent across the whole basin, have different names in the Muja Sub-basin compared with the other two. Various correlations between the upper and middle members, and between specific seams within the members of the eastern sub-basins, have been hypothesized, but no correlations are yet formally accepted. In the middle and upper members, the seams split, vary in thickness, and contain erosional washouts; as a consequence correlation is difficult. The coal seams are generally less than 4 m thick, although the Hebe seam in the Muja Sub-basin is 13 m thick. The coals are sub-bituminous; a typical analysis shows 25% moisture, 6% ash, 24% volatile matter, 45% fixed carbon, and a specific energy of 20 MJ/kg (Kristensen and Wilson, 1986). Petrographically, the coals of the Muja Member are dominated by vitrinite and inertinite, and pyrite is most abundant in the cleats (joints) (Sappal, 1982).

Geophysical measurements suggest the maximum thicknesses of preserved Permian sediments are 1100 m, 850 m, and 580 m in the Cardiff, Muja, and Shotts Sub-basins, respectively.

Structurally, both the Cardiff and Muja Sub-basins are half grabens in which drag effects have created asymmetric synclines, and faulting is common.

SAMPLING AND ANALYSIS

The seams, and the numbers of samples taken from them, are listed in Table 1. This table should be studied in conjunction with Figure 2. Where possible, samples were taken from the working faces of operating mines; elsewhere drill core was used. The geographic location of sample points is given in Figure 3 and, in composite section, in Figure 4. Many of the sampled faces have subsequently been destroyed by mining. Lack of suitable material meant that large parts of the basin were not sampled.

With one exception (at the Ewington opencut), the faces sampled were freshly exposed, or less than one year old. (Previous work by Davy and Wilson, 1984, showed that there was no significant change in composition in that time). All faces were cleaned before sampling. Drill core, on the other hand, varied in age up to several years. Apart from changes due to oxidation of pyrite, there were no other signs of chemical alteration of drill-core samples. Six samples

TABLE 1. COAL SEAMS SAMPLED, ABBREVIATIONS USED IN SUBSEQUENT TABLES AND FIGURES, AND NUMBERS OF SAMPLES (EXCLUDING SHALY COAL) TAKEN FROM EACH SEAM

Cardiff Sub-basin	Abbrev.	n	Muja Sub-basin	Abbrev.	n	Shotts Sub-basin	Abbrev.	n
Cardiff Member			**Muja Member**			**Premier Member**		
Cardiff No. 1	CA1	7	Ate	A	6	Premier 1	P1	1
Thin seam	CA1.5	2	Bellona	B	6	2	P2	4
Cardiff No. 2	CA2	13	Ceres	C	12	3	P3	6
Thin seam	CA2.5	1	Diana (Upper)	DU	4	4	P4	8
Cardiff	CA	25	Diana	D	6	5	P5	1
Neath	N	27	Thin seam	DE	1	6	P6	1
			Eos	E	12	Juno	JU	2
			Flora	F	7	Premier 7	7	1
'Ben'		7	Galatea	G	9			
			Hebe	H	25	CP5(a)		1
			Iona	I	8	CP10		3
Collieburn Member						CP20		2
						CP30		1
Wyvern	W	21	**Chicken Creek Member**					
Collieburn No. 2	CO2	13						
			Gryps	GR	3	**Ewington Member**		
			Chiron	CH	3			
			Thin seam	MU	2	Moira	MA	7
			Middle	M	4	Stockton	S	12
			Thin seam above			Wallsend	WA	6
			Centaur	CENTU	1	Seam below		
			Centaur	CENT	20	Wallsend		
						(? No. 5)	BWA	5
						Thin seam	BWA2	1

A complete stratigraphy showing approximate correlations is given in Figure 2. An additional 4 samples of thin coals of uncertain stratigraphic location, and 22 shaly coals (ash 20–30%) were examined.

(a) Position of the CP5 seam with respect to 'P' seams uncertain.

were taken from the Stockton seam at the disused Ewington opencut (Fig. 3). For these samples the exposed coal was 'cut back' to provide fresh material.

Exposed seams were channel-sampled to give a succession of samples equivalent to 1 m of vertical thickness through the seam. The samples used by Davy and Wilson (1984) were also included; most of these were channel samples taken through the total thickness of the seam. Each sample taken from an opencut face weighed at least 2 kg.

Sampling of drill core was less successful. Much coal had been removed for proximate–ultimate analysis, including the more likely correlation candidates, and

only small amounts of coal remained at the top and bottom of the seams. Such coal rarely amounted to more than 20 cm in length and 50–250 g by weight. A few thin seams, present in some holes, were sampled in their entirety.

Some of the inter-seam sediments, mainly claystones but including a few sandstones, were sampled for comparison with adjacent coals, and were examined in a similar manner.

In all, 334 coal and shaly coal, and approximately 200 inter-seam sediment samples were chemically analysed. Ninety samples were examined mineralogically.
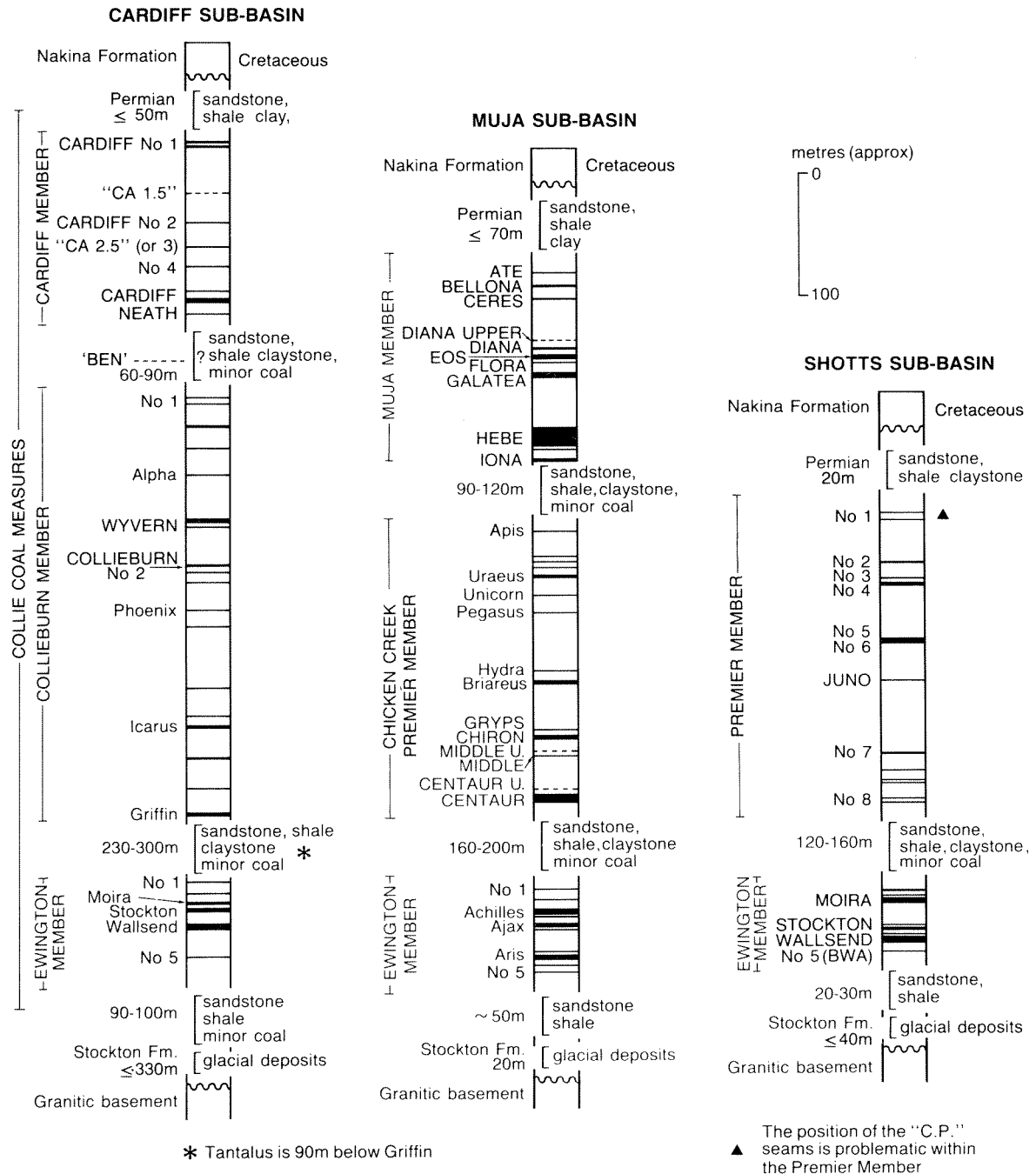

Figure 2. Stratigraphic succession of the main coal seams, Collie Basin.

4

Analytical methods for the orientation samples are given in Davy and Wilson (1984). Pre-analysis treatment and the analytical methods themselves were modified for the later samples. Details of the revised methods are given in Davy and Wilson (in press). Analysis was carried out at the Western Australian Government Chemical Laboratories (GCL); most determinations resulted from inductively coupled plasma atomic-emission spectrometry (ICPAES), or X-ray fluorescence spectrometry (XRF) on ash of coal previously pulverised to below 75 microns. For the subsequent discussion, results have been back calculated to 'raw' coal. Cerium, Li, and Y were only determined for the later samples; Ag, Sb, Sn, and TiO_2 only for the orientation samples. The pH of 20 coals, measured as a slurry of 1 part coal to 3 parts water, was determined using an Orion pH meter.

Sixty-five samples were examined mineralogically at the GCL using various techniques (X-ray diffraction, scanning electron microscopy, heavy-mineral studies). The remainder were examined in the Geological Survey using conventional thin sections and heavy-mineral

separates. Separation of the latter was effected using tetrabromoethane with a density of 2.96 g/cm^3. One sample was submitted to the Central Research Laboratories of the Broken Hill Co. Pty Ltd, in Newcastle, NSW, for mineralogical examination.

PRESENTATION OF RESULTS

The analyses of all samples collected, together with the actual values recorded for the ashed samples and summary statistics for each major seam, are given by Davy and Wilson (in press). Interpretation has been assisted by statistical calculations and graphical plots; pertinent diagrams and tables are reproduced in this paper.

Table 2 gives a statistical summary of all the coals (ash <20%) analysed, and Tables 3A to 3G give a summary for the individual members. Table 2 gives not only the range of values, but also arithmetic and geometric means and values for various percentiles. The 90th percentile is close to the upper limit of the normal
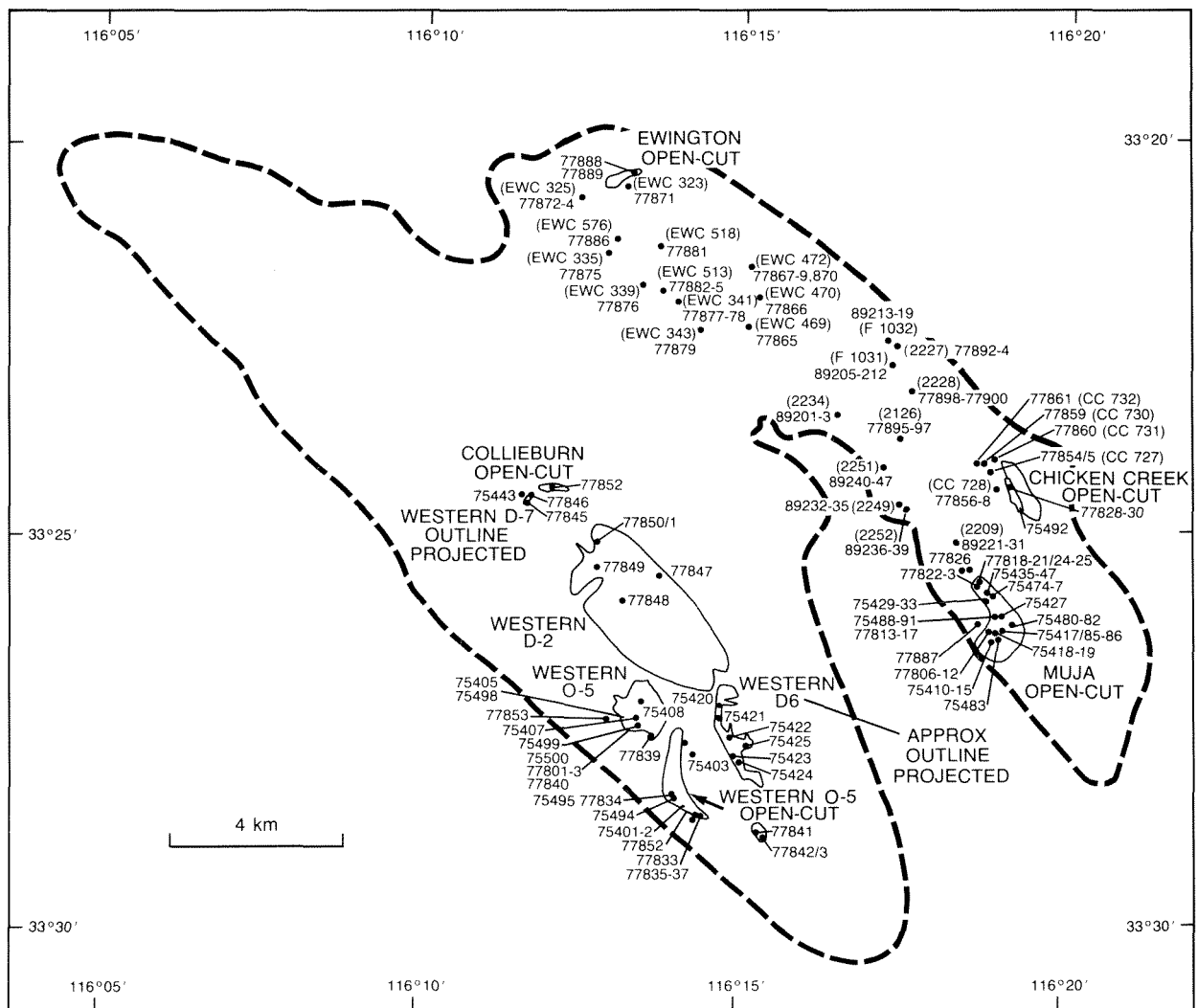

Figure 3. Geographic location of the samples studied. Where taken from drill core, hole number is shown in brackets.

range for most elements (Pb is an exception). Many seams have isolated high values for individual elements (cf. the 90th percentile value with the maximum reported). These high values tend to exaggerate the arithmetic mean, and the geometric mean (or alternatively, the 50th percentile–median) gives a better idea of the 'average' value.

Cobalt values reported are maxima, since there may have been contamination from the tungsten carbide mill used in grinding.

In the subsequent discussion, seams, and samples taken from them, are normally identified by the seam name alone.

GENERAL COMPOSITIONAL FEATURES OF COALS

Of all the samples collected as coal, 22 proved to be shaly coal (20–30% ash) and 40 contained between 10% and 20% ash. The large majority (272 samples), therefore, are low-ash coals: this is reflected in the averages shown in Tables 2 and 3. Many components are present in small amounts, in some cases close to, or below, the detection limits. Rubidium is excluded from most tables as it rarely reaches 5 ppm and, because of detection limits, could not be calculated at lower levels. Most components have a wide scatter even within an individual seam, although its extent varies from seam to seam. The extent of the scatter can be represented by the coefficient of variation (100 times the standard deviation divided by the arithmetic mean). The value of this coefficient increases with the degree of scatter. Though the figures for this coefficient are not reproduced in full, they indicate that B, S, Zr, and CaO have the least scatter, whilst K_2O, Pb, and Ge have the highest scatter, of the components measured. The ash content (by definition less than 20% in coal) has, in consequence, an artificially low scatter.

TABLE 2. SUMMARY OF CHEMICAL DATA FOR ALL COALS SAMPLED (n = 312)

| | Range | | | $\bar{x}$ | Geometric mean | Percentiles | | | |
						25th	50th	75th	90th
			Percentage						
Ash	1.5	–	19.3	6.0	5.2	3.4	5.2	8.0	14.0
SiO_2	0.1	–	11.3	2.4	1.6	0.9	1.9	3.7	5.9
Al_2O_3	0.2	–	9.8	1.8	1.5	0.9	1.4	2.1	3.3
Fe_2O_3	<0.02	–	7.0	0.55	0.29	<0.2	0.35	0.66	1.2
			Parts per million						
MgO	10	–	5 890	700	470	240	500	920	1 250
CaO	20	–	12 000	930	640	350	660	1 200	1 850
Na_2O	<30	–	4 470	350	230	125	260	400	540
K_2O	<10	–	2 320	160	60	20	50	140	450
P_2O_5	<10	–	7 450	780	230	45	300	950	2 100
As	<0.1	–	36	0.7	0.4	0.3	0.4	0.6	1.2
B	1	–	14	3.4	3.2	3.2	3.7	4.3	5
Ba	7	–	1 015(a)	183	96	40	110	255	500
Be	<0.5	–	12	1.7	1.1	0.6	1.5	3	4
Ce (b)	3	–	1 457	69	34	20	36	75	130
Cl	<10	–	4 900	152	78	43	95	175	310
Co	<5	–	321	15	8.3	4.5	8.5	13.5	21
Cr	<5	–	117	11	7.1	<5	7.2	12.5	24
Cu	<1	–	741	11	5.8	4.3	6	8.5	15
Ge	<0.1	–	47	2.7	0.6	<0.2	0.5	2	7
La	1	–	585	34	17	7	17	39	68
Li	<0.1	–	9	0.7	0.3	0.1	0.4	0.9	2
Mn	<2	–	667	22	6.7	<3	5.5	27	60
Mo	<0.2	–	6	1.1	0.5	<0.2	1.0	2	3
Nb	<1	–	71	3.9	2.7	2	3	5	8
Ni	2	–	161	21	16	11	17	27	38
Pb	<1	–	595	30	4.7	2	4	9	80
Rb	<5	–	17	<5	<5	<5	<5	<5	<5
S	400	–	50 000	5 010	3 750	2 400	3 500	5 500	9 000
Sr	2	–	863	110	38	10	42	125	330
Th	<0.4	–	26	4.2	2.5	2	3.3	5.5	10
U	<1	–	58	1.4	0.8	<1	<1	1	2
V	2	–	279	17	9.7	5.7	9	16	40
Y (b)	<5	–	217	22	11	4	14	29	47
Zn	<2	–	273	28	17	8	17	38	66
Zr	3	–	436	29	22	16	23	34	53

Coal is defined as having less than 20% ash, coaly shale reaches 29.8% ash, and in the Collie Basin there is continuous variation up to 27.5% ash.

(a) One coaly shale (21.7% ash, 77828 D) contains 1950 ppm Ba, 11 ppm Be, 3322 ppm Ce, 141 ppm Cr, 1850 ppm La, 1125 ppm Sr, 35 ppm U, and 960 ppm Y.
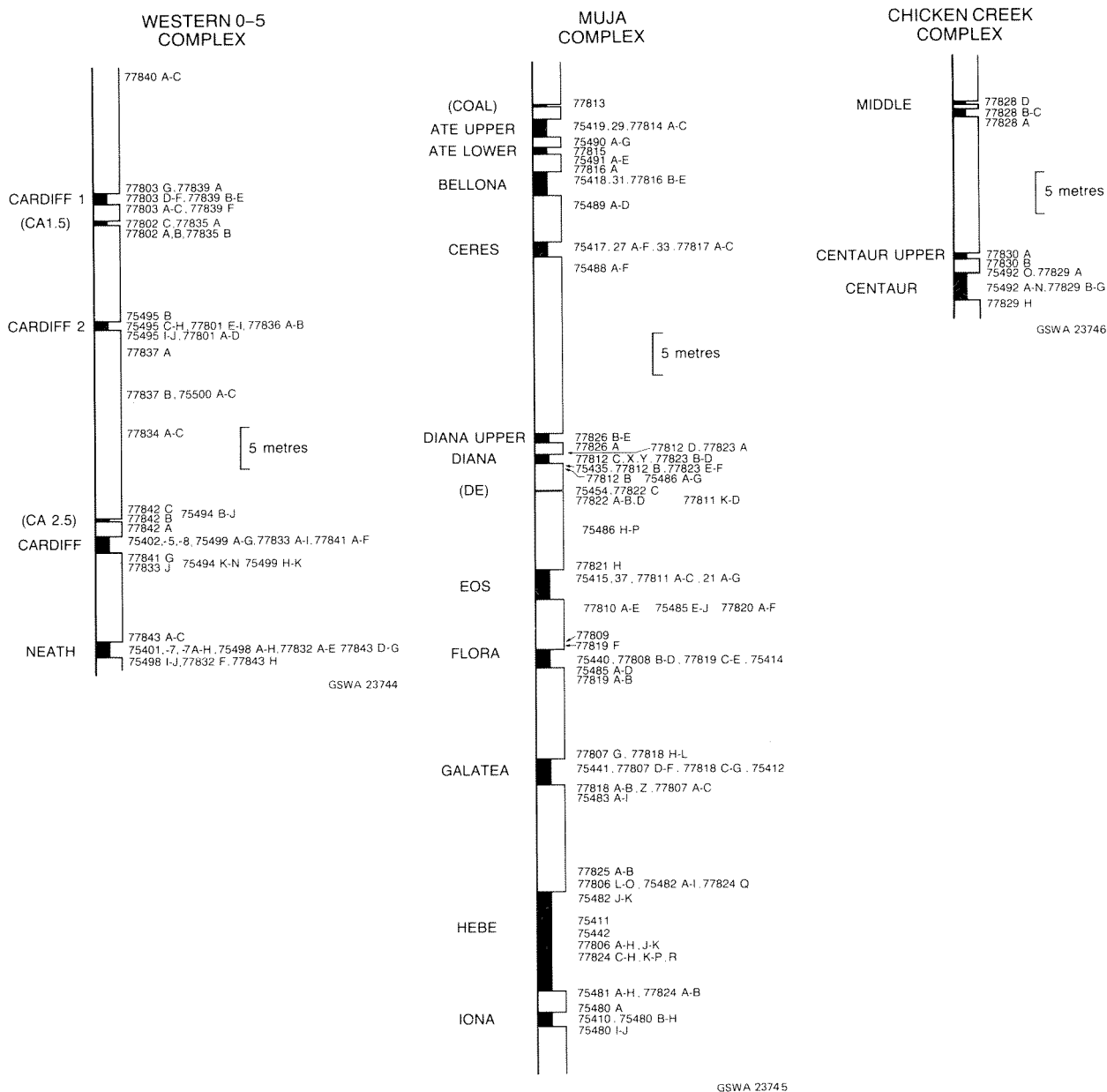
(b) 274 samples

WESTERN 0–5 COMPLEX

77840 A-C

CARDIFF 1
(CA1.5)
77803 G . 77839 A
77803 D-F . 77839 B-E
77803 A-C . 77839 F
77802 C . 77835 A
77802 A,B . 77835 B

CARDIFF 2
75495 B
75495 C-H . 77801 E-I . 77836 A-B
75495 I-J . 77801 A-D
77837 A

77837 B . 75500 A-C

77834 A-C   ⌐ 5 metres

(CA 2.5)
77842 C
77842 B   75494 B-J
77842 A
CARDIFF
75402,-5,-8 . 75499 A-G . 77833 A-I . 77841 A-F
77841 G
77833 J   75494 K-N   75499 H-K

NEATH
77843 A-C
75401,-7,-7A-H . 75498 A-H . 77832 A-E 77843 D-G
75498 I-J . 77832 F . 77843 H

GSWA 23744

MUJA COMPLEX

(COAL)   77813
ATE UPPER   75419 , 29 . 77814 A-C
ATE LOWER   75490 A-G
75815
75491 A-E
77816 A
BELLONA   75418 , 31 . 77816 B-E

75489 A-D

CERES   75417 , 27 A-F . 33 . 77817 A-C
75488 A-F

⌐ 5 metres

DIANA UPPER   77826 B-E
77826 A   77812 D . 77823 A
DIANA   77812 C, X, Y . 77823 B-D
75435 . 77812 B . 77823 E-F
77812 B   75486 A-G
(DE)   75454 . 77822 C
77822 A-B,D   77811 K-D

75486 H-P

77821 H
75415 , 37 . 77811 A-C . 21 A-G
EOS
77810 A-E   75485 E-J   77820 A-F
77809
77819 F
FLORA   75440 . 77808 B-D . 77819 C-E . 75414
75485 A-D
77819 A-B

GALATEA
77807 G . 77818 H-L
75441 . 77807 D-F . 77818 C-G . 75412
77818 A-B , Z . 77807 A-C
75483 A-I

77825 A-B
77806 L-O . 75482 A-I . 77824 Q
75482 J-K
75411
75442
HEBE
77806 A-H , J-K
77824 C-H . K-P , R

75481 A-H . 77824 A-B
75480 A
IONA   75410 . 75480 B-H
75480 I-J

GSWA 23745

CHICKEN CREEK COMPLEX

MIDDLE   77828 D
77828 B-C
77828 A

⌐ 5 metres

CENTAUR UPPER   77830 A
77830 B
75492 O . 77829 A
CENTAUR   75492 A-N . 77829 B-G
77829 H

GSWA 23746

Figure 4. **Composite sections, showing location of samples in the profiles.**

Of the 26 seams studied from which 4 or more samples were collected, only Bellona, Ceres, Galatea, P3, P4, Wallsend, and the seam below Wallsend have over half their components with a coefficient of variation less than 50%. Most seams, therefore, have a highly variable trace-element composition.

Two compositional features stand out: a bimodal distribution of Pb; and the high $Al_2O_3 : SiO_2$ ratio of many samples.

High Pb values (> 50 ppm) occur in all samples from Cardiff No. 1, Cardiff No. 2, a thin seam (referred to as CA 1.5) between these two seams, and a seam currently identified as Ben. The highest value in these seams is 480 ppm (in 77801 I) from Cardiff No. 2. The high Pb content is not confined to the coals, but is also present in shales both above and below the coals; the seat earth below Ben has the highest Pb value (1875 ppm, 77853 K) of all. Seams showing consistently high Pb levels are restricted to the southwest Cardiff Sub-basin (Fig. 5). Isolated high values occur in other seams but are not restricted to any specific geographical area or stratigraphic interval. The highest Pb content of any coal sample is 595 ppm (77871, Moira).

Though the majority of samples have SiO_2 in excess of Al_2O_3, over 100 coals contain more Al_2O_3 than SiO_2. In many cases the ratio is very high (e.g. 77803 F, Cardiff No. 1, $Al_2O_3 : SiO_2 = 7.6$) and values in excess of unity occur in both high and low ash coals (e.g. 77826 D, Diana Upper, 18.0% ash, $Al_2O_3 : SiO_2 = 3.5$). Samples with $Al_2O_3 : SiO_2$ greater than 2 are most common in the lower part of the Muja Member (Diana Upper to Iona), in Middle and Centaur, in the Chicken

7

TABLE 3. SUMMARY DATA FOR EACH COAL–BEARING MEMBER

	A. CARDIFF MEMBER (n = 75)			B. COLLIEBURN MEMBER (n = 34)			C. 'BEN' (n = 7)			D. MUJA MEMBER (n = 96)		
	Range	$\bar{x}$	Geometric mean	Range	$\bar{x}$	Geometric mean	Range	$\bar{x}$	Geometric mean	Range	$\bar{x}$	Geometric mean
Percentage												
Ash	1.24 – 18.3	6.2	5.5	1.7 – 12.0	5.6	4.7	4.0 – 0.8	0.4	7.4	1.5 – 18.0	4.6	4.0
SiO_2	0.3 – 10.0	2.7	2.1	0.1 – 8.7	2.2	1.1	0.6 – 7.4	3.0	2.1	0.1 – 7.5	1.7	1.2
Al_2O_3	0.1 – 7.2	2.0	1.6	0.2 – 5.7	1.4	1.2	2.3 – 6.0	3.8	3.5	0.7 – 9.8	1.5	1.3
Fe_2O_3	0.02 – 1.2	0.37	0.25	0.05 – 1.7	0.56	0.41	<0.1 – 0.2	<0.1	<0.1	<0.02 – 6.0	0.30	0.15
Parts per million												
MgO	70 – 2 390	677	479	80 – 2 180	616	404	210 – 400	277	262	10 – 4 480	600	410
CaO	80 – 3 420	813	529	210 – 2 900	1 331	1 158	220 – 410	300	294	110 – 2 960	745	602
Na_2O	20 – 4 210	308	203	70 – 500	237	203	90 – 620	299	257	10 – 1 670	391	331
K_2O	<10 – 1 110	117	55	10 – 950	127	51	30 – 2 320	630	175	<10 – 1 590	105	45
P_2O_5	<10 – 2 060	402	111	130 – 7 200	2 553	1 625	10 – 140	54	38	10 – 5 650	811	366
As	<0.1 – 1	0.34	0.27	0.1 – 2	0.42	0.33	0.2 – 0.8	0.4	0.4	0.1 – 36	0.96	0.44
B	1 – 14	3.6	3.3	2 – 6	3.6	3.5	1 – 4	2	2	2 – 7	3.6	3.5
Ba	7 – 1 015	199	76	54 – 988	37	303	15 – 74	35	29	11 – 745	143	85
Be	<0.5 – 3	1.0	0.75	<0.5 – 4	1.3	0.98	1 – 2	2	2	<0.5 – 4	1.5	1.1
Ce	(a) 4 – 1 457	113	43	(c) 3 – 149	26	13	78 – (590)	174	130	(e) 3 – 502	54	33
Cl	<10 – 4 900	224	92	20 – 310	113	93	<10 – (690)	159	60	<10 – 540	106	68
Co	<5 – 321	29	14	<5 – 25	8.2	6.8	2 – 7	5	4	<5 – 84	9.5	6.8
Cr	<5 – 39	7.4	5.8	<5 – 22	6.1	4.7	6 – 32	15	13	<5 – 87	8.1	5.4
Cu	1 – 741	17	6.2	<1 – 15	5.0	4.0	3 – (95)	26	15	<1 – 38	6.5	5.0
Ge	<0.1 – 38	2.9	0.50	<0.1 – 6	0.57	0.24	2 – 13	5	4	<0.1 – 41	2.3	0.56
La	<5 – 585	49	20	1 – 80	15	6.8	48 – (284)	94	77	1 – 320	28	17
Li	<0.1 – 3	0.48	0.27	<0.1 – 2	0.30	0.17	0.1 – 2	0.6	0.4	<0.1 – 2	0.40	0.23
Mn	<2 – 79	18	6.7	<2 – 39	9.0	5.7	<2 – 18	5		<2 – 36	6.4	3.3
Mo	<0.1 – 5	0.8	0.29	<0.1 – 3	0.73	0.27	0.6 – 2	1.1	1.0	<0.1 – 6	1.1	0.63
Nb	1 – 10	3.6	3.0	<0.5 – 7	3.2	2.2	<2 – 19	7	4	<0.5 – 71	4.7	2.9
Ni	<1 – 54	16	13	2 – 31	13	11	14 – 25	20	20	2 – 138	22	17
Pb	<1 – 480	63	6.9	<1 – 28	4.9	2.7	91 – (439)	199	178	<1 – 318	14	4.0
Rb	<5 – 6	<5	<5	<5 – 9	<5	<5	<5 – 17	<5		<5 – 8	<5	<5
S	650 – 25 400	3 350	2 880	2 190 – 18 500	6 920	6 060	2 130 – 4 080	2 981	2 917 S	1 190 – 42 200	3 640	2 890
Sr	2 – 380	77	23	26 – 863	329	227	4 – 13	8	8	2 – 544	90	43
Th	<0.4 – 26	4.4	2.8	<0.4 – 16	2.1	0.93	4 – 30	13	10	<0.4 – 24	3.6	2.4
U	<1 – 58	1.7	0.68	<1 – 3	0.6	0.55	<1 – 25	6	3	<1 – 7	0.84	0.63
V	1 – 90	14	9.6	2 – 38	8.2	5.6	3 – 39	16	12	<1 – 279	16	8.8
Y	(b) <5 – 413	28	12	(d) <5 – 56	8.7	4.1	19 – (109)	35	28	(f) <5 – 103	19	12
Zn	<2 – 63	17	11	<5 – 112	30	20	<1 – 17	9	6	<5 – 149	36	24
Zr	3 – 81	26	23	5 – 63	23	17	16 – 75	43	38	5 – 436	31	21

(a) n = 62; (b) n = 62; (c) n = 76; (d) n = 27; (e) n = 76; (f) n = 76.   'Ben' is included separately, since it may now correlate with the Cardiff Member.

TABLE 3. (continued)

	E. CHICKEN CREEK MEMBER (n = 34)				F. PREMIER MEMBER (n = 29)				G. EWINGTON MEMBER (n = 29)			
	Range		$\bar{x}$	Geometric mean	Range		$\bar{x}$	Geometric mean	Range		$\bar{x}$	Geometric mean
Percentage												
Ash	1.8 –	17.6	5.4	4.4	3.34 –	19.2	7.9	7.2	3.2 –	15.9	8.7	8.2
SiO_2	0.2 –	9.7	1.9	1.0	0.5 –	11.3	3.6	2.7	1.0 –	8.4	4.0	3.6
Al_2O_3	0.6 –	5.9	1.9	1.4	0.64 –	3.8	1.5	1.3	0.63 –	7.6	2.2	1.9
Fe_2O_3	0.10 –	2.5	0.43	0.31	0.21 –	3.4	1.3	1.2	0.06 –	7.0	1.1	0.70
Parts per million												
MgO	100 –	5 890	899	623	120 –	1 230	623	490	60 –	5 370	1 050	616
CaO	170 –	1 780	569	482	220 –	3 190	965	792	120 –	12 000	1 840	1 010
Na_2O	<30 –	4 470	664	397	50 –	280	156	139	<30 –	1 000	178	100
K_2O	<10 –	1 340	133	33	<10 –	2 170	294	132	10 –	670	137	76
P_2O_5	<10 –	2 950	487	201	<10 –	3 300	767	271	<10 –	3 240	270	59
As	<0.1 –	11	0.68	0.32	0.3 –	4	1.5	0.95	0.2 –	4	0.62	0.46
B	2 –	5	3.0	2.9	2 –	6	3.4	3.3	2 –	6	2.7	2.6
Ba	12 –	556	119	80	12 –	704	202	136	11 –	850	132	77
Be	0.7 –	9	2.3	1.8	<0.5 –	4	1.7	1.4	<0.5 –	11	3.1	1.5
Ce	16 –	648	87	54	5 –	109	30	20	6 –	125	48	37
Cl	<10 –	720	255	172	<10 –	310	95	64	<10 –	650	99	39
Co	2 –	83	8.5	4.8	2 –	85	16	11	3 –	63	11	8.9
Cr	<5 –	42	11	8.1	6 –	67	15	12	7 –	117	26	19
Cu	1 –	20	6.2	5.1	4 –	28	7.9	6.8	4 –	435	24	9.8
Ge	<0.1 –	38	3.5	0.90	<0.1 –	11	2.7	1.1	<0.2 –	35	3.2	0.55
La	6 –	364	45	26	3 –	65	18	12	4 –	61	26	21
Li	<0.1 –	4	0.80	0.41	0.1 –	9	1.3	0.69	0.1 –	6	2.0	1.1
Mn	<2 –	53	12	8.2	<1 –	196	54	19	<1 –	667	71	21
Mo	<0.1 –	6	1.9	1.2	0.5 –	4	1.7	1.5	<0.2 –	6	1.1	0.71
Nb	<0.5 –	32	4.1	2.4	1 –	9	2.9	2.3	(1) –	11	2.9	2.4
Ni	5 –	161	20	14	7 –	119	28	23	13 –	70	29	26
Pb	<1 –	52	7.7	4.0	<0.5 –	24	5.5	3.1	<0.4 –	595	33	4.4
Rb	<5 –	9	<5	<5	<5 –	10	<5	<5	<5 –	<5	<5	<5
S	1 190 –	21 600	5 040	4 080	5 040 –	31 700	10 900	9 510	400 –	50 000	5 770	3 670
Sr	3 –	340	52	27	5 –	615	140	63	2 –	637	62	16
Th	<0.4 –	9	3.2	1.9	<1 –	11	3.8	3.0	<2 –	16	5.2	4.2
U	<1 –	4	1.0	(0.78)	<1 –	7	1.9	1.2	<1 –	19	2.2	1.1
V	3 –	100	23	11	4 –	121	21	13	5 –	97	22	13
Y	8 –	215	33	25	2 –	67	15	8.5	3 –	108	22	15
Zn	6 –	273	37	22	4 –	199	38	19	4 –	64	18	13
Zr	8 –	67	23	19	11 –	67	31	29	13 –	89	35	31

Creek Member, and in all major seams in the Cardiff Sub-basin with the exception of Neath (though even this seam has one high Al_2O_3 : SiO_2 sample). However, no seam has all samples showing Al_2O_3 exceeding SiO_2.

In other seams there are rare, isolated high Al_2O_3 : SiO_2 ratios, but SiO_2 is usually in excess of Al_2O_3 as is normal in most coals. There are no very high Al_2O_3 : SiO_2 ratios in the Premier Member coals in the Shotts Sub-basin; the highest recorded was in 77869 B (CP20) which showed an Al_2O_3 : SiO_2 ratio of 1.3.

MINERALOGY OF COAL AND COAL ASH

Mineralogical studies have shown that quartz, kaolinite, and zircon are present in all the coals studied, though, in some cases, concentrations are so low that they cannot be detected by X-ray diffraction. A listing of all minerals recognized (from XRD, SEM, heavy-mineral studies, or conventional thin-section microscopy) is given in Table 4. Of the seams examined, those of 'CP' and the Chicken Creek Member are relatively free of minerals other than the three noted above.

Centaur is the only seam in the Chicken Creek Member containing detrital minerals other than quartz, kaolinite, and zircon.

Some goethite may be an oxidation product of pyrite, and these two minerals rarely occur together. However, S, though present at the 1000 ppm level, has not been identified in minerals other than pyrite, and, rarely, a barium–strontium sulphate. Many samples have no obvious mineral that contains sulphur. Hematite has been detected together with goethite in Wallsend and may, as well as some of the goethite, be authigenic. Analyses of pyrite from Iona show it to be free of most trace elements, however it does contain up to 250 ppm Ni.

The barium–strontium sulphate mineral appears slightly unusual in that SEM studies suggest equal proportions of Ba and Sr. The mineral approximates to barytocelestite $(BaSr(SO_4)_2)$; although rare, similar material has been recorded previously (Deer and others, 1962, v. 5, p. 197).

The high Al_2O_3 : SiO_2 ratio is explained by the presence of crystalline gibbsite in two samples and an
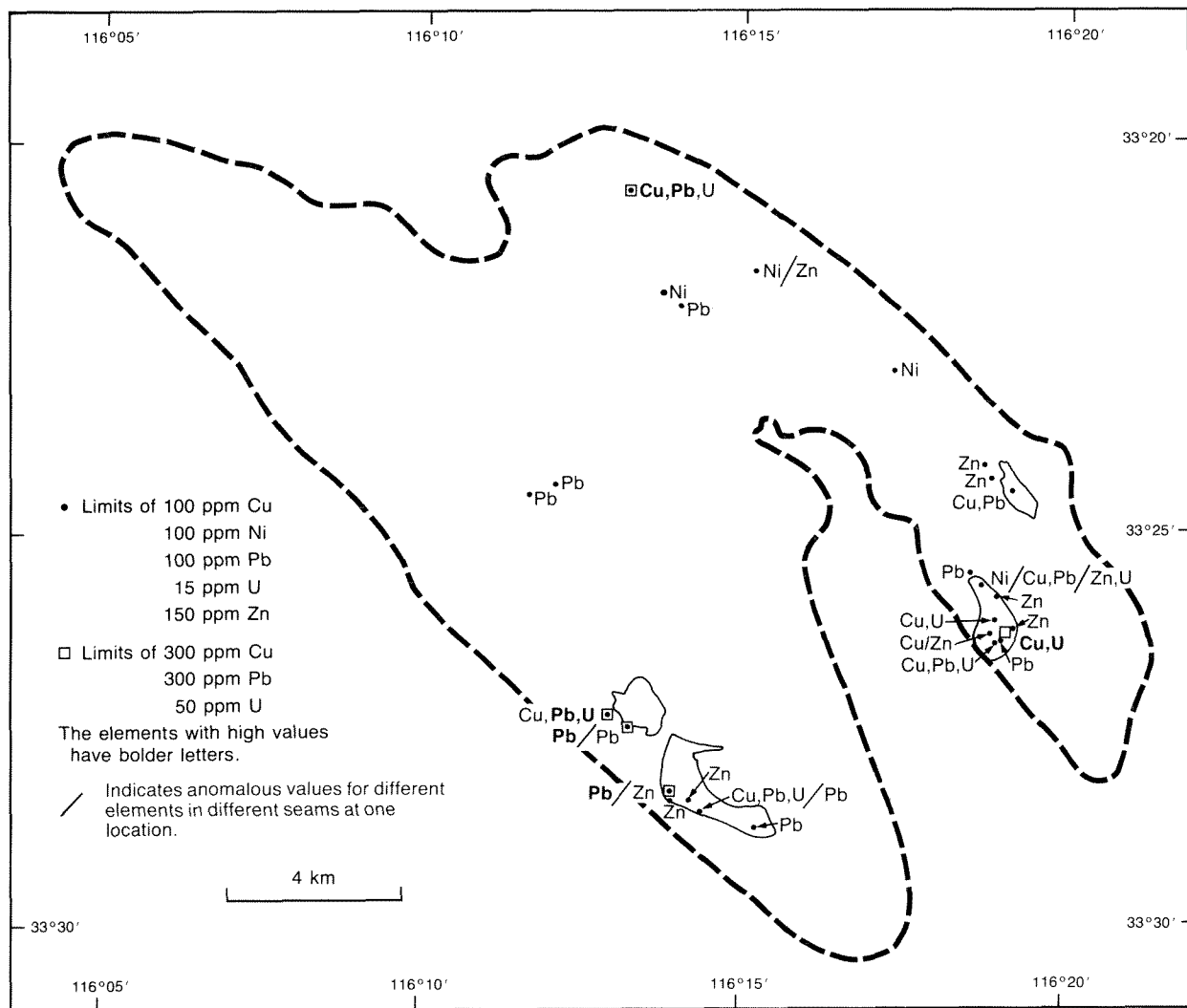
Figure 5. Geographic location of samples with high levels of selected trace elements.

10

TABLE 4.   MINERALS IDENTIFIED IN COAL SEAMS AT COLLIE

	Kaolinite	Quartz	Zircon	Al-Mineral	Amphibole	Barytocelestite	Biotite	Epidote	Garnet	Gibbsite	Goethite	Hematite	Kyanite	Leucoxene	Monazite	Phosphate	Pb-Mineral	Pyrite	Rutile	Siderite	Staurolite	Tourmaline
Ate	x	x	ej		x		x	x	x									x	x			c
Bellona	x	x	ehi		x													x	x		x	ad
Ceres	x	x	ef		x		x	x							x			x			x	a
Diana Upper	x	x	fgh	x									x					x				
Diana	x	x	fc		x													x		x	x	
Eos	x	x	efg				x			x								x				
Flora	x	x	efgh	x		x				x								x	x			
Galatea	x	x	efghj		x		x						x	x				x	x		x	bc
Hebe	x	x	ef	x	x													x				
Iona	x	x	eg					x			x							x	x			d
Gryps	x	x	e															x				
Chiron	x	x	eg															x				
Middle	x	x	efi	x							x							x				
Centaur Upper	x	x	efh								x											
Centaur	x	x	efgh		x		x							x	x							
Cardiff 1	x	x	ehi	x											x		x	x				
Cardiff 1.5	x	x	e	x				x	x									x		x	x	d
Cardiff 2	x	x	ef	x			x				x				x		x	x		x		
Cardiff 2.5	x	x	i		x					x												
Cardiff	x	x	e								x				x			x				
Neath	x	x	efhi								x							x				
'Ben'	x	x	g	x	x	x	x								x		x	x				
Wyvern	x	x	egh	x	x	x			x		x					x		x				
Collieburn 2	x	x	i	x	x	x			x		x					x		x				
Moira	x	x	g		x													x				b
Stockton	x	x	e	x				x			x				x			x				
Wallsend	x	x	g						x		x	x						x				
Below Wallsend 1	x	x	e																	x		
Below Wallsend 2	x	x	e		x															x	x	
P1	x	x	g															x				a
P2	x	x	g	x			x	x	x									x				
P3	x	x	g					x	x		x	x	x		x			x				ad
P4	x	x	eg	x			x	x	x		x	x	x					x			x	c
JU	x	x	eg						x									x				
CP 5	x	x	eg															x				
CP 10	x	x	eg															x				
CP 20	x	x	eg															x				

a = yellow to olive   b = olive to green   c = yellow to brown
d = yellow to blue–green   e = colourless, unzoned, terminated   f = colourless, zoned, terminated
g = yellow   h = unterminated, colourless, with inclusions   i = metamict (malacon)
j = red–brown

GSWA 24724

11

essentially amorphous aluminium (hydroxide) mineral, which can be considered as a protogibbsite, in many others.

No mineral has been found to explain the high Pb contents. The high Pb levels have been confirmed, but SEM analysis suggests that the Pb is dispersed, probably with Al, throughout the coal. Lead has a high correlation with Ce and La overall (see later discussion), but no rare-earth Pb mineral has been found, and monazite (where examined) shows no detectable Pb.

Siderite is the only carbonate identified. At the most common pH (2.6–4.7, Table 5), carbonate minerals are unstable.

TABLE 5. pH VALUES AND SELECTED OTHER COMPONENTS FOR SAMPLES OF COAL

Sample	Seam (a)	pH	SiO_2	Al_2O_3	Fe_2O_3	Co	Mn
			(Percentage)			(ppm)	
75427 A	C	4.3	1.6	1.3	0.06	<5	<2
77808 D	F	3.9	3.6	2.2	0.27	14	6
77819 E	F	4.2	0.6	2.0	0.16	15	5
77821 E	E	4.2	0.2	1.0	0.07	<5	<2
77823 C	D	3.8	0.5	1.0	0.37	18	3
77824 P	H	4.1	0.7	1.0	0.11	9	3
77826 D	DU	4.7	4.9	9.8	0.20	<5	2
77828 C	M	6.0	1.8	5.8	0.20	<5	<2
77829 D	CENT	4.3	0.8	0.9	0.26	<5	14
77830 A	CENTU	3.4	1.7	1.6	0.65	10	11
77835 A	CA1.5	4.2	1.6	7.2	0.08	<5	<2
77836 A	CA2	4.8	1.3	3.4	0.03	<5	2
77845 E	CO2	3.5	1.1	1.5	0.57	6	7
77846 E	CO2	3.4	0.4	1.4	0.37	5	2
77847 A	W	3.1	0.9	1.5	0.16	10	<2
77848 E	W	2.6	1.0	1.4	0.89	10	17
77853 K	(b) BEN	4.2	14.3	12.9	5.4	<7	<10
77869 B	CP20	2.6	1.0	1.3	2.7	–	<2
77896	P3	2.7	6.3	1.8	0.60	8	6
89244	S	3.4	5.0	2.6	0.71	7	51

(a) Seam abbreviations as given in Table 1.   (b) Shaly coal, ash 20–30%.

Kaolinite, as seen under the microscope, is partly the alteration product of feldspar, partly detrital (comminuted ?after mica), and partly authigenic where large sheaves of grains fill cavities in coal. Quartz in the coal, when seen in thin section, appears detrital.

Several colour varieties of zircon and tourmaline have been identified. In the case of zircon there are also variations in shape, in the degree of crystallinity, and in the presence or absence of inclusions and zoning. Any given sample usually contains only one variety of tourmaline, but may have several varieties of zircon.

INTER-SEAM SAMPLES

The bulk of the inter-seam sediments is derived from detritus which originally comprised quartz, feldspar, and mica. Feldspar grains are now altered to kaolinite, and micas are now largely a mixture of clays (kaolinite, illite, and chlorite). Other kaolinite is authigenic, formed in the interstices between detrital grains.

Other minerals identified in these sediments are similar to those in the coal, although no aluminium hydroxide and no sulphate minerals have been recognized.

No attempt has been made to identify base-metal or uranium-bearing minerals. Quartz is largely detrital, but overgrowths are not uncommon. There is an even greater variety in the types of zircon present. For example, shaly sandstone between Galatea and Hebe (77806 N) contains 6 different zircon types:

(a) colourless, irregular, unzoned and without inclusions;

(b) colourless, irregular, unzoned but with abundant inclusions;

(c) red-brown, rounded and zoned;

(d) red-brown, metamict grains;

(e) colourless, zoned, euhedral grains without inclusions;

(f) pink, zoned, and well formed.

The last mentioned are the least common. There are fewer garnets than zircons.

The minerals identified in inter-seam sediments in this project differ somewhat from those identified by Glover (1952), who found the heavy fraction to be dominated by garnet and lesser amounts of zircon. Among the minor components Glover identified apatite, chloritoid, spinel, and anatase, none of which have been identified in the samples collected for this study. Hornblende and apatite were not present in Glover's samples, although they are present in trace amounts in our samples.

Chemical analyses show the inter-seam sediments to have low $Al_2O_3 : SiO_2$ ratios, and low absolute amounts of MgO, CaO, Na_2O, and K_2O, all of which are commonly present at less than 0.5% (1% for K_2O in a few samples). Many samples of both claystone and sandstone in fact contain less than 0.1% of these components. However, the values for these alkali and alkaline-earth oxides are (generally) slightly higher, and for SiO_2 and Al_2O_3 considerably higher, than in nearby coals. Other elements normally higher in claystone than in coal include As, B, Cr, Li, Nb, Rb, Th, U, V, Zr, and possibly Pb. The Rb:Sr ratio of coal is very low since Rb is below detection (5 ppm), but exceeds 1 for most claystones. Similarly, K_2O:Rb ratios are much higher in the coals because of the differences in Rb content. Other components varying little between claystone and coal include Cl, Ge, Fe_2O_3, and P_2O_5, (sometimes also Ba and Be) whilst wide internal variations mask any differences between claystone and coal for Ce, Cu, La, Sr, Y, and Zn. The values of a few elements, Co, Ni, and S, are commonly lower in the claystones than in the coal.

Sandstones are depleted in most components other than SiO_2, and possibly Zr, compared with the claystones.

12

Some inter-seam sediments have unusually high trace-element values. The high Pb content in the seat earth underlying Ben has already been mentioned. This sample, 77853 K, also contains 280 ppm Cu, 105 ppm U, and relatively high levels of Ba, Ce, Cl, La, and Y. The maximum value of Zn (960 ppm in 75482 E) occurs in the 'Hebe Shale' (Park, 1982) above the Hebe seam. In shales below Diana, Cu values up to 960 ppm (75486 I) and U values up to 150 ppm (75486 J) have been determined. Chlorine has a maximum value of 0.91% in a seat earth below Cardiff No. 2 (77801 D). A shaly coal, 5 cm thick, above Middle at Chicken Creek (77828 D) contains 1950 ppm Ba, 3320 ppm Ce, 230 ppm Cu, 1850 ppm La, 260 ppm Pb, 35 ppm U, and 960 ppm Y, and together with similar material below Ben, is the most 'mineralized' of the samples collected. Copper and Zn behave antipathetically; when Cu levels are high Zn levels are usually low, in many cases below detection.

Most inter-seam sediments however, are not mineralized but have trace-element contents at the 'Clarke' level (e.g. as given in Krauskopf, 1979) or below.

DISCUSSION

COMPARISON OF THE COMPOSITION OF COLLIE SEAMS WITH OTHER COALS

Some comparisons of the mean values and/or ranges of values are effected in Tables 6 and 7. Analyses of sub-bituminous coals are rare, and the 'US' and 'World' data of Table 6 are for bituminous coals. Table 7 gives comparisons of Collie with various types of Australian coals, including the Leigh Creek sub-bituminous–brown coal of South Australia.

The comparisons illustrate the variability of the compositions of coals. In comparison with the 'US' and 'World' bituminous coals, Collie coals are very depleted in As, B, Li, Mn, Mo, S, and Ca and are enriched in Ce, La, Th, and Y. The differences must relate, in part at least, to the nature of detrital source material, and the high values of Ce, for example, may be attributed to the granitic hinterland of the Yilgarn Craton. Bituminous coals from the United States have characteristics similar to those of Collie in that, while the highest values may indeed be high, mean values are usually quite low.

Table 7 indicates that the trace elements are normally substantially higher at Collie than in the brown coals from the Latrobe Valley of Victoria, though the reverse is true for Ca, Na, Mg, and Cl. On the whole, Collie coals have lower concentrations of trace elements than the Leigh Creek coals (except Ce and Sr), and there is no consistent pattern in the comparison with Australian bituminous coals.

The low values of B, Ca, K, and Mn, and the wide scatter of values of Pb, Sr, and Zn, reflected by the differences between the arithmetic and geometric means, stand out in the Collie coals in comparison with other Australian coals.

ELEMENT RELATIONSHIPS

The elements now present in the coals can be considered in three groups:

    (a) detritus;

    (b) organic;

    (c) chemical precipitates.

In addition, there has been authigenic growth of minerals at the expense of both detritus and chemical precipitates.

Nicholls (1968) suggested that resolution into detrital or organic origin could be made by interpretation of plots of a given component against the ash content, where the component concerned was plotted as the log concentration either of the 'whole' coal, or of the coal ash. Plots of the present data made in these ways (for those seams where there are an adequate number of samples) suggest that B, Mo, Ni, and Zn are the only components relatable to the organic part of the coal. Conversely, Si, Al, Zr, K, Cu, Ce, La, Li, Nb, Pb, V, Y, and Ca are commonly found to plot as detritus-related components.

However, few components behave consistently. Boron is the only element always relatable to the organic fraction (Fig. 6A). Silica, except in Cardiff No. 1, is the only component always relatable to the detrital fraction (Fig. 6B). Some elements, such as Cr or Th, which might be expected to relate solely to detritus do not, on this basis, do so (Fig. 6C). Some plots show convincing trends, but one or two samples per seam plot away from this trend, which indicates that some other process has operated selectively within the seam (Fig. 6D).

As Nicholls' plots do not help identify chemical precipitation, and the overall patterns may be obscured by excessive scatter, further clarification has been sought from correlation coefficients, cluster analysis, and the determined mineralogy.

Overall correlations are given in Table 8 (where the data have been log-transformed) for all coals except those used by Davy and Wilson (1984). Similar tables compiled for individual seams are not reproduced. Again some general patterns are clear. Chromium, Cu, Li, Nb, Th, V, Zr, Si, Al, and K are clearly relatable to the ash content and may be presumed to be detrital. Other groupings indicated include Ce, La, Y, and Pb; Ba, Sr, Ca, and P; Fe and S (and Mn, where Mn is more closely related to Fe than to S). The Ce group is also related to the ash content, but with lower correlations than the main detrital group.

These groupings may be interpreted partly in terms of minerals, and Table 9 gives the inferred or expected origins of the minerals. The ash-group elements appear to be related to the ubiquitous quartz–kaolinite–zircon minerals, with K hidden in degraded illite or in kaolinite; the Ce-group may be related to monazite, although there is a negative relationship with P; and the alkaline-earth elements and P may be related to the

observed sulphates and carbonates and, possibly, to an undetected phosphate mineral, possibly a modified apatite. No mineral has been found to account for the high overall correlation of rare earths with Pb. In fact, Pb correlates strongly with rare earths only in the Cardiff Member; elsewhere the correlation is mainly with Al and the more definite detrital group. Iron and S combine in pyrite, but Mn possibly relates more to Fe (hydroxides). There is no strong correlation of S with either Ba or Sr. Components which show no strong correlations with others include MgO (which is probably distributed between silicates and carbonates), Na$_2$O (which is probably present in silicates and in salt), and As, Ni, and Zn (which are probably distributed between the organic fraction, and pyrite and iron oxides).

Clustering, using the methods of Davis (1986), gives better definition to the groupings, and highlights the independent relationships of Ge, B, Co, and Mo (Fig. 7). Chlorine in this diagram also plots separately, in contrast with the correlation matrix (Table 8), where Cl has significant positive correlations with U, Cu, Ce, La, Y, and Na. Beryllium, Ni, and Zn form a subgroup not readily identified from the correlation matrix, which suggests an association of Be with organics or sulphides.

Thin-section studies show the alkaline-earth (and P) and Fe and S groups to be largely chemical precipitates; there is a detrital component for Ba and Sr in some seams. Minerals recognized as at least partly authigenic appear to have had no significant effect on the redistribution of the elements (except rarely for the alkaline earths) and, in all probability, the authigenic minerals have been formed by the mobilization and reprecipitation of nearby components already present in the coals and shales.

SEAM VARIATIONS

Variations within seams are generally more extreme than those between seams and it has not been possible to chemically fingerprint any individual seam.

Some of the difficulties of characterization are shown by samples 77888 A to C and 77889 A to C, collected from Stockton in the Ewington open-cut. The sample

TABLE 6. COMPARISON OF COMPOSITION OF COLLIE COALS WITH SOME USA AND WORLD DATA

| | COLLIE | | | USA (a) | | | World |
	$\bar{x}$	Geometric mean	90th percentile	Range		Average	average (b)
				Percentage			
Si	1.1	0.75	2.8	0.58	– 6.09	2.6	2.8
Al	0.95	0.80	1.8	0.43	– 3.04	1.4	1.0
Fe	0.39	0.20	0.84	0.34	– 4.32	1.6	1.0
				Parts per million			
Mg	422	283	754	1 000	– 2 500	1 200	200
Ca	665	458	1 323	500	– 26 700	5 400	10 000
Na	259	170	400	0	– 2 000	600	200
K	133	50	448	200	– 4 300	1 800	100
P	343	101	92	<100	– 1 400	–	500
S	5 010	3 750	9 000		–	20 000	20 000
As	0.7	0.4	1.2	0.5	– 106	15	3.0
B	3.4	3.2	5	1.2	– 356	50	75
Ba	183	96	500		–	150	500
Be	1.7	1.1	4	0	– 31	2	3
Ce	69	34	130		–	7.7	11.5
Cl	152	78	310	0	– 5 600	207	1 000
Co	15	8.3	21	0	– 43	7	5
Cr	11	7.1	24	0	– 610	15	10
Cu	11	5.8	15	1.8	– 185	19	15
Ge	2.7	0.6	7	0	– 819	0.71	5
La	34	17	68	0	– 98	6.1	10
Li	0.7	0.3	2		–	20	65
Mn	22	6.7	60	6	– 181	100	50
Mo	1.1	0.5	2	0	– 73	3	5
Nb	3.9	2.7	8		–	4.5	–
Ni	21	16	38	0.4	– 104	15	15
Pb	30	4.7	80	4	– 218	16	25
Rb	<5	<5	<5		–	2.9	100
Sr	110	38	330		–	100	500
Th	4.2	2.5	10		–	1.9	–
U	1.4(c)	0.8(c)	2(c)	<10	– 1 000	1.6	1
V	17	9.7	40	0	– 1 281	20	25
Y	22	11	47	<0.1	– 59	10	10
Zn	28	17	66	0	– 5 600	39	50
Zr	29	22	53	8	– 133	30	–

(a) taken from Valkovic (1983, Table 1, p. 58) (b) taken from Valkovic (1983, Table 2, p. 59-60) (c) estimated; many values below detection

14

TABLE 7. COMPARISON OF COMPOSITION OF COLLIE COALS WITH SOME OTHER AUSTRALIAN COAL

	Sub-bituminous coal Collie (n = 312)			Bituminous coal NSW and Qld (n = 40)			Brown/sub-bituminous coal Leigh Creek, SA (n = 5)			Brown coal Latrobe Valley, Vic. (n = 28)		
	Range	x̄	Geometric mean	Range	x̄	Geometric mean	Range	x̄	Geometric mean	Range	x̄	Geometric mean
Percentage												
Si	<0.05 – 5.1	1.1	0.75	–	–	–	–	–	–	(a) 0.11 – 3.51	0.34	0.20
Al	0.1 – 3.1	0.95	0.80	0.79 – 5.5	2.8	2.5	0.6 – 3.76	2.6	2.0	.0070 – 1.31	0.30	0.080
Fe	<0.01 – 4.9	0.39	0.20	0.09 – 3	0.83	0.65	0.49 – 1.88	1.41	1.2	.0055 – 0.49	0.175	0.075
Parts per million												
Mg	6 – 3 550	422	283	–	–	–	–	–	–	<700 – 4 700	1 900	1 300
Ca	14 – 8 580	665	458	400 – 18 000	4 000	2 500	8 100 – 16 300	10 900	10 300	(a) 100 – 10 700	4 400	1 200
Na	<22 – 3 310	259	170	110 – 3 600	570	380	3 600 – 8 100	6 200	5 900	370 – 2 200	950	880
K	<8 – 1 925	133	50	110 – 6 900	1 800	1 100	750 – 4 000	2 400	1 700	<39 – 120	75	68
P	<4 – 3 280	343	101	(c) 30 – 4 000	310	–	–	–	–	(a) <3 – 77	13	8
S	400 – 50 000	5 010	3 750	–	–	–	–	–	–	–	–	–
As	<0.1 – 36	0.7	0.4	0.19 – 16	2.4	1.2	2.1 – 3.7	2.8	2.7	<0.09 – 1.31	0.17	0.12
B	1 – 14	3.4	3.2	(c) 1.5 – 300	60		(b) 60 – 300	200		(a) 2 – 30	10	7
Ba	7 – 1 015	183	96	33 – 980	210	150	220 – 440	315	308	1.74 – 172	63	34
Be	<0.5 – 12	1.7	1.1	(c) <0.4 – 8	1.5	–	–	–	–	(a) <0.05 – 0.7	0.11	0.07
Ce	3 – 1 457	69	34	9 – 46	11	10	12.8 – 56	34	29	0.06 – 50.7	10.3	3
Cl	<10 – 4 900	152	78	24 – 1 900	360	200	2 600 – 4 900	3 800	3 600	380 – 1 300	780	730
Co	<5 – 321	15	8.3	1.6 – 20	5.9	4.4	2.9 – 7.1	4.8	4.6	0.05 – 2	0.60	0.36
Cr	<5 – 117	11	7.1	2 – 56	12.5	10	5.4 – 4.1	29	21	0.08 – 19	2.2	0.4
Cu	<1 – 741	11	5.8	(c) 2.5 – 40	15	–	(b) 3 – 40	15	–	(a) 0.2 – 9.5	1.3	0.6
Ge	<0.1 – 47	2.7	0.6	(c) <0.3 – 30	6	–	<1 – 6	2	–	–	<0.3	<0.3
La	1 – 585	34	17	4.2 – 24	12	11	6.3 – 30	19	16	0.034 – 14.2	1.30	0.31
Li	<0.1 – 9	0.7	0.3	–	–	–	–	–	–	(a) <0.06 – 1.3	0.14	0.09
Mn	<2 – 667	22	6.7	<5.4 – 410	120	73	31 – 240	150	145	0.45 – 55	21	8
Mo	<0.1 – 6	1.1	0.5	(c) <0.3 – 6	1.5	–	(b) <0.6 – 2.5	1.5	–	(a) <0.2 – 0.4	0.2	0.2
Nb	<1 – 71	3.9	2.7	–	–	–	–	–	–	–	–	–
Ni	2 – 161	21	16	(c) 0.8 – 70	15	–	(b) 4 – 25	10	–	(a) 0.1 – 6.8	2.4	1.7
Pb	<1 – 595	30	4.7	(c) 1.5 – 60	10	–	<2.5 – 20	4	–	(a) <0.1 – 9	0.8	0.3
Rb	<5 – 17	<5	<5	–	–	–	–	–	–	–	–	–
Sr	2 – 863	110	38	34 – 270	140	120	400 – 700	510	500	<6 – 250	82	51
Th	<0.4 – 26	4.2	2.5	0.57 – 7.9	3.7	3.0	2.1 – 17.4	9.2	6.6	<0.008 – 3.46	0.29	0.04
U	<1 – 58	1.4	0.8	0.28 – 2.5	1.3	1.1	0.43 – 3.8	2.1	1.5	<0.06 – 1.20	0.35	0.14
V	2 – 279	17	9.7	13 – 90	32	28	4.3 – 49	28	19	<10 – 25	3.5	3.3
Y	<5 – 217	22	11	(c) 1 – 25	7	–	(b) 2.5 – 40	15	–	–	–	–
Zn	<2 – 273	28	17	15 – 45	27	25	15 – 40	28	26	0.5 – 13	3.5	2.0
Zr	3 – 436	29	22	(c) 6 – 400	100	–	(b) 25 – 250	80	–	–	–	–

Data for non-Collie coals from Fardy and others (1984), except (a) from Bone and Schaap (1981), Table 5; (b) from CSIRO (1963); (c) from Swaine (1979)
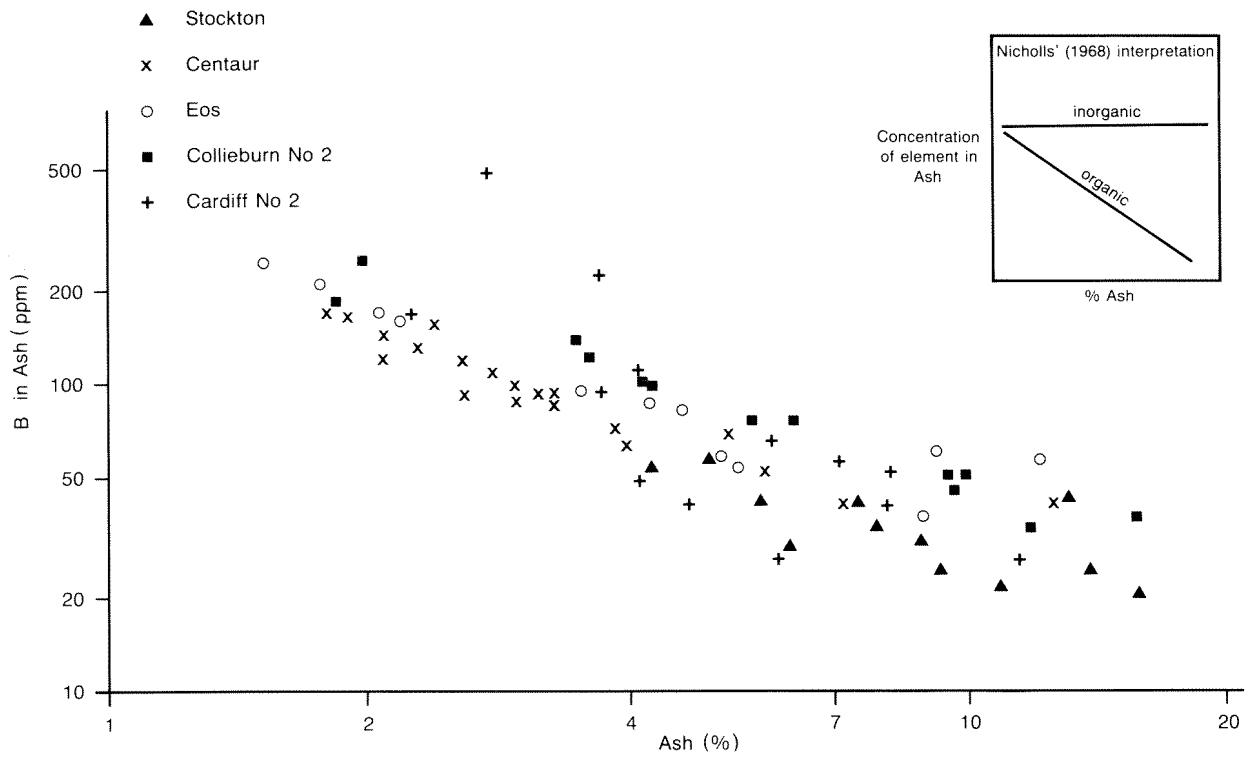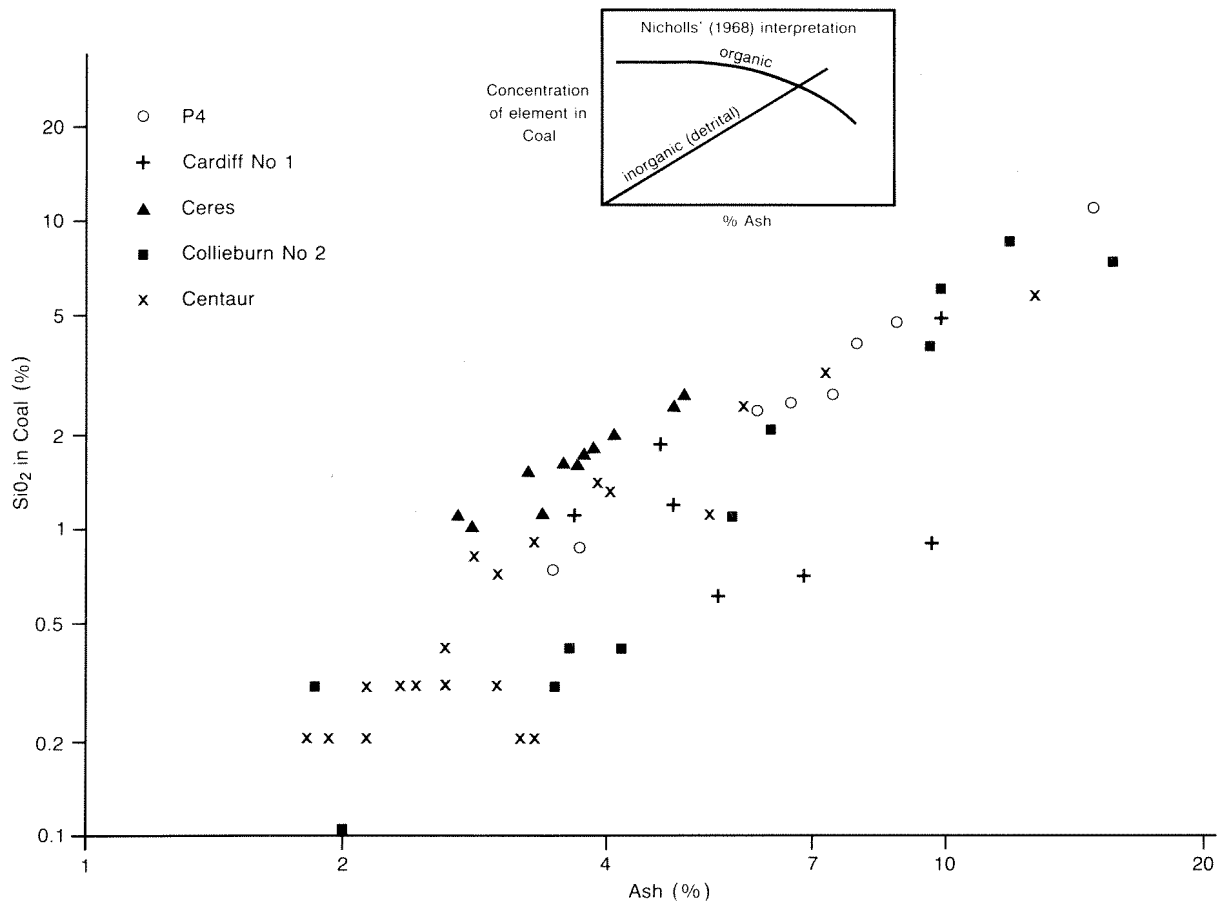
Figure 6. Plots for various seams showing the relationships of selected components to ash content.

16
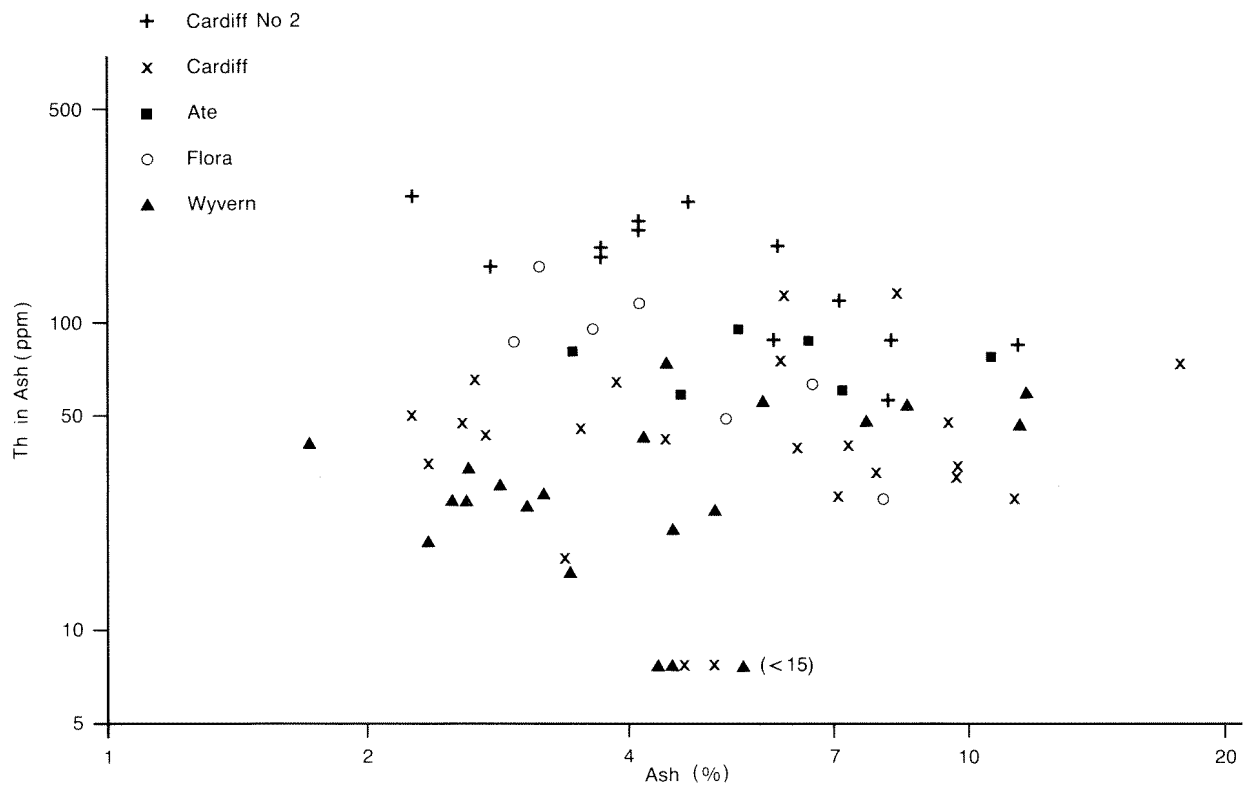
(C) Thorium in ash

GSWA 23750
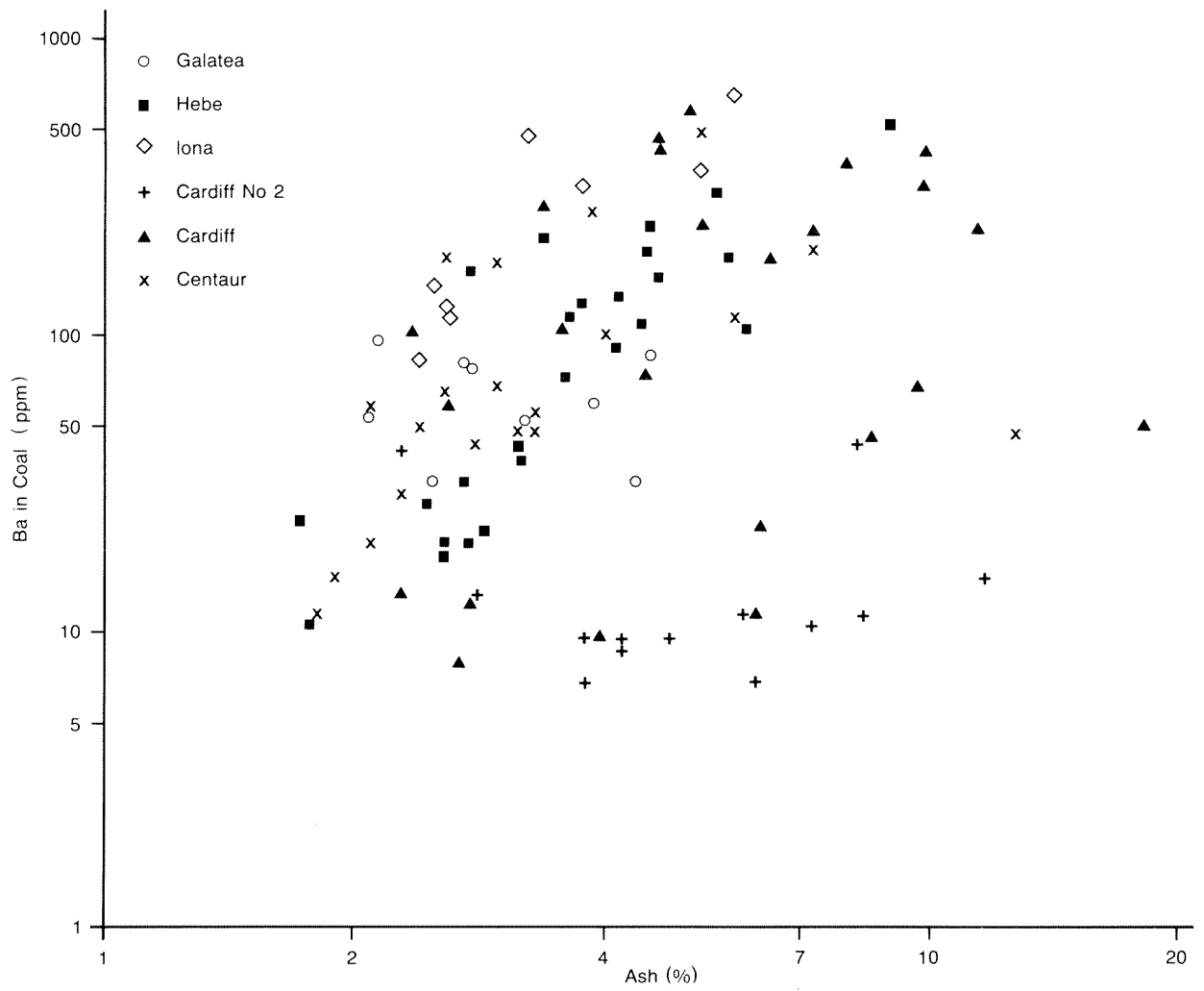
(D) Barium in Coal

GSWA 23751

17

TABLE 8. CORRELATION MATRIX FOR CHEMICAL COMPONENTS OF COLLIE COALS

	Ash	As	B	Ba	Be	Ce	Cl	Co	Cr	Cu	Ge	La	Li	Mn	Mo	Nb	Ni	Pb	S	Sr	Th	U	V	Y	Zn	Zr	SiO_2	Al_2O_3	Fe_2O_3	MgO	CaO	Na_2O	K_2O	P_2O_5
Ash																																		
As	–																																	
B	–	–																																
Ba	.20	–	–																															
Be	.38	–	–	–																														
Ce	.23	–	–	–	–																													
Cl	–	–	–	–	–	.65																												
Co	–	.21	–	–	–	–	–																											
Cr	.46	.23	–	–	.58	.23	–	–																										
Cu	–	–	–	–	–	.62	.73	–	.34																									
Ge	–	–	–	.21	.20	–	–	–	.47	–																								
La	.25	–	–	–	–	.98	.58	–	.22	.54	–																							
Li	.60	–	–	.20	–	–	–	–	–	–	–	–																						
Mn	.31	–	–	–	–	–	–	–	–	–	–	–	.53																					
Mo	–	.39	–	–	–	–	–	–	.30	.23	.44	–	–	–																				
Nb	.41	–	–	–	.20	–	–	–	–	–	–	–	–	–	–																			
Ni	.26	.65	–	–	.51	–	–	.34	.48	–	.50	–	–	–	.43	–																		
Pb	–	–	–	-.23	–	.42	.26	–	.21	.38	.33	.46	–	–	.29	–	–																	
S	–	.60	–	–	–	–	–	–	.24	–	–	–	–	–	.44	–	.47	–																
Sr	–	–	–	.87	–	–	–	–	–	–	–	–	–	–	–	–	–	–	–															
Th	.59	–	–	–	.26	.46	.39	–	.55	.41	.38	.46	–	–	.23	.56	.29	.52	–	–														
U	.21	–	–	–	–	.73	.74	–	.33	.88	–	.66	–	–	.27	–	–	.45	–	–	.48													
V	.31	–	–	–	.33	–	–	–	.70	–	.66	–	–	–	.34	.25	.38	.20	–	–	.53	–												
Y	.23	–	–	–	.31	–	–	–	.37	.68	–	.90	–	–	.28	–	.21	.37	–	–	.45	.73	.27											
Zn	–	–	–	–	.41	–	–	–	.21	–	–	–	–	–	–	.22	.41	–	–	–	–	–	.30	–										
Zr	.50	–	–	–	.24	–	–	–	.36	–	.24	–	.22	–	–	.89	–	–	–	–	.61	–	.30	–	–									
SiO_2	.90	–	–	–	.32	–	–	–	.33	–	–	–	.60	.30	–	.37	–	–	–	–	.45	–	.22	–	–	.45								
Al_2O_3	.78	–	–	–	.28	.55	.37	–	.39	.29	–	.59	.33	–	–	.44	–	.31	–	–	.72	.37	.35	.50	–	.48	.55							
Fe_2O_3	.29	.59	–	–	.21	–	–	.23	.31	–	–	–	.27	.47	.31	–	.43	–	.82	–	–	–	–	–	–	–	–	–						
MgO	.34	–	–	–	.21	–	–	–	–	–	–	–	.29	–	–	–	–	–	–	–	–	–	.21	–	–	–	–	–	.37					
CaO	.28	–	–	.45	–	–	–	–	–	–	–	–	–	–	–	–	–	–	–	.42	–	–	–	–	–	–	–	.26	–	.62				
Na_2O	.21	–	–	–	–	.57	.55	–	–	.43	–	.59	–	–	–	–	–	–	–	–	.27	.41	.26	.65	–	–	–	.46	–	.51	–			
K_2O	.66	–	.26	–	–	–	–	–	.37	–	–	–	.44	–	–	.36	–	–	–	–	.58	–	.32	–	–	.32	.66	.54	–	–	–	.34		
P_2O_5	–	–	–	.82	–	–	–	–	–	–	–	–	–	–	–	–	–	–	–	.96	–	–	–	–	–	–	–	–	–	–	–	–	.34	

Only values in excess of 0.2 (probability significance level of >99.5%) are recorded. Data were log-transformed before calculation.

TABLE 9. ORIGIN OF MINERALS PRESENT

Detrital	Chemical	Alteration products	Authigenic or partly authigenic
Quartz, amphibole, garnet, kyanite, monazite, mica, staurolite, zircon, rutile	Pyrite, siderite	Goethite, ?hematite	'Aluminium minerals'
	Some barytocelestite	Some kaolinite, leucoxene	Some barytocelestite, some kaolinite, 'lead mineral', some 'phosphate', ?some tourmaline
Some barytocelestite, some kaolinite, some tourmaline			

sites were only 50 m apart, and the positions in the seam were comparable, yet there are significant differences in abundance of no fewer than 17 components (Table 10). Since the Ewington open-cut is disused, these differences might be attributable to weathering, despite the care taken in sampling. However, other samples of Stockton, collected from drill core, show major variations in a further three components.

The ranges, and the arithmetic and geometric means of individual elements have been plotted, by sub-basin, on bar diagrams and illustrate the wide variations within the seams as well as the overlap of compositions between seams (Figs 8A to 8E). There are a few seams where, for certain elements, there is no apparent overlap (though this may simply be a function of the restricted numbers of samples analysed). It may be easier, when given the analysis of an unknown coal, to identify seams from which it has not been derived than to determine positively the seam of origin.

Absolute concentrations of a given element can vary substantially in unequivocally fresh material collected at different localities. Thus, Moira sampled in one part of the Shotts Sub-basin has very different Pb contents from the same seam sampled elsewhere in the same sub-basin (Fig. 8C). Barium is another element which varies substantially depending on the sampling locality.

Figures 9A and 9B show that the patterns of distribution of an element through the thickness of a seam may be dissimilar at different sampling sites. For the most part, those components which relate to the ash content show sympathetic (though not exactly similar) profiles through seams at different localities. The patterns of distribution of ash and ash-related elements, however, differ from seam to seam, and can become quite complex, particularly when the seams split and stony bands appear within the seams (Fig. 9A, Hebe). Boron, Ni, and Zn, as befits their dominant relationship with the organic fraction of the coal, have relatively little scatter at different points within a seam (Ni, Fig. 9B).

The overall low ash content, the irregular distribution of that ash, and the variation of detrital components within the seams, indicate non-systematic depositional conditions for the formation of the seams. There is no indication that detritus is more prominent at the base of a seam than elsewhere. Also, there is no indication that chemical deposition is restricted to zones with low detritus. The variation in abundances from place to place, and within individual seams, gives limited support to previously formulated ideas of deposition in local stagnant swamps formed in fluvial conditions, where streams were of low energy, braided, and periodically changed position in the floodplain (Lowry, 1976; Park, 1982; Wilson, in press). A few seams have
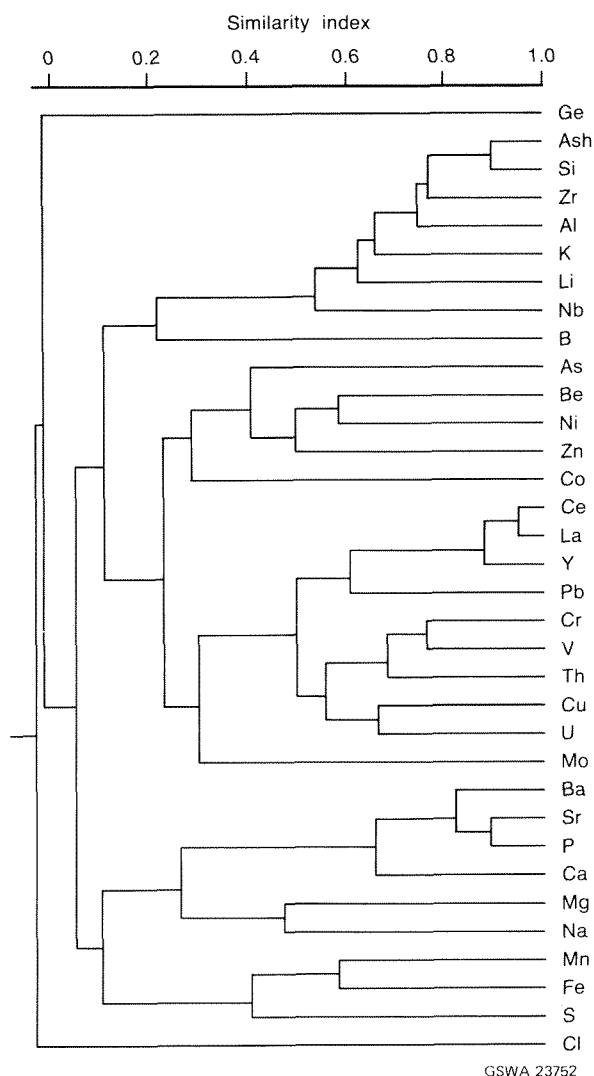
Figure 7. Cluster analysis dendrogram for all coals.

GSWA 23752

TABLE 10. ANALYSES OF SIX SAMPLES FROM THE STOCKTON SEAM

	77888A	B	C	7789A	B	C
Percentage						
Ash	13.2	15.9	8.9	5.0	5.8	4.3
SiO_2	2.5	4.3	3.1	2.4	2.8	2.0
Al_2O_3	5.9	7.6	3.6	1.3	1.7	1.5
Fe_2O_3	0.69	0.71	0.06	0.46	0.32	0.3
Parts per million						
MgO	5 210	5 370	3 840	90	60	60
CaO	12 000	11 100	4 790	150	120	180
Na_2O	1 000	910	690	<30	<30	<30
K_2O	110	130	120	20	20	10
P_2O_5	40	20	40	30	20	20
S	400	500	1 100	1 500	1 600	1 700
As	0.7	0.6	0.3	1	0.6	0.6
B	6	3	3	3	2	2
Ba	99	91	48	12	12	11
Be	6	6	3	2	3	1
Ce	84	93	48	58	48	31
Cl	650	560	350	150	110	130
Co	13	7	8	9	9	9
Cr	28	37	25	15	13	9
Cu	16	19	9	8	5	7
Ge	<0.3	<0.4	<0.2	<0.2	<0.2	<0.3
La	57	60	28	34	36	20
Li	0.7	0.6	0.3	0.2	0.2	0.2
Mn	<4	<4	<4	<4	<4	<4
Mo	1	0.6	0.4	0.5	0.1	0.7
Nb	7	11	6	3	3	2
Ni	70	48	30	33	29	27
Pb	16	16	11	4	3	4
Rb	<5	<5	<5	<5	<5	<5
Sr	166	144	67	2	2	3
Th	11	12	8	4	4	3
U	3	3	2	<1	<1	<1
V	12	14	14	9	7	6
Y	39	32	14	30	26	13
Zn	14	10	23	18	35	18
Zr	66	96	52	31	33	19

Other samples from this seam show major differences in

Ba (values 16-128 ppm)   Mn (values 2–667 ppm)   S (values 1 500–8 250 ppm)
Cl (values <10–90 ppm)   Li (values 0.3–6 ppm) Fe_2O_3 (values 0.13–4.5%)

indications of increasing detritus towards the top of the seam (e.g. Cardiff No. 2), but, for the most part, coal deposition is terminated abruptly with the coal composition not heralding any impending change.

SECULAR TRENDS BETWEEN SEAMS

The internal variation within seams obscures to some degree the variations between seams. Nevertheless (and bearing in mind the small numbers of samples collected from some seams), the bar diagrams (Figs 8A to 8E) can be used to examine evolutionary patterns in the sub-basins.

Cardiff Sub-basin

The Cardiff Sub-basin shows the most obvious patterns. In the Collieburn Member, Wyvern Seam has lower mean values for ash content, Al, P, B, Ba, Ce,

La, Sr, and V, and higher mean values for Fe, Mg, Ca, Th, and Zn than Collieburn No. 2. In the Cardiff Member, trends are pronounced and persist through four major seams. There is an overall decrease upwards from Neath to Cardiff No. 1 in Si, Fe, Mg, Ca, P, and Sr and a corresponding increase in Al, Ce, Cl, Cr, La, Ni, Th, V, Y, and possibly, Cu. For a few elements there is a peak (As) or a minimum (K, Ba, Nb) at Cardiff No. 2. In some cases the progression appears to carry straight through from Collieburn No. 2 to Cardiff No. 1 (e.g. Ca, P, Ba, and Sr). In addition, Cardiff Nos 1 and 2 are high in Ge and Pb in comparison with the lower seams.

The bar charts show that the seam currently identified as Ben is out of order in the above progression. These diagrams, and a principal component plot (Fig. 10, discussed later), show that Ben is compositionally closest to Cardiff No. 1 or Cardiff No. 2, usually the latter. If the observed trends are real, Ben is misidentified.

20

The main secular contrast is between decreasing alkaline earths (and P), and increasing rare earths. The trends are independent of differences in the amount of ash and presumably reflect changes in source material. Support for this comes from the contrasting behaviour in more definitely ash-related elements where Al, V, and Th have trends opposite to those of K and Nb.

Muja Sub-basin

In the Muja Sub-basin there are too few samples in the upper part of the Chicken Creek Member for trends to be significant. There is, however, an apparent tendency for Si, Al, As, and Ni to increase, and for Cl to decrease upwards.

Elemental patterns in the Muja Member are complex; there are no consistent increases or decreases through the member, though Si has an irregular tendency to increase upwards (Fig. 8A). In general, trends between two to three seams are present within a relatively narrow range of composition. These ill-defined trends generally 'peak' at Galatea–Flora, Diana–Diana Upper, and Ate. Arsenic reaches an absolute maximum value for the member in Diana. Other, more typical, behaviour is illustrated in Figures 8B to 8E.

Shotts Sub-basin

Seams in the Shotts Sub-basin, including the Ewington Member, have not been adequately sampled for the definition of secular trends. However, the lower part of the Premier Member may have lower Mg, Ca, P, Ba, Mn, and Sr than either the upper part of the member, or the underlying Ewington Member.

CORRELATIONS BETWEEN SEAMS

Early work at Collie recognized the presence of the Ewington Member in all sub-basins (Lord, 1952; Low, 1958). It was also believed that the Collieburn and Muja Members were correlatives 'on a large scale' (Lowry, 1976), but that individual seams from these members do not correlate across the Stockton Ridge. Similarly, the Premier Member seams of the Shotts Sub-basin are considered the equivalent of those in the Chicken Creek (Premier) Member of the Muja Sub-basin, but are separately named. Correlation of the individual seams between the two sub-basins has not yet been agreed (Park, 1982; Kristensen and Wilson, 1986).

Recent palynological work (J. Backhouse, personal communication, 1987) has suggested that the lower part of the Chicken Creek Member (Gryps to Centaur) is
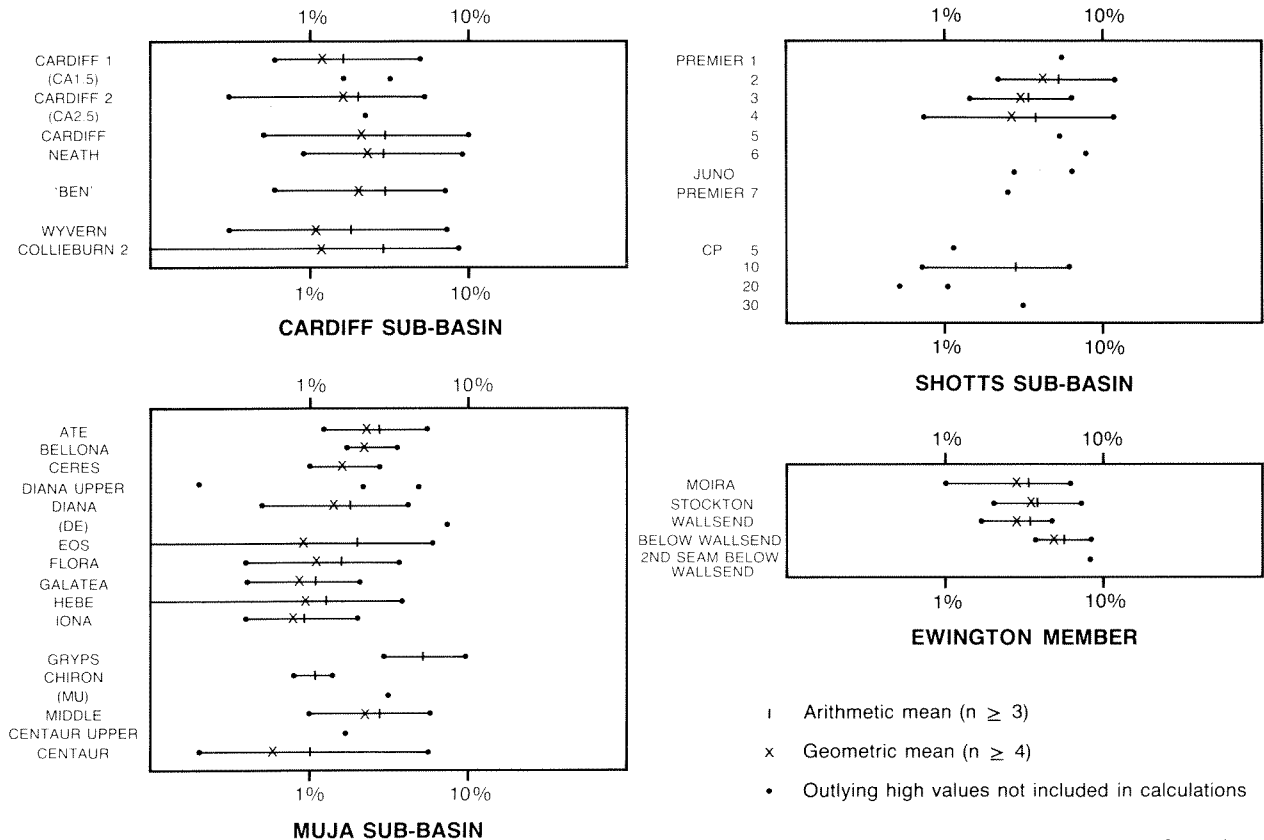
Figure 8A. Distribution of SiO$_2$ within each coal seam.
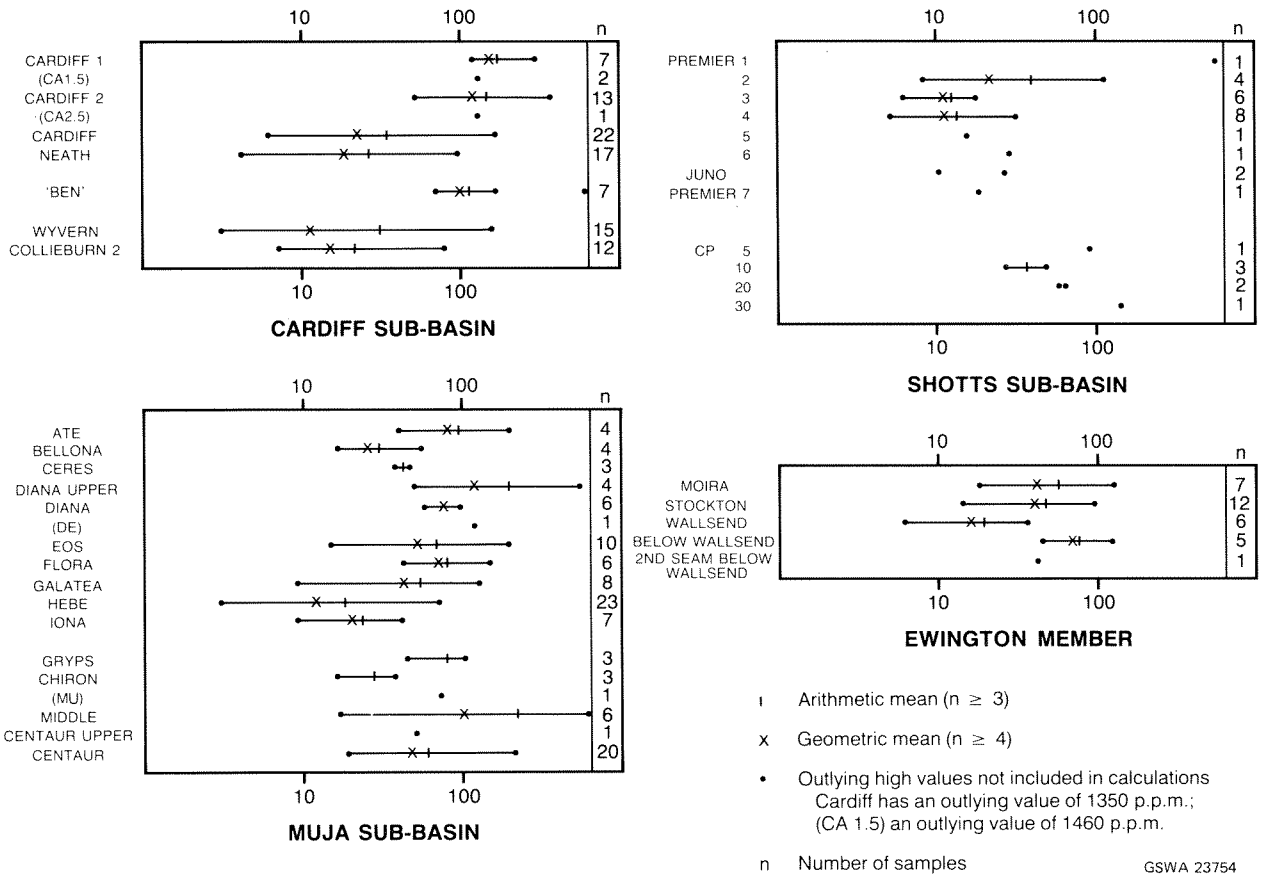
Figure 8B. Distribution of Ce within each coal seam.
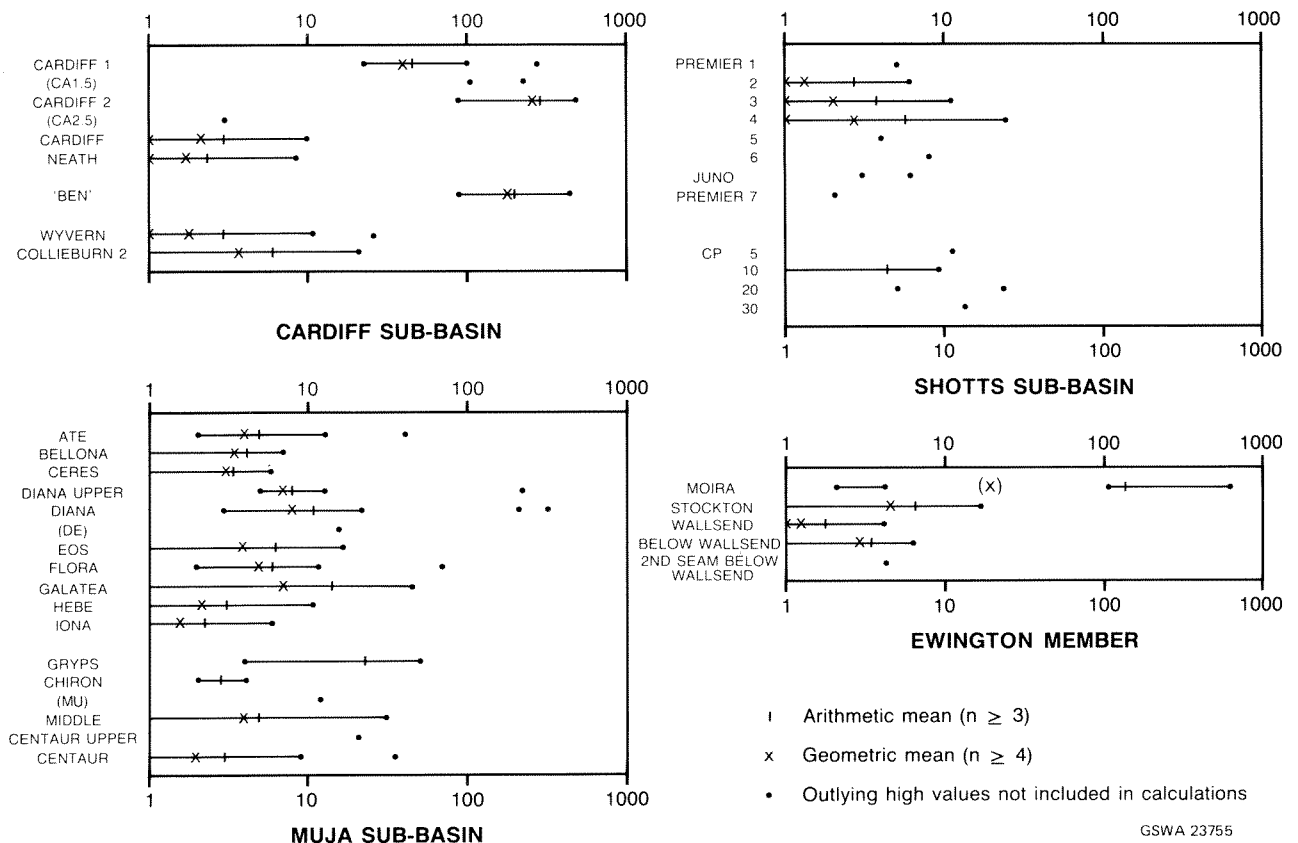
Figure 8C. Distribution of Pb within each coal seam.
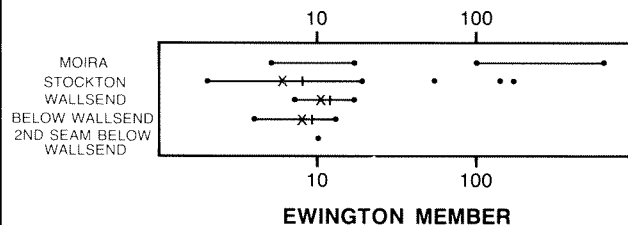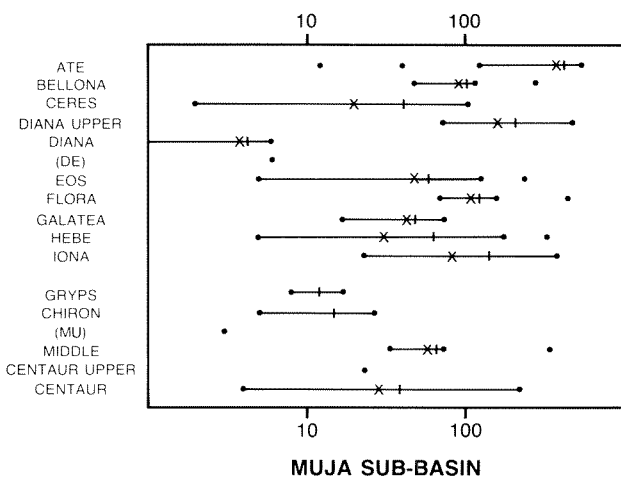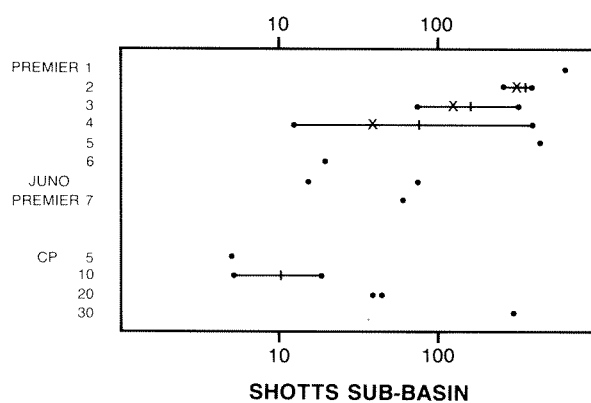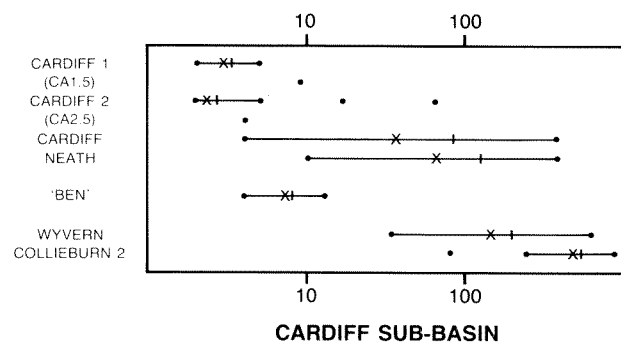
Figure 8D. Distribution of Sr within each coal seam.
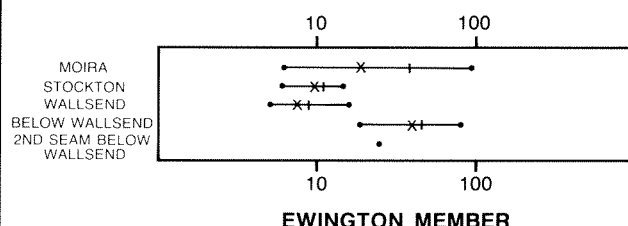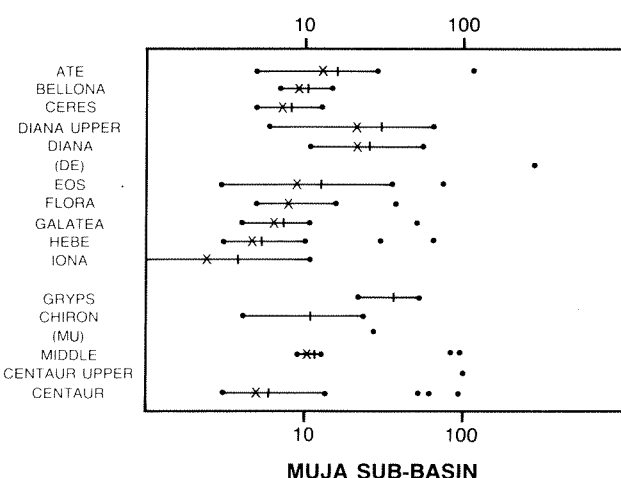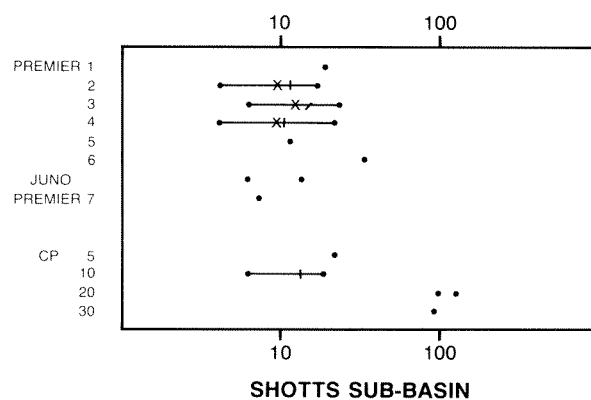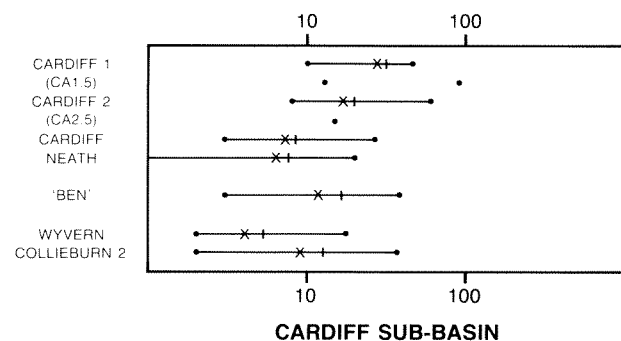
Figure 8E. Distribution of V within each coal seam

23

broadly comparable with Tantalus in the Cardiff Sub-basin, and that the Hebe–Iona seams of the Muja Member are equivalent to the Wyvern–Collieburn No. 2 levels of the Collieburn Member.

Unfortunately, in this study it has not been possible to compare the Premier Member with the Chicken Creek Member, since the seams considered to be potentially correlatable were only accessible in one or other of the sub-basins. Equally, as Tantalus was not available, no comparisons could be made of the Chicken Creek Member with potentially equivalent seams in the Cardiff Sub-basin.

Comparisons have been made of the Muja Member with the Collieburn and Cardiff Members using multi-variate principal component analysis (Davis, 1986). Figure 11 shows a comparison of Hebe and Iona with Wyvern and Collieburn No. 2. The indications from the diagram are that Iona, rather than Hebe, is more likely to correlate with Wyvern. Some samples of Hebe

overlap the Wyvern field, but there is little correspondence between Hebe and Collieburn No. 2. The diagram shows, however, the wide scatter of points and the paucity of samples from Iona (samples at one locality only). Thus the possible correlation can only be considered as supportive of Backhouse's work.

On the assumption that the palynological correlation is valid, a comparison of the coals above Wyvern–Iona suggests that Diana is the only possible Muja Member seam which could correlate with Cardiff Nos 1 and 2, and that Hebe has some similarities with Cardiff and Neath (Fig. 10). Eos, Flora, and Galatea show little correspondence; Eos and Galatea form groups which, whilst they fall within the range of Cardiff and Neath, do not closely resemble these seams. Flora, using this form of analysis, appears extremely variable.

These uncertainties of correlation are compounded when the different secular patterns of the Muja, and the Collieburn and Cardiff Members are considered. Wilson
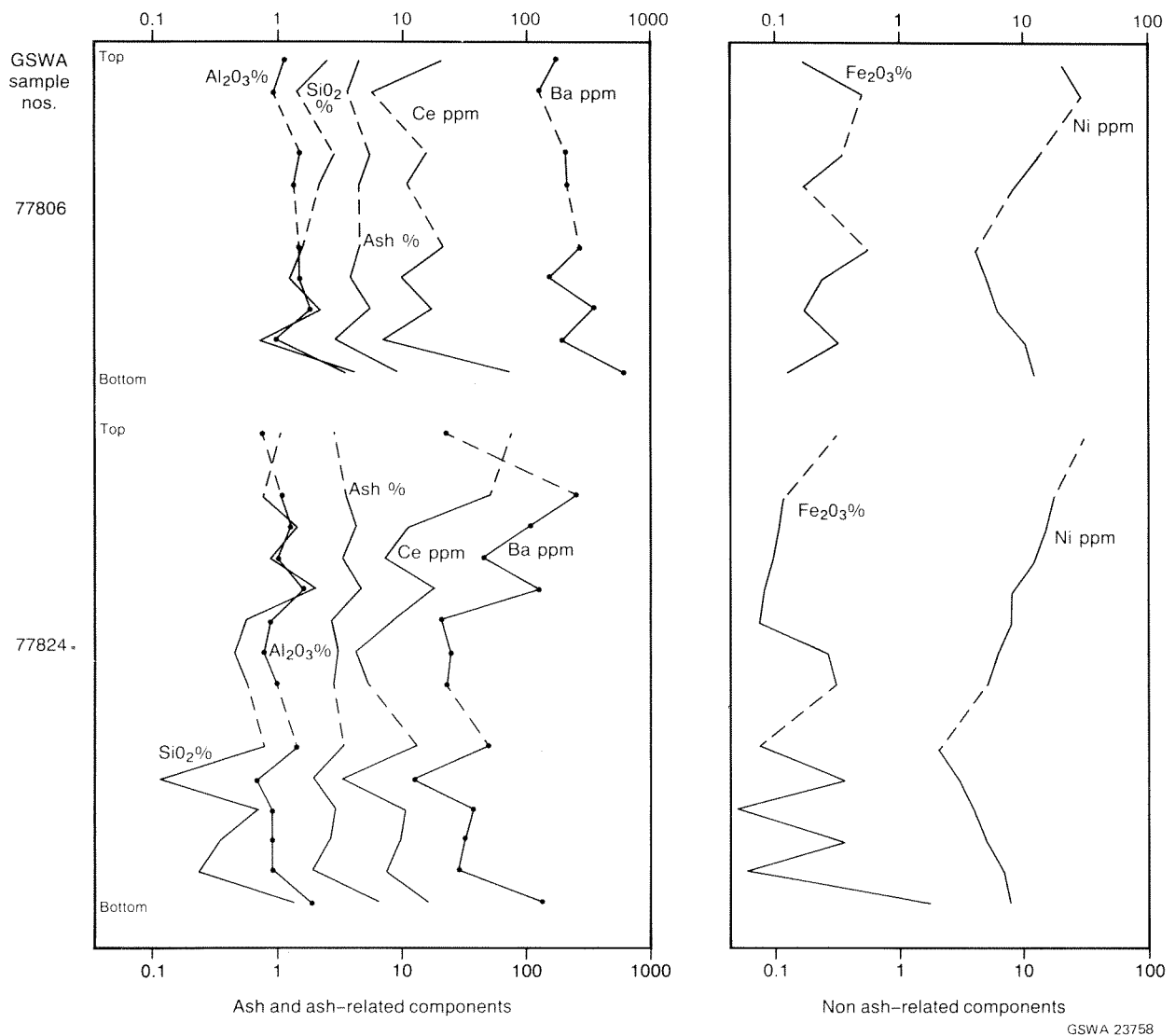
Figure 9A. Vertical section through Hebe seam (selected components).

24

(1989) has shown that deposition of Permian coal measures took place over a considerable area in the southwestern Yilgarn Craton, and it is only subsequent faulting and erosion which has isolated the Collie Basin. The lateral impersistence of seams, and variations in trace element characteristics, are believed to be related to the inherent variability of fluvial systems. Additional studies are clearly necessary before satisfactory correlations can be accepted.

POTENTIAL ENVIRONMENTAL PROBLEMS

Environmental problems relating to coals come from elements which are volatile when coal is burned, and from elements whose presence in the ash left after combustion is potentially dangerous.

Of the elements studied, Pb appears to offer the greatest environmental concern. No estimate has been made of losses during ashing, but the residues left,

particularly from Cardiff Nos 1 and 2 (and Ben), can contain over 1000 ppm Pb, up to a maximum over 1% Pb in one sample (77801 I) of Cardiff No. 2. Any use of ashes derived from these coals as back-fill, or for other rehabilitation purposes, must ensure that no Pb is released to the environment (including groundwater, vegetables, fodder crops, and pasture). As isolated samples of other seams also contain high levels of Pb, continued routine monitoring of this element (already being undertaken by the State Electricity Commission of Western Australia) is warranted.

Other potentially toxic pollutants, discussed by Lim (1979), and determined in this study, include As, Be, Co, Cu, Mo, Ni, and V. Uranium may also be included. These are particularly significant at Collie when the use or disposal of ash is considered. Though absolute levels in the coals are normally low, because the ash content is itself low, the residues in the ash can be quite high (Table 11). These levels are generally higher than
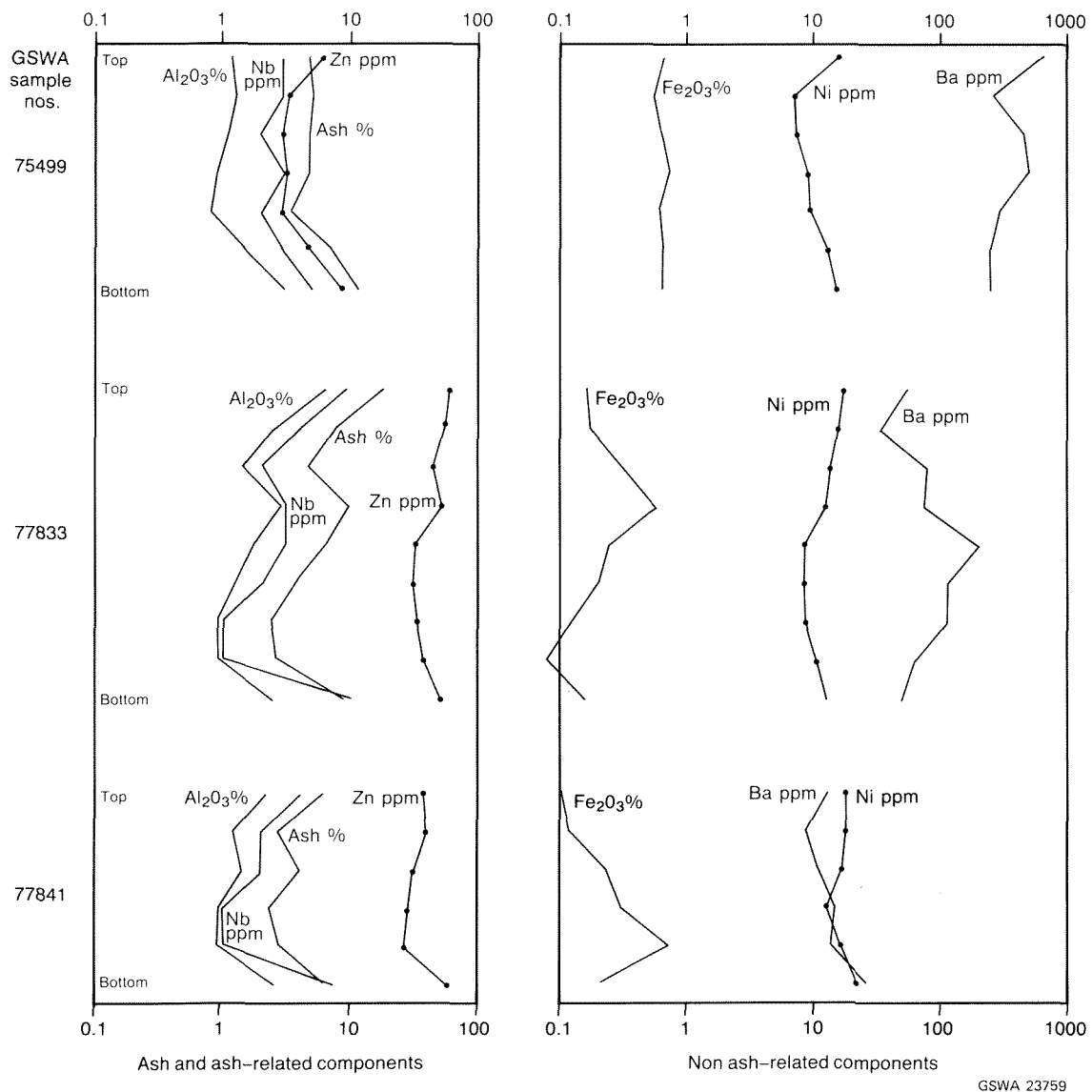
GSWA 23759

Figure 9B. Vertical section through Cardiff seam (selected components).

25
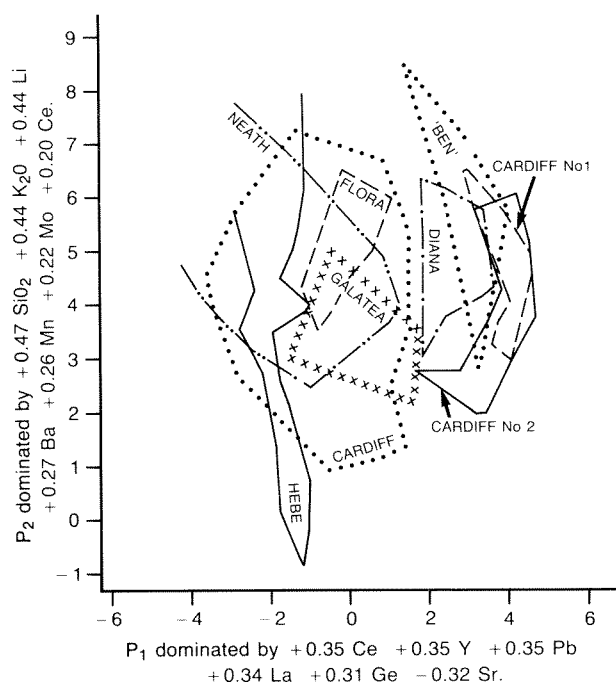
GSWA 23760

Figure 10. Principal-component plot for coals between Diana and Hebe, and between Cardiff No. 1 and Neath.

complete before deposition). These more soluble components have apparently been removed totally from the Collie Basin. Less soluble components, such as SiO_2 and Al_2O_3, though partly mobilized, have moved no great distance (being redeposited variously as gibbsite, authigenic kaolinite, or overgrowths on quartz). Whilst conditions are still favourable for some leaching, it is likely that the most intense activity occurred during the Miocene period at the time of the main surface lateritization and/or bauxitization.

The Collie Coal Measures show kaolinitic alteration and authigenic growth throughout their full structural thickness. These features cannot be due wholly to direct weathering and probably reflect deep circulating groundwater effects (though hydrothermal effects are possible).

natural trace elements in soils or shales (Vinogradov, 1959; Krauskopf, 1979). Given alkaline pH conditions, elements such as Cu, B, and Mo, at least, may become accessible to plants (Lim, 1979), and testing of the leaching potential of the ash is desirable before disposal.

POST-DEPOSITIONAL ALTERATION

The aluminium oxide and hydroxide minerals in the coal constitute *prima facie* evidence for incipient bauxitization. This is presumably more evident in the coals because of a high primary Al_2O_3 : SiO_2 ratio. Most coals with high Al_2O_3 : SiO_2 ratios are relatively near-surface (the ratios are lower in the deeper coals of the Shotts Sub-basin) which is consistent with a bauxitization pattern. The pH values of the coal slurries (Table 5) suggest that Fe, and trace elements such as Co and Mn, would be leached more quickly than Al. The present chemical state seems consistent with the general conditions for bauxitization in a reducing environment proposed by Norton (1973, fig. 3B, area 3). However, the range of pH values obtained (2.6–6.0) suggests that a variety of dissolution and reprecipitation processes may be active, resulting in the production of a wide diversity of end products. The lack of Ca, Mg, Na, and K in both interseam sediments and coal, and the virtual absence of Rb in coal, attest to a leaching process which probably began during the erosion of source rocks, prior to deposition of the sediments, but which was completed post-deposition (feldspar grains would have lost their shape if alteration had been

TABLE 11. A COMPARISON OF THE MEAN COMPOSITION OF COLLIE COAL ASH WITH WORLD AVERAGES FOR SHALES AND SOILS

	Mean content in ash	Mean content in shale (Krauskopf 1979)	Mean content in soils (Vinogradov 1959)
Percentage			
SiO_2	36.7	50.9	70.6
Al_2O_3	30.2	17.4	13.5
Fe_2O_3	8.9	6.7	5.4
MgO	1.2	2.3	1.0
CaO	1.7	3.5	1.9
Na_2O	0.62	1.2	0.85
K_2O	0.20	3.0	1.6
P_2O_5	1.5	0.17	0.18
S	9.6	0.25	0.09
Parts per million			
As	12	105	
B	71	100	10
Ba	3 088	600	500
Be	29	3	6
Ce	1 156	70	50
Cl	3 193	170	100
Co	281	20	8
Cr	194	100	200
Cu	195	50	20
Ge	54	1.5	1
La	627	40	40
Li	11	60	30
Mn	323	850	850
Mo	26	2	2
Nb	64	15	–
Ni	408	80	40
Pb	581	70	10
Sr	1 885	400	300
Th	69	12	6
U	20	3.5	1
V	286	130	100
Y	403	35	50
Zn	568	90	50
Zr	479	180	300

26
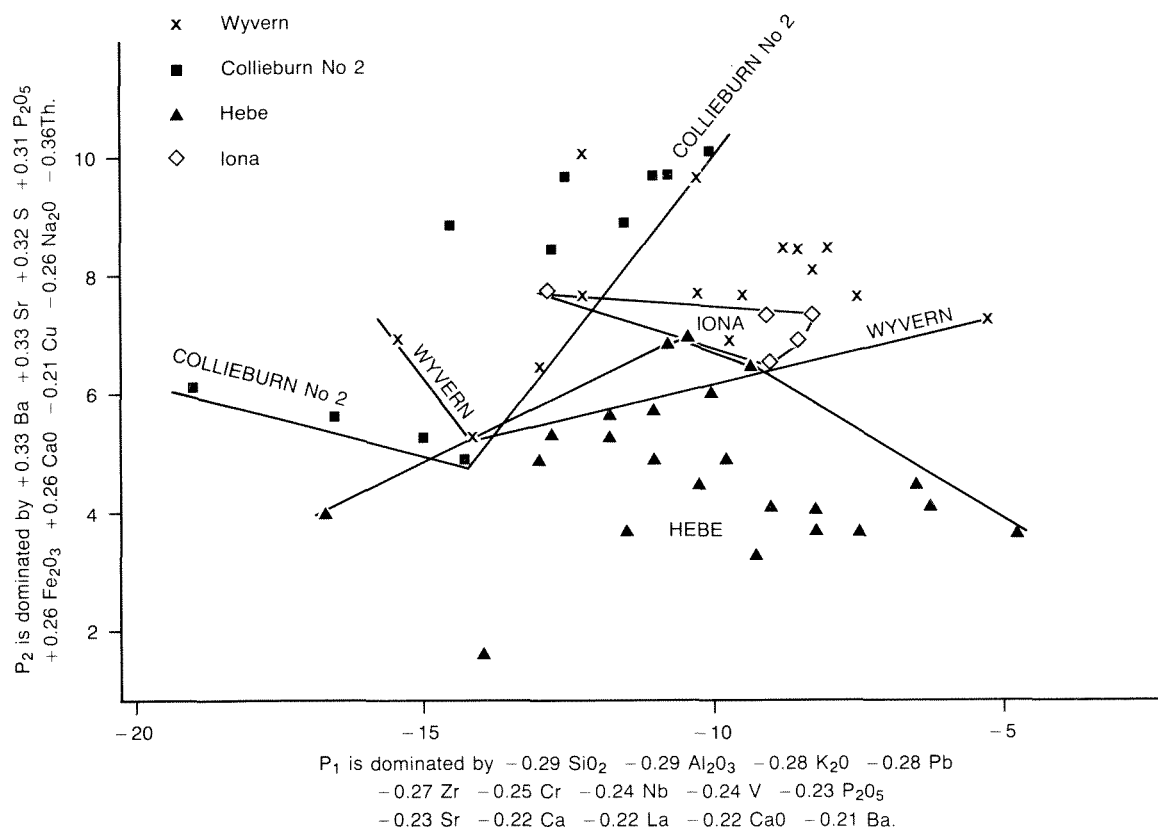
Figure 11. Principal-component plot showing samples from Hebe, Iona, Wyvern, and Collieburn No. 2.

ECONOMIC SIGNIFICANCE AND SOURCE OF DETRITUS

Though there are enhanced values of base metals and uranium in some coals and interseam sediments, there is no direct suggestion that any beds are sufficiently mineralized as to constitute an orebody. The presence, in the shale below Diana in the Muja open-pit, of what may be construed as an incipient roll-front, (however U correlates more strongly with Cu than with the more usual Mo or V) means that there is some potential for finding U mineralization within the Permian sediments. In addition, the presence of high U content, together with the high levels of Pb located elsewhere, may point to the presence of mineralized source rocks.

Uranium is well known for its capacity to travel in solution and form secondary, or even tertiary, deposits (Gruner, 1956) and its origins probably lie in 'hot' granitoids located outside the Collie Basin. The presence of 'hot' granitoids may be further suspected from the presence, in certain coals and claystones, of high levels of Ce, La, and Y, which are usually deemed to have originated in fractionated granitoids, alkaline granitoids, pegmatites derived from such granitoids, or carbonatites.

Lead content is not universally high, either in the coal or in interseam sediments. Localized 'high' spots therefore indicate a specific source of lead. Localization of high values further suggests a source at no great distance from the basin, since Permian glacial or fluvial activity might be presumed to 'smear' the distributions. The consistently high Pb content in Cardiff Nos 1 and 2, in the thin seams of coal between Cardiff No 1 and Cardiff, and in sediments between these seams (all located close to the southwest margin of the basin), strongly points to a nearby source that was exposed and eroded while the Cardiff Member was being deposited. Since this source was apparently exposed for an appreciable period (to contribute to some 65–75 m of sediment) it may have been totally eroded. Nevertheless some remnants may remain awaiting discovery.

Lead, Ba, and Sr are at relatively high levels in some sediments and, if hydrothermal processes have played a part in the development of kaolinite, these 'high' values may result from leakages of fluids along basin-margin faults.

However, the source of high values of elements of economic interest other than U, and perhaps Ba and Sr, is more likely to be detritus. Both this study and that of Glover (1952) indicate mixed origins for this material. These include metasediments (represented by quartzite pebbles, kyanite, staurolite, and garnet), granitoids (quartz, feldspar, zircon, monazite), and mafic rocks (hornblende, epidote). The degree of angularity of some of the grains implies only one cycle of erosion

27

(Glover, 1952), and Glover notes that the large quantities of garnet found in some interseam sediments are 'probably rather near the source of origin'.

Two studies of palaeocurrent directions (Wilde and Walker, 1978; Wilson, 1989) suggest that the source of detritus in the vicinity of Cardiff Nos 1 and 2 in particular, and for the Cardiff Member in general, was from the east through to the south, southeasterly being dominant. The same quadrant dominates palaeocurrents in the Muja Member and, although sandstones underlying the U-bearing shale below Diana show fluvial depositional currents from the east (Wilson, in press), this direction should be considered purely local within an overall northwesterly dipping palaeoslope. Thus, the sources of both Pb and U may be sought south to east of the Collie Basin; the Pb from a source perhaps west or south of the Stockton Ridge, the U from a source south or east of Muja. As the coals and sediments which contain both the Pb and the U include minerals derived from metasediments, the sources may lie in the Balingup Metamorphic Belt (Wilde and Walker, 1982). This belt is exposed between Donnybrook and Bridgetown and includes the pegmatites at Greenbushes, some 50 km to the south. Moreover, gneissic and migmatitic rocks, which may relate to this belt and which may include derivatives of sedimentary and volcanic rocks, extend east of Bridgetown. These are appropriate rocks for primary sources for the Pb and U. The Greenbushes deposits contain rare-earth minerals (M. Pryce, personal communication, 1987), and analyses of the coal and interseam sediments for As, Sb, and Sn may indicate whether a Greenbushes-type pegmatite is a likely source for the rare earths of the coal, or whether some alternative source must be sought. The association of the high Pb content with above average Cu level suggests that a sulphidic volcanogenic source may be needed for the Pb.

Similarly, in the quadrant southeast of the coalfield, there is an abundance of poorly exposed granitoids, among which may occur plutons more fractionated than the rest and thus containing potential sources of U.

Most of the area of possible source rocks is covered by laterite and other more recent sediments, so the source rocks, if still present, may be no longer directly exposed. Exploration for such rocks might be directed through a pisolitic laterite study of the type suggested by Smith (1987), and Smith and others (1987).

CONCLUSIONS

The principal conclusions from this project are as follows:

(1) The Collie coals generally have low trace-element concentrations. However, individual seams and occasional samples in other seams may have high trace-element values.

(2) Collie coals have unusually low ash and silicate components. They are very low in As and B, and are high in Ce, La, and Y compared with other 'World' coals. The reported values are usually similar to those reported for Australian bituminous coals. Most trace elements are more abundant in Collie coals than in Victorian brown coals, but are generally quite similar in abundance to Leigh Creek coal. However, 'silicate' components are higher at Leigh Creek.

(3) It has proved impossible to 'fingerprint' seams because of compositional variation within seams. It may be easier, when given the analysis of an unknown coal, to identify seams from which it has not been collected than to identify positively the specific seam from which it was taken.

(4) Correlation of the seams between the sub-basins has not proved possible with the samples to hand, except that the data available support a correlation, based on palynological grounds, of Iona in the Muja Sub-basin with Wyvern in the Cardiff Sub-basin. Diana is the only seam of the Muja Member which has potential for correlation with the upper part of the Cardiff Member.

(5) There are some systematic secular trends in the abundances of certain elements — namely the alkaline and rare-earth elements, particularly in the Cardiff Sub-basin.

(6) Lead levels in the upper seams of the Cardiff Member are high, up to 480 ppm (equivalent to 1% Pb in the ash, 77802 I, Cardiff No. 2). The maximum Pb value in any coal is 595 ppm. Use of the ash from these coals for rehabilitation purposes could conceivably constitute a health hazard.

(7) Al_2O_3 : SiO_2 ratios of many coal samples are very high and there is an excess of Al_2O_3 above that required for the formation of clay minerals (e.g. kaolinite). The authigenic nature of the Al mineral, and the recognition of at least some crystalline gibbsite, implies incipient bauxitization, probably at the time of production of the Darling Range bauxitic laterite in the Miocene. The near absence of Rb, and low values of Na_2O and K_2O, coupled with visibly altered feldspar, also indicate that post-depositional leaching has been active. These last components have apparently been largely removed from the area; other components, such as Al_2O_3 and SiO_2 have been mobilized but redeposited at no great distance.

(8) The minerals present indicate mixed origins; they are related variously to detrital input, chemical deposition, and authigenic diagenetic growth.

(9) Many components, including Al, Si, K, Cr, Cu, Li, Nb, Th, V, and Zr, and, to a lesser extent, Ce, La Pb, and Y, can be related to ash and are of presumed detrital origin. Other components, notably B, can be related to the organic component of the coals. Some elements (e.g. Mg, Na) are partitioned between minerals of different origins, and Ba and Sr, though present as barytocelestite, have a mixed chemical–detrital origin. Other elements, such as Zn, are found in association with different minerals in different seams.

(10) The distributions of high Pb and U values may have economic significance. If nothing else they point to the possibility of mineralized source rocks. The geographic localization of the high Pb values suggests that the source of this Pb may have been close to the southern margin of the Cardiff Sub-basin. The high U values suggest the presence of fractionated granitoids in a source area east of Muja. A possible fractionated granitoid source is also postulated for the high rare-earth content of some of the coals and interseam sediments. Any remnants of these source rocks, which still exist, may now be concealed under laterite or other cover.

(11) The relative lack of detritus or detrital minerals, and associated low values of trace elements in the coals are extra evidence in support of the previously stated concept of coal deposition, in situ, in very low-energy swamp conditions within a braided-fluvial complex.

(12) On the basis of its composition, the seam sampled as Ben, in the southwestern part of the Cardiff Sub-basin, is probably part of either Cardiff No. 1 or Cardiff No. 2.

ACKNOWLEDGEMENTS

REFERENCES

BONE, K.M., and SCHAAP, H.A., 1981, Trace elements in Latrobe Valley brown coal: environmental and geochemical implications: SEC Victoria, Report S0/80/15 (restricted unpublished report).

BROWN, H.R., and SWAINE, D.J., 1964, Inorganic constituents of Australian coals: Journal Institute Fuel, v. 37, p. 422–440.

CHATTERJEE, P.K., and POOLEY, F.D., 1977, An examination of some trace elements in New South Wales coals: Australasian Institute of Mining and Metallurgy, Proceedings, No. 263, p. 19–30.

CLARK, M.C., and SWAINE, D.J., 1962. Trace elements in coal (1) New South Wales coals, (2) Origin, mode of occurrence and economic importance: CSIRO, Division of Coal Research, Technical Communication 45.

CSIRO, 1963, Characteristics of coals from lobe D, Leigh Creek coalfield, South Australia: CSIRO Division of Coal Research, Location Report 34.

DAVIS, J.C., 1986, Statistics and data analysis in geology: Wiley, New York, 646 p.

DAVY, R., and WILSON, A.C., 1984, An orientation study of the trace — and other — element composition of some Collie coals: Western Australia Geological Survey, Record 1984/3.

DAVY, R., and WILSON, A.C., in press, Chemical analyses of samples from the Collie Coal Measures: Western Australia Geological Survey, Record 1989/17.

DEER, W.A., HOWIE, R.A., and ZUSSMAN, J., 1962, Rock-forming minerals, v. 5, Non-silicates: Longmans, London, 371 p.

DOOLAN, K.J., TURNER, K.R., KNOTT, A.C., and WARBROOKE, P., 1984, A study of the feasibility of elemental analyses as an aid in coal seam discrimination: BHP Co. Pty Ltd, Central Research Labs., Report CRL/R/17/84 (unpublished).

FARDY, J.J., McORIST, G.D., and FARRAR, Y.J., 1984, The analysis of coals and fly ash for trace elements and natural radioactivity: Australian Coal Science Conference, Proceedings, Churchill, Victoria, p. 159–166.

GLOVER, J.E., 1952, Petrology of the Permian and Tertiary deposits of Collie, Western Australia in 'Collie Mineral Field', by J.H. LORD: Western Australia Geological Survey, Bulletin 105, Part 1, Appendix III, p. 202–239.

GLUSKOTER, H.J., RUCH, R.R., MILLER, W.G., CAHILL, R.A., DREHER, G.B., and KUHN, J.K., 1977, Trace elements in coal; occurrence and distribution: Illinois State Geological Survey, Circular 499.

GRUNER, J.W., 1956, Concentration of uranium in sediments by multiple migration accretion: Economic Geology v. 57, p. 495–520.

HARRIS, L.A., BARRETT, H.E., and KOPP, O.C., 1981, Elemental concentrations and their distribution in two bituminous coals of different palaeoenvironments: International Journal Coal Geology, v. 1, p. 175–193.

HART, R.J., and LEAHY, R.M., 1983, The geochemical characterisation of coal seams from the Witbank Basin: Geological Society South Africa, Special Publication, v. 7, p. 169–174.

HAWLEY, J.E., 1955, Spectrographic study of some Nova Scotian coals: Canadian (Institute) Mining Metallurgy Bulletin, v. 48, no. 523, p. 712–726.

KNOTT, A.C., and WARBROOKE, P., 1983, Characterisation of a range of Australian raw coals: BHP Co. Pty Ltd, Central Research Laboratories, Report CRL/R/21/83 (unpublished).

KRAUSKOPF, K.B., 1979, Introduction to geochemistry: McGraw-Hill, New York, 2nd edition, 617 p.

KRISTENSEN, S.E., and WILSON, A.C., 1986, A review of the coal and lignite resources of Western Australia, in 'Geology and Exploration', edited by D.A. BERKMAN: Commonwealth Mining and Metallurgy Institute Congress/Australasian Institute Mining and Metallurgy, Publication 13, Melbourne, Australia, p. 87–97.

LIM, M.Y., 1979, Trace elements from coal combustion atmospheric emissions: IEA Coal Research, London, Report ICTIS/TRO5, 58 p.

LORD, J.H., 1952, Collie Mineral Field: Western Australia Geological Survey, Bulletin 105, part 1.

LOW, G.H., 1958, Collie Mineral Field: Western Australia Geological Survey, Bulletin 105, part 2.

LOWRY, D., 1976, Tectonic history of the Collie Basin, Western Australia: Geological Society Australia Journal, v. 23, p. 95–104.

NICHOLLS, G.D., 1968, The geochemistry of coal-bearing strata, in 'Coal and coal-bearing strata', edited by D.G. MURCHISON and T.S. WESTOLL: Oliver and Boyd, Edinburgh, p. 269–307.

NORTON, S.A., 1973, Laterite and bauxite formation: Economic Geology, v. 68, p. 353–361.

PARK, W.J., 1982, The geology of the Muja Sub-basin, a model for the Collie Basin, Western Australia, in 'Coal resources: origin, exploration and utilization in Australia', edited by C.W. MALLET: Geological Society of Australia, Symposium Proceedings, p. 319–340.

SAPPAL, K.K., 1982, Petrography of Collie coal from the Muja Sub-basin, Western Australia: Australasian Institute Mining Metallurgy, Conference, Proceedings, Melbourne, Victoria, p. 433–439.

SMITH, R.E., 1987, Current research at CSIRO Australia on multi-element laterite geochemistry for detecting concealed mineral deposits: Chemical Geology, v. 60, p. 205–214.

SMITH, R.E., PERDRIX, J.L., and DAVIS, J.M., 1987, Dispersion into pisolitic laterite from the Greenbushes mineralized Sn-Ta pegmatite system, Western Australia: Journal Geochemical Exploration, v. 28, p. 251–265.

SWAINE, D.J., 1979, Trace elements in Australian bituminous coals and fly ashes, *in* 'Combustion of pulverized coal, the effect of mineral matter', *edited by* I. McSTEWART and T.F. WALL: Colloquium Department Engineering, University of Newcastle, N.S.W., p. W3-14-18.

USGS, 1982, Chemical impurities in coal, *in* Geological Survey Research, 1981: U.S. Geological Survey, Professional Paper 1275, 30 p.

VALKOVIC, V., 1983, Trace elements in coal, vol. 1: CRC Press, Boca Raton, Florida.

VINOGRADOV, A., 1959, The geochemistry of rare and dispersed chemical elements in soils, 2nd edition, revised: New York, Consultants Bureau, 209p.

WILDE, S.A., and WALKER, I.W., 1978, Palaeocurrent directions in the Permian Collie Coal Measures, Collie, Western Australia: Western Australia Geological Survey, Annual Report 1977, p. 41–43.

WILDE, S.A., and WALKER, I.W., 1982, Collie, Western Australia: Western Australia Geological Survey 1:250 000 Geological Series Explanatory Notes, 39 p.

WILSON, A.C., (in press), Collie Basin, *in* Geology and Mineral Resources of Western Australia: Western Australia Geological Survey, Memoir 3.

WILSON, A.C., 1989, Palaeocurrent patterns in the Collie Coal Measures — the implications for sedimentation and basin models: Western Australia Geological Survey, Professional Papers, Report 25.

GEOLOGY AND GROUNDWATER RESOURCES OF THE SUPERFICIAL FORMATIONS BETWEEN PINJARRA AND BUNBURY, PERTH BASIN

by A. C. Deeney

ABSTRACT

The geology and hydrogeology of the superficial formations of the coastal plain between Pinjarra and Bunbury have been investigated by drilling on a 4 km grid. A total of 151 bores were drilled at 74 sites to a depth of between 2 and 54 m. Additional bores were drilled at five sites and pumping tests were carried out to determine aquifer characteristics.

The superficial formations unconformably overlie Mesozoic sediments and comprise a number of formations of Quaternary age which form a stratigraphically complex sequence up to 90 m thick.

The superficial formations form an unconfined aquifer which consists predominantly of sand and limestone in the west, and clay and sand in the east where the clay (Guildford Formation) forms an important aquitard in the upper part of the aquifer. The saturated thickness of the aquifer is generally 20–30 m. It can be divided into three regional flow systems, namely Myalup, Waroona, and Serpentine, from which groundwater discharges to the Peel Inlet, the Harvey Estuary and the coastal lakes across saline interfaces, and to the Murray, Harvey, Wellesley, and Collie River Systems. Substantial quantities of groundwater discharge locally to drains and to the underlying Mesozoic sediments, and are lost by evapotranspiration from the shallow water table.

The groundwater salinity in the Myalup flow system is generally less than 1000 mg/L TDS. In the northern part of the Waroona flow system and the southern part of the Serpentine flow system, the salinity is generally less than 1500 mg/L TDS. Groundwater in the remainder of the Waroona flow system is brackish to saline and there is considerable local and seasonal variation in the groundwater salinity. The high groundwater salinity of up to 22 900 mg/L TDS in this area is probably the result of long term flood irrigation using imported irrigation water.

Groundwater in the area is predominantly of the sodium chloride type. Some groundwater in calcareous sediments (Jandakot Beds) and from the crest of the Yanget and Mialla groundwater mounds, which are developed in the Myalup flow system, is of the calcium bicarbonate type.

Generally, the groundwater would require treatment for turbidity, hardness, colour, hydrogen sulphide, and iron before use as public water supplies.

Estimates of groundwater throughflow range from 1.6 x 10^6 m^3 per annum for the Serpentine flow system to 19.1 x 10^6 m^3 per annum for the Myalup flow system which is the most prospective area for further development. These estimates provide a conservative basis for decisions concerning groundwater development since they only represent a proportion of the annual recharge to the aquifer.

KEYWORDS: Swan Coastal Plain; hydrogeology; geology; groundwater; salinity; stratigraphy

INTRODUCTION

LOCATION

The area investigated comprises about 1600 km^2 of predominantly agricultural land located on the Swan Coastal Plain 110 km south of Perth (Fig. 1). It extends for 80 km from the Murray and South Dandalup Rivers in the north, to the Collie River in the south, and is bounded by Harvey Estuary, the coastal lakes and Leschenault Inlet in the west, and by the Darling Scarp in the east.

The regional centres of population, Mandurah and Bunbury, are situated just outside the area and draw water from local groundwater resources. Water supplies for the smaller towns within the area, with the exception of Australind, are obtained from dams located east of the Darling Scarp. Groundwater from the superficial formations is widely used for stock and domestic supplies; large-scale irrigation is restricted to a few small areas of arable land near the coast.

PURPOSE AND SCOPE

The work was carried out to investigate the hydrogeology of the superficial formations; to establish a network of monitoring bores to measure the natural water level and salinity variations in the aquifer; and to assess the extent of high salinity groundwater in the Waroona, Harvey, and Collie irrigation areas (Fig. 1). Subsequently, the scope of the project was extended to include estimation of the quantity of phosphorus discharged by groundwater to the Peel Inlet–Harvey Estuary system. This was a matter of concern, particularly in the longer term, because of excessive algal growth in Peel Inlet due to the input of phosphorus derived from fertilizer.

INDIAN OCEAN

50   Harvey Shallow bore

A1–G8   Lake Clifton bores

BS2   Bunbury Shallow bore

M11   Mandurah bore

HL2   Harvey Line bore

BPL/2   Binningup Line bore

HIA1.2   Harvey Irrigation Area bore

HIS1/180   Harvey Irrigation Scheme bore

P175   Private bore

CS1   Cable Sands bore

PWD1/180   Public Works Department bore

WHS4   Waroona High School No. 4 bore

PIN 1   Pinjarra 1

PC1   Preston 1

LP1   Lake Preston 1

PB1   Preston Beach bore

AE3   Alcoa (Pinjarra) bore

AWA   Alcoa (Wagerup) bore

Waroona Irrigation Area

Harvey Irrigation Area

Collie Irrigation Area

Principal groundwater irrigation areas

5 km

GSWA 23673

Figure 1. Locality map

32

Lithological, geophysical, and hydrogeological data from previously drilled boreholes have been used in the interpretation of the geology and hydrogeology where appropriate.

PREVIOUS WORK

Sanders (1974) attempted to assess the cause of salinization in his review of the geology and hydrology of the superficial formations of the Harvey–Waroona area which was based on information obtained from a bore census. Between 1974 and 1979, 52 monitoring bores were drilled in the superficial formations for the Department of Agriculture to investigate the relationship of soil salinity to the hydrogeology in the Harvey–Waroona area (George and Furness, 1979). In 1980, seven exploratory bores were drilled by the Public Works Department, near Harvey, to investigate the possibility of obtaining a groundwater supply for irrigation (Wharton, 1980).

Sixty-one exploratory bores were drilled during 1978 and 1979 to investigate the hydrogeology of the superficial formations along the western margin of the coastal plain and to estimate the water balances of the coastal lakes (Commander, 1988).

Commander (1982) included an assessment of the superficial formations in his outline of the groundwater resources of the Mandurah–Bunbury region.

In 1911, an unsuccessful 675 m deep bore was drilled near Cookernup by the West Australian Government, for town water supply. Systematic investigation by the Geological Survey of the deep aquifers in the area commenced in 1962 near Mandurah and Pinjarra (Commander, 1975) and was extended to Bunbury (Commander, 1984) and along two east–west drilling lines at Binningup (Deeney, 1989a) and near Waroona (Deeney, 1989b).

Information on the deep aquifers is also available from three petroleum exploration wells drilled in the late 1960s and early 1970s (Jones and Nicholls, 1966; Lehman, 1966; Young and Johanson, 1973), and a number of bores drilled for industrial and town water supplies near Pinjarra, Waroona, Australind, and Point Grey.

INVESTIGATION PROGRAM

A network of 151 monitoring bores was constructed at 74 sites on a 4 km grid between 1981 and 1983 (Fig. 1). The bores were drilled by the Mines Department Drilling Branch with an Edson 5000 rig using the mud-flush rotary method and occasionally a free flight auger. Drilled diameters ranged from 127 to 152 mm. Cuttings samples were taken at 3 m intervals and are stored in the GSWA core library.

Bores were completed with 80 mm PVC casing which was slotted adjacent to the monitoring interval, and was stabilized with a gravel pack in the annulus. Protective steel casing, about 1 m long and 100–154 mm in diameter, fitted with a locking cap, was

cemented at the surface. Bore depths ranged from 2 m to 54 m and 1 to 3 bores were constructed at each site. A summary of the bore data is given by Deeney (1988) and Sadgrove and Deeney (1989).

The deepest bore at each site was drilled at least 2 m into the underlying Mesozoic sediments and backfilled to locate a 5–6 m monitoring interval in the basal section of the superficial formations. The other bores were completed with 3–4 m monitoring intervals located at the water table and at an intermediate level between the water table and the base of the superficial formations. Gamma-ray, and in a few cases single point resistance, logs were run in the deepest bore at each site prior to the installation of casing. Palynological examination of Mesozoic sediments was carried out by GSWA staff and samples containing macrofossils were submitted for palaeontological examination at the West Australian Museum. Results are given in Sadgrove and Deeney (1989).

The bores were developed and sampled by airlift or bailing. Because of concern about the groundwater-borne phosphorus input to the Peel Inlet–Harvey Estuary system, a detailed chemical sampling program was carried out between April and August 1983 which included field measurement of some unstable parameters. Water samples were analysed by the Chemistry Centre of WA. Chemical analyses are tabulated by Deeney (1988, Appendix 3).

All of the bores have been levelled to Australian Height Datum (AHD) by the Mines Department Surveys and Mapping Division. Water levels have been measured at monthly intervals for about 3 years since completion.

Test production bores were drilled at sites 2, 15, 32, 48, and 67. The production bores were completed with 154 mm steel casing and 154 mm or 100 mm stainless steel screens, and were located about 30 m from the monitoring bores used for observation during the pumping tests. A short pumping test program was carried out at each site. It consisted of a six-stage continuous step-drawdown test, to determine the bore efficiency, followed by an 8 hour constant rate test. Flow rates were adjusted using preset valves during the step tests and measured using a weir tank fitted with a 90° v-notch weir. Water levels were measured using pressure transducers connected to chart recorders and checked using hand-held electric probes.

CLIMATE AND LAND USE

The area has a Mediterranean climate, with hot dry summers and cool wet winters. The average annual rainfall is about 900 mm along the coast, increasing to about 1100 mm along the Darling Scarp. Rainfall generally exceeds evaporation during the five months, May to September. The average annual evaporation is about 1400 mm.

Most of the land has been cleared for agriculture; in the Waroona, Harvey, and Collie irrigation areas (Fig. 1) pastures are irrigated using water from dams east of

the Darling Scarp. In a number of areas adjacent to the Old Coast Road (Fig. 1) crops are irrigated using groundwater. The remainder comprises small areas of native vegetation, State Forest (pine plantations), and urban areas.

PHYSIOGRAPHY AND DRAINAGE

The area lies on the Swan Coastal Plain which is bordered by the Darling Scarp and the coastline (Fig. 1). The coastal plain can be divided into four geomorphic units in this area. These have been named by McArthur and Bettenay (1974) as the Quindalup Dune System, the Spearwood Dune System, the Bassendean Dune System, and the Pinjarra Plain, and they correspond respectively to the Safety Bay Sand, the Tamala Limestone, the Bassendean Sand, and the Guildford Formation (Fig. 2).

The three sets of dunes are parallel to the present coastline, and lakes and swamps commonly occur in the low-lying interdunal depressions (Fig. 3). The Quindalup Dunes occur along a coastal strip, generally less than 2 km wide, and reach a maximum elevation of about 40 m above sea level. They are backed by the Spearwood Dunes which form prominent parallel ridges reaching a maximum elevation of 70 m above sea level. The Bassendean Dunes form low hills, reaching a maximum elevation of about 30 m above sea level, in a zone up to 11 km wide between the Spearwood Dunes and the Pinjarra Plain or the Darling Scarp.

The Pinjarra Plain is developed in front of the Darling Scarp near which it reaches a maximum elevation of about 80 m above sea level. It is a piedmont and alluvial plain which extends westwards to the Bassendean Dunes and locally through to the Spearwood Dunes.

The area is drained by the Murray, Harvey, and Collie river systems, flowing from the Darling Scarp to the estuaries and coastal inlets. The Harvey River Main Drain, the Harvey River Diversion Drain, the Mangosteen–Wellesley River Diversion Drain, and numerous smaller drains have been constructed to lower the water table in the eastern and central parts of the coastal plain. The majority of these discharge into the rivers, although a few flow directly into Peel Inlet and the Indian Ocean. The drained area is shown on Figure 3.

Most of the runoff occurs during winter in response to rainfall; the low flows in the rivers during the summer consist predominantly of groundwater discharging as baseflow.

GEOLOGY

SETTING

The area lies within the Perth Basin, which in this area contains about 8000 m of Phanerozoic sediments (Playford and others, 1976), and is bounded in the east by the Darling Fault and the Precambrian rocks of the Yilgarn Block.

The formations comprising the Cainozoic succession (Table 1) in this area are referred to collectively as the superficial formations (Allen, 1976). They range in thickness from about 12 m to 90 m and rest on a gentle westerly sloping erosional surface. They unconformably overlie Mesozoic sediments on the coastal plain, and Precambrian rocks along the Darling Scarp. The unconformity surface is irregular and ranges in elevation from +50 m AHD near the Darling Scarp to -28 m AHD near the coast (Fig. 4). Three prominent east–west erosional channels in the Mesozoic sediments are located east of and probably beneath Peel Inlet, at the southern end of the Harvey Estuary, and west of Harvey.

STRATIGRAPHY

The stratigraphic succession in the area is given in Table 1. The superficial formations form a stratigraphically complex sequence and their inferred relationships are shown in Figure 5.
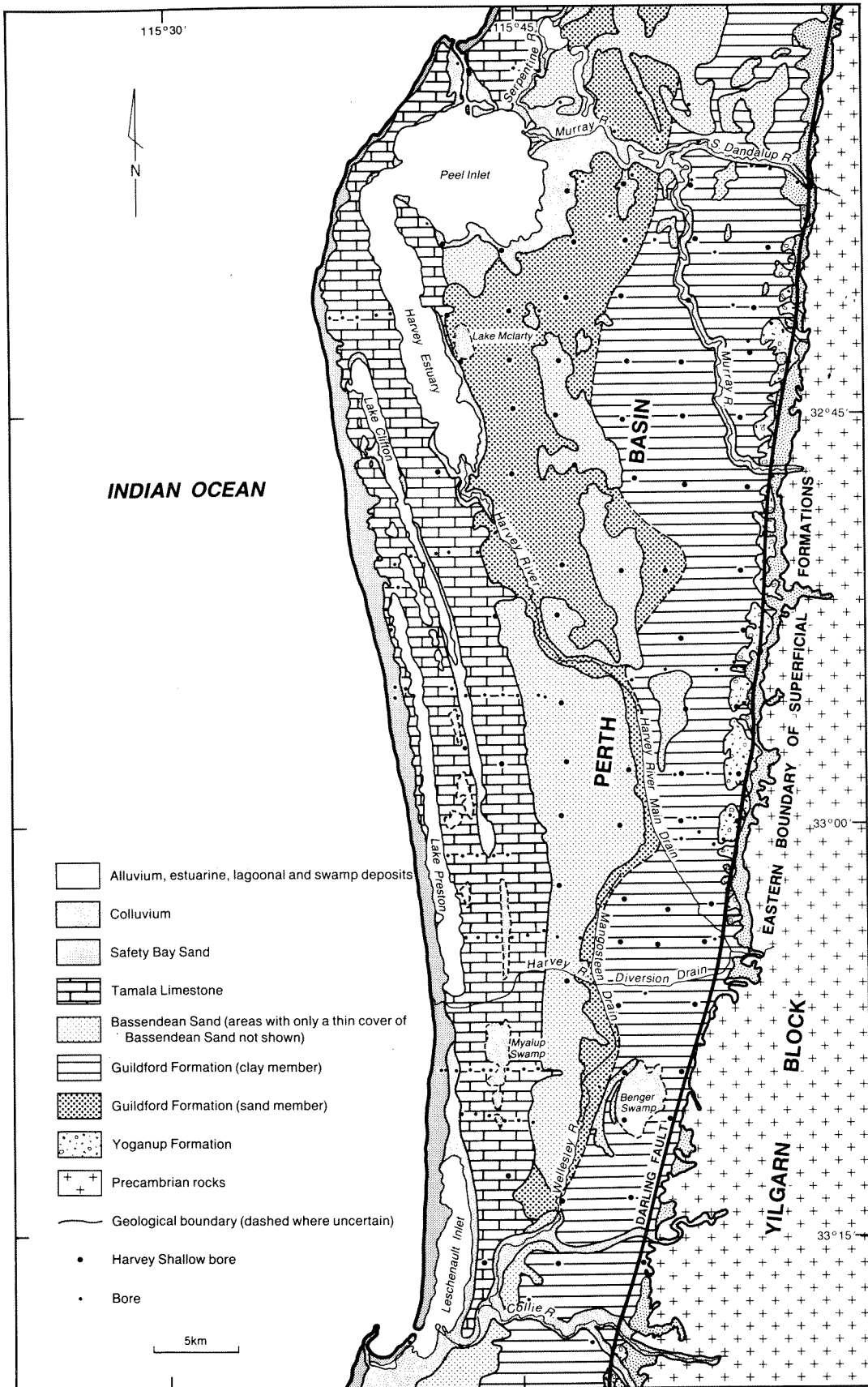
The Leederville Formation occurs below the superficial formations over most of the area. In the northwest, the superficial formations unconformably overlie the Osborne Formation and in the northeast they unconformably overlie the Cockleshell Gully Formation (Fig. 4).

Yoganup Formation

The Yoganup Formation (Low, 1971) consists of white and orange-brown, poorly sorted, subangular to subrounded, fine to very coarse sands and clayey sands. The sands are ferruginized and leached, consist predominantly of quartz with minor amounts of weathered feldspar, and are associated with silts and clays. A basal gravel containing pebbles of granite and laterite up to 2 cm in diameter was encountered in many bores. Traces of carbonaceous material were sometimes found near the top of the sequence. The samples obtained during drilling generally contained traces of heavy minerals; strand lines rich in heavy minerals are known to occur in the formation along the Darling Scarp (Baxter, 1982).
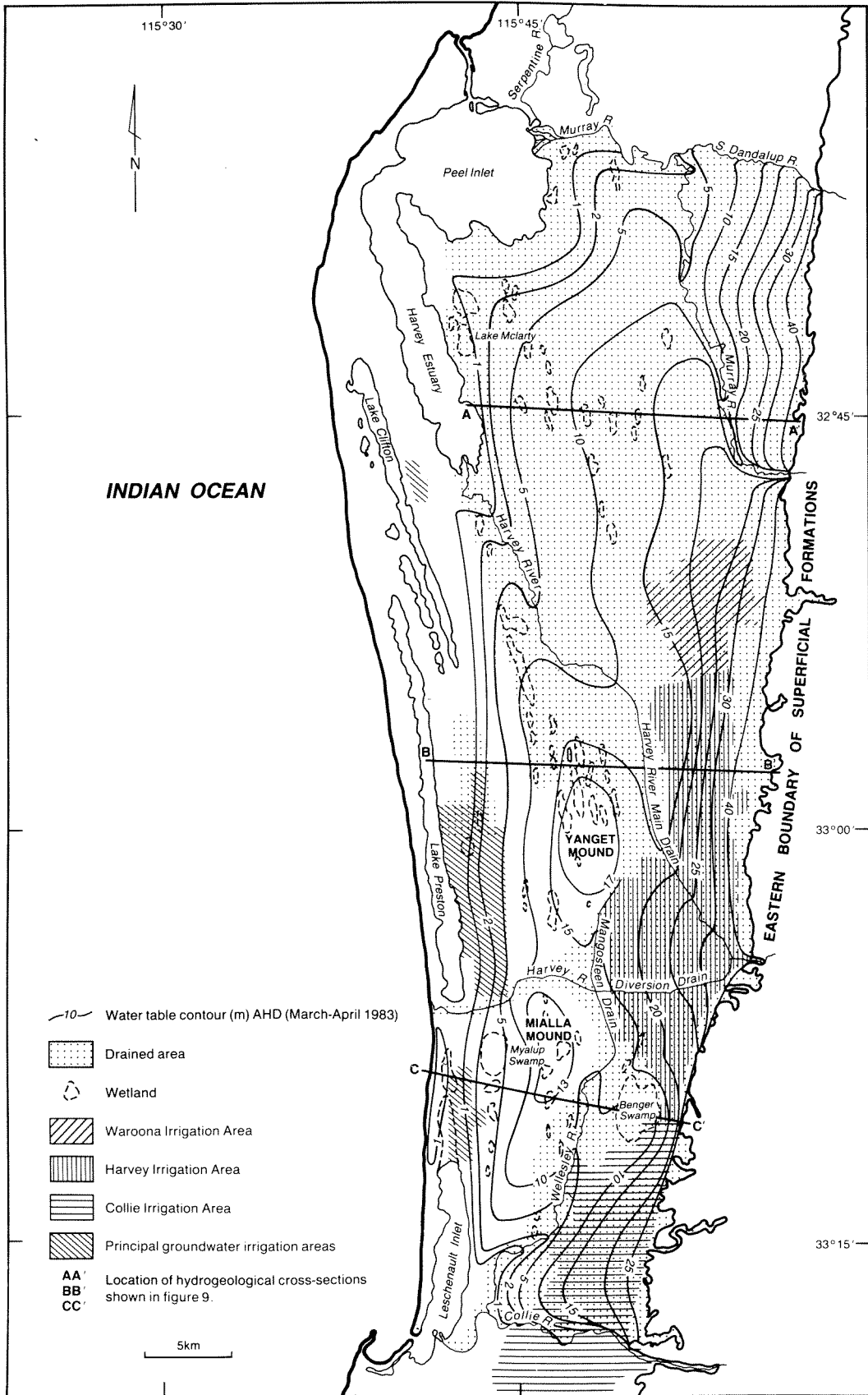
The Yoganup Formation rests unconformably on Mesozoic sediments of the Perth Basin and Precambrian rocks of the Yilgarn Block, and is unconformably overlain by the Guildford Formation. The Yoganup Formation occurs adjacent to the Darling Scarp (where it is locally exposed) and extends westwards to interfinger with the Jandakot Beds (Fig. 5).

The Yoganup Formation is more extensively developed in the north, where it extends 7–10 km west of the Darling Scarp, than in the south, where it extends westwards for 0.5–4 km. The formation ranges in thickness from 1 to 25 m, owing both to its mode of deposition and the effects of post-depositional erosion (Fig. 6). It extends from about -20 m AHD to about +70 m AHD and is thickest at the foot of the Darling Scarp.

Legend

Alluvium, estuarine, lagoonal and swamp deposits

Colluvium

Safety Bay Sand

Tamala Limestone

Bassendean Sand (areas with only a thin cover of Bassendean Sand not shown)

Guildford Formation (clay member)

Guildford Formation (sand member)

Yoganup Formation

Precambrian rocks

Geological boundary (dashed where uncertain)

• Harvey Shallow bore

• Bore

5km

INDIAN OCEAN

Peel Inlet

Lake Mclarty

PERTH BASIN

YILGARN BLOCK

EASTERN BOUNDARY OF SUPERFICIAL FORMATIONS

DARLING FAULT

Harvey Estuary

Lake Clifton

Lake Preston

Leschenault Inlet

Harvey River

Murray R.

S. Dandalup R.

Serpentine R.

Harvey River Main Drain

Mangosteen Drain

Diversion Drain

Wellesley R.

Collie R.

Myalup Swamp

Benger Swamp

115°30'

115°45'

32°45'

33°00'

33°15'

GSWA 23674

Figure 2. Geology

35

Figure 3. Water table contours

GSWA 23675

N

INDIAN OCEAN

Serpentine R.
Murray R.
Peel Inlet
Lake Mclarty
S. Dandalup R.
Murray R.
Harvey Estuary
Lake Clifton
Harvey River
Harvey River Main Drain
Lake Preston
Mangosteen Drain
Harvey Diversion Drain
Myalup Swamp
Benger Swamp
Wellesley R.
Leschenault Inlet
Collie R.

DARLING FAULT
EASTERN BOUNDARY OF SUPERFICIAL FORMATIONS

32°45'
33°00'
33°15'

—-5— Structure contour on the base of the superficial
        formations (dashed where uncertain) (m AHD)

-------- Geological boundary

Osborne Formation

Leederville Formation

Cockleshell Gully Formation

Precambrian rocks

5km

GSWA 23676

Figure 4. Structure contours on the base of the superficial formations
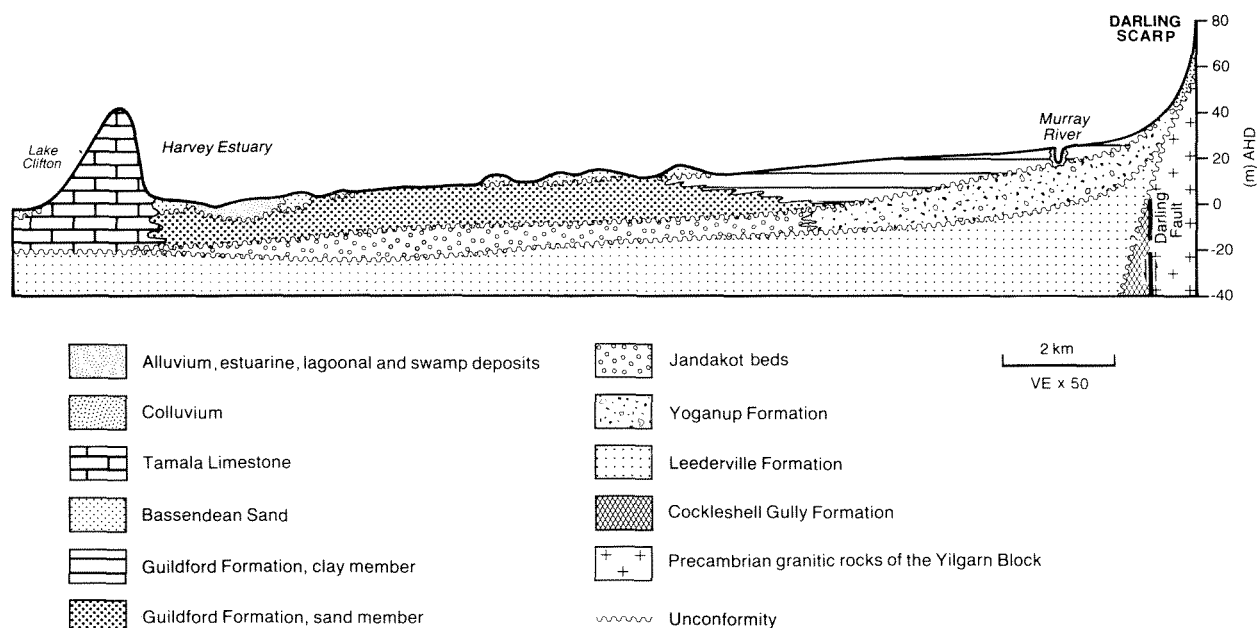
Figure 5. Diagrammatic geological section showing stratigraphic relationships of superficial formations

Wilde and Walker (1979) and Baxter (1982) have suggested that the Yoganup Formation is of Early Pleistocene age.

The Yoganup Formation is a shoreline deposit associated with a buried prograding coastline in which leached and ferruginized sands and clayey sands represent a system of dunes, beach ridges, and deltaic deposits (Baxter 1982).

Jandakot beds

The Jandakot beds (Darragh and Kendrick, 1971) consist of grey, poorly sorted, subrounded, medium-grained sand to very fine gravel, fine sand, silt, clay, calcarenite, and limestone, generally with abundant fossils. They occasionally contain minor amounts of glauconite, phosphatized shell fragments and phosphatic nodules, and often contain carbonaceous material and traces of heavy minerals.

The Jandakot beds rest unconformably on Mesozoic sediments. They are unconformably overlain by the Guildford Formation in the central part of the coastal plain and by the Tamala Limestone in the west (Fig. 5).

The Jandakot beds can be traced continuously in the subsurface from Pinjarra southwards to within about 5 km of Australind (Fig. 6). They are absent in the southernmost part of the project area and have not been encountered in the Perth Basin south of the project area (Commander, 1984; Hirschberg, 1989).

The Jandakot beds extend from about -30 m AHD to +5 m AHD and from the contact with the Yoganup Formation in the east to within about 7 km of the coast.

Their thickness ranges from 2.5 to 25 m, reflecting the influence of pre-depositional topography and post-depositional erosion (Fig. 6).

The Jandakot beds generally contain small gastropods and bivalve fragments, echinoid spines, large benthic foraminifers, and fragments of brachiopod shells and calcareous marine algae. They are probably of Early Pleistocene age (Darragh and Kendrick, 1971) and were probably deposited in an estuarine to shallow-marine environment.

The Jandakot beds are considered to be an estuarine to marine facies equivalent of the Yoganup Formation on the basis of their position in the stratigraphic sequence, their depositional environment, and their age.

Guildford Formation

The Guildford Formation (Low, 1971) can be subdivided into a clay member (in the east) and a sand member (in the west) that are laterally equivalent (Figs 2 and 5).

The clay member consists of brown or grey clay and sandy clay together with thin beds of arenaceous material ranging in grade from fine sand to very fine gravel. Occasionally, the clays are ferruginized and those occurring close to the Darling Scarp are often multi-coloured — purple, red-brown, green, yellow, and grey.

The sand member consists predominantly of grey, poorly sorted, fine to very coarse-grained quartz sand, together with minor beds of brown or grey clay and clayey sand, and traces of heavy minerals. Generally,

38
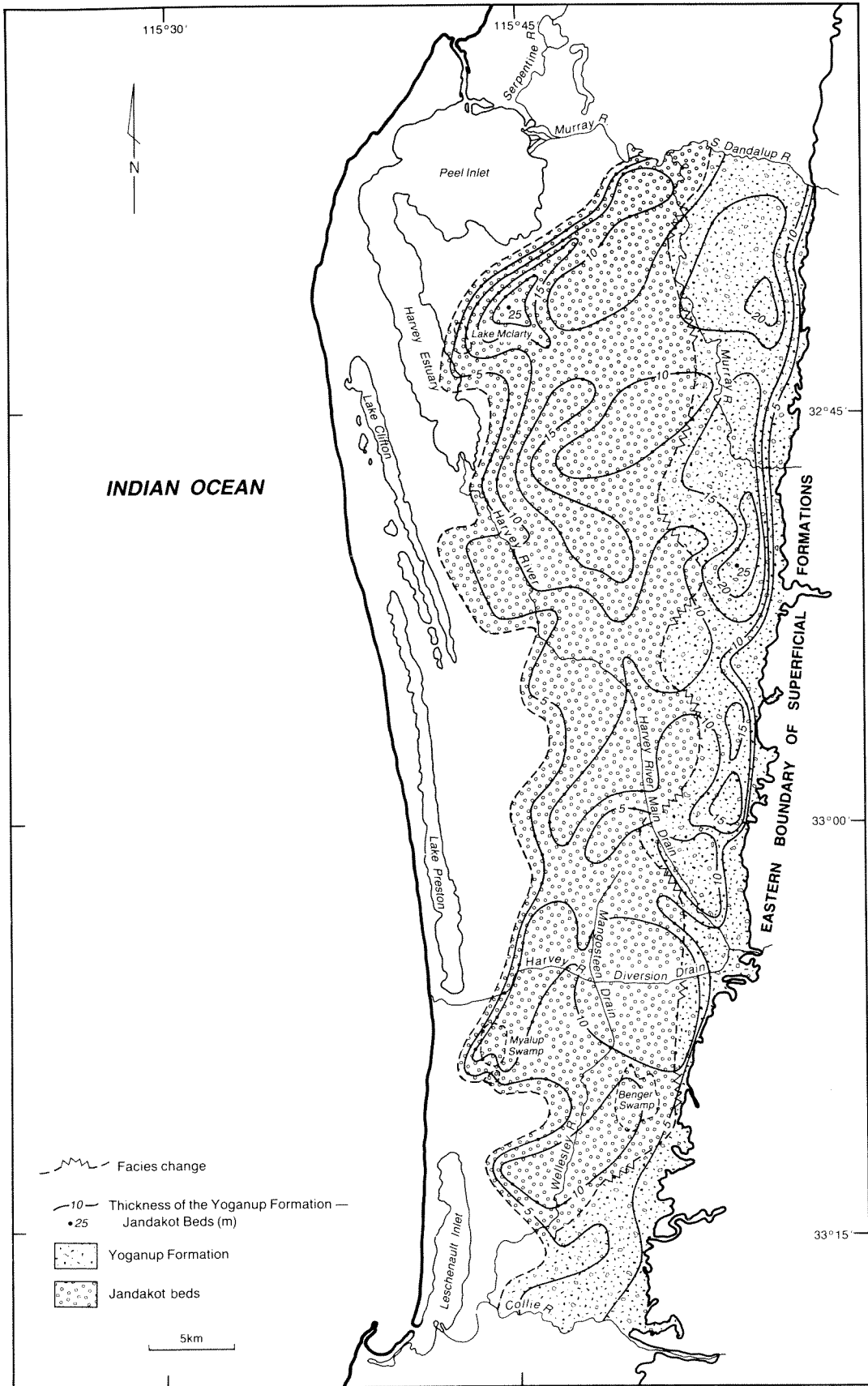
Figure 6. Yoganup Formation–Jandakot Beds: extent and thickness

TABLE 1. STRATIGRAPHY AND LITHOLOGY OF COASTAL PLAIN AREA

Age	Stratigraphic unit and lithology		
	West	Central	East
QUATERNARY Holocene	Alluvium, estuarine, lagoonal, and swamp deposits (15); (sand, silt, clay, and peat)		
Pleistocene Middle-Late	Safety Bay Sand (50) (sand, calcareous and unlithified)		(a) Colluvium (5) (lithic sand, silt, clay, laterite, laterite debris)
	—— UNCONFORMITY ——		
	Tamala Limestone (90)	Bassendean Sand (15?); (sand)	
Early-Middle		—————— UNCONFORMITY ——————	
	(limestone, sand, calcarenite, minor clay, minor fossils)	Guildford Formation sand member (30) (sand, minor clay, calcareous sand, and fossils)	Guildford Formation clay member (27) (clay, sandy clay)
		—— UNCONFORMITY ——	
Early	Jandakot beds (25) (sand, silt, clay, minor limestone, fossiliferous)		Yoganup Formation (25) (sand, clayey sand)
	—— UNCONFORMITY ——		
CRETACEOUS Early-Late	Osborne Formation (siltstone and clay)		
	—— UNCONFORMITY ——		
Early	Leederville Formation (sand, siltstone, clay, shale)		
	—— UNCONFORMITY ——		
JURASSIC Early-Middle	Cockleshell Gully Formation (sand, siltstone, clay, shale)		

Notes: (a) Colluvium ranges in age from Tertiary to recent. (b) Figures in brackets are estimated maximum thicknesses in metres.

a layer of coffee-brown ferruginized (limonitic) sand is present near the water table. Layers of calcareous sand were found in the sequence at sites 2, 10, 19, 20, 23, 24, 27, 28, 42, and 50. However, the sampling methods employed during the investigation preclude precise determination of the depth at which the calcareous sands occur and in some cases these sediments may belong to the underlying Jandakot Beds.

The Guildford Formation unconformably overlies the Jandakot beds, the Yoganup Formation, and granitic rocks of the Yilgarn Block. It is unconformably overlain by the Bassendean Sand and alluvium on the coastal plain, and by colluvium along the Darling Scarp (Fig. 5). The stratigraphic relationship between the Guildford Formation and the Tamala Limestone is uncertain.

The Guildford Formation extends westwards from the foot of the Darling Scarp to within 10 km of the coast. The clay member occurs in the eastern part of the coastal plain and extends from about -5 m AHD to about +70 m AHD. The clay member generally attains its maximum thickness close to the foot of the Darling Scarp and ranges from 2 m to 27 m thick. The sand and clay members interfinger in the central part of the coastal plain. The sand member extends from about -25 m AHD to about +20 m AHD and ranges in thickness from 4 to 30 m.

Macrofossils and fine shell debris were found in the sand member at two sites — 2 and 19. The most characteristic fossils recovered were internal moulds of small marine gastropod shells which may be of Middle Pleistocene age (G. W. Kendrick, written communication, 1983).

The lithology, geometry, and location of the sediments comprising the clay member suggest that they were deposited as alluvial fans, derived from weathering of the Yilgarn Block. The alluvial fans grade laterally, at their distal end, into the fluvial and shallow-marine sediments of the sand member.

Bassendean Sand

The Bassendean Sand (Playford and Low, 1972) consists of white to pale-grey and occasionally brown, moderately sorted, fine- to medium-grained quartz sand containing traces of heavy minerals. It unconformably overlies the Guildford Formation.

The Bassendean Sand forms a thin cover over much of the coastal plain east of the Spearwood Dunes and a discontinuous zone of low hills in the central region of the coastal plain (Figs 2 and 5). It may reach a maximum thickness of 15 m and is of eolian origin.

The Bassendean Sand may be of Middle to Late Pleistocene age (Playford and others, 1976).

Tamala Limestone

The Tamala Limestone (Playford and others, 1976) comprises limestone, calcarenite, and sand, with minor clay and shell beds.

The Tamala Limestone unconformably overlies Cretaceous sediments in the west and the Jandakot Beds along its eastern margin (Fig. 4). It is unconformably overlain by the Safety Bay Sand in the west and may interfinger with the Bassendean Sand in the east. The nature of the contact between the Tamala Limestone and the Guildford Formation is uncertain. On the basis of its position, lithology, and age, the marine sequence in the Tamala Limestone may interfinger with the sand member of the Guildford Formation.

The Tamala Limestone occurs in the west (Fig. 2) and extends from about -28 m AHD to +70 m AHD. It has a maximum thickness of about 90 m.

Macrofossils recovered from the Tamala Limestone have been assigned a Middle Pleistocene age (G. W. Kendrick, written communication, 1983). The formation is predominantly of eolian origin. However, below approximately +3 m AHD it is composed mainly of marine and lacustrine sediments (Commander, 1988).

Bores 58A and 59A, located on the southern shore of the Peel Inlet, penetrated a sequence of grey-green and orange-brown clay containing nodules or thin layers of gypsum and dolomite, overlying orange-brown calcareous sand and sandy limestone with dolomite, anhydrite and clay. G.W. Kendrick (written communication, 1983) has suggested a Middle Pleistocene age for the macrofossil assemblage obtained from bore 59A. The sequence may represent a sabkha-type deposit. These deposits have been tentatively assigned to the Tamala Limestone on the basis of their location and lithology. The sand and limestone are lithologically similar to the marine sequence in the Tamala Limestone, but are also similar to the sand member of the Guildford Formation.

Safety Bay Sand

The Safety Bay Sand (Playford and others, 1976) consists of unlithified calcareous sand, and unconformably overlies the Tamala Limestone. It forms a narrow strip of stable and mobile dunes along the coastline (Fig. 2) and has a maximum thickness of about 50 m. The Safety Bay Sand is of Holocene age (Playford and others, 1976).

Colluvium

The colluvium consists of fragments of Precambrian rocks and laterite, and the grain size ranges from coarse pebbly sand to poorly sorted silty sand and clay. It overlies the Yoganup Formation, the Guildford Formation, and Precambrian rocks (Fig. 5).

Deposits of colluvium occur along the Darling Scarp (Fig. 2) and are finer grained at the foot than on the slopes. The thickness of these deposits varies considerably and may exceed 5 m.

Alluvium, estuarine, lagoonal, and swamp deposits

Alluvium, consisting mainly of grey and brown silt and clayey sand, occurs along the rivers and their tributaries (Fig. 5).

Estuarine and lagoonal deposits comprising black, brown, and grey humic sandy clay, silt, marl, clayey sand, sand, and calcarenite unconformably overlie the Tamala Limestone and the Guildford Formation. They occur on the floor and margins of the Peel Inlet, the Harvey Estuary, and the coastal lakes.

Swamp deposits, consisting of dark grey to black, fine sand, silt and clay, and containing peat and diatomite, occupy the floors and margins of wetlands.

These deposits are of Holocene age.

HYDROGEOLOGY

### AQUIFER RELATIONSHIPS AND AQUIFER PARAMETERS

The superficial formations, which consist predominantly of clay and sand in the east, and of sand and limestone in the west, form an unconfined aquifer extending westwards from the Darling Scarp to the coast. In the east, the Guildford Formation clay member, which covers an area of approximately 730 km^2 (Fig. 7), forms an important aquitard in the upper part of the aquifer. The water table is generally within 1–2 m of the ground surface, except beneath the Bassendean and Spearwood Dunes where it can be up to 30 m deep. The aquifer is underlain by Mesozoic sediments which generally have low permeability, though locally both upward and downward leakage occurs.

Analysis of the pumping tests shows that the superficial formations form an aquifer that is inhomogeneous and anisotropic. The distribution of isopotentials at the end of the pumping, and the variation in lithology, indicate that it is a multilayer aquifer which is divisible into aquitards and aquifers.

Type curves generated from solutions for semi-confined and semi-unconfined aquifers match the data curves. Although neither model adequately describes the response of the aquifer to pumping (it lies between the two), the former is thought to be more appropriate if the hydraulic head distribution at the end of pumping is considered.

The results obtained using the solutions of Walton (1962) are considered to be reasonable estimates of the transmissivity, hydraulic conductivity, and coefficient of elastic storage of the pumped aquifer (Table 2). The calculated values of the hydraulic conductivity of the aquitard provide estimates of the vertical hydraulic conductivity of the sediments overlying and underlying the pumped aquifer, since the direction of flow in these sediments was approximately vertical.

The pumping-test analyses show that the vertical hydraulic conductivity of the superficial formations is lower than the horizontal hydraulic conductivity, and that values may differ by a factor of between 10 and 1000. Generally, this is due to the stratification and
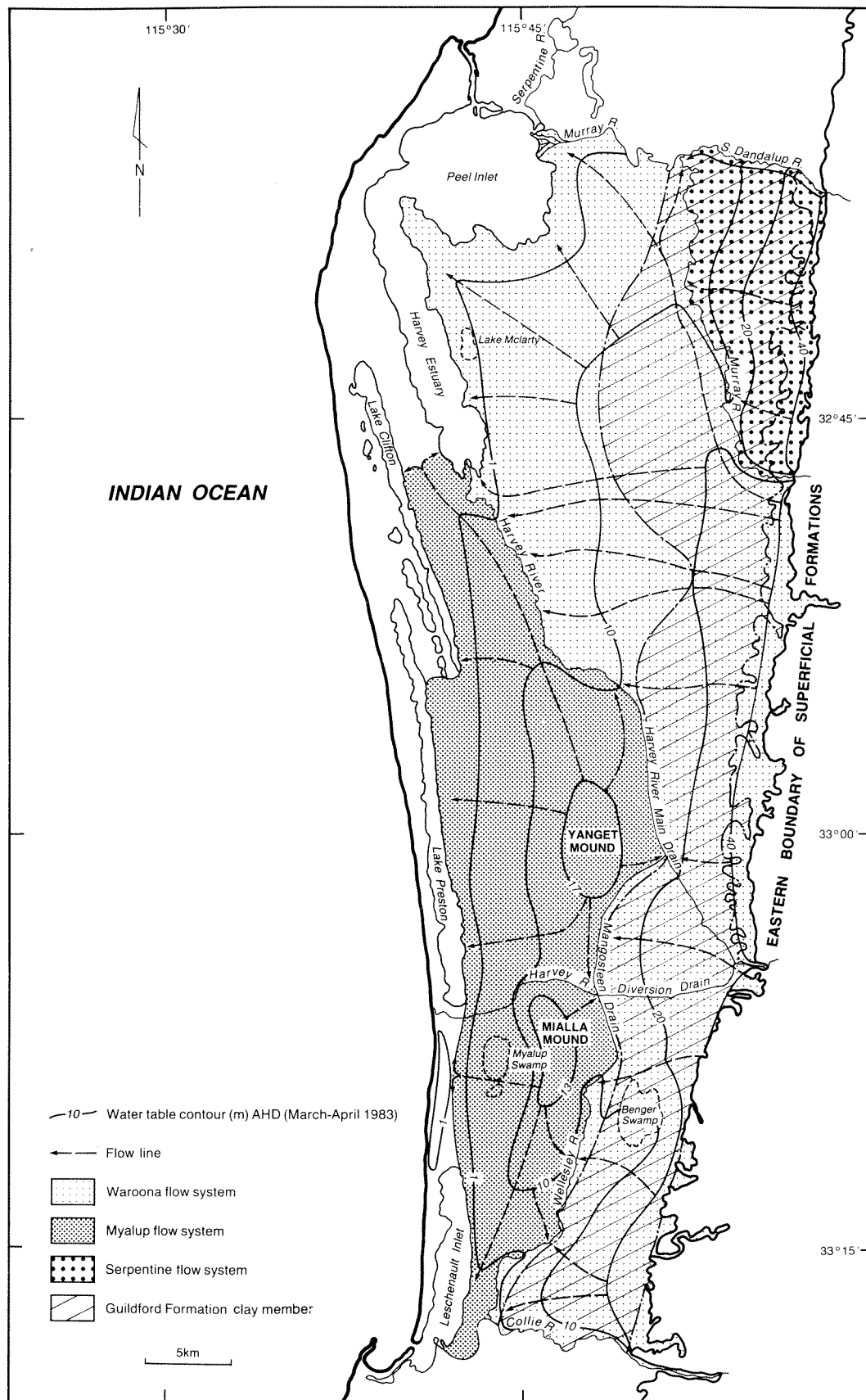
Figure 7. Regional groundwater flow systems
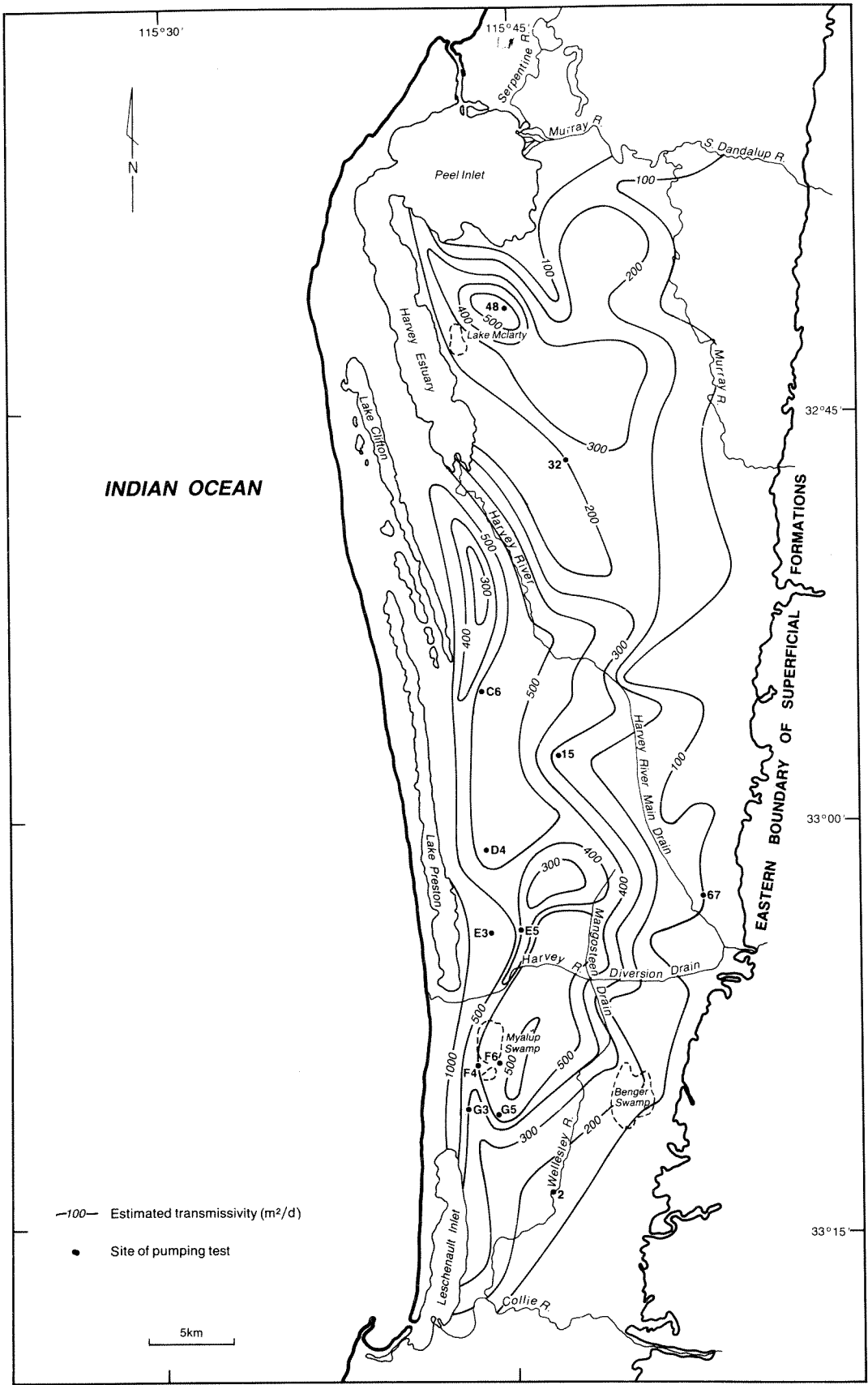
GSWA 23679

Figure 8. Estimated transmissivity of the superficial formations

GSWA 23680

43

TABLE 2. PUMPING-TEST RESULTS

Boresite	Pumping rate (m³/d)	Drawdown in observation bores after 8 h pumping (m)		Pumped aquifer	Saturated thickness (m)	Aquitard	Saturated thickness (m)	Trans-missivity (m²/d)	Hydraulic conductivity of aquifer (m/d)	Hydraulic conductivity of aquitard (m/d)	Coefficient of elastic storage (aquifer)
		Water table	Base of superficial formations								
HS2	278	0.1	2.645	Jandakot beds	7	Guildford Formation (sand member)	13.5	38	5	4.7×10^{-3}	1.4×10^{-4}
HS15	1095	0.127	2.087	Jandakot beds and Guildford Formation (sand member)	10	Guildford Formation (sand member)	18.5	97	10	3.3×10^{-1}	2.4×10^{-4}
HS32	194	0.003	0.932	Jandakot beds	8	Guildford Formation (sand member)	17.5	23	3	2.9×10^{-1}	2.7×10^{-4}
HS48	1168	0.220	0.782	Jandakot beds	25	Guildford Formation (sand member)	9	409	16	1.6×10^{-1}	3.2×10^{-3}
HS67	220	0.217	1.442	Yoganup Formation	7	Guildford Formation (clay member)	20.5	57	8	1.3×10^{-2}	2.2×10^{-4}

variation in lithology. Locally, layers readily identifiable as aquitards are present. These are formed by silts and clays which do not persist laterally.

Aquifer transmissivities were estimated from lithological logs (Table 3) and were also obtained from pumping-test analyses described in this paper and by Commander (1988). The transmissivity generally increases from east to west (Fig. 8), varies locally, and ranges from 50 to 1150 m^2/d. The wide range of values obtained reflects the variation in lithology and, to a lesser extent, the saturated thickness of the aquifer, which is 20–40 m throughout most of the area, except where it decreases close to the Darling Scarp and the southern margin of the Peel Inlet.

TABLE 3. HYDRAULIC CONDUCTIVITY VALUES

Lithology	Hydraulic conductivity (m/d)
Sand	
Fine to very fine gravel	30
Fine to very coarse	30
Medium to coarse	30
Fine to coarse	15
Medium	15
Fine to medium	10
Fine	4
Very fine to fine	2
Very fine	1
Silt	1
Slightly silty/clayey sand	5
Clayey sand	1
Sandy clay	1
Slightly sandy clay	0.5
Clay	0.01
Limestone	50

Source: Freeze and Cherry (1979)

FLOW SYSTEMS

Three regional flow systems can be recognized in the superficial formations: these are the Waroona, Myalup, and Serpentine flow systems. They are separated by discharge boundaries (Fig. 7).

The flow systems have been defined on the basis of the water-table configuration and the geology, and the relationships between the flow systems are illustrated in Figures 7 and 9.

The Waroona flow system occupies an area of approximately 960 km^2. It is bounded by the Peel Inlet, the Harvey Estuary, the Harvey River and Main Drain, the Mangosteen Drain, and the Wellesley River in the west; the Murray River in the north and east; the Darling Scarp in the east; and the Collie River in the south.

In the eastern part of the Waroona flow system the superficial formations consist predominantly of clay. The aquifer transmissivity, though variable, is low. Transmissivity is higher in the west where the superficial formations consist mainly of sand.

The Myalup flow system extends over an area of about 510 km^2. It is bounded in the west by the coastal lakes and Leschenault Inlet, and in the south by the Collie River. The northern boundary of the flow system between Lake Clifton and Harvey Estuary (Fig. 7) has been arbitrarily selected to coincide with the approximate position of a saline interface in the aquifer, since only thin lenses of fresh water occur northwest of this position. The rivers and drains which form the western boundary of the Waroona flow system also form the eastern boundary of the Myalup flow system.

The aquifer transmissivity is generally higher in the Myalup flow system than in the other flow systems since the superficial formations consist predominantly of sand and limestone.

The Serpentine Flow system (Davidson, 1984) extends northwards from the investigation area to the Serpentine River and is bounded by the Serpentine River in the west and by the Darling Scarp in the east. Only the southern part of the flow system, which extends over an area of about 150 km^2 south of the south Dandalup River (Fig. 7), is described in this report. In this southern part of the flow system, the superficial formations consist predominantly of clay and the aquifer transmissivity is low.

RECHARGE, WATER LEVEL VARIATION, GROUNDWATER FLOW, AND DISCHARGE.

Recharge

The superficial formations are recharged directly by rainfall. Recharge rates vary across the coastal plain as a result of the variation in lithology, depth to the water table, and topographic gradient. Generally, recharge rates are likely to be higher in the central part of the coastal plain than in the east or west because of the low clay content of the sediments, shallow water table, and low topographic gradient.

Most of the recharge to the Yoganup Formation occurs in a discontinuous zone along the foot of the Darling Scarp where the Formation is exposed, or the overlying sediments are thin (Fig. 7). Downward flow through the Guildford Formation clay member is probably small.

In the area extending from Waroona to the Collie River (Fig. 3), flood irrigation and leakage from the irrigation channels provides an additional source of recharge to the Guildford Formation clay member and causes temporary waterlogging during the summer.

Inflow to the superficial formations occurs locally by upward leakage from the Leederville Formation, and from the Harvey River Diversion Drain close to the contact between the Tamala Limestone and the Guildford Formation sand member (Fig. 3).

Water level variation and seasonal range

Bore hydrographs for site 46 and the monthly rainfall at Harvey are shown in Figure 10, for the period October 1981 to June 1985. Hydrographs are given by Deeney (1988). Variations in water level can usually be correlated with variations in rainfall. Peaks in the groundwater hydrographs occur 1–3 months after peaks in the rainfall histogram (Fig. 10), and the length of the time lag increases with increasing depth to the water table. Generally, the response of bores screened in the base of the aquifer corresponds closely with the response of the the water table bores.

The water table fluctuates seasonally and intersects the ground surface in many parts of the area during winter to maintain numerous wetlands (Fig. 3), the largest of which is Benger Swamp. Generally, the seasonal range in water table level is 1–2 m (Fig. 11). The greatest seasonal range (2.0–4.2 m) occurs close to the Darling Scarp, and the least range (0.2–0.9 m) occurs in the Tamala Limestone. Seasonal ranges in potentiometric head generally correspond to those at the water table, except locally, where there is a significant head difference between the water table and the base of the aquifer.

Groundwater flow

The water-table elevation generally decreases from east to west and follows the topography except within the Spearwood Dunes. The presence of watercourses, lakes, and inlets has resulted in the formation of a
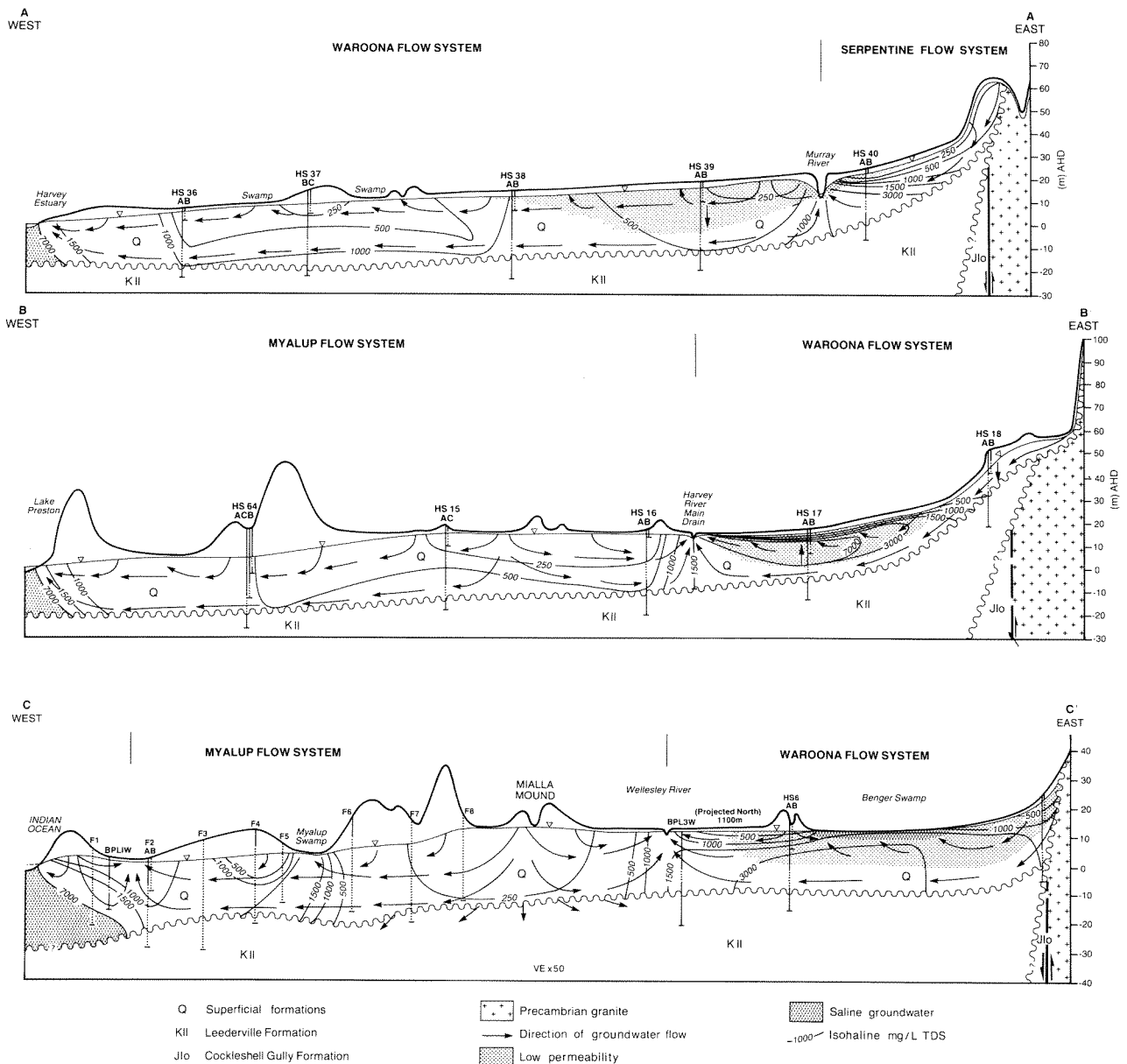
Figure 9. Hydrogeological cross sections (locations shown on Fig. 3)

46

complex groundwater flow regime which includes a number of groundwater divides, and the Yanget and Mialla mounds (Fig. 3).

The hydraulic gradient is low in the central part of the coastal plain. It increases close to the Darling Scarp where the aquifer thickness decreases and the topographic gradient increases, and close to the Peel Inlet and the Harvey Estuary where the aquifer thickness also decreases. There is also a steep hydraulic gradient in the Tamala Limestone close to the contact with the Guildford Formation sand member (Commander, 1988).

In the Waroona flow system, groundwater flow is in a westerly direction from the Darling Scarp, and in a north-easterly direction from the groundwater divide adjacent and parallel to the Murray River (Fig. 7). The saturated thickness of the aquifer is generally 20–30 m, reaches a maximum of 45 m west of Harvey, and decreases to 10 m along the southern margin of the Peel Inlet. The transmissivity is estimated to be generally less than 200 m^2/d in the eastern part of the flow system and increases to about 500 m^2/d in the northwest.

Groundwater flow in the Serpentine flow system is westwards from the Darling Scarp. The saturated thickness is generally about 20 m and decreases close to the scarp. The transmissivity is estimated to be less than 100 m^2/d.

In the Myalup flow system, groundwater flows from the Yanget and Mialla mounds to the coastal lakes in the west, and to the rivers and drains in the east. The saturated thickness of the aquifer decreases from about 30 m in the east to about 20 m in the west. The transmissivity generally exceeds 400 m^2/d and reaches a maximum in excess of 1000 m^2/d adjacent to the eastern side of Lake Preston.

Generally, there is a downward head difference between the water table and the base of the superficial formations of about 0.1–1 m, except close to the scarp where it increases to 8 m. Locally, upward head differences of 0.1–1 m are present close to discharge boundaries, and in other areas, as a result of confinement by the Guildford Formation clay member and clays in the Jandakot beds.

The widespread occurrence of significant head differences reflects the vertical anisotropy of the aquifer, and the predominance of downward head differences indicates that regular recharge occurs throughout the area. In the drained area (Fig. 3) that covers most of the coastal plain except for the Spearwood and the Quindalup Dunes, much of the water recharged is probably intercepted by the drains before it reaches the lower part of the aquifer.

Groundwater discharge

Groundwater discharges from the superficial formations to the major watercourses, inlets, and coastal lakes which form the flow system boundaries, and also to the large number of drains and smaller rivers which are present in the central and eastern parts of the area. The presence of the Guildford Formation clay member

prevents groundwater discharge from the basal section of the aquifer to the rivers and drains which flow across it. The Murray River has completely eroded the Guildford Formation clay member to expose the Yoganup Formation, and groundwater discharges to it from the Waroona flow system and from the Serpentine flow system.

Significant quantities of groundwater are removed by evapotranspiration from the swamps and areas where the water table is at shallow depth. Groundwater discharge from the Guildford Formation clay member occurs mainly by evapotranspiration.

Discharge to the Mesozoic sediments by downward leakage occurs locally throughout the project area. A large volume of water is probably discharged from the Myalup flow system by downward leakage, and this may occur over most of the area between the Harvey and Wellesley Rivers in the east and the Spearwood Dunes in the west (Deeney, 1988, 1989b).

Groundwater salinity

Fresh groundwater with a salinity of less than 500 mg/L TDS is more extensive at the water table than at the base of the aquifer (Figs 12 and 13). In the basal section of the aquifer it is restricted to areas in the central part of the Myalup flow system and to a discontinuous zone adjacent to the Darling Scarp in the Serpentine and Waroona flow systems. Fresh groundwater with a minimum measured concentration of 90 mg/L TDS occurs near the crest of the Yanget Mound in the Myalup flow system where the groundwater salinity is generally less than 1000 mg/L TDS. In the northern part of the Waroona flow system the groundwater salinity is generally less than 1500 mg/L TDS. Groundwater salinity adjacent to the discharge zones ranges up to about 4000 mg/L TDS.

The groundwater salinity in the Guildford Formation clay member is generally higher than in the underlying sediments. Locally, the salinity close to the water table varies from fresh to saline (>7000 mg/L TDS) over much of the project area. The salinity at a particular location is probably influenced by the presence or absence of Bassendean Sand overlying the clay and may be a function of the distance from a discharge zone.

In the Guildford Formation clay member, south of Waroona, the groundwater is generally brackish (1500–7000 mg/L TDS) to saline with a maximum measured concentration of 22 900 mg/L TDS; north of Waroona the groundwater is generally fresh to brackish.

A comparison of the two sets of chemical analyses (one sampled on completion of drilling, the other from mid-1983) shows that differences in TDS concentrations of 1000–15000 mg/L are common in bores screened in the Guildford Formation clay member. These differences are probably due mainly to seasonal changes in the position of the water table within the aquifer and also to the sampling method employed. The
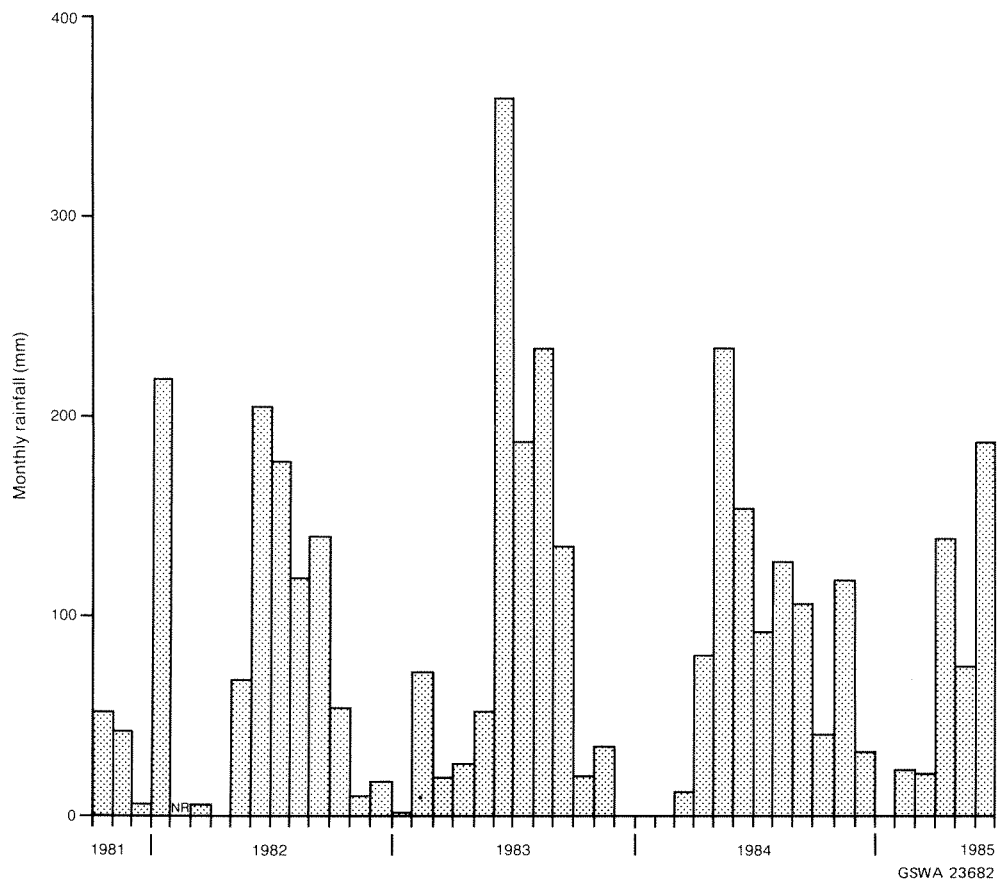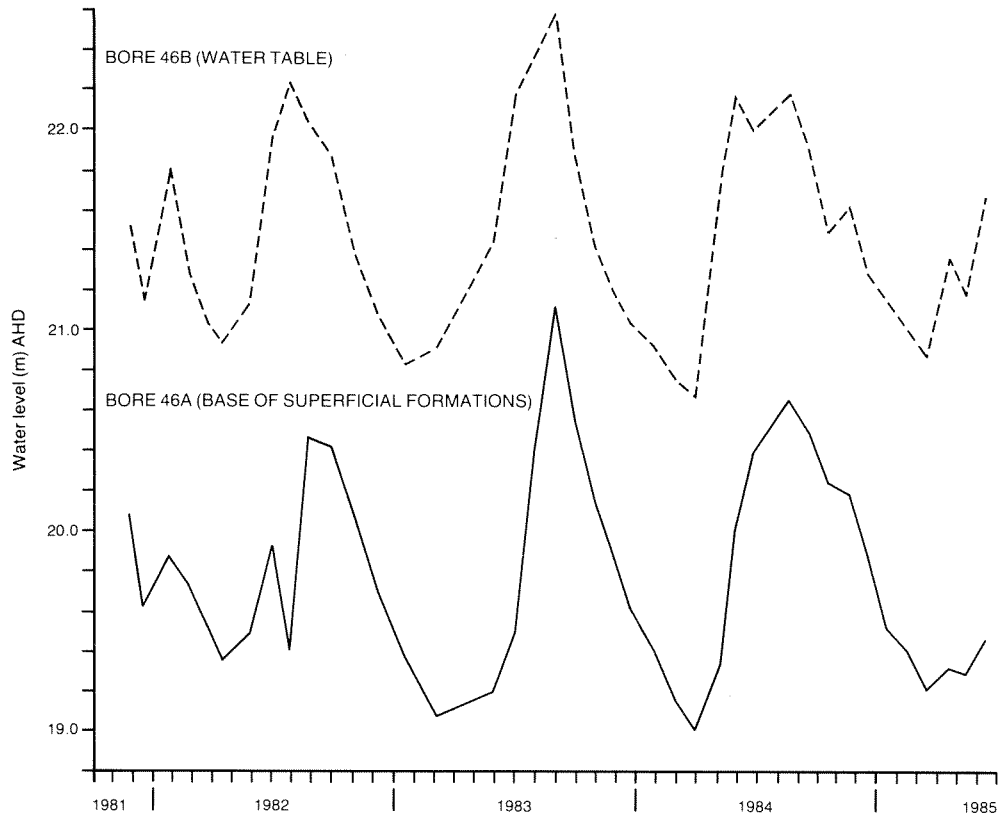
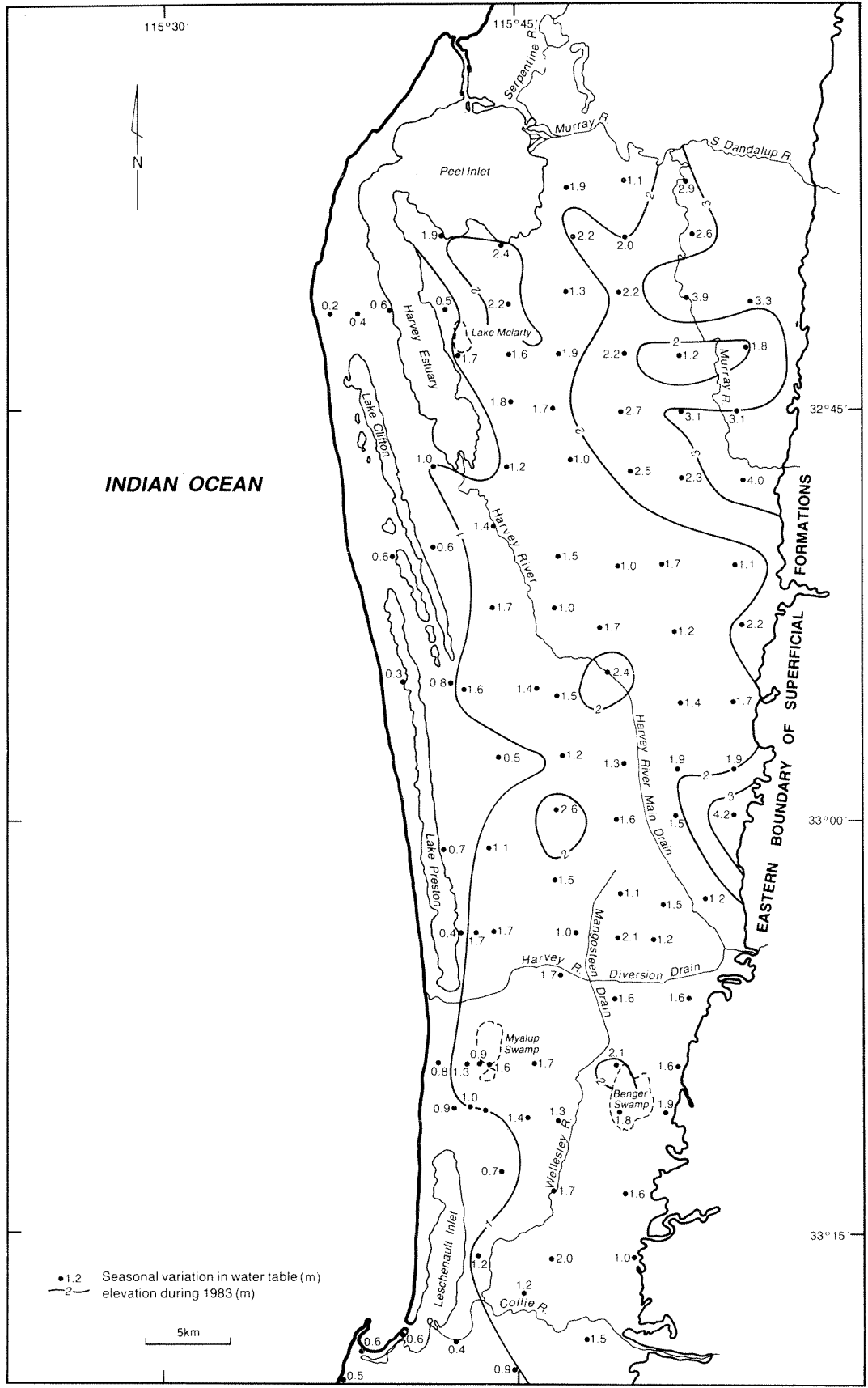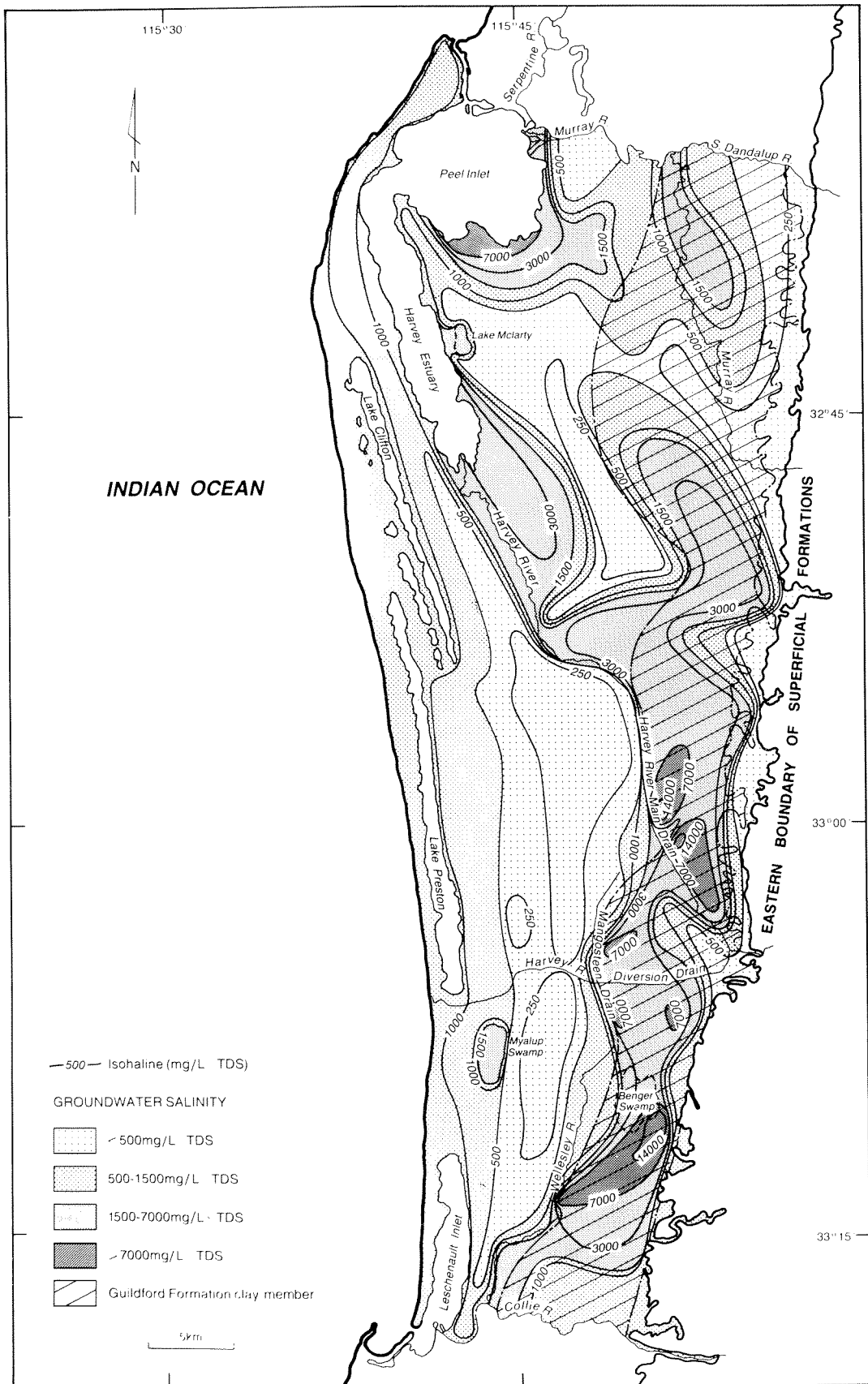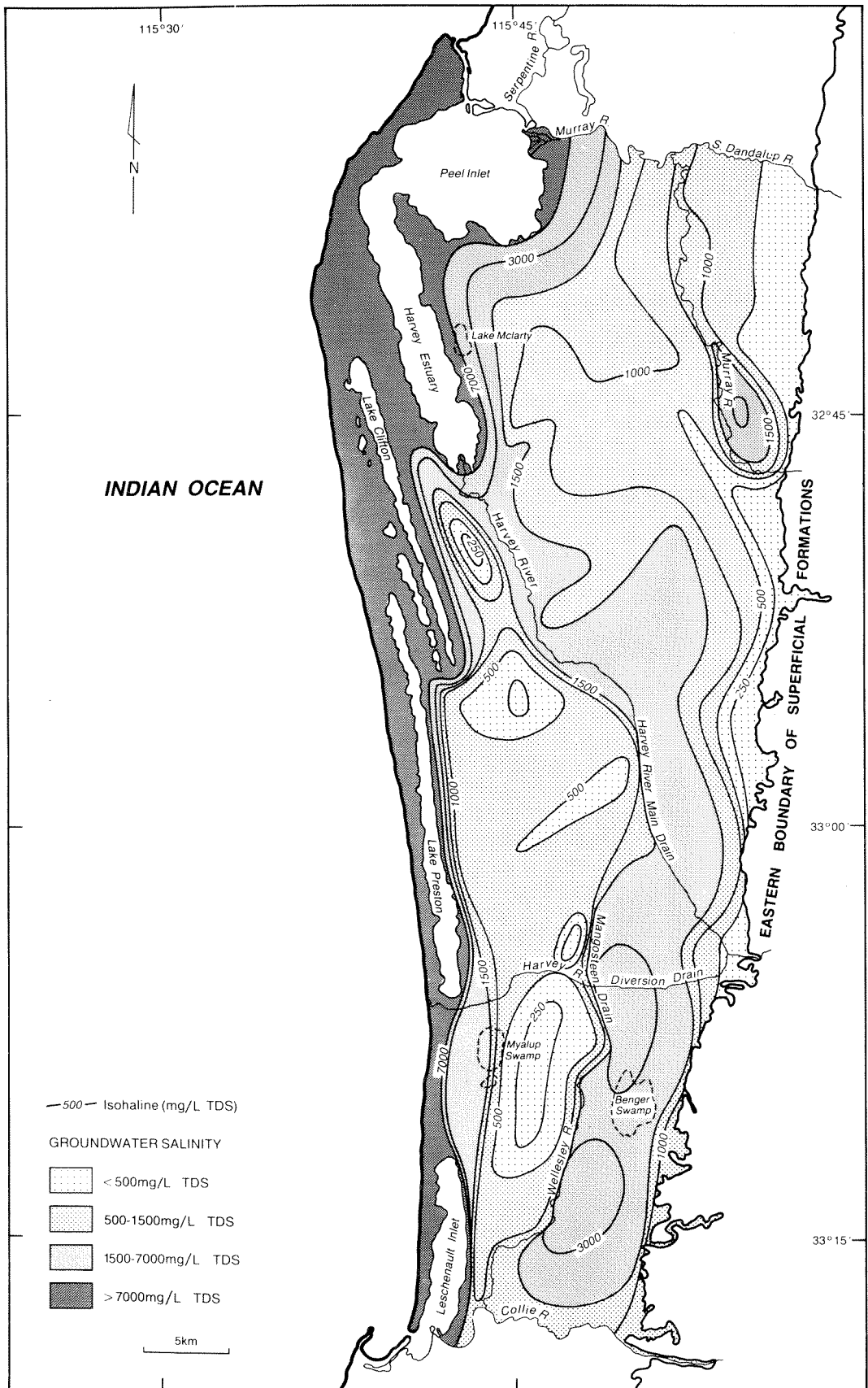**Figure 10. Monthly rainfall at Harvey and bore hydrographs for site 46 (October 1981–June 1985)**

48

Figure 11. Seasonal variation in water table elevation during 1983

49

Figure 12. Groundwater salinity at the water table

Figure 13. Groundwater salinity at the base of the superficial formations

51

salt content of the soil profile probably varies considerably with depth; therefore, variation in water level would result in the dissolution and deposition of stored salt on a seasonal basis.

Groundwater in the sediments underlying the Guildford Formation clay member is brackish, except in the north and east where it is fresh to brackish. Generally, the groundwater salinity in these sediments is lower than, or approximately equal to, the salinity in the Guildford Formation member clay and the salinity distribution is similar.

In the project area the groundwater salinity generally increases in the direction of groundwater flow. However, other factors strongly influence the salinity distribution, and these include the variation in permeability, evapotranspiration from the shallow water table, irrigation in the Waroona–Collie River area, downward leakage through the Guildford Formation clay member, and upward leakage locally from Mesozoic sediments.

A saline interface is present along the western boundaries of the Waroona and Myalup flow systems and extends 0.5–1 km inland at the base of the aquifer, except at Point Grey where it underlies the whole of the peninsula. Hypersaline groundwater with a salinity of 101 000 mg/L TDS is present in the aquifer on the southern side of the Peel Inlet near the base of the Point Grey peninsula and may have formed in a sabkha-type environment. Evaporative concentration of seawater in the aquifer probably formed the hypersaline groundwater, and precipitation of the evaporite minerals found in the sediments has enriched it in magnesium with respect to seawater. Hypersaline groundwaters with salinities up to 64 000 mg/L TDS also occur in the aquifer beneath the coastal lakes (Commander, 1988).

Groundwater chemistry

The concentrations of the major ions in the Harvey Shallow bores and selected Lake Clifton bores have been plotted as a percentage of their total milliequivalents per litre on a Piper Trilinear Diagram (Fig.
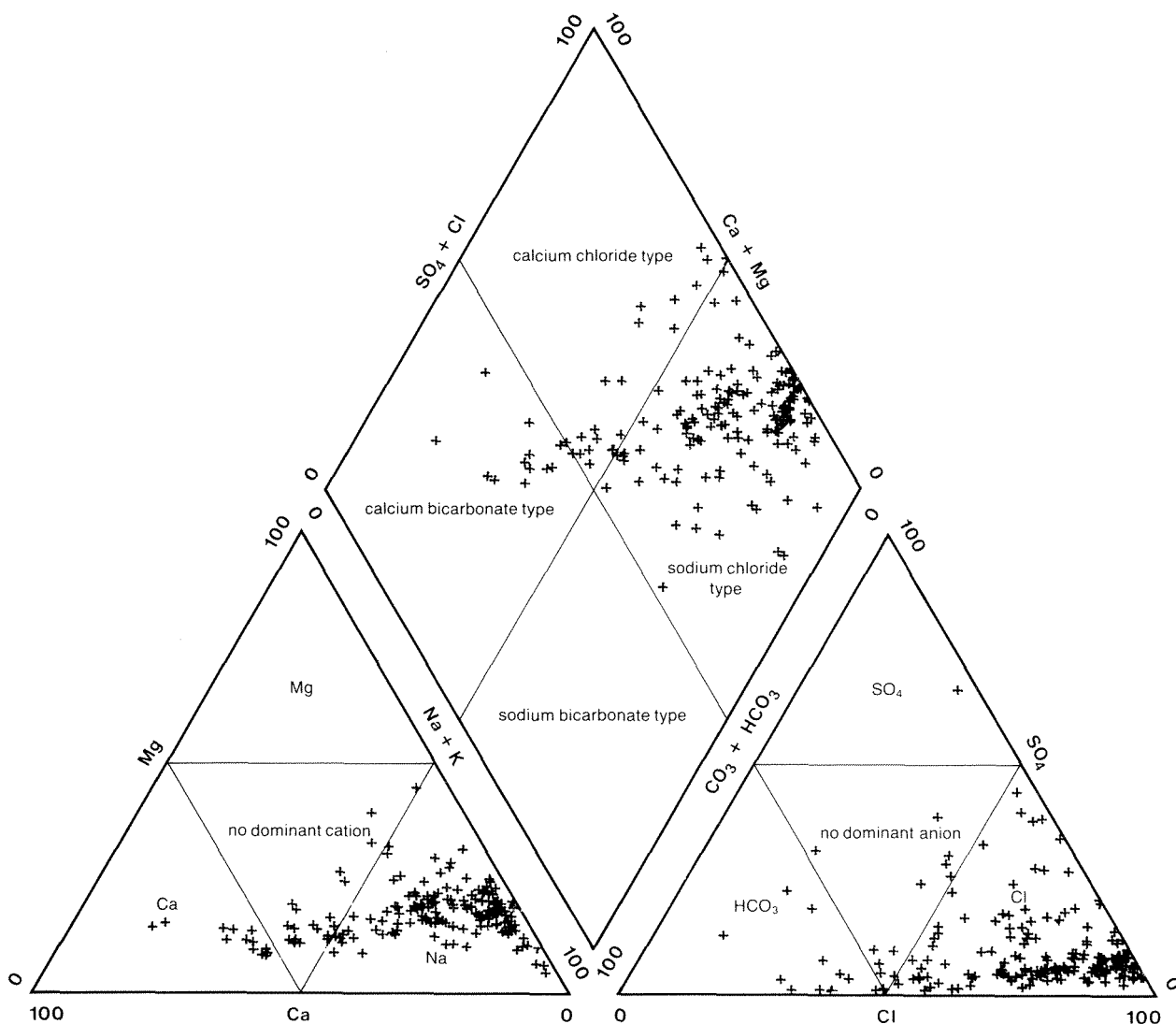

Figure 14. Piper Trilinear Diagram — Harvey Shallow bores

GSWA 23686

52

14). Most of the waters are of the sodium chloride type and a few are of the calcium bicarbonate type. The remainder are transitional between the sodium chloride type and the calcium bicarbonate or calcium chloride types. Generally, the percentages of sodium and chloride increase and the percentages of calcium and bicarbonate decrease with increasing salinity.

Groundwaters from the water-table bores near the crests of the mounds and divides in the Myalup flow system are of the calcium bicarbonate type. Generally, groundwaters from the water-table bores exhibit higher percentages of calcium and bicarbonate than those from bores screened in the basal section of the aquifer. This distribution probably reflects the shorter distances that the waters have flowed since entering the aquifer.

A few of the groundwaters from the Jandakot Beds are also of the calcium bicarbonate type; however, the majority of the groundwaters from the Jandakot Beds, together with those from the Tamala Limestone, are transitional between this type and the sodium chloride type. This is probably due to the presence of carbonate in these sediments.

Generally, sulphate ranges from 5 to 40% of the total anions, and the percentage of sulphate at the water table is generally higher than at the base of the aquifer. The sulphate in groundwater is derived from rainfall and from the calcium sulphate (anhydrite) which, together with phosphate, is applied extensively to the land on the Pinjarra Plain and the Bassendean Dunes. The higher percentage of sulphate (68%) present at the water table at site 55 is probably due to point source pollution. Conditions suitable for sulphate reduction and the formation of hydrogen sulphide (pH<7.0, negative redox potential) occur generally in the aquifer. The biochemical reduction of sulphate may account for the lower percentages of sulphate at the base of the aquifer.

Previous work (Deeney, 1985) has shown that phosphorus concentrations at the water table are extremely variable; they range from less than 10 μg/L to 3 000 μg/L and the major source of phosphorus is fertilizer.

The distribution of phosphorus in the deeper groundwaters is more uniform and generally bears little similarity to its distribution at the water table. It was concluded that the phosphorus in the deeper groundwaters may be largely derived from phosphate contained in the Jandakot Beds. It was also concluded that the quantity of phosphorus discharged by groundwater was not significant in comparison to that discharged by rivers and drains.

Nitrate concentrations in the aquifer are generally less than 0.1 mg/L (as nitrogen). Locally, elevated concentrations of nitrate up to 5.8 mg/L (N) may be associated with point source pollution. Ammonia concentrations are generally less than 1 mg/L (N) and reach a maximum of 3.7 mg/L (N) locally.

Silica concentrations range from 3–100 mg/L, generally exceed 20 mg/L, and commonly exceed 50 mg/L.

During the sampling program it was observed that groundwaters were generally reduced; redox potentials (Eh) were in the range +100 to -200 mV. Values of pH ranged from 3.7 to 8.6. They were generally between 6.5 and 8 in groundwaters from the Tamala Limestone, and between 5 and 7 in groundwaters from the rest of the aquifer. Groundwaters are commonly coloured brown due to the presence of organic acids and contained dissolved hydrogen sulphide.

Iron concentrations show a wide variation, generally being in the range 1–5 mg/L. Many are very high and the maximum concentration recorded was 78 mg/L. The principal variables which influence the solubility of iron in groundwater include the pH, Eh, and the concentration of sulphate and bicarbonate. A considerable ferrous iron concentration can be maintained under the Eh–pH regime existing in the aquifer; however, the reasons for the observed distribution of iron, particularly the very high concentrations, are uncertain.

In most cases, turbidity, hardness, colour, and hydrogen sulphide and iron concentrations would require that groundwater be treated before introduction to the public water supply.

## GROUNDWATER RESOURCES

Groundwater throughflow

Groundwater throughflow has been estimated for each flow system using a flow net and the transmissivity contours shown in Figure 8. Each flow system has been subdivided into flow sections which are separated by bounding flow lines (Fig. 15) and include a number of flow channels.

The total throughflow of each flow system (Table 4) ranges from 1.6 x 10^6 m^3 per annum for the Serpentine flow system, to 19.1 x 10^6 m^3 per annum for the Myalup flow system.

Groundwater throughflow as a percentage of annual rainfall for each flow system (Table 4) was estimated by dividing the total throughflow by the average annual rainfall over the area of the flow system. These estimates range from 1% for the Serpentine flow system to 4% for the Myalup flow system.

Groundwater recharge as a percentage of annual rainfall was estimated using the chloride balance equation, and assuming that all the chloride in groundwater originates directly from rainfall. This assumption is considered to be valid only for the crests of the Yanget and Mialla mounds. In these areas the chloride ion concentration in groundwater close to the water table ranges from 20 to 50 mg/L. The chloride ion concentration in rainfall, 3–11 km from the coast, is about 12 mg/L (Hingston and Gailitis, 1977). Estimates of groundwater recharge based on these figures range from 24% to 60% of annual rainfall.

A comparison of the figures obtained for groundwater recharge and groundwater throughflow in the Myalup flow system indicates that throughflow may represent only 7–17% of the recharge to the aquifer. This is
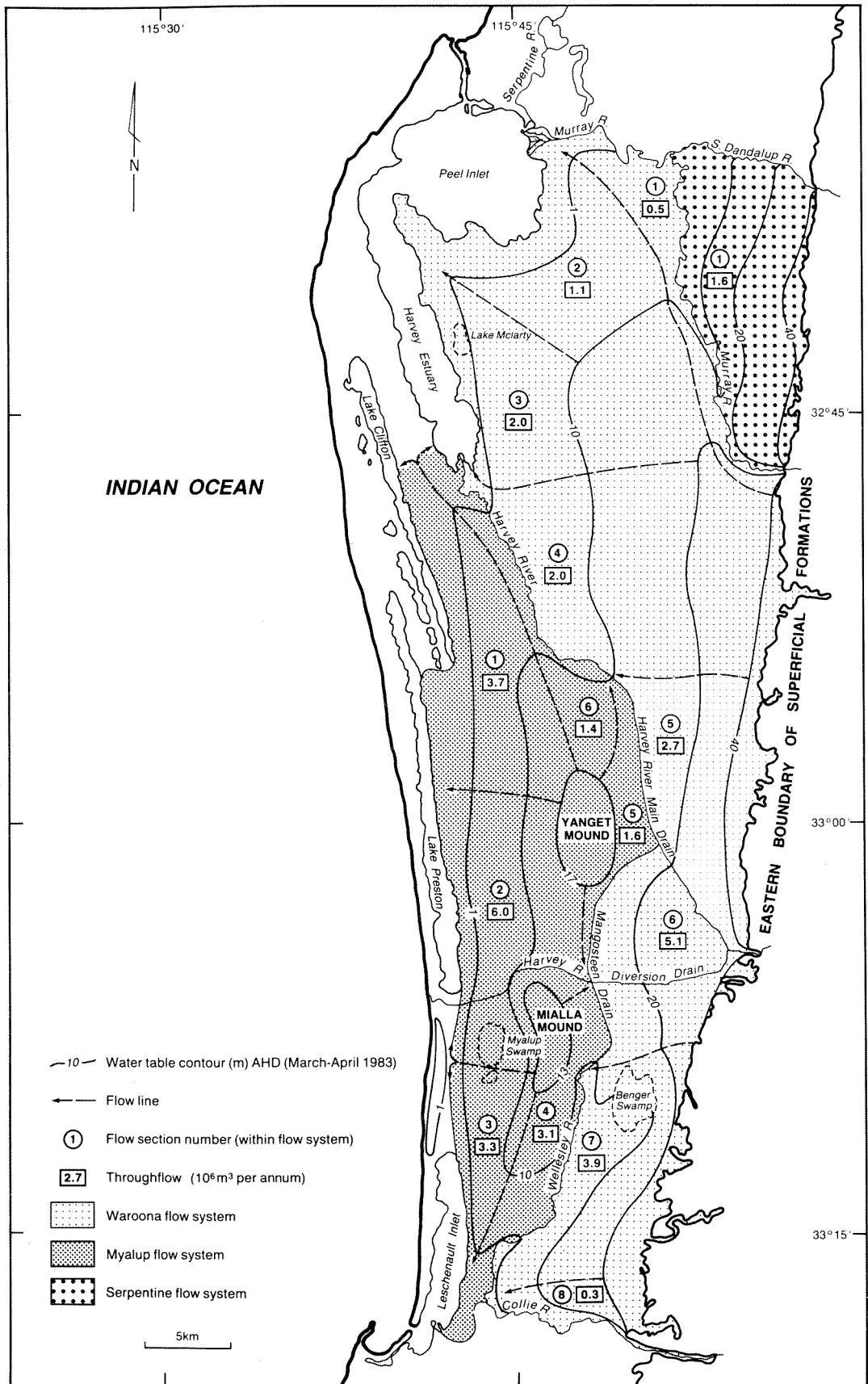
Figure 15. Regional groundwater flow systems and flow sections

because discharge locally to drains and to the underlying Mesozoic sediments, together with losses by evapotranspiration, are substantial and are greater than the total throughflow.

Groundwater development

The Myalup flow system contains a large resource of fresh groundwater and is the most prospective area for further development. It is also an area where it is inferred that significant recharge to the underlying Leederville Formation occurs by downward leakage. A large resource of fresh to brackish groundwater is present in the northern part of the Waroona flow system in the area where the Guildford Formation clay member is absent. Elsewhere development is limited by salinity and yield, though locally, small supplies of fresh groundwater are available from the upper part of the aquifer.

Throughflow estimates provide a conservative basis for decisions concerning groundwater allocation as the throughflow probably represents only a small proportion of the annual recharge to the aquifer. Pumping in areas of shallow water table would substantially reduce local discharge and losses by evapotranspiration by lowering the water table, and would thus effectively increase the renewable groundwater resource.

EFFECTS OF IRRIGATION

Waroona flow system

Flood irrigation of pastures in the Waroona, Harvey, and Collie Irrigation areas (Fig. 3) has taken place for

more than 30 years using water from dams east of the Darling Scarp. Currently, the application of imported irrigation water, at an average rate of about 900 mm per annum, results in the addition of about 6000 kg/ha of salt each year. In comparison, the annual accession of salts from rainfall is about 216 kg/ha (Hingston and Gailitis, 1977), and from fertilizer is about 300 kg/ha. The estimates given for irrigation rates, concentrations of salts in irrigation waters, and accession of salts from fertilizer application are based on information supplied by the WA Department of Agriculture and the Water Authority of WA. Evaporation increases the concentration of salts, and groundwater throughflow is insufficient to flush them effectively owing to the low permeability of the sediments.

Groundwater in the irrigation areas is brackish to saline and the salinity is generally much higher than in the area north of Waroona (Fig. 12) where there is no widespread irrigation. No significant differences were found in the lithology of the Guildford Formation clay member which underlies both areas and it is likely that irrigation has caused a significant increase in the groundwater salinity.

Irrigation is also likely to have caused groundwater levels to rise. The effects are not particularly pronounced on a regional scale, however, they are apparent in the area immediately west of Harvey (Fig. 3). Consequently, pastures in the irrigation areas are susceptible to secondary salinization.

Myalup flow system

Groundwater from the superficial formations is used to irrigate lucerne and vegetables in the areas shown on

TABLE 4. ESTIMATES OF GROUNDWATER THROUGHFLOW

Flow system	Area (km²)	Flow section	Throughflow (10⁶ m³ p.a.)	Discharge area	Total throughflow (10⁶ m³ p.a.)	Average rainfall over flow system (10⁶ m³ p.a.)	Total throughflow as a percentage of average annual rainfall
Myalup	510	1	3.7	Coastal lakes	19.1	510 (1.0)	4
		2	6.0	Coastal lakes			
		3	3.3	Leschenault Inlet			
		4	3.1	Wellesley River and Mangosteen Drain			
		5	1.6	Harvey River Main Drain and Mangosteen Drain			
		6	1.4	Harvey River and Main Drain			
Waroona	960	1	0.5	Murray River	17.6	960 (1.0)	2
		2	1.1	Peel Inlet			
		3	2.0	Harvey Estuary			
		4	2.0	Harvey River			
		5	2.7	Harvey River Main Drain			
		6	5.1	Harvey River Main Drain, Mangosteen Drain and Wellesley River			
		7	3.9	Wellesley River			
		8	0.3	Collie River			
Serpentine	150	1	1.6	Murray River	1.6	165 (1.1)	1

Note: Average rainfall figure in brackets is in m p.a.

Figure 3. In the areas east and south of Lake Preston, groundwater from the Leederville Formation is also used. Application rates vary from 600 to 1400 mm per annum for lucerne, and from 1000 to 2700 mm per annum for vegetables. The salinity of the irrigation water ranges from 800 to 1500 mg/L TDS.

Abstraction of groundwater for irrigation generally involves the recycling of water and results in an increase in groundwater salinity due to the evaporative concentration of salts. The presence of a saline interface in the superficial formations close to, and in some cases beneath, the irrigation areas constitutes a potential problem since pumping may result in movement of the interface and an increase in the salinity of the groundwater abstracted.

Commander (1983) reported that the groundwater salinity in the irrigation areas was gradually increasing. He concluded that the increases, which ranged from 100 to 900 mg/L TDS over a period of 5 years, were caused by the recycling of salts and that movement of the saline interface during the irrigation season had caused a temporary, though marked, increase in salinity in the area east of Lake Clifton.

Increases in the groundwater salinity are likely to continue in the irrigation areas and may necessitate the temporary suspension or, in some areas, the cessation of cultivation.

CONCLUSIONS

The superficial formations form an anisotropic, inhomogeneous, unconfined aquifer which has a saturated thickness of about 20–30 m. In the basal section of the aquifer, the Jandakot beds extend southwards almost to Australind and are considered to be a marine facies of the Yoganup Formation. A sand member and a clay member of the Guildford Formation are recognized; the clay member forms an important aquitard in the upper part of the aquifer. The sand member is probably of Middle Pleistocene age and may interfinger with the basal marine sequence in the Tamala Limestone.

There are three regional groundwater flow systems (Waroona, Myalup, and Serpentine) in the superficial formations from which groundwater discharges to the Peel Inlet, the Harvey Estuary, the coastal lakes, and the Murray, Harvey, Wellesley, and Collie river systems.

The Myalup flow system is the most prospective part of the aquifer for further development and contains the only major resource of fresh groundwater. The groundwater salinity generally ranges from 90 to 1000 mg/L TDS and the total throughflow is estimated to be 19.1 x 10⁶ m³ per annum. The northern part of the Waroona flow system contains a large resource of fresh to brackish groundwater in which salinity is generally less than 1500 mg/L TDS. Elsewhere, development of groundwater resources is limited by low yield and by generally higher salinity, although small supplies of fresh groundwater are often available from the upper part of the aquifer.

Irrigation using water from dams east of the Darling Scarp has caused a significant increase in the groundwater salinity in the Waroona, Harvey, and Collie irrigation areas. Pastures in these areas are susceptible to secondary salinization as a result of rising water levels.

The groundwater salinity in a number of areas close to the eastern side of the coastal lakes is gradually increasing as a result of irrigation using groundwater. These trends are likely to continue and may affect the future viability of irrigation in these areas.

REFERENCES

ALLEN, A.D., 1976, Outline of the hydrogeology of the superficial formations of the Swan Coastal Plain: Western Australia Geological Survey, Annual Report 1975, p. 31.

BAXTER, J.L., 1982, History of mineral sand mining in Western Australia, in Reference Papers: Exploitation of Mineral Sands. Western Australia School of Mines, WAIT-AID Ltd, Perth.

COMMANDER, D.P., 1975, The hydrogeology of the Mandurah-Pinjarra area: Western Australia Geological Survey, Record 1975/3.

COMMANDER, D.P., 1982, An outline of the Groundwater Resources of the Mandurah-Bunbury Region: Western Australia Geological Survey, Hydrogeology Report 2412 (unpublished).

COMMANDER, D.P., 1983, Effects of irrigation on the groundwater regime in the south west coastal groundwater area: Western Australia Geological Survey, Hydrogeology Report 2483 (unpublished).

COMMANDER, D.P., 1984, The Bunbury shallow-drilling groundwater investigation: Western Australia Geological Survey, Report 12, p. 32–52.

COMMANDER, D.P., 1988, Geology and Hydrogeology of the "Superficial formations" and coastal lakes between Harvey and Leschenault Inlets (Lake Clifton Project): Western Australia Geological Survey, Report 23, p. 37–50.

DARRAGH, T.A. and KENDRICK, G.W., 1971, Zenatropsis ultima sp. nov., terminal species of Zenatropsis lineage (Bivalvia: Mactridae): Royal Society Victoria Proceedings, v. 84, p. 87–91.

DAVIDSON, W.A., 1984, A flow-net analysis of the unconfined groundwater in the "Superficial formations" of the southern Perth area, Western Australia: Western Australia Geological Survey, Record 1984/9.

DEENEY, A.C., 1985, The phosphorus discharged by groundwater to the Peel Inlet-Harvey Estuary system, Western Australia: West Australia Department Conservation and Environment, Bulletin 195, p. 19–34.

DEENEY, A.C., 1988, Geology and groundwater resources of the superficial formations of the coastal plain between Pinjarra and Bunbury: Western Australia Geological Survey, Hydrogeology Report 1988/5.

DEENEY, A.C., 1989a, The geology and hydrogeology of the Binningup Borehole Line: Western Australia Geological Survey, Report 25, p. 7–16.

DEENEY, A.C., 1989b, Hydrogeology of the Harvey Borehole Line: Western Australia Geological Survey, Report 26, p. 59–68.

FREEZE, R.A., and CHERRY, J.A., 1979, Groundwater: New Jersey, Prentice-Hall, Inc., 604p.

GEORGE, P.R., and FURNESS, L.J., 1979, Groundwater Hydrology of the Harvey Irrigation Area: Report prepared for 26th Annual Meeting and Study Tour of the Australian National Committee of the International Commission on Irrigation and Drainage.

HINGSTON, F.J., and GAILITIS, V., 1977, Salts in rainfall in Western Australia (1973-74): Australia CSIRO Division of Land Resources Management, Technical Memorandum 7/1.

HIRSCHBERG, K-J., 1989, Busselton shallow-drilling groundwater investigation: Western Australia Geological Survey, Report 25, p. 17–38.

JONES, D.K., and NICHOLLS, J., 1966, Pinjarra No. 1 well completion report: Western Australian Petroleum Pty Ltd Petroleum Search Subsidy Act Report 65/4176 (unpublished).

LEHMAN, P.R., 1966, Preston No. 1 Corehole completion report: West Australian Petroleum Pty Ltd Report (unpublished).

LOW, G.H., 1971, Definition of two new Quaternary formations in the Perth Basin: Western Australia Geological Survey, Annual Report 1970, p. 33–34.

McARTHUR, W.M., and BETTENAY, E., 1974, Development and distribution of the soils of the Swan Coastal Plain, W.A.: Australia, CSIRO Soil Publication No. 16.

PLAYFORD, P.E., and LOW, G.H., 1972, Definitions of some new and revised rock units in the Perth Basin: Western Australia Geological Survey, Annual Report 1971, p. 44–46.

PLAYFORD, P.E., COCKBAIN, A.E., and LOW, G.H., 1976, Geology of the Perth Basin, Western Australia: Western Australia Geological Survey, Bulletin 124.

SADGROVE, G.W., and DEENEY, A.C., 1989, Harvey Shallow Project bore completion reports: Western Australia Geological Survey, Hydrogeology Report 1989/19.

SANDERS, C.C., 1974, Geology and Hydrology of the Harvey-Waroona area: Western Australia Geological Survey, Hydrogeology Report 1213 (unpublished).

WALTON, W.C., 1962, Selected analytical methods for well and aquifer evaluation: Illinois State Water Survey, Bulletin 49, 81p.

WHARTON, P.H., 1980, Harvey Irrigation Scheme, Supplementary water supply investigation: Western Australia Geological Survey, Hydrogeology Report 2217 (unpublished).

WILDE, S.A., and WALKER, I.W., 1979, Explanatory notes on the Collie 1:250 000 Geological Sheet, Western Australia: Western Australia Geological Survey, Record 1979/11.

YOUNG, R.J.B., and JOHANSON, J.N., 1973, Lake Preston No. 1 well completion report: Western Australian Petroleum Pty Ltd Report (unpublished).

HYDROGEOLOGY OF THE HARVEY BOREHOLE LINE, PERTH BASIN

by A. C. Deeney

ABSTRACT

The Harvey Line comprises eight bores drilled between 1982 and 1985 at four sites on an east–west line across the Perth Basin near Waroona. They were drilled to a maximum depth of 810 m and have an aggregate depth of 2749 m.

The Cockleshell Gully Formation (Early to Middle Jurassic) has been block faulted, and it dips at a low angle to the northwest. It is unconformably overlain by the Leederville Formation, which has been gently folded to form a broad synclinal structure. Flat-lying superficial formations unconformably overlie the Mesozoic sediments.

The Leederville Formation and the Cockleshell Gully Formation form multi-layered aquifers which are largely composed of fine-grained sediments in the east. The Leederville Formation is recharged locally by downward leakage from the superficial formations, and groundwater flow is westwards. Groundwater with a salinity of less than 500 mg/L TDS occurs only in the superficial formations. The saline groundwaters present in the superficial formations near the coast and beneath Lake Preston do not appear to extend into the Leederville Formation. Groundwater with a salinity range of 500–1500 mg/L TDS is present in the upper part of the Leederville Formation. Brackish groundwater with a salinity in the range 2300 to 7000 mg/L TDS extends downwards from the lower part of the Leederville Formation into the Cockleshell Gully Formation to a depth of -450 m AHD in the west and about -300 m AHD in the east. Groundwater in the remainder of the Cockleshell Gully Formation is saline and flow rates are very low. The potential for development of the groundwater resources is limited.

KEYWORDS: Perth Basin; hydrogeology; geology; groundwater; stratigraphy

INTRODUCTION

The Harvey Line consists of eight exploratory bores at four sites (designated HL1 to HL4) drilled along an east–west line across the coastal plain near Waroona, 43 km south of Mandurah (Figs 1 and 2).

The investigation is part of a long-term drilling program to evaluate the deep groundwater resources of the Perth Basin, and was funded jointly by the Commonwealth and the State under the National Water Resources (Financial Assistance) Act, 1978. Elsewhere, the nearest deep exploratory bores are along the Binningup Line, 26 km to the south (Deeney, 1989a), and in the Mandurah–Pinjarra area 40 km to the north (Commander, 1974). Other deep bores close to the Harvey Line are the Lake Preston No. 1 oil exploration well and exploratory water-supply bores for Wagerup Alumina Refinery and Preston Beach. Additional information concerning the shallow groundwater resources was obtained from nearby bores drilled for the Lake Clifton Project (Commander, 1988) and the Harvey Shallow Project (Deeney, 1989b).

PHYSIOGRAPHY, CLIMATE, AND LAND USE

The Harvey Line bores are situated on the Swan Coastal Plain which is formed by alluvial, shallow-marine, shoreline, and coastal-dune deposits, extending from the Darling Scarp to the Indian Ocean. The coastal plain can be divided into four physiographic units in this area: an alluvial plain developed in front of the Darling Scarp, and three sets of stabilized dunes parallel to the coastline with lakes and swamps in the low-lying interdunal depressions.

The coastal plain in the vicinity of the Harvey Line is drained by the Harvey River and a number of drains which discharge into the river.
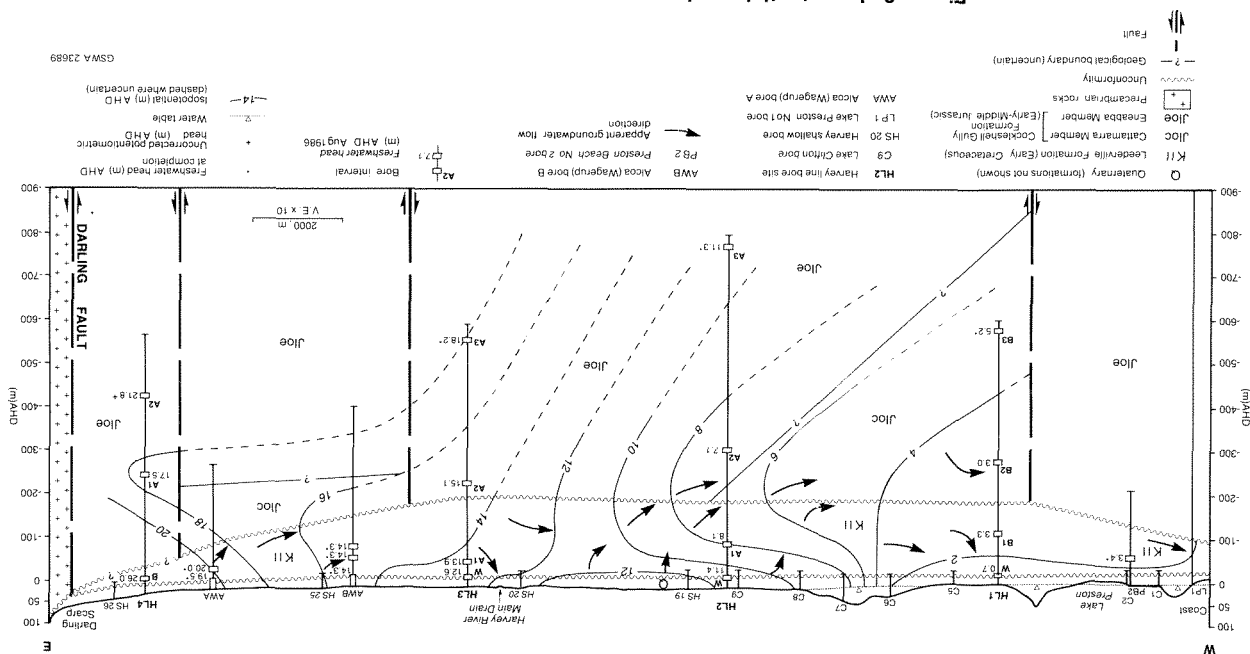
The climate of the area is Mediterranean. The average annual rainfall ranges from about 900 mm near the coast to about 1100 mm at the Darling Scarp. Rainfall generally exceeds evaporation during the five months from May to September. The average annual evaporation is about 1400 mm.

Most of the land east of HL2 has been cleared for agriculture. Pastures east of the Harvey River are irrigated, using water from dams located on the Darling Plateau. Native vegetation covers most of the coastal plain west of HL2, apart from an area of pine plantations between HL2 and the Old Coast Road.

INVESTIGATION PROGRAM

The bores were drilled between 1982 and 1985 by the Mines Department Drilling Branch. Water-supply bores (designated W) were drilled first at every site. A 600–800 m deep exploratory bore (designated A) was then drilled at each site with the Department of Mines Midway Skytop rig using the mud-flush rotary method. One bore (HL4B) was also drilled to 50 m to provide for additional monitoring. HL1A was abandoned at a

The map shows a coastal region of Western Australia with the following labeled features:

MANDURAH

FALCON BAY

PEEL INLET

INDIAN OCEAN

HARVEY ESTUARY

LAKE CLIFTON

LAKE PRESTON

PLAIN

COASTAL

SWAN

Bore locations: M1, M2, M3, M4, M5, M6, M7, M8, M9, M10, M11, M12, M13, M14, M15, M16, M17, M18

Murray R, North Dandalup River, PINJARRA

Old Bunbury Road, Old Coast Road, Harvey River

WAROONA

HS 25, HS 26, HS 20, HS 19, HL 1, HL 2, HL 3, HL 4, AWB AWA

PB2, C1, C2, C5, C6, C7, C8, C9, LP1

SCARP

PLATEAU

DARLING

Harvey River Main Drain, Mangosteen Drain

HARVEY

Diversion Drain, River

BINNINGUP, BPL1, BPL2, BPL3, BPL4

Wellesley River, Benger Swamp, BENGER

33°00', 115°45'

5 km

N

HL1	Harvey line bore	
BPL1	Binningup line bore	
M1	Mandurah bore	
C1	Lake Clifton bore	
HS 20	Harvey shallow bore	
AWA	Alcoa (Wagerup) A bore	
AWB	Alcoa (Wagerup) B bore	
LP1	Lake Preston No 1 oil well	
PB2	Preston Beach No 2 bore	

STRUCTURAL UNITS

DANDARAGAN TROUGH, HARVEY RIDGE, DARLING FAULT, YILGARN BLOCK

GSWA 23687

Figure 1. Locality map and structural subdivisions

60

Figure 3. Isopotentials and apparent groundwater flow directions

depth of 62.5 m because of drilling difficulties, and a second bore (HL1B) was constructed. A summary of the bore data is given in Table 1.

Cutting samples were collected, at 3 m intervals, from the exploratory bores. On completion of drilling, a suite of geophysical logs was run in each bore including gamma-ray and long- and short-normal resistivity logs. About 20 sidewall cores were recovered from siltstones or clays in each bore. The bores were completed with 154 mm steel casing and pressure cemented. Three intervals in bores HL1B, HL2A and HL3A, and two intervals in bore HL4A, (numbered sequentially from the top down) were selected for perforation with shaped charges in order to collect water samples and measure potentiometric heads.

In bores HL1B, HL2A, and HL3A, the lower interval was perforated, developed, and abandoned prior to the perforation of the middle and upper intervals. A string of 80 mm galvanized-iron pipe (extending below the lower interval) was installed, with 12 m of flame-cut slots opposite the middle interval, and compressible packers set above and below the middle interval to seal the annulus. This bore construction allows the middle and upper intervals to be monitored, observation of the upper interval being facilitated by the installation of 25 mm galvanized-iron pipe in the annulus. The 80 mm

Figure 2. Geological section

TABLE 1. BORE DATA

Bore	Interval	AMG Zone 50 Easting	AMG Zone 50 Northing	Commenced	Completed	Total depth (m bns)	Elevation (m) AHD Natural surface	Elevation (m) AHD Top of casing	Perforation interval (m bns)	Formations	Water level (m btc) 5.8.86	Potentiometric head (m) AHD 5.8.66 Fresh-water	Potentiometric head (m) AHD 5.8.66 Environmental	Salinity(a) (mg/L TDS)	Airlift yield (m³/d)	Status of bore
HL1A(b)		378700	6357200	25.2.83	14.3.83	62.5	–	–	–	–	–	–	–	–	–	Abandoned
HL1B	1	378700	6357200	14.3.83	8.4.83	605	1.617	2.325	117–123	Kll	+ 0.895	3.3	3.2	2 360	640	Observation
	2							2.219	279–285	Jlo	+ 0.56	3.0	2.8	2 270	30	Observation
	3							–	582–588	Jlo	9.71(e)	5.2	2.5	30 500	10	Abandoned
HL1W		378700	6357200	16.11.82	18.11.82	21	–	1.769	13–19(c)	Q	1.10	0.7	0.7	716	290	Observation
HL2A	1	384800	6356700	16.5.83	16.6.83	810	13.155	13.712	105–111	Kll	5.60	8.1	8.1	1 390	930	Observation
	2							13.843	324–330	Jlo	7.23	7.1	6.9	3 550	360	Observation
	3							–	786–792	Jlo	20.09(e)	11.3	7.5	31 400	100	Abandoned
HL2W		384800	6356700	18.11.82	22.11.82	31	–	13.175	25–31(c)	Q,Kll	1.79	11.4	11.4	479	460	Observation
HL3A	1	390500	6358000	8.4.83	16.5.83	603	12.794	13.301	61–66	Kll	+ 0.62	13.9	13.9	1 560	50	Observation
	2							13.240	241–247	Jlo	0.06	15.1	14.5	11 700	<1	Observation
	3							–	568–574	Jlo	8.45(e)	18.2	12.1	32 500	1 270	Abandoned
HL3W		390500	6358000	22.11.82	24.11.82	30	–	13.049	23–29(c)	Kll	0.415	12.6	12.6	2 310	110	Observation
HL4A	1	397700	6359200	14.3.84	16.4.84	598	33.042	33.464	273–282	Jlo	16.62	17.5	16.9	4 790	350	Observation
	2			6.12.84	14.12.84			33.471	459–465	Jlo	11.92	21.8(f)	21.8(f)	–	<1	Observation
HL4B		397700	6359200	14.12.84 19.4.85	19.12.84 22.4.85	50	33.042	33.471	38–48(c)	Kll	7.47	26.0	26.0	1 690(g)	<1	Observation
HL4W1		397700	6359200	24.11.82	26.11.82	25	–	–	18–24(c)	Q,Kll	8.1(e)	–	–	479	<1	Abandoned
HL4W2		397700	6359200	29.11.82	02.12.82	50	–	–	14–50(d)	Q,Kll	8.1(e)	–	–	–	<1	Abandoned

(a) Airlift samples taken at completion, TDS by calculation
(b) HL1A was drilled to a depth of 62.5 m and abandoned due to drilling difficulties
(c) Screened interval
(d) Slotted PVC

(e) Approximate static water level measured at completion
(f) Not corrected for the density distribution resulting from the salinity variation with depth
(g) Bailed sample

bns — Below natural surface
btc — Below top of casing
Q — Superficial formations
Kll — Leederville formation
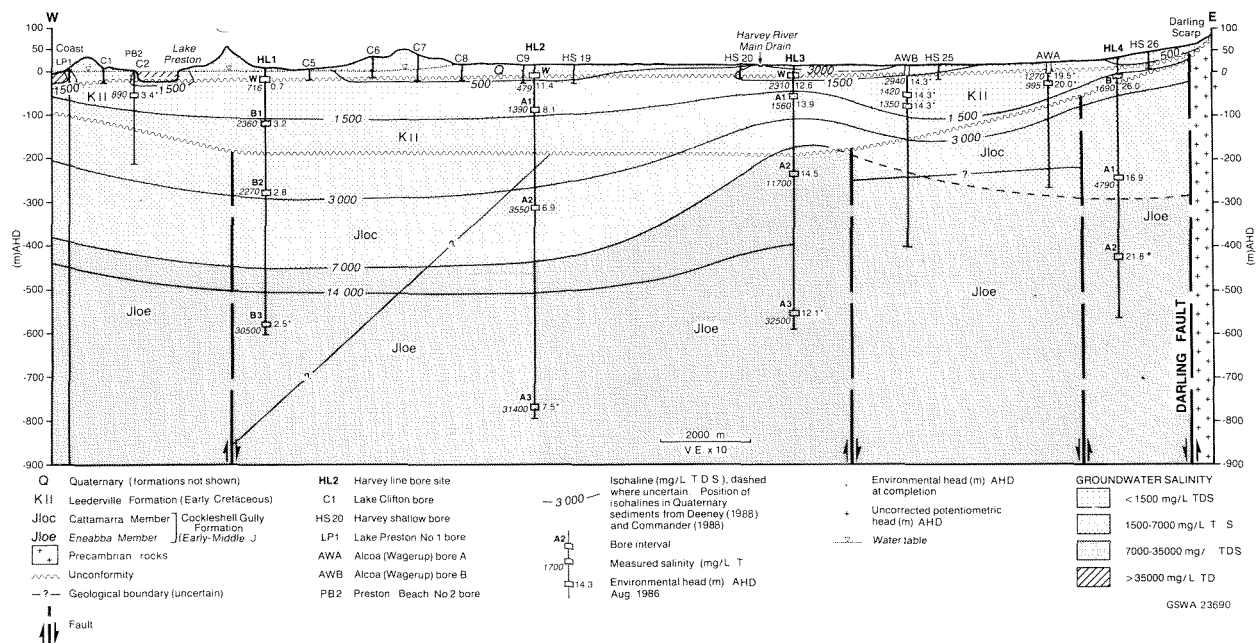Jlo — Cockleshell Gully Formation

Figure 4. Groundwater salinity and environmental heads

and 25 mm pipes in HL1B, and the 25 mm pipe in HL3A have been fitted with gate valves to control artesian flows.

A similar bore construction was employed in HL4A, except that only one packer was used to seal the annulus between the two monitoring intervals. HL4B was completed with 100 mm PVC casing coupled to a 50 mm galvanized-iron screen. The water-supply bores were completed with 100 mm steel casing and in-line stainless-steel screens.

Each interval was developed by airlifting and surging to obtain a clear uncontaminated water sample for chemical analysis by the Government Chemical Laboratories (Table 2). Flow rates from HL3A2, HL4A2 and HL4B were insufficient to allow full development. A comparison of the measured salinities of the samples with the salinities estimated from the long-normal resistivity logs indicates that the sample from HL4A2 is not representative of the formation waters, but that those from HL3A2 and HL4B probably are representative of the formation waters. Water levels in all the monitoring intervals have been measured once a month since completion. Using the method of Lusczynski (1961), values of potentiometric head given in Table 1 and Figures 3 and 4 have been corrected for the density distribution resulting from salinity variations with depth. Values given in Figure 3 have been converted to fresh-water heads to allow comparison in a horizontal direction, and values given in Figure 4 have been converted to environmental heads to allow comparison in a vertical direction. The differences between measured and corrected heads ranged up to 18 m.

After completion, gas-cut artesian flows were observed from the middle and upper intervals in HL1B. The gas could not be readily identified due to the small quantities involved. Information from the Binningup Line bores (Deeney, 1989a) suggests that it may be natural gas. The quantity of gas appears to have increased during the monitoring period, due perhaps to accumulation in the bore casing. This may have affected the measured potentiometric heads.

GEOLOGY

SETTING

The Harvey Line of bores was drilled in the southernmost part of the Dandaragan Trough. The trough is a structural subdivision of the Perth Basin (Playford and others, 1976) and is a deep graben bounded on the east by the Darling Fault and in the South by the Harvey Ridge (Fig. 1). The Harvey Ridge is probably fault bounded and extends northwest from the Darling Fault. The Perth Basin contains about 5000 m of Phanerozoic sediments in this area (Playford and others, 1976).

STRATIGRAPHY

Sediments encountered in the Harvey Line bores range in age from Early Jurassic to Holocene. The formations recognized are given in Table 3 and are described below.

Cockleshell Gully Formation

The Cockleshell Gully Formation (Willmott, 1964) has been subdivided into two members. The Eneabba Member was encountered in HL2A, HL3A, and HL4A, and the Cattamarra Member was encountered HL1B and HL2A (Fig. 2).

63

TABLE 2. CHEMICAL ANALYSES OF WATER SAMPLES (mg/L)

Bore interval	Sample number(a)	pH	EC mS/m @25°C	TDS	TH	TA	Ca	Mg	Na	K	CO$_3$	HCO$_3$	Cl	SO$_4$	NO$_3$	SiO$_2$	B	F
HL1B1	78497	8.5	439	2 360	800	227	187	81	590	13	12	253	1 220	116	<1	18	–	0.2
HL1B2	78498	8.3	418	2 270	260	277	51	32	763	26	3	332	090	125	<1	12	–	1.0
HL1B3	75728	8.0	4 650	30 500	4 400	115	556	723	10 200	241	<2	140	17 800	918	<1	2	–	–
HL1W	75288	7.9	138	716	310	252	90	21	150	4	<2	308	262	26	<1	9	0.08	0.3
HL2A1	78494	8.4	271	1 390	350	195	68	45	394	16	9	220	679	55	<1	13	–	0.2
HL2A2	78495	8.1	644	3 550	280	217	59	32	1 240	26	<2	265	1 840	203	<1	13	–	1.3
HL2A3	78496	7.8	4 500	31 400	5 900	102	1 230	692	9 560	44	<2	125	18 100	1 610	<1	9	–	0.2
HL2W	75289	7.5	87.5	479	280	275	90	14	68	4	<2	336	117	2	<1	16	0.07	0.1
HL3A1	78492	8.5	290	1 560	320	230	50	47	461	19	3	275	749	83	1	13	–	0.2
HL3A2	78493	7.3	1 900	11 700	1 700	98	648	12	3 840	50	<2	119	6 710	418	<1	3	–	0.2
HL3A3	75865	7.2	4 330	32 500	8 800	33	3 180	205	9 070	34	<2	40	19 100	910	<1	15	–	0.2
HL3W	75290	7.6	420	2 310	700	307	104	106	626	10	<2	375	1 120	139	<1	15	–	0.2
HL4A1	79767	7.7	859	4 790	420	102	127	25	1 700	8	<2	125	2 740	109	<1	14	0.2	1.3
HL4B	16774(b)	7.6	318	1 690	186	170	35	24	565	14	<2	207	880	60	<1	8	0.36	0.4

Analyses carried out by Government Chemical Laboratories, Perth
(a) Airlift samples taken at completion
(b) Bailed sample

EC Electrical conductivity
TDS Total dissolved solids by calculation @ 180°C

TH Total hardness as calcium carbonate
TA Total alkalinity as calcium carbonate

The Eneabba Member consists of angular to subangular, weakly cemented quartz sandstone containing accessory pyrite and garnet, and weakly consolidated siltstone and shale. The siltstone and shale are micaceous and generally multi-coloured being purple, red-brown, green, yellow, blue-black, and grey. They contain minor to trace amounts of carbonaceous material.

The Cattamarra Member is composed of angular to subangular, weakly cemented quartz sandstone containing accessory pyrite, and weakly consolidated siltstone and shale. The siltstone and shale are generally grey, brown, or olive-green, and micaceous. Carbonaceous shales and low-grade coal were common in the cuttings samples from HL1B, but could not be identified on the geophysical logs.

In HL1B, HL2A, and HL3A, individual beds in the Cattamarra and Eneabba Members of the Cockleshell Gully Formation are up to 40 m thick, and the sandstones are poorly sorted and generally fine to very coarse grained. In HL4A, the sandstones are moderately sorted and very fine to fine grained, and the beds are only about 5 m thick. These differences between the sequences in the western bores and the easternmost bore are readily apparent on the gamma-ray logs which show a smaller range and a more uniform response with depth in HL4A. Individual beds cannot be correlated between bores.

The Cockleshell Gully Formation is about 2000 m thick (Playford and others, 1976), of which a maximum thickness of 607 m was intersected in HL2A. It is unconformably overlain by the Leederville Formation.

Owing to oxidation of the sediments, few of the samples yielded palynomorphs. Only sidewall cores from HL1B yielded assemblages. These are dominated by *Classopolis* pollen grains and appear to belong to the *C. chateaunovi* Assemblage sub-zone of Filatoff (1975). This indicates an age of Early to Middle Jurassic (Pleinsbachian–Aalenian, probably upper Toarcian) and a non-marine environment of deposition (Backhouse, 1983a). This evidence supports the conclusions drawn on the basis of lithology and indicates that the sequence in HL1B belongs to the Cattamarra Member.

Leederville Formation

The Leederville Formation (Cockbain and Playford, 1973) was encountered in all the exploratory bores and consists of quartz sandstone, siltstone, and shale. The sandstones are grey, silty, weakly cemented, poorly sorted, generally fine to very coarse grained, and frequently contain trace amounts of heavy minerals. They often include thin layers of lime-cemented and pyrite-cemented sandstone. The siltstones and shales are generally dark grey, mottled olive-green or brown, and in HL4A they are multi-coloured, which indicates that the sequence has been weathered prior to deposition of the superficial formations. They are usually micaceous and contain minor to trace amounts of carbonaceous material. In HL1B and HL2A the sandstones are up to 20 m thick, whereas in HL3A and HL4A they are about 6 m thick. Individual beds cannot be correlated between bores.

The Leederville Formation is approximately 175 m thick in HL1B, HL2A, and HL3A. It thins both to the east and to the west being 37 m thick in HL4A and 77 m thick in Lake Preston No. 1 (Young and Johanson, 1973). The Leederville Formation is unconformably overlain by the superficial formations.

Few of the sidewall cores yielded palynomorphs owing to the weathering of the sediments. The palynomorphs indicate a non-marine, fluviatile to backswamp environment of deposition and can be placed in the *B. limbata* Zone (Backhouse; 1983a,b,c). This indicates an age of Early Cretaceous (Valanginian to Aptian, probably Hauterivian to Barremian) which is consistent with the Leederville Formation. The South Perth Shale is not recognized as a separate unit in this part of the Perth Basin and the whole of the Early Cretaceous sequence is thought to belong to the Leederville Formation.

Superficial formations

Following Allen (1976), the Cainozoic sediments of the Swan Coastal Plain in this area are referred to as the superficial formations. They have been described by Commander (1988) and Deeney (1989b).

TABLE 3. STRATIGRAPHIC SUCCESSION IN THE HARVEY LINE BORES

Age	Formation	Thickness (m)				Summary lithology	Remarks
		HL1	HL2	HL3	HL4		
Quaternary	Superficial formations	23	26	21	20	Sand, sandy clay, clay, limestone, calcarenite	Unconfined aquifer, groundwater is fresh to brackish
			UNCONFORMITY				
Early Cretaceous	Leederville Formation	165	177	183	37	Sandstone, siltstone, shale	Multi-layered aquifer, groundwater is marginal to brackish
			UNCONFORMITY				
Early–Middle Jurassic	Cockleshell Gully Fm Cattamarra Member Eneabba Member	417	38 569	399	543	Sandstone, siltstone, shale	Multi-layered aquifer, groundwater is brackish to saline

The superficial formations consist of sand, limestone, silt, and clay, and exhibit a marked variation in lithology both laterally and vertically. They form a stratigraphically complex sequence which comprises sediments of marine, littoral, alluvial, and eolian origin. In the western and central parts of the coastal plain they consist of sand and limestone with minor amounts of silt and clay. These deposits interfinger with a sequence which consists of clay, clayey sand, and minor amounts of gravel adjacent to the Darling Scarp.

The superficial formations form a flat-lying sequence which ranges in thickness from about 20 m to 70 m and extends westwards from the Darling Scarp. They rest unconformably on a gentle westward-sloping erosional surface.

STRUCTURE

The inferred geological structure along the Harvey Line is shown in Figure 2. The Cockleshell Gully Formation dips northwestwards at a low angle (Playford and others, 1976) and has been block faulted along northeasterly trending faults. It has been downfaulted against Precambrian granitic rocks of the Yilgarn Block by the Darling Fault. The positions of the faults shown in Figure 2 have been determined from geological evidence obtained during drilling, and from geological sections and structure-contour maps based on seismic surveys, given in Playford and others (1976).

The Leederville Formation unconformably overlies the Cockleshell Gully Formation and has been gently folded to form a broad synclinal structure. This structure may have formed as a result of flexure and differential compaction of sediments over faults marginal to the Harvey Ridge, as suggested by Cope (1972).

HYDROGEOLOGY

Superficial formations

The anisotropic unconfined aquifer formed by the superficial formations has a saturated thickness of about 25 m (Fig. 3) and has been discussed in detail by Commander (1988) and Deeney (1989b).

The aquifer is recharged directly by rainfall, and a large proportion of infiltration is lost by evapotranspiration.

Groundwater flow is generally westwards from the Darling Scarp, and the seasonal variation in water-table level is generally in the range 0.5–2.0 m. Groundwater discharges locally to water courses and swamps, to the Leederville Formation, and across saline interfaces to Lake Preston and the Indian Ocean (Fig. 4).

The groundwater is generally fresh to marginal and has a salinity of between 150 and 1500 mg/L TDS (Fig. 4). In the clayey sediments near HL3A, and locally, close to discharge areas, it is brackish and has a salinity of between 1500 and 4000 mg/L TDS. Hypersaline groundwater (48 000 mg/L TDS) occurs in the aquifer beneath Lake Preston (Commander, 1988).

Groundwater in the aquifer west of the Harvey River Main Drain constitutes an important resource in view of the limited quantity of good quality water in the deeper aquifers.

Leederville Formation

The Leederville Formation forms a multi-layered aquifer in which the percentage of sandstone increases westwards from about 40% at HL4 to about 80% at HL1. It ranges in thickness from about 37 m at HL4 to 183 m at HL3.

The Leederville Formation is recharged by downward leakage from the superficial formations. The main recharge area is inferred to be between the Harvey River Main Drain and Lake Clifton bore C6, where the superficial formations consist predominantly of sand and where there is a downward potentiometric gradient (Fig. 3). East of the Harvey River Main Drain there is likely to be little recharge, because the superficial formations consist predominantly of clay, and the potentiometric heads in the Leederville Formation are approximately equal to the heads in the superficial formations.

Groundwater flow in the Leederville Formation is westwards and discharges offshore. Onshore, discharge may also occur into the superficial formations near HL3, and in the area between Lake Clifton bore C6 and the coast, where the potentiometric heads in the Leederville Formation are higher than those in the superficial formations (Fig. 3). In the low-lying parts of this area, gas-cut artesian flows may be encountered. Artesian flows may also be encountered near HL3.

Groundwater with a salinity of between 500 mg/L and 1500 mg/L occurs in the upper part of the aquifer (Fig. 4). In the lower part of the aquifer, the groundwater salinity is generally less than 3000 mg/L TDS, except near HL3A where it may exceed 7000 mg/L TDS. The saline and hypersaline groundwaters present in the superficial formations near the coast and beneath Lake Preston appear not to extend into the Leederville Formation.

Groundwater in the Leederville Formation is of the sodium chloride type and normally contains dissolved iron in concentrations which would require treatment for domestic, industrial, or public water-supply purposes. Concentrations of fluoride are generally less than 0.4 mg/L (Table 2).

The natural seasonal variation in potentiometric head is 0.5–1.0 m (Fig. 5). Current abstraction from the aquifer is small and there is some potential for further development of the upper part of the aquifer, west of the Harvey River Main Drain, for irrigation or industrial supplies. Elsewhere, higher salinities and lower yields limit the use of the aquifer for water supplies.

Cockleshell Gully Formation

The Cockleshell Gully Formation forms a confined multi-layered aquifer which is composed of fine- to

66

very coarse-grained sandstone interbedded with siltstone and shale in the western and central parts of the coastal plain, and of siltstone and shale interbedded with fine-grained sandstone in the eastern part. The percentage of sand increases from about 50% at HL4, to 60% at HL3, and 70% at HL2 and HL1.

The Cockleshell Gully Formation is recharged by leakage from the Leederville Formation under a downward potentiometric head gradient (Fig. 3). The main recharge area is inferred to be west of HL3 where the Leederville Formation consists predominantly of sandstone. Downward leakage east of HL3 is probably small owing to the predominance of siltstone and shale in the Leederville Formation. The apparent groundwater flow direction is westwards and discharge may occur into the Leederville Formation in the vicinity of HL3 (Fig. 3). Groundwater movement is likely to be very slow at depth where the groundwater is saline. Gas-cut artesian flows may be encountered in low-lying areas between Lake Clifton bore C5 and the coast.

Seasonal variations in potentiometric head of about 0.3 m occur in phase with, and largely as a result of, variations in head in the overlying aquifers (Fig. 5).

The groundwater salinity in the Cockleshell Gully Formation ranges from 2270 to 32 500 mg/L TDS (Fig. 4). Brackish groundwater with a salinity in the range 2300 to 7000 mg/L TDS extends to a depth of about -450 m AHD west of HL3, and -300 m AHD east of HL3. The remainder of the aquifer contains saline groundwater. Groundwater in the Cockleshell Gully Formation is of the sodium chloride type.

There are no bores producing water from the Cockleshell Gully Formation; future development is limited by the lack of low salinity groundwater and also by low yields in the east. However, because of the high salinity and the presence of relatively thick beds of sandstone, the formation may be suitable for liquid-waste injection at depth in the west.

GROUNDWATER TEMPERATURE

Temperature logs were run to the base of the 80 mm pipe in each deep bore, 2 to 3 years after completion of drilling, to ensure that natural geothermal gradients had been re-established. Generally, temperature gradients ranged from 2.1°C to 2.9°C per 100 m; higher
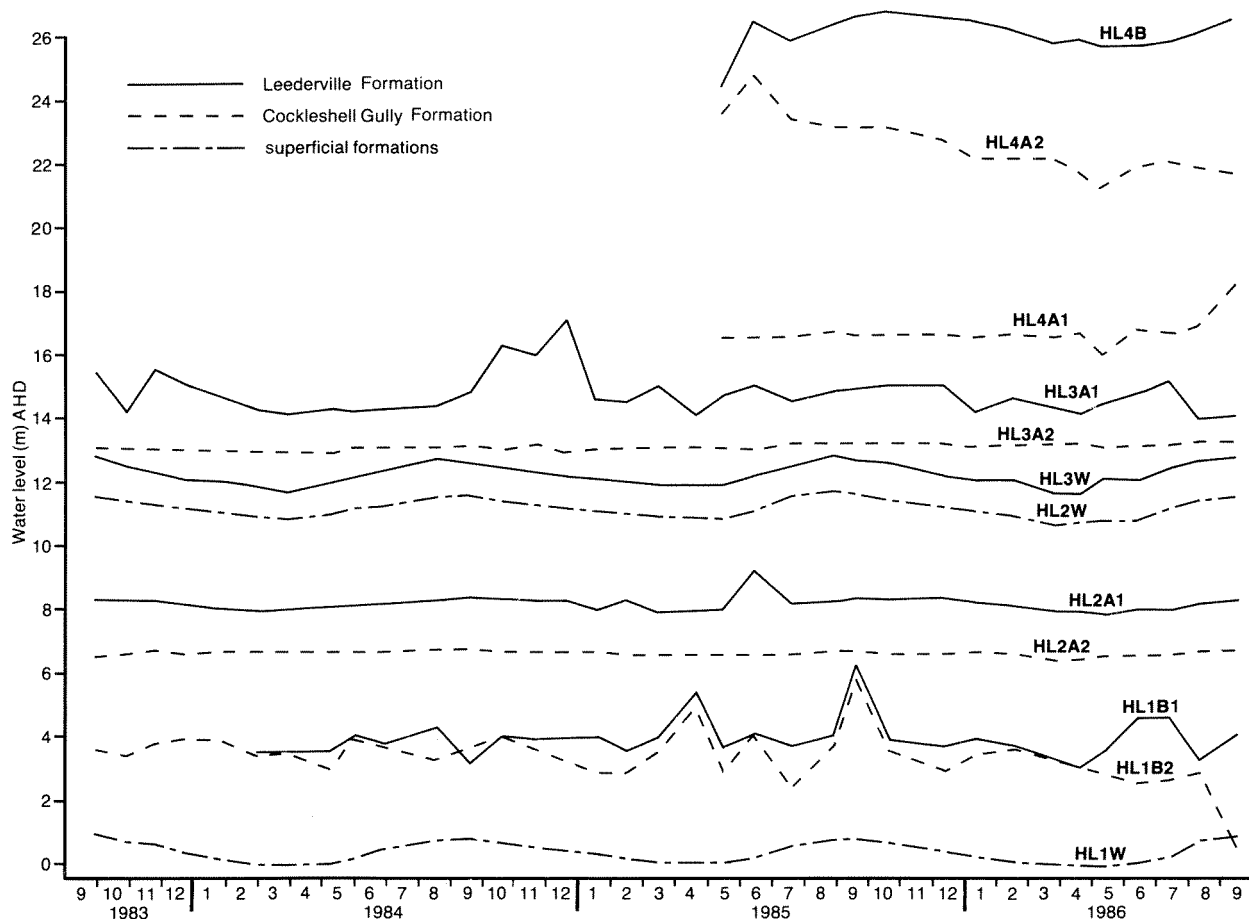

Figure 5. Hydrographs

GSWA 23691

67

gradients of up to 5.8°C per 100 m were associated with shales of low thermal conductivity. The results are shown as isotherms in Figure 2.

CONCLUSIONS

Drilling of the Harvey Line bores has provided new information on the deep aquifers of the Perth Basin near Waroona. In the eastern part of the area, the Leederville Formation and the Cockleshell Gully Formation consist predominantly of fine-grained sediments and borehole yields are likely to be low. In the west, both formations have a higher proportion of sand.

Fresh groundwater with a salinity of less than 500 mg/L TDS occurs only in the superficial formations. The upper part of the Leederville Formation contains marginal groundwater that has a salinity range of 500–1500 mg/L TDS. Groundwater in the lower part of the Leederville Formation and the upper part of the Cockleshell Gully Formation is brackish (2300–7000 mg/L TDS). Groundwater at depth in the Cockleshell Gully Formation is saline (7000–32500 mg/L TDS). There is only limited potential for further development of groundwater resources.

REFERENCES

ALLEN, A.D., 1976, Outline of the hydrogeology of the superficial formations of the Swan Coastal Plain: Western Australia Geological Survey, Annual Report 1975, p. 31–42.

BACKHOUSE, J., 1983a, Palynology of Harvey Line 1B: Western Australia Geological Survey, Palaeontology Report 12/1983 (unpublished).

BACKHOUSE, J., 1983b, Palynology of Harvey Line 2A: Western Australia Geological Survey, Palaeontological Report 15/1983 (unpublished).

BACKHOUSE, J., 1983c, Palynology of Harvey Line 3A: Western Australia Geological Survey, Palaeontological Report 19/1983 (unpublished).

COCKBAIN, A.E., and PLAYFORD, P.E., 1973, Stratigraphic nomenclature of Cretaceous rocks in the Perth Basin: Western Australia Geological Survey, Annual Report 1972, p. 26–31.

COMMANDER, D.P., 1974, Hydrogeology of the Mandurah–Pinjarra area: Western Australia Geological Survey, Annual Report 1973, p. 20–25.

COMMANDER, D.P., 1988, Geology and hydrogeology of the superficial formations and coastal lakes between Harvey and Leschenault Inlets (Lake Clifton Project): Western Australia Geological Survey, Report 23, Professional Papers.

COPE, R.N., 1972, Tectonic style in the southern Perth Basin: Western Australia Geological Survey, Annual Report 1971, p. 46–60.

DEENEY, A.C., 1989a, Hydrogeology of the Binningup borehole line, Perth Basin: Western Australia Geological Survey, Report 25, Professional Papers.

DEENEY, A.C.,1989b, Geology and groundwater resources of the superficial formations between Pinjarra and Bunbury, Perth Basin: Western Australia Geological Survey, Report 26, Professional Papers, p. 31–57.

FILATOFF, J., 1975, Jurassic palynology of the Perth Basin, Western Australia: Palaeontographica B, 154, p. 1–113.

LUSCZYNSKI, N.J., 1961, Head and flow of groundwater of variable density: Journal Geophysical Research, v. 66, no. 12, p. 4247–4256.

PLAYFORD, P.E., COCKBAIN, A.E., and LOW, G.H., 1976, Geology of the Perth Basin, Western Australia: Western Australia Geological Survey, Bulletin 124.

WILLMOTT, S.P., 1964, Revisions to the Mesozoic stratigraphy of the Perth Basin: Australia Bureau Mineral Resources Petroleum Search Subsidy Acts Publication 54, Appendix 1, p. 11–17.

YOUNG, R.J.B., and JOHANSON, J.N., 1973, Lake Preston No. 1 well completion report: Western Australian Petroleum Pty Ltd Report (unpublished).

A MAJOR THRUST IN THE KING LEOPOLD OROGEN, WEST KIMBERLEY REGION

by T. J. Griffin

ABSTRACT

A major thrust, the Inglis Fault, in the Inglis Gap–Lennard Gorge area of the King Leopold Ranges, forms the boundary between the deformed early Proterozoic Kimberley Basin succession of the Gibb River Terrane, and the adjacent Hooper Terrane, an early Proterozoic crystalline complex. This terrane boundary, previously mapped as a major unconformity, contains a chaotic mixture of chloritic schist and broken quartz veins, and dips gently to the northeast. It overlies cleaved schist and porphyritic granitoid of the Hooper Terrane, and is overlain by tightly folded, cleaved massive sandstone of the Gibb River Terrane. The latter contains thin ductile shear zones, parallel to the Inglis Fault, which have disrupted the cleavage and indicate reverse movement. The Gibb River Terrane and the Hooper Terrane were brought together during southwesterly directed convergence in the King Leopold Orogeny.

KEYWORDS: King Leopold Orogen, Gibb River Terrane, Hooper Terrane, Inglis Fault, thrust faults, listric faults, folding.

INTRODUCTION

The Kimberley region in the extreme north of Western Australia contains 200 000 km² of Proterozoic rocks. These are readily divided into two groups which occupy distinct areas (Fig. 1):

(1) the Kimberley Basin succession, which occupies the 160 000 km² of the Kimberley Plateau and its rugged margin, consists of mainly flat-lying sedimentary units; and

(2) crystalline rocks in the adjacent low-lying areas around the southwestern and southeastern margins of the Kimberley Basin succession which consist of low- to high-grade metamorphics, felsic volcanics, and granitoids.

This paper deals with the southwestern contact between the Kimberley Basin succession and the adjacent crystalline complex in the West Kimberley.

Previous work in the area refers to the contact beneath the Kimberley Basin rocks as an unconformity (Roberts and others, 1965, 1968; Gellatly and Derrick, 1967; Gellatly and others, 1968; Gellatly and Halligan, 1971; Derrick and Playford, 1973; Gellatly and Sofoulis, 1973; Gellatly and others, 1974, 1975; Plumb and others, 1985). However, recent field work indicates that the contact is faulted, and has a generally moderate to shallow dip to the northeast. The contact is a zone of reverse faulting.

The recognition that a faulted boundary, rather than an unconformity, separates the relatively stratiform Kimberley Basin succession from the contrasting geology of the crystalline rocks to the southwest (Griffin and Myers, 1988) has widespread implications. It is appropriate to consider these two regions as separate geological terranes (Jones and others, 1983, 1986). The Gibb River Terrane consists of the Kimberley Basin succession, and the Hooper Terrane consists of the crystalline rocks of the King Leopold Orogen (Fig. 1). These two terranes were brought together during the orogeny responsible for the latest deformation in the King Leopold Ranges. This tectonic belt is called the King Leopold Orogen (Fig. 2).

HOOPER TERRANE

The stratigraphy of the crystalline basement complex of the Hooper Terrane in the King Leopold Orogen is correlated with the better exposed Lamboo Complex in the east Kimberley in Figure 3.

METASEDIMENTARY ROCKS

The oldest of the Hooper Terrane rocks are sandstone, shale, siltstone, and minor amounts of acid volcanics, that have been tightly folded and metamorphosed at greenschist to upper amphibolite grades (Gellatly and others, 1968, 1974). Quartzite and calcareous rocks are rare. The base of the sequence is not exposed; the top is overlain by a sequence of acid volcanics (Gellatly and others, 1974, 1975).

The lowest unit comprises quartz wacke, quartz–feldspar wacke, and quartz–muscovite–biotite (–andalusite) phyllite. This is overlain by interbedded quartz–muscovite–biotite schist and phyllite, and has dacitic tuff interbeds at the base. The upper part includes dacitic and rhyolitic crystal-lithic tuff and ignimbrite, and minor amounts of andesite and subvolcanic intrusives. Thin beds of conglomerate and volcaniclastic sandstone occur locally (Plumb and others, 1985).
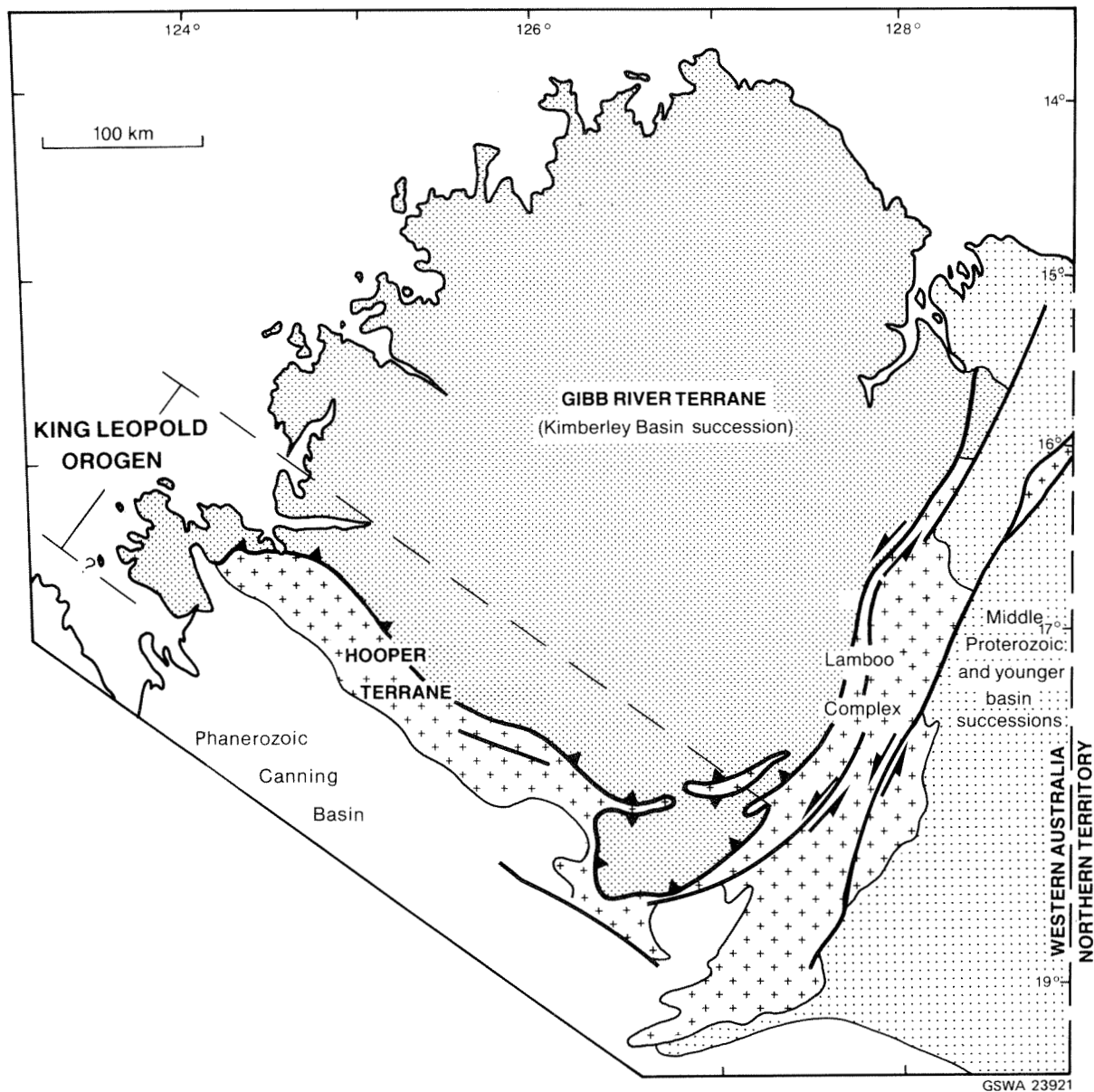
Figure 1. Major elements of the early Proterozoic geology of the Kimberley region, Western Australia.

These rocks have been correlated with the Halls Creek Group in the East Kimberley, and, in particular, with the Olympio Formation at the top of the Halls Creek Group (Fig. 3) (Gellatly and others, 1968, 1974, 1975; Hancock and Rutland, 1984; Plumb and others, 1985). A small area of high-grade metamorphics in the centre of the complex (Gellatly and others, 1974) includes quartz–sillimanite–feldspar–biotite gneiss, and cordierite–quartz–biotite–garnet gneiss. These rocks could be correlatives of the Tickalara Metamorphics of the Lamboo Complex in the East Kimberley.

EARLY INTRUSIVE ROCKS

Amphibolitized dolerite and gabbro sills are widespread (Fig. 2). They are usually porphyritic and include minor amounts of ultramafic rocks. The largest
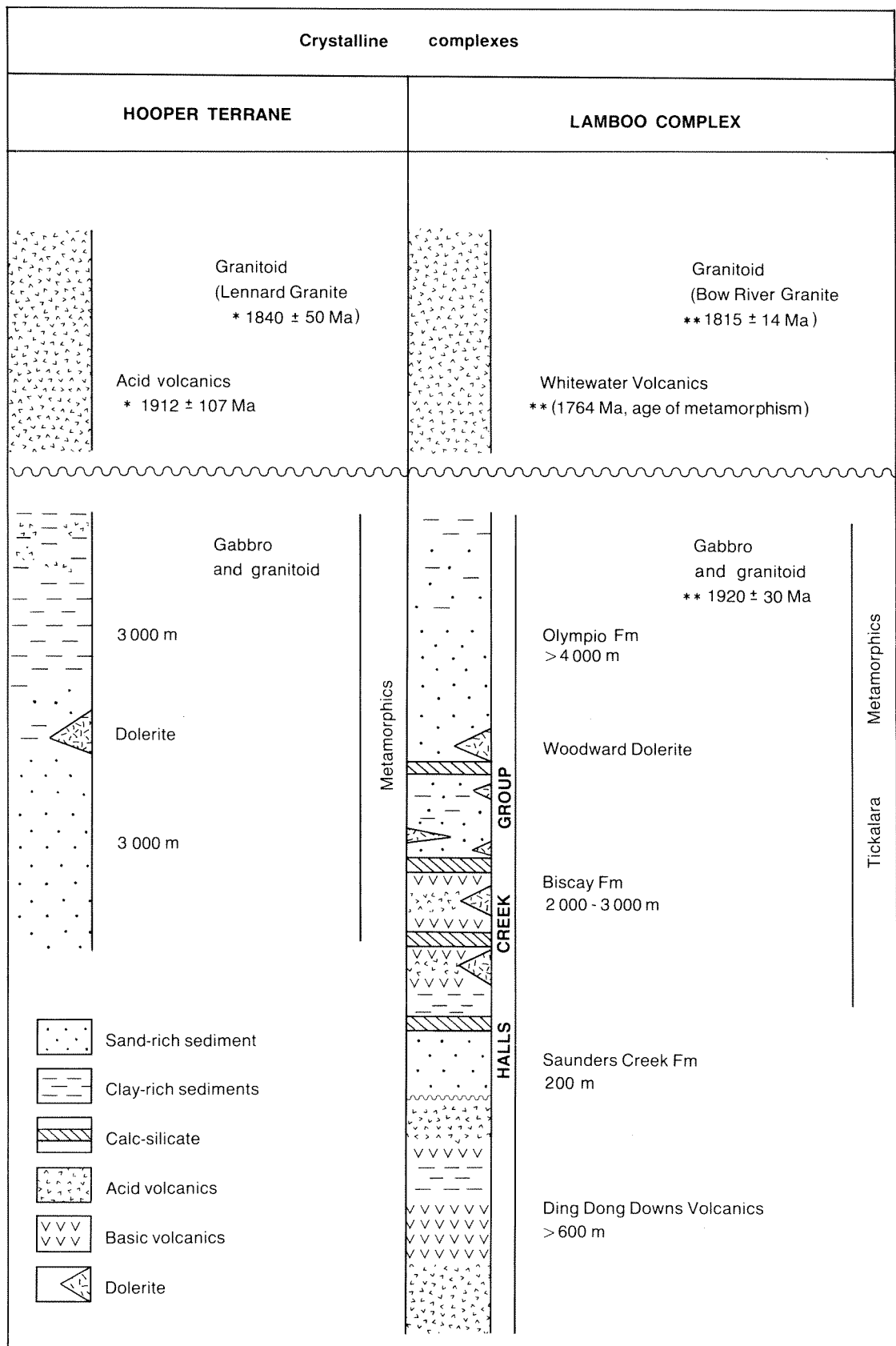
sill complex is in the central part of the terrane. It consists of seven folded sills that have an average thickness of 250 m and are separated by 30–90 m thick units of sedimentary rock (Gellatly and others, 1974). Contacts are generally sharp and concordant with the bedding in the metasedimentary rock sequences.

The Wombarella Quartz Gabbro is a lopolith of layered orthopyroxene- and biotite-bearing quartz gabbro, and porphyritic tonalite, that outcrops as an elliptical body (5 km long) in the west-central part of the terrane. Deformation and metamorphism on the margins has produced minor amounts of gneissic material that was derived from these rocks (Gellatly and others, 1968, 1974). The Kongorow Granite is a widespread complex of porphyritic granite together with minor amounts of gneiss and migmatite, which
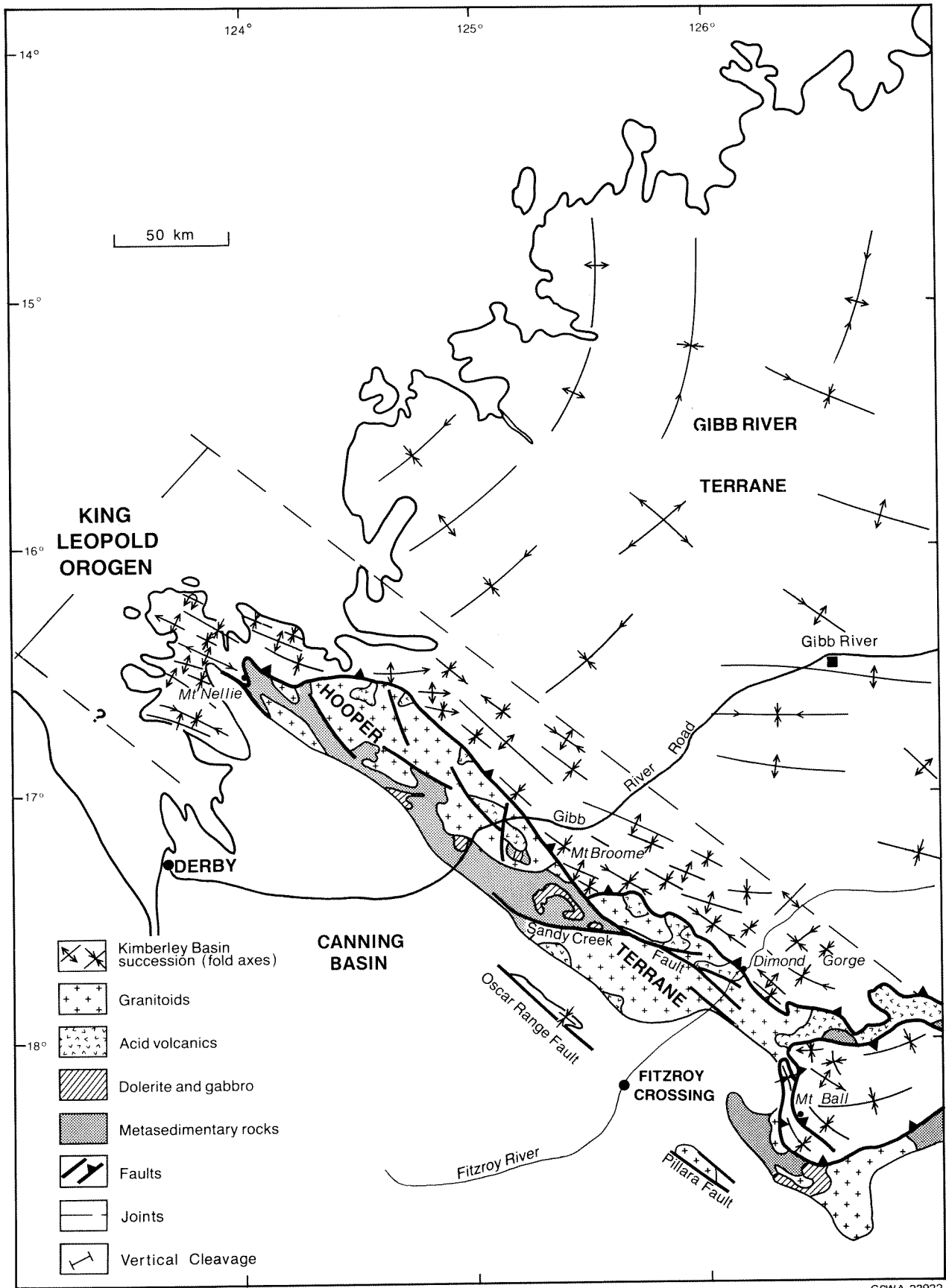
Figure 2. Geological map of the West Kimberley showing the broad distribution of rock types in the exposed Hooper Terrane, and the orientation and intensity of folding in the Gibb River Terrane.

71

Crystalline complexes	
HOOPER TERRANE	LAMBOO COMPLEX

HOOPER TERRANE

Granitoid
(Lennard Granite
* 1840 ± 50 Ma)

Acid volcanics
* 1912 ± 107 Ma

Gabbro
and granitoid

3 000 m

Dolerite

3 000 m

Metamorphics

LAMBOO COMPLEX

Granitoid
(Bow River Granite
** 1815 ± 14 Ma)

Whitewater Volcanics
** (1764 Ma, age of metamorphism)

Gabbro
and granitoid
** 1920 ± 30 Ma

Olympio Fm
> 4 000 m

Woodward Dolerite

Biscay Fm
2 000 - 3 000 m

Saunders Creek Fm
200 m

Ding Dong Downs Volcanics
> 600 m

Metamorphics

HALLS CREEK GROUP

Tickalara

Legend:
- Sand-rich sediment
- Clay-rich sediments
- Calc-silicate
- Acid volcanics
- Basic volcanics
- Dolerite

* (Rb-Sr) Page (1976; after Bennet and Gellatly, 1970)
** (Rb-Sr) Page (1976; after Bofinger, 1967)

GSWA 23923

Figure 3. Summary of the stratigraphy of the Kimberley crystalline complexes (after Dow and Gemuts, 1969; Gellatly and others, 1974; Plumb and others, 1985).

intruded the metamorphics and the Wombarella Quartz Gabbro (Gellatly and others, 1968, 1974; Gellatly and Halligan, 1971; Derrick and Playford, 1973; Gellatly and Sofoulis, 1973).

Other minor phases of granitoid have been assumed to represent early intrusion into the metamorphics (Gellatly and others, 1968, 1974).

ACID VOLCANIC ROCKS

The acid volcanics consist mainly of rhyodacitic tuff, agglomerate, and minor amounts of lava and tuffaceous sediment. They form steeply dipping sheets in narrow belts adjacent to granitoid. Broken quartz, plagioclase, and potash-feldspar crystals are abundant. These rocks give a Rb–Sr isochron age of about 1910 Ma (Page, 1976).

Four units are recognized: a basal well-bedded sequence of rhyodacitic tuff and tuffaceous sedimentary rocks; a biotite-rich ash-flow tuff; a crystal-poor ash-flow tuff; and an upper crystal-rich tuff that has more than 50% crystal fragments, and minor amounts of agglomerate. The relationship with the underlying metasedimentary and metamorphic rocks is uncertain. A conglomerate in the north-central part of the complex contains dolerite pebbles, presumably derived from the underlying sequence (Gellatly and others, 1968, 1974), which suggests that the basal contact is probably an unconformity. The acid volcanics have been correlated with the Whitewater Volcanics in the Lamboo Complex (Fig. 3) (Gellatly and others, 1968, 1974) where they rest unconformably on Olympio Formation at the top of the Halls Creek Group, but never on lower horizons (Dow and Gemuts, 1969; Derrick and Playford, 1973).

LATE INTRUSIVE ROCKS

Sixteen different granitoid units have been identified which intrude the acid volcanics and earlier granitoids and metamorphics. The late granitoids dominate the Hooper Terrane and include large porphyry bodies (such as Mount Disaster Porphyry), and porphyritic and non-porphyritic phases that have a wide range in grain size. Tonalite, granodiorite, monzogranite, and syenogranite are abundant; quartz gabbro is present as small bodies. These rocks are dated at about 1840 Ma (Rb–Sr isochron; Page, 1976). Pegmatite and aplite occur as a minor phase in some intrusive bodies.

Dolerite dykes are widespread and are particularly abundant in McSherrys Granodiorite, the Lennard Granite, and metamorphics in the centre of the terrane. The dykes are largely unaltered, less than 500 m apart, and range from 1 to 7 m wide. They are generally less than 3 km long. The younger dykes contain fine, even-grained, very dark dolerite that is quarried as 'black granite' ornamential stone.

STRUCTURE

The Hooper Terrane is dominated by several lineaments, parallel to the long axis of the terrane, which presumably represent major faults — although the displacement on these has not been determined. The rocks are characterized on air-photos by abundant prominent joints that fall broadly into steeply dipping northerly and north-northwesterly trending sets. At outcrop scale, all rock types contain strongly foliated zones that are either vertical or dip steeply to the southwest. Mylonite is present in many of the more intensely deformed zones, which are generally 5–20 cm wide. The lineations in the mylonite are always steep. Aligned and rotated phenocrysts, quartz rodding, and biotite streaking define the lineation. Biotite and chlorite form ragged lenticular aggregates that outline the foliation in both intrusive and extrusive acid igneous rocks. The metasedimentary rocks contain small-scale, tight-to-isoclinal folds of varied orientation which indicate that deformation of these rocks occurred prior to intrusion of the late granitoids (Gellatly and others, 1974)

GIBB RIVER TERRANE

STRATIGRAPHY

Basement to the Kimberley Basin is unknown in the King Leopold Orogen. The early Proterozoic Kimberley Basin succession consists of the Speewah Group and the overlying Kimberley Group (Fig. 4). The less extensive Bastion Group overlies the Kimberley Group in the northeast, and the Crowhurst Group (<1 km thick) overlies the Kimberley Group in the southeast.

The Speewah and Kimberley Groups are well exposed in the King Leopold Orogen. The Speewah Group is up to 1.7 km thick and the Kimberley Group is up to 4 km (Plumb and Gemuts, 1976; Plumb and others, 1981, 1985). In addition, up to 1 km of Hart Dolerite forms sills at several stratigraphic levels in both the Speewah and Kimberley Groups.

A feature of the basin is its uniform stratigraphy, both in thickness of units and lithology (Plumb and Gemuts, 1976; Plumb and others, 1981, 1985). They suggested that the extent of the sedimentary basin may not have been appreciably greater than the presently preserved structural basin. However, where the Kimberley Basin succession crossed over the crystalline basement, in the northwest at Mount Nellie and the southeast at Mount Ball, the Speewah Group is very thin, whereas the Kimberley Group transgresses these areas with little change (Plumb and Gemuts, 1976).

The Speewah Group is exposed only on the upturned southeastern and southwestern margins; its extent beneath the central part of the basin is unknown. This group is interpreted as a broad transgressive–regressive event: fluvial sands (lower O'Donnell Formation) grade to alternating or interfingering fluvial and shallow-marine sands and silts (upper O'Donnell Formation), then to deep-water silts (Luman Siltstone). Fluvial sands reappear at the base of the Kimberley Group (Plumb and Gemuts, 1976; Plumb and others, 1981, 1985).

The Kimberley Group is dominated by mature and laterally uniform formations that consist of quartz sandstone, tholeiitic basalt, and red and green siltstone.

The Kimberley Group is thought by Plumb and Gemuts (1976) and Plumb and others (1981, 1985) to have been deposited in a broad semi-enclosed shallow-marine basin. Sediment dispersal was by strong unidirectional longshore currents that flowed towards the south-southeast.

The Hart Dolerite extends throughout the 160 000 km^2 of the Kimberley Basin succession. It is dated at about 1762 ± 15 Ma (Rb–Sr isochron; Page and others, 1984), and has a composite thickness of up to 1 km that is exposed over several sills. The rocks show typical tholeiitic compositions and differentiation trends. Granophyre, up to 250 m thick, is at the top in the thickest sills (Plumb and Gemuts, 1976; Plumb and others, 1985).

STRUCTURE

The central part of the Gibb River Terrane is only mildly deformed, and forms broad dome-and-basin interference patterns. Deformation intensifies markedly to the southwest, near the limit of the basin succession (Fig. 2). This zone of folding and faulting on the southwest margin of the Gibb River Terrane is part of the King Leopold Orogen. It is characterized by northwest-trending faults and tight folds that have steep axial planes.

A strong, generally vertical cleavage can be recognized low in the sequence, in particular in the coarse sandstone. This cleavage is axial planar to the open-to-tight folds which are well exposed at Lennard River Gorge (Fig. 5). At the southern end of Dimond Gorge

|		UNIT	ROCK TYPES	REMARKS
	700 m	Pentecost Sandstone	Quartz and feldspathic sandstone, ferruginous siltstone and sandstone, glauconitic sandstone	Cross-bedded clay pellets
	150 m	Elgee Siltstone	Massive red siltstone, sandstone, green shale	Mud cracks, shale pellets
	200 m	Warton Sandstone	Quartz and feldspathic sandstone, minor shale	Cross-bedded, ripple marks, clay pellets
	700 m	Carson Volcanics	Tholeiitic basalt, feldspathic sandstone, siltstone, chert	
	1200 m	King Leopold Sandstone	Quartz sandstone, granule sandstone, conglomerate, micaceous siltstone	Cross-bedded, moderately well sorted
	50 m	Luman Siltstone	Micaceous siltstone, shale, minor sandstone	Mud cracks, ripple marks, cross-beds
	400 m	Lansdowne Arkose	Feldspathic and quartz sandstone, arkose, micaceous siltstone	Cross-bedded, ripple marks, clay pellets. Intruded extensively by Hart Dolerite
	50 m	Valentine Siltstone	Chloritic laminated siltstone	Tuff and rhyolite to east
	200 m	Tunganary Formation	Feldspathic and quartz sandstone, arkose, siltstone and phyllite	Cross-bedded ripple marks. Intruded extensively by Hart Dolerite
	520 m	O'Donnell Formation	Coarse quartz sandstone, quartz granule sandstone, minor phyllite and siltstone, fine arkose, and pebble conglomerate	Cross-bedded granule sandstone

GSWA 23924

Figure 4. Summary of the stratigraphy of the Kimberley Basin succession from the Mount Broome area (see Fig. 2) (from Plumb and Gemuts, 1976; Plumb and others, 1981, 1985).
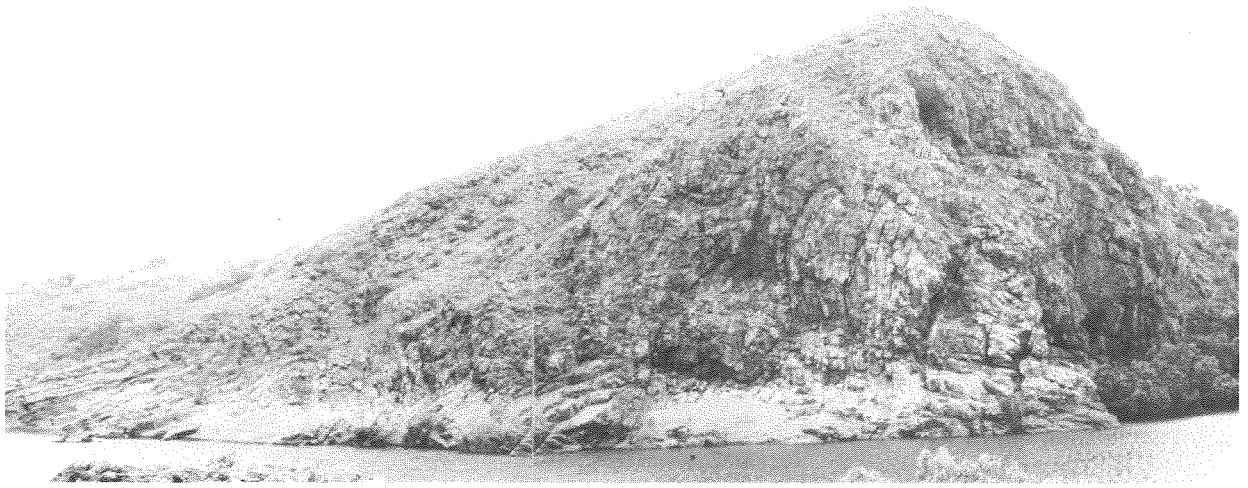
Figure 5. A tight fold of bedded sandstone from the Kimberley Basin succession on the southwest margin of the Gibb River Terrane, east bank of the Lennard River Gorge.
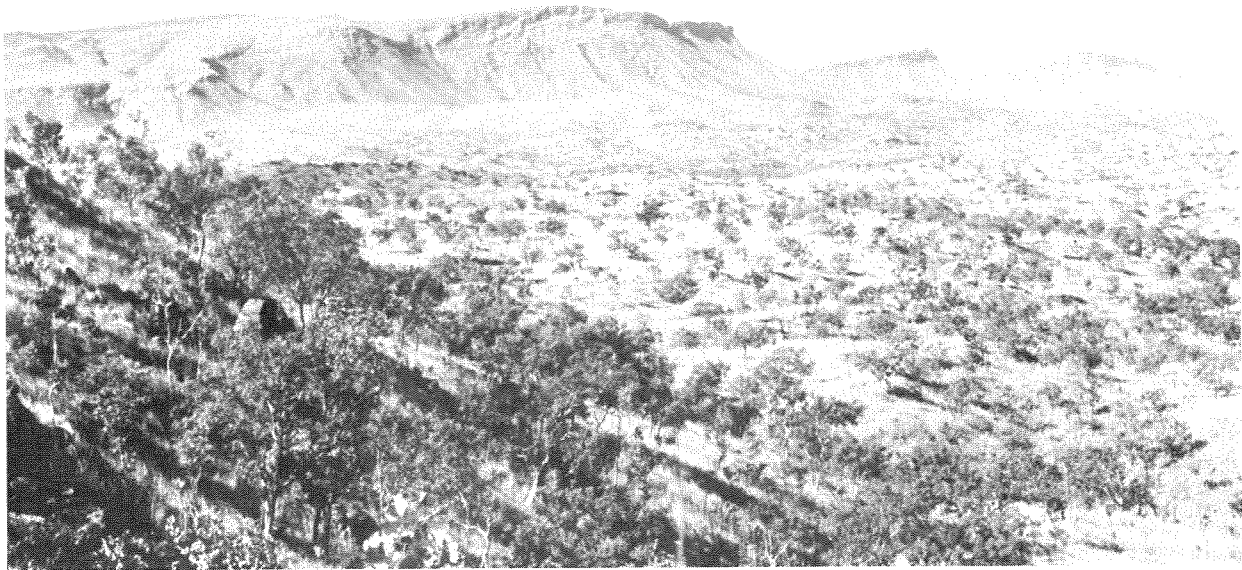
Figure 6. The sandstone scarp of the Gibb River Terrane above the low-lying country of the Hooper Terrane; looking southeast from Inglis Gap.

GSWA 23927

Figure 7. Faults and tight folds in a sandstone sequence of the Gibb River Terrane adjacent to the Hooper Terrane, on the east bank of the Fitzroy River, south Dimond Gorge.

these tight folds are associated with overturned folds and steep faults, some of which are reverse faults (Fig. 7).

The faulted contact between the Gibb River Terrane and Hooper Terrane has formed a prominent scarp along the southwestern margin of the Gibb River Terrane (Fig. 6).

At Inglis Gap, low-angle reverse faults dip to the northeast, and disrupt the steep cleavage. The rock at Inglis Gap is a coarse, cross-bedded sandstone and pebble sandstone. Faulting within the sandstone at Inglis Gap has produced thin, ductile shear zones, some of which contain broken and boudinized quartz (Fig. 8). The lineation in these zones plunge 35° towards 055°. Further to the northeast these low-angle reverse faults disrupt and repeat the stratigraphy (Fig. 9).

Steep north-trending faults that cut the southwest margin of the Gibb River Terrane appear to have resulted from intermittent reactivation of old faults in the Hooper Terrane.

THE TERRANE BOUNDARY

The boundary between the generally sedimentary successions of the Gibb River Terrane and the crystalline rocks of the Hooper Terrane is a zone of intense shearing, and is interpreted as a major thrust fault, the Inglis Fault (Griffin and Myers, 1988). This fault has been observed at two localities. At Inglis Gap (on the Gibb River road) it is very poorly exposed in a roadside gutter as a highly kaolinized shear zone (10–20 cm wide) that has a shallow dip to the northeast. Cleaved quartz sandstone outcrops above the zone, and a strongly schistose pink and white spotted clayey rock below. This clayey rock was derived from porphyritic granitoid which is widespread in the Hooper Terrane. The almost vertical cleavage in the altered granitoid has been dragged to the southwest and indicates thrusting of the Gibb River Terrane over the Hooper Terrane.

This fault motion is consistent with the sense of movement that is indicated by the refracted cleavage in the small ductile shear zones within the sandstone (Fig. 8).

A better exposure is at the southern end of the Lennard Gorge. Here the Inglis Fault is a horizontal shear zone (0.5–1.0 m wide) that consists of a chaotic mixture of quartz–chlorite–biotite schist and broken quartz veins (Fig. 10). Jointed massive quartz sandstone with a vertical cleavage, trending 340°, lies above the tectonic zone. This sandstone is part of the tightly folded sequence seen in Figure 5. Chlorite–biotite schist (cleavage dipping 80° to 025°) is exposed beneath the fault and is part of the metasedimentary sequence of the Hooper Terrane. On the east bank, the Inglis Fault is curved and has an apparent shallow to moderate dip to the northeast. A listric fault system associated with the Inglis Fault accounts for both small-scale and large-scale structures observed along the southwestern margin of the Gibb River Terrane. Structures related to this thrusting event may also exist in the Hooper Terrane.

AGE OF DEFORMATION IN THE KING LEOPOLD OROGEN

The King Leopold Orogen includes the fold belt on the southwestern margin of the Gibb River Terrane, the thrusted contact between the Gibb River and Hooper Terranes, and the crystalline complex of the Hooper Terrane. Initial deformation post-dated deposition and mafic igneous activity of the early Proterozoic Kimberley Basin succession, but pre-dated late Proterozoic glacial successions that unconformably overlie the early Kimberley Basin succession. Subsequent deformation, with a very similar style, post-dated these glacials (Plumb and Gemuts, 1976; Plumb and others, 1981; Coats and Preiss, 1980; Griffin, in press).

76
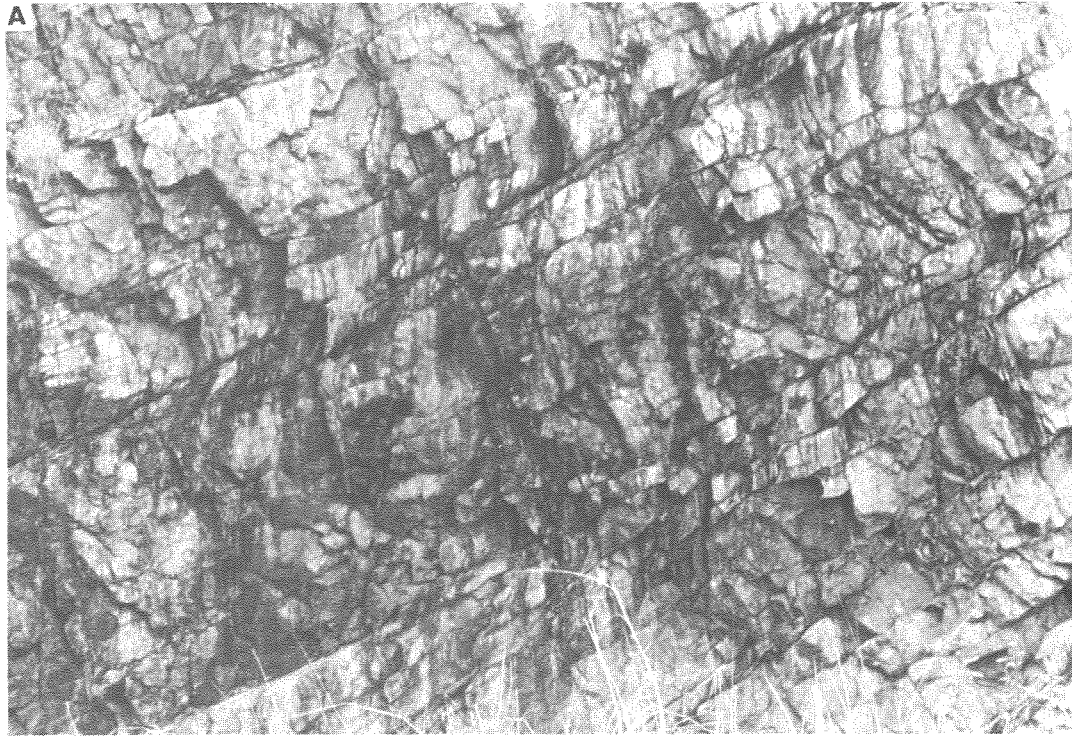
GSWA 23928

Figure 8. Reverse faults in massive sandstone and pebble sandstone of the Gibb River Terrane, less than 10 m above the faulted contact with the Hooper Terrane; road cutting at Inglis Gap. A — The prominent cleavage in the sandstone has been refracted in small shear zones which indicates reverse dextral movement. The rock face is 3 m high. B — Close-up of a shear zone (ball point pen is 15 cm long).
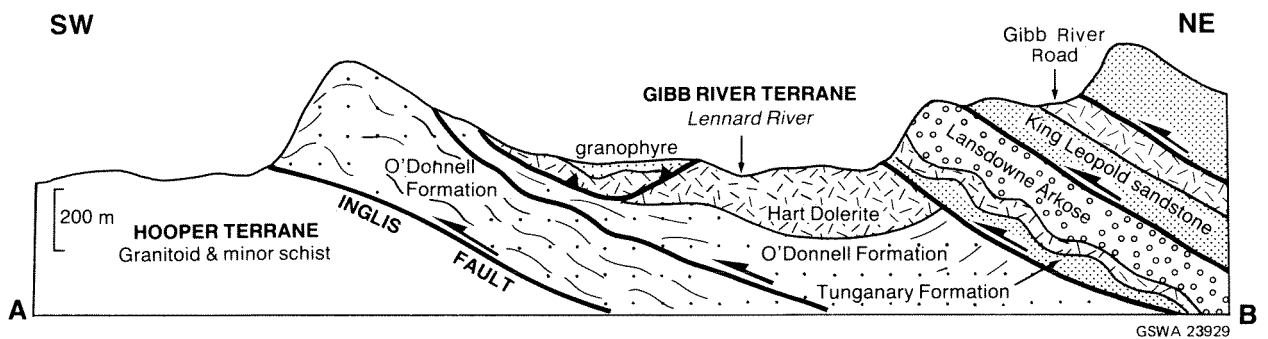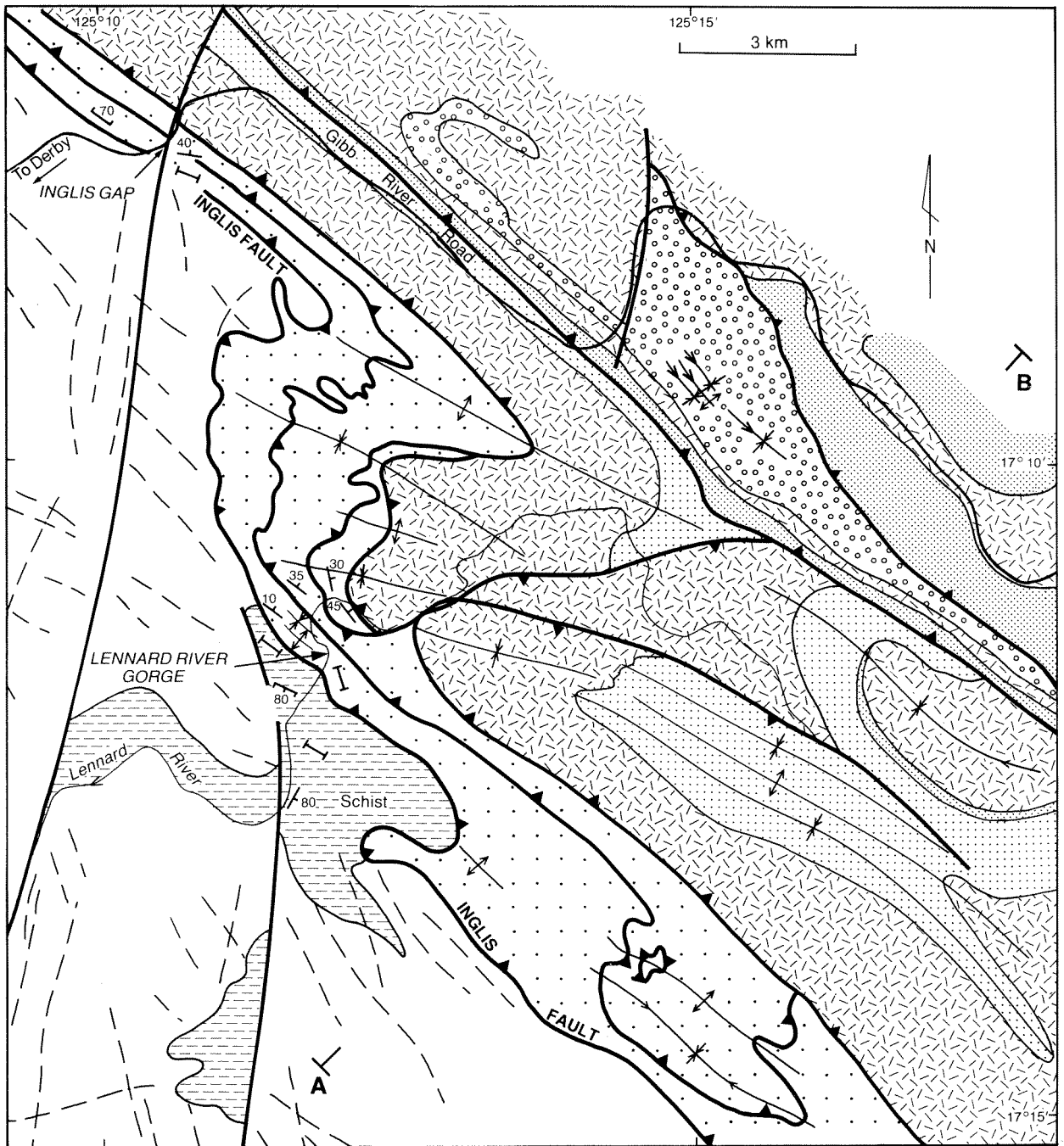
77

Figure 9. Geology of the southwestern margin of the Gibb River Terrane, Inglis Gap–Lennard River Gorge area.

78

Figure 10. The Inglis Fault thrust zone between the Gibb River Terrane and the Hooper Terrane in Lennard River Gorge, west bank. Jointed massive sandstone outcrops above chaotic quartz–chlorite–biotite schist and broken quartz veins within the zone.

CONCLUSION

The fold belt on the southwest margin of the Gibb River Terrane includes zones of tight folding and reverse faulting (Fig. 10). These rocks were moved from the northeast and thrust over the crystalline complex of the Hooper Terrane. The deformation becomes more intense in the Gibb River Terrane towards the crystalline complex (Fig. 2). Further work is required to determine whether the Gibb River Terrane is native or exotic.
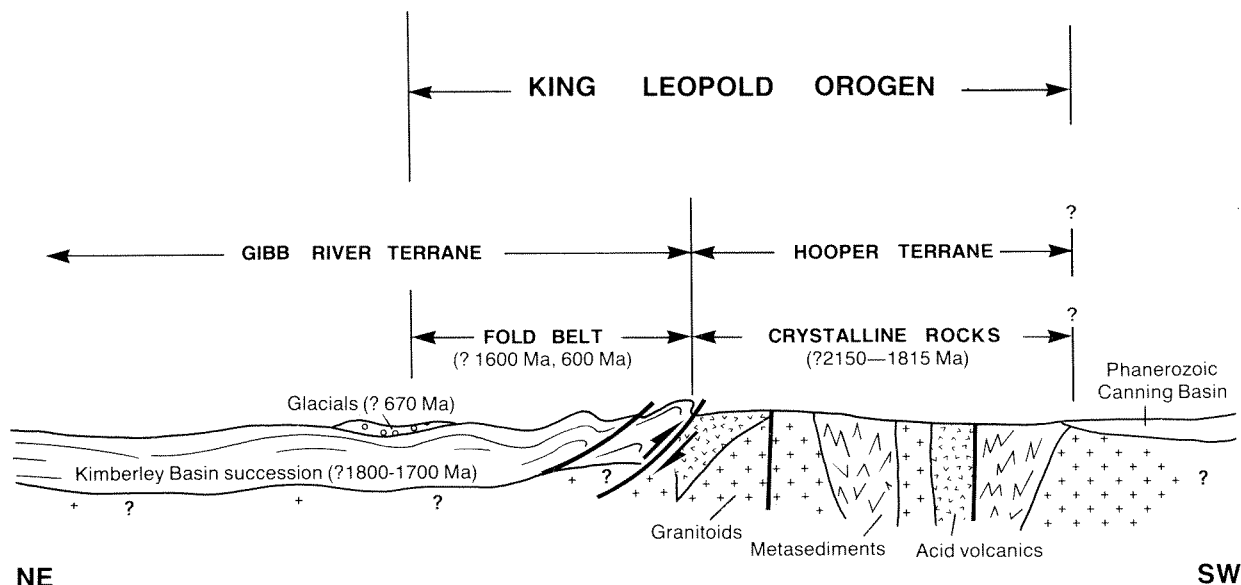
Although the regional rock relationships are broadly consistent with an unconformity, no detailed description of that unconformity has been given by previous workers (Roberts and others 1965, 1968; Gellatly and others, 1968, 1973, 1974, 1975; Gellatly and Halligan, 1971; Gellatly and Sofoulis, 1973; Derrick and Playford, 1973; Plumb and others, 1985). The recognition that the boundary is faulted explains the absence of that description. Movement on the Inglis Fault explains why parts of the succession are locally absent, such as in the southeast where the Carson Volcanics rest directly on crystalline basement in an area where the underlying King Leopold Sandstone is consistently thick (Roberts and others, 1968). In the same region, curved faults which are shown on the Lennard River 1:250 000 geological sheet (Derrick and Playford, 1973) may

more logically be interpreted as low angle reverse faults (Fig. 2), and part of a listric fault system that repeats the stratigraphy on a major terrane boundary thrust.

The boundary between the Gibb River Terrane and the Hooper Terrane varies from straight to scalloped (Fig. 2). The scalloped sections are likely to be in areas where the decollement has a shallow to flat orientation, whereas the straight sections are probably dominated by a steep decollement zone.

In the East Kimberley, the effect of the tectonism that formed the King Leopold Orogen was probably largely reflected in sinistral strike-slip movements in the crystalline complex. Major strike-slip faults with sinistral movement in the Proterozoic are prominent in the east Kimberley (Fig. 1) and subsequent intermittent movements are recorded in Palaeozoic and younger rocks (Dow and Gemuts, 1969; Plumb and Gemuts, 1976; Plumb and others, 1981).

Although detailed observations are restricted to a relatively small section of the contact between the Gibb River Terrane and the Hooper Terrane, the conclusions appear to apply to, and are compatible with previous reports of, the geology along the whole length of the contact. The boundary is interpreted as a major thrust fault, the Inglis Fault, along which the Gibb River Terrane was thrust onto the Hooper Terrane within the King Leopold Orogen (Fig. 11).

Figure 11. Diagrammatic cross section illustrating the structural relations of the major components of the King Leopold Orogen.

REFERENCES

BENNETT, R., and GELLATLY, D. C., 1970, Rb–Sr age determinations of some rocks from the West Kimberley Region: Australia BMR, Record 1970/20 (unpublished).

BOFINGER, V. M., 1967, Geochronology of the East Kimberley area of Western Australia: Australian National University, Ph.D. thesis.

COATS, R. P., and PREISS, W. V., 1980, Stratigraphic and geochronological reinterpretation of the late Proterozoic glaciogenic sequences in the Kimberley region, Western Australia: Precambrian Research, v. 13, p. 181–208.

DERRICK, G. M., and PLAYFORD, P. E., 1973, Lennard River, W.A.: Western Australia Geological Survey, 1:250 000 Geological Series Explanatory Notes.

DOW, D. B., and GEMUTS, I., 1969, Geology of the Kimberley region, Western Australia — The East Kimberley: Western Australia Geological Survey, Bulletin 120.

GELLATLY, D. C., and DERRICK, G. M., 1967, Lansdowne, W.A.: Western Australia Geological Survey, 1:250 000 Geological Series Explanatory Notes.

GELLATLY, D. C., DERRICK, G. M., and PLUMB, K. A., 1975, The geology of the Lansdowne sheet area, Western Australia: Australia BMR, Report 152.

GELLATLY, D. C., and HALLIGAN, R., 1971, Charnley, W.A.: Western Australia Geological Survey, 1:250 000 Geological Series Explanatory Notes.

GELLATLY, D. C., and SOFOULIS, J., 1973, Yampi, W.A.: Western Australia Geological Survey, 1:250 000 Geological Series Explanatory Notes.

GELLATLY, D. C., SOFOULIS, J., DERRICK, G. M., and MORGAN, C. M., 1968, The older Precambrian geology of the Lennard River sheet area, Western Australia: Australia BMR, Record 1968/126 (unpublished).

GELLATLY, D.C., SOFOULIS, J., DERRICK, G.M., and MORGAN, C. M., 1974, The older Precambrian geology of the Lennard River sheet area, Western Australia: Australia BMR, Report 153.

GRAY, G.G., 1986, Native terranes of the Central Klamath Mountains, California: Tectonics, v. 5, p. 1043–1054.

GRIFFIN, T.J., in press, King Leopold and Halls Creek Orogens, in Geology and mineral resources of Western Australia: Western Australia Geological Survey, Memoir 3.

GRIFFIN, T. J., and MYERS, J. S., 1988, Geological Note — A Proterozoic terrane boundary in the King Leopold Orogen, Western Australia: Australian Journal of Earth Sciences, v. 35, p. 131–132.

HANCOCK, S. L., and RUTLAND, R. W. R., 1984, Tectonics of the early Proterozoic geosuture — The Halls Creek Orogenic Sub-province, northern Australia: Journal of Geodynamics, v. 1, p. 387–432.

JONES, D.L., HOWELL, D.G., CONEY, P.J., and MONGER, J.W.H., 1983, Recognition, character and analysis of tectonostratigraphic terranes in western North America, in Accretionary tectonics in the circum-Pacific regions edited by M. HASHIMOTO and S. UYEDA: Tokyo, Terra Science Publishing Co., p. 21–35.

JONES, D. L., SILBERLING, N. J., and CONEY, P. J., 1986, Collision tectonics in the Cordillera of western North America — examples from Alaska, in Collision Tectonics edited by M. P. COWARD and A. C. RIES: Geological Society of America, Special Publication 19, p. 367–387.

PAGE, R. W., 1976, Reinterpretation of isotopic ages from the Halls Creek Mobile Zone, northwestern Australia: Australia BMR, Journal of Australian Geology and Geophysics, v. 1, p. 79–81.

PAGE, R. W., McCULLOCH, M.T., and BLACK, L. P., 1984, Isotopic record of major Precambrian events in Australia: International Geological Congress, 27th, Moscow, 1984, Proceedings v. 5, p. 25–72.

PLUMB, K.A., ALLEN, R., and HANCOCK, S.L., 1985, Excursion guide — Proterozoic evolution of the Halls Creek Province, Western Australia: Conference on tectonics and geochemistry of early to middle Proterozoic fold belts, Darwin, N.T., 1985, Excursion Guide, Australia BMR, Record 1985/25 (unpublished).

PLUMB, K. A., DERRICK, G. M., NEEDHAM, R. S., and SHAW, R. D., 1981, The Proterozoic of northern Australia, *in* Precambrian of the southern hemisphere *edited by* D.R. HUNTER: Amsterdam, Elsevier, Developments in Precambrian Geology 2, p. 202–307.

PLUMB, K. A., and GEMUTS, I., 1976, Precambrian geology of the Kimberley region, Western Australia: International Geological Congress, 25th, Sydney, N.S.W., 1976, Excursion Guide no. 44C.

ROBERTS, H. G., HALLIGAN, R., and GEMUTS, I., 1965, The geology of the Mount Ramsey 1:250 000 sheet area SE/52-9, Western Australia: Australia BMR, Record 1965/156 (unpublished).

ROBERTS, H.G., HALLIGAN, R., and PLAYFORD, P.E., 1968, Mount Ramsay, W.A.: Western Australia Geological Survey, 1:250 000 Geological Series Explanatory Notes.

THE CHEMISTRY OF PLUTONIC FELSIC ALKALINE ROCKS IN THE EASTERN GOLDFIELDS PROVINCE

by W. G. Libby

ABSTRACT

More than thirty small, mildly alkaline, Archaean, felsic, plutonic bodies are sparsely scattered in a north–south belt, 800 km long by 100 km wide, through the Eastern Goldfields Province of Western Australia. The suite is heterogeneous but in its characteristic development it is low in quartz, which ranges between 0% and 20%, and contains strongly coloured green clinopyroxene. Microprobe analyses of moderately to strongly coloured varieties identified the two dominant pyroxenes as aegirine-augite and sodian ferro-salite to ferro-augite; paler varieties which were not analysed may be more diopsidic. The aegirine-augite at some localities is accompanied by riebeckitic to richteritic amphibole. Whole-rock samples have an alkalinity index which is high but rarely exceeds 1.0. The rocks are low in normative quartz and in some places contain normative aegirine; they are richer in total alkalis than are samples of associated subalkaline granite. Trace elements show a low degree of magmatic evolution, without notable enrichment in rare-earth or other incompatible elements. Light rare-earth elements are moderately enriched relative to chondrite, but the Eu anomaly is slight to non-existent.

Enrichment in alkalis relative to Si, Al, and Ca, coupled with low initial Sr isotopic ratio, small Eu anomalies, LREE enrichment, and a primitive chemical signature, is compatible with derivation from an alkali-enriched mafic rock in the lower crust or mantle, with little upper-crustal development, perhaps leaving residual garnet.

KEYWORDS: Eastern Goldfields; chemistry; plutonic rocks; alkali igneous rocks

INTRODUCTION

Alkaline igneous rocks are not only of interest for their unusual and diverse rock types, but also as both hosts and sources of mineral deposits. Further, they may be used in interpreting the geological conditions under which economic deposits may be formed. Within the Eastern Goldfields Province, the Mount Weld carbonatite provides a regolith of ore-grade apatite (Willett, Duncan, and Rankin, 1986) and in the Kimberley Province, alkaline (lamproitic) intrusions host commercial diamond mineralization (Jaques, Lewis, and Smith, 1986). It has been established that there is a preferential association of base-metal (especially copper) and precious metal (especially gold) deposits with alkaline rocks in North America in rocks ranging in age from Precambrian to Tertiary (Mutschler and others, 1985). The late Archaean mildly alkaline rocks of the Eastern Goldfields, which are the subject of this paper, however, have not yet been shown to be productive.

Felsic alkaline rocks were recognized in the Eastern Goldfields of Western Australia as early as 1915 by Jutson, but were first studied as a group by Libby (1978), and Lewis and Gower (1978). They have been reviewed recently by Jaques and others (1985). Earlier comprehensive studies were limited to the southern two-thirds of the belt of occurrence and emphasized petrographical aspects of the rocks, whereas the present study considers the entire belt and considers their chemical composition. The alkaline rocks are found to be relatively primitive, in terms of chemical evolution within the crust. They bear a special relationship with certain evolved subalkaline rocks associated with the adamellites of Mount Boreas, and with a suite of amphibole-bearing granites, but a complete understanding of the alkaline rocks requires more detailed field mapping.

Samples for analysis were collected by the GSWA in the course of regional mapping of the Eastern Goldfields, and by the author during 1979. D. F. Blight contributed samples from Gilgarna Rock on KURNALPI*. All new chemical analyses were performed by the Government Chemical Laboratories, Perth.

GEOLOGICAL SUMMARY

The Eastern Goldfields Province is a granite–greenstone terrane with a marked north-northwest grain defined by elongation of greenstone belts and zones of shearing. There is a range of granitic rock masses, from large to small. The larger masses (the external granites of Sofoulis, 1963) are in part gneissic, while the smaller, ovoid bodies (the internal granites) in part have gneissic margins. The general geology of a substantial part of the province was studied in detail recently by Hallberg (1985).

The Archaean felsic alkaline rocks in the eastern part of the Yilgarn Craton form scattered small bodies. They are restricted to the Eastern Goldfields Province and distributed from the Fitzgerald Peaks on LAKE JOHNSTON in the south, to the Teague Ring Structure at

---

*Names of 1:250 000 geological sheets are printed in capitals to distinguish them from similar place names.

Lake Teague on NABBERU 800 km to the north (Fig. 1). The belt of alkaline rocks is little more than 100 km wide, apparently delimited on the west by the Ida lineament (and extensions) and less clearly delimited on the east where outcrop is poorer and the rocks less well known. Hallberg (1985) suggested that the alkaline rocks in the Laverton–Leonora area are further restricted to tectonically active zones within the province. The rocks mainly have a coarse texture, but a few bodies are fine grained or porphyritic; possibly some have been metamorphically recrystallized.
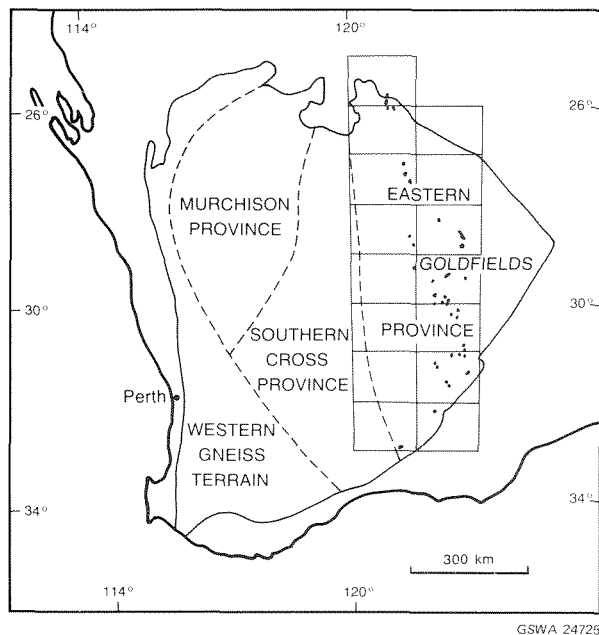

Figure 1. Alkaline rock localities in the Eastern Goldfields Province of the Yilgarn Craton and index to Figure 2.

Not all alkaline rocks in the area belong to the Archaean alkaline suite. Proterozoic and presumed Proterozoic bodies of alkaline affinity are found both within and around the Eastern Goldfields Province at: Shamba Kappa Homestead (Thom and others, 1977) and Lake Shaster (Libby and Lipple, 1978) in the Albany–Fraser Province; Bobbies Point (van de Graaff and Bunting, 1975) at the eastern margin of the Yilgarn Craton; and (carbonatite) at the eastern margin of the Archaean alkaline province near Mount Weld (Hallberg, 1985; Willett and others, 1986).

PETROGRAPHY

The petrography of alkaline rocks south of latitude 28° south was described by Libby (1978) and is treated here only where substantial numbers of samples or significant samples have subsequently become available. North of this line there are four principal alkaline localities: the area around Mount Blackburn; the area north and east of Woorana Well; the area around Red Mountain; and the area within and near the Teague Ring Structure. The first three are on SIR SAMUEL, the final one on NABBERU. All localities are discussed

in the descriptions of SIR SAMUEL (Bunting and Williams, 1979) and NABBERU (Bunting and others, 1982). Monzogranite (the Mount Boreas adamellite) which may be related to the alkaline suite, extends in an essentially continuous strip from Mount Boreas on LAVERTON across DUKETON. Small masses similar to the Boreas adamellite (Bunting and Williams, 1979; Stuckless and others, 1981) are common within the northern part of the Eastern Goldfields, in part cutting rocks of the alkaline suite as dykes (Bunting and Williams, 1979). Further rocks of Boreas type are identified in the southernmost alkaline locality at the Fitzgerald Peaks. Another suite of doubtful affinity includes hornblende monzogranite to soda-rich syenogranite as at Mount MacDonald, in areas south and southwest of the Teague Ring Structure (where it is pyroxene bearing), and elsewhere in smaller masses.

Petrographic nomenclature follows Streckeisen (1973) except that potassic and intermediate granites are distinguished with the names syenogranite and monzogranite, at the division point between quartz syenite and quartz monzonite. The term 'alkaline' is used for rocks with alkali-rich mafic minerals, or with sufficient alkalis that the feldspar:quartz ratio in a felsic rock is greater than in normal granite. The term 'subalkaline' applies to rocks which are not alkaline.

Plagioclase determination, unless indicated otherwise, is by the optical a-normal method.

For initial inclusion in the suite of materials to be studied as alkaline rocks, samples were required to show one of the following characteristics: quartz less than 20% of the rock by volume; alkaline pyroxene or alkaline amphibole as a primary or major phase; or mesoperthitic (hypersolvus) alkaline feldspar. In general, the rocks with one or more of these features tend to form coherent chemical trends and encourage the belief that a suite of related rocks exists. The petrographic features of the various localities are summarized in Figure 2.

The alkaline rocks which were studied are mainly coarse grained or coarsely seriate. Some are porphyritic or porphyritic with a seriate groundmass. In general, the alkaline rocks have less quartz than average granite, but they are rarely quartz free. The typical mafic mineral is green clinopyroxene, ranging in colour from pale green through deep emerald-green to the olive-green of aegirine-augite. At most localities the pyroxene is very weakly alkaline with about 2% Na_2O, but it is rich in Fe and straddles the boundary between the fields of sodian Ca-ferroaugite and sodian ferrosalite. At a few localities it is more sodic and analyses as aegirine-augite.

As well as pyroxene, a few localities have a bluish alkaline amphibole. Such an amphibole at McAuliffe Well was established by microprobe as richterite, zoned to magnesioriebeckite. At Twin Peaks the amphibole at one locality is magnesiohornblende. Much of the feldspar is mesoperthite, but many samples have two discrete feldspars or combinations, such as mesoperthitic cores surrounded by microcline or albite ('transsolvus' feldspar).

84

The plagioclase is always sodic but may range from nearly pure albite to (optical and normative) sodic oligoclase in the two-feldspar rocks. In a few cases, inset grains of coarse subhedral mesoperthite have striking oscillatory zoning which is traced by variations in exsolution. In such cases, less coarse groundmass feldspar is separated into discrete Na- and K-feldspar grains, often seriate. It is seldom clear whether discrete groundmass grains are primary or the result of post-magmatic recrystallization. Titanite (sphene) typically has variable birefringence and an orange colour.

Other minerals are uncommon, although apatite is abundant in some samples and fluorite is rarely visible. Feldspathoids, and those more unusual minerals that are characteristic of strongly alkaline rocks, have not yet been described from the Archaean alkaline rocks of the area.

FITZGERALD PEAKS

This locality has been described in detail by Lewis and Gower (1978). At this point only a table (Table 1) summarizing the petrography is included, which establishes the heterogeneity of the unit from samples collected previously by the GSWA. Plagioclase extinction angle is by the a-normal method. A negative sign indicates 'obtuse' extinction; that is, a composition more sodic than about An_{20}. 'Boreas' under 'Rock type' indicates a rock generally of the Boreas type; that is, a biotite adamellite with prominent metamict allanite and coloured titanite with reduced birefringence.

RED LAKE

The Red Lake locality is east of the Kalgoorlie–Menangina road at the southern boundary of EDJUDINA, about 18 km south of Menangina Homestead. The rock has a doubtful relationship to the alkaline suite. It is dominantly a plagioclase–clinopyroxene rock. Quartz is a minor constituent or is absent, and microcline is normally subordinate to plagioclase. Hornblende is commonly present. The clinopyroxene ranges from pale green to bright apple-green. Where measured (a-normal extinction angle) plagioclase is clearly albite, but zoning (sample 59029A) and epidote in altered cores indicate that it is, or has been, locally more calcic. The relatively calcic cores in some samples are sharply zoned, with a broad alkalic rim, suggesting magmatic mixing or metamorphism. Clear igneous textures are not common, but sharp euhedral oscillatory zoning of plagioclase (with K-feldspar) in one sample (59029C) discourages contemplation of a wholly metamorphic origin. In one sample a large, stumpy, subhedral grain was identified as orthopyroxene. In another sample a very coarse inset of microcline encloses clinopyroxene.

Analysed clinopyroxene is similar to that from most of the alkaline localities, but has less Na than that at the most alkaline localities (McAuliffe Well and Mount Blackburn).
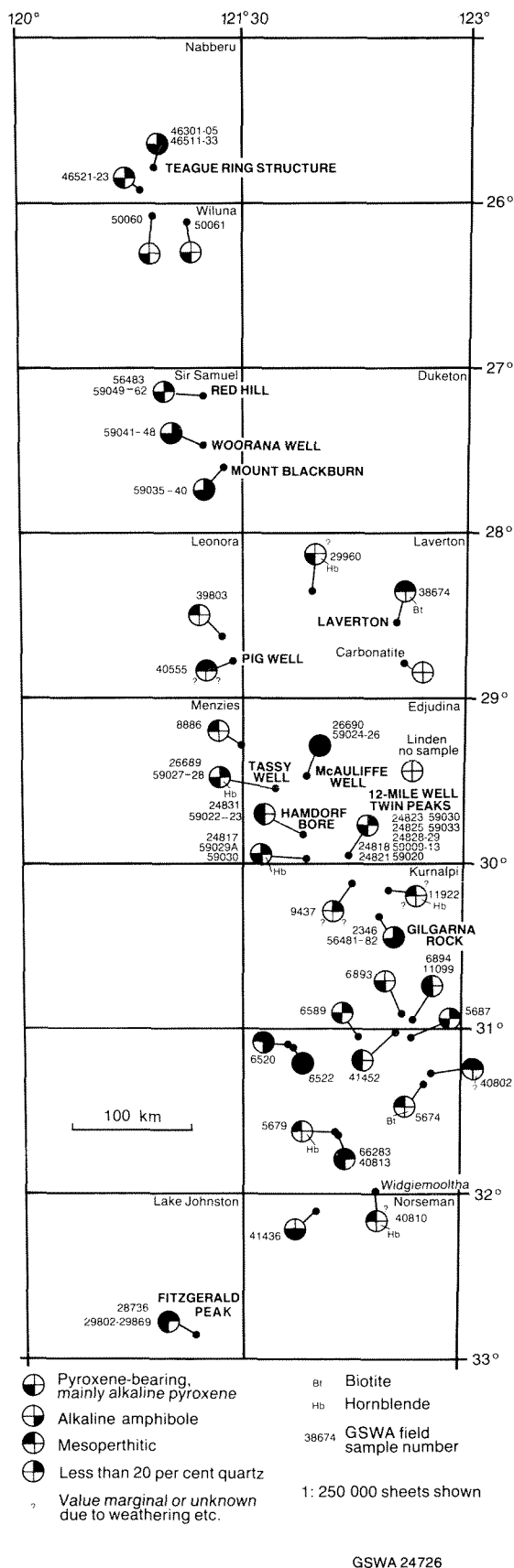
Figure 2. Petrographic summary and index to localities of alkaline rocks in the Eastern Goldfields Province.

TABLE 1. PETROGRAPHY — FITZGERALD PEAKS

Sample	Plagioclase extinction	Rock type	Mafic minerals	Alkali feldspar	Titanite
28927	-12	Quartz syenite	Aeg-aug, biot, alk amph	Complex	Some
29802	- 9	Quartz syenite	Aeg-aug, alk amph	Complex	Abundant
29803	-15	Alkali leucogranite	Aeg-aug	Mesoperthite	No
29805	- 7	Boreas	Biot	Discrete	Abundant
29806	-14	Quartz syenite	Aeg-aug	Complex	No
29807	-14	Quartz syenite	Aeg-aug, biot	Mesoperthite	Minor
29808	- 1	Boreas	Biot	Discrete	Abundant
29810	-10	Leucogranite	None	Discrete	No
29811	-14	Quartz syenite	Aeg-aug	Mesoperthite	No
29812	-13	Leuco quartz syenite	None	Mesoperthite	No
29813	-14	Quartz syenite	Aeg-aug, biot	Mesoperthite	Abundant
29815	-13	Leucogranite	None	Mesoperthite	Some
29817	-13	Alkali leucogranite	Aeg-aug, alk amph	Mesoperthite	Abundant
29818	-14	Quartz syenite	Aeg-aug	Mesoperthite	Some
29819	-13	Alkali granite	Wth cpx	Complex	Some
29820	- 8	Granite	Biot (hb)	Discrete	Rare
29821	-13	Syenite	Aeg-aug	Mesoperthite	Abundant
29822	-14	Syenite	Biot, cpx, alk amph	Complex	Abundant
29823	-15	Alkali granite	Aeg-aug	Mesoperthite	Abundant
29824	-15	Alkali leucogranite	None	Mesoperthite	Rare
29825	-16	Quartz syenite	Aeg-aug	Mesoperthite	Abundant
29826	-14	Alkali leucogranite	Probably cpx, wth	Mesoperthite	Rare
29828	- 9	Quartz syenite	Amph	Discrete	Abundant
29830	- 6	Alkali leucogranite	Pale amph after cpx	Discrete	Some
29831	-13	Quartz syenite	Aeg-aug, secondary amph	Complex	Abundant
29832	-14	Quartz syenite	Aeg-aug, amph	Mesoperthite	Some
29833	- 9	Quartz syenite	Aeg-aug	Complex	Abundant
29834	- 7	Alkali leucogranite	None, wth	Discrete	No
29835	- 7	Pyroxene granite	Colourless cpx	Discrete	Some
29836	-14	Alkali leucogranite	Pale amph after cpx	Complex	No
29837	-14	Quartz syenite	Alk amph after cpx	Mesoperthite	Some
29839	-13	Alkali leucogranite	Alk amph prob after cpx	Complex	No
29840	-13	Alkali granite	Pale green cpx, alk amph	Complex	Some
29841	-13	Syenite	Aeg-aug	Complex	Rare
29843	-14	Syenite	Aeg-aug	Mesoperthite	Abundant
29844	-15	Mafic-rich syenite	Aeg-aug	Discrete	No
29845	- 6	Quartz syenite	Pale cpx, alk amph	Complex	Rare
29846	- 5	Alkali quartz monzonite	Pale cpx, amph	Discrete	Common
29847	- 4	Leuco hornblende granite	Olive-green hb, cltd biot	Discrete	Some
29848	- 5	Hornblende quartz monzonite	Olive-green hb	Discrete	Some
29849	-12	Alkali leucogranite	None	Mesoperthite	No
29850	- 4	Syenite	Aeg-aug, alk amph	Discrete	Some
29851	-11	Syenite	Pale-green cpx, cltd biot	Discrete	No
29852	-12	Syenite	Aeg-aug	Complex	Very abundant
29853	-10	Quartz syenite	Aeg-aug	Complex	Some
29855	- 9	Quartz syenite	Pale amph, rare biot	Discrete	No
29857	-12	Quartz syenite	Green amph	Complex	No
29858	-16	Leuco quartz syenite	Aeg-aug	Complex	Some
29859	-14	Alkali leucogranite	Wth, some amph	Complex	Some
29860	-11	Alkali granite	Wth, some amph	Discrete	Some
29861	-11	Quartz syenite	Pale cpx	Complex	Abundant
29862	-10	Alkali granite	Wth, some amph	Discrete	Some
29863	-14	Quartz syenite	Pale cpx	Complex	Some
29864	- 9	Alkali granite	Pale cpx	Discrete	Abundant

Aeg : aegirine	Aug : augite	Cpx : clinopyroxene
Alk : alkali	Biot : biotite	Hb : hornblende
Amph : amphibole	Cltd : chloritized	Wth : weathered

TWELVE MILE WELL

The Twelve Mile Well locality, about 18 km southeast of Menangina Homestead on EDJUDINA, was described by Libby and de Laeter (1981). Feldspars are discrete and weakly seriate. The albite to microcline ratio tends to be high, some samples approaching albitite. Mafic xenoliths and schlieren are abundant, including a mafic raft 20 m in length (sample 59011E) which consists largely of fibrous pale-green amphibole with less epidote and microcline.

HAMDORF BORE

The locality at Hamdorf Bore is a rocky outcrop, about 100 m in diameter, southeast of the road from Cement Well to Hamdorf Bore, about 2 km southwest of Hamdorf Bore. The locality is about 14 km north-northeast of Menangina Homestead. The alkaline body seems to be a small plug, with associated dykes, intruded into an igneous hornblende–biotite monzogranite. The main body is quartz syenite with zoned

TABLE 2. REPRESENTATIVE MICROPROBE ANALYSES OF PYROXENE AND AMPHIBOLE

Sodian ferrosalite to sodian ferroaugite:

	Twelve Mile 59011A	Twin Peaks 59014B	Hamdorf 59022D	Red Lake 59029F	Woorana 59042A	Woorana 59044C	Woorana 59045B	Red Hill 59058C	Red Hill 59061
SiO_2 (%)	52.40	51.51	50.48	50.41	52.25	50.77	51.83	51.28	52.16
Al_2O_3	0.77	0.82	0.60	0.69	1.01	0.86	0.81	1.12	0.69
FeO^*	13.20	11.07	16.38	14.21	17.57	16.11	17.55	14.02	14.57
MnO	0.31	0.28	0.73	0.39	nd	0.48	0.81	0.92	0.41
MgO	9.85	11.01	7.45	9.02	7.45	7.97	7.20	9.56	9.19
CaO	21.34	21.63	19.36	21.66	19.86	19.74	20.50	21.36	20.65
Na_2O	1.93	1.20	2.19	1.00	1.99	2.13	2.02	1.11	1.97
Total	99.80	97.52	97.19	97.38	100.13	98.06	100.72	99.37	99.64

Aegirine-Augite:

	McAuliffe 59024A	McAuliffe 59024D	McAuliffe 59024E	Mt Blackburn 59035C
SiO_2 (%)	52.39	52.31	51.80	53.80
TiO_2	nd	0.17	0.15	0.32
Al_2O_3	0.51	0.64	0.55	0.64
FeO^*	22.91	20.83	22.62	19.66
MnO	0.48	0.57	0.56	0.33
MgO	4.28	5.71	4.48	6.47
CaO	9.76	11.75	9.68	11.50
Na_2O	8.67	7.15	8.34	8.22
Total	99.00	99.13	98.18	100.94

Amphibole:

	Magnesio-hornblende	Calcian magnesio-hornblende	Richterite	Richterite	Actinolitic hornblende	Magnesio-hornblende	Actinolite
	Twin Peaks 59014B	McAuliffe 59024A	McAuliffe 59024D	McAuliffe 59024E	McAuliffe 59026	MacDonald 59064	Red Hill 59061
SiO_2 (%)	45.91	52.64	51.87	53.39	51.37	49.67	53.45
TiO_2	0.65	0.30	0.54	0.31	0.65	0.53	nd
Al_2O_3	6.09	1.40	2.30	1.09	3.83	5.70	1.22
FeO^*	16.00	16.05	14.61	12.31	12.70	17.23	12.89
MnO	0.26	0.58	0.66	0.72	0.62	nd	0.43
MgO	12.09	12.61	13.58	15.08	15.31	12.53	15.31
CaO	10.93	3.62	6.65	6.12	11.10	11.90	11.13
K_2O	0.83	0.76	0.78	0.99	0.54	0.78	0.41
Na_2O	1.71	6.33	4.71	5.74	2.01	1.27	1.11
Total	94.47	94.29	95.70	95.75	98.13	99.61	95.93

FeO^* : Total Fe as FeO.
nd : Not detected

alkali-feldspar megacrysts, and mafic minerals consisting of sodian ferrosalite and an assortment of amphiboles, including dark blue-green hornblende (optically, hastingsite). Zoning of coarse grains suggests igneous crystallization, but microcrystalline feldspar (intergranular to coarse grains) may be secondary, possibly indicating healing of cataclastic mortar after final emplacement. Sample 59022D carries fluorite and perhaps close to 1% carbonate. Fluorite is visible in the field. See Table 2 for microprobe analysis of sodian ferrosalite in sample 59022D.

McAULIFFE WELL

The first description of syenite at the McAuliffe Well locality was by Honman (1917) who attributed recognition of the rock type to Jutson. The locality was mentioned by name by Williams and others (1976) and by Hallberg (1985, p. 61). McAuliffe Well is 10 km east of Yerilla Homestead on EDJUDINA. It was mapped by Williams and others (1976) as an oval body, about 1 by 2 km, elongated to the northeast. It is one of the largest and best-exposed alkaline bodies in the central and southern parts of the Eastern Goldfields Province.

The typical rock at McAuliffe Well is made up of aegirine-augite, richterite to magnesioriebeckite, a single alkali feldspar and interstitial quartz, with a few accessories. All phases are euhedral against quartz, and the mafic minerals seem generally interstitial to feldspar, but may locally be euhedral against the outer zones of feldspar. The quartz matrix varies from coarse to fine, giving the rock an overall seriate texture. The feldspar shows sharp oscillatory, euhedral zoning marked by alternation of sheets of microcline and albite. The alternation of alkali feldspars could justify the name hypersolvus mesoperthite. However, the case for hypersolvus crystallization is not firmly established; Bonin (1986, p. 55) has shown that alternation of Na- and K-feldspar in alkali feldspars of alkaline rocks can result from alternating crystallization of albite and K-feldspar as well as from rhythmic exsolution. The euhedral aspect of the zoning is consistent with such an origin without excluding exsolution.

Some parts of the body are petrographically subalkaline; the amphibole in parts of the south and northwest appears, optically, to be hornblendic rather than sodic. This identification is confirmed at locality 59026 by microprobe (Table 2). Where the amphibole loses its dusky pale-blue colour and becomes green, the pyroxene tends to be altered and declines in abundance. Also, the feldspar becomes more irregularly and patchily zoned and a discrete plagioclase phase appears. There is a small amount of secondary epidote. These effects do not everywhere coincide and sample 59026, though containing hornblende, retains the typical single euhedral, zoned feldspar. In all parts of the body, quartz is subordinate, perhaps 10% of the rock.

Microprobe analyses of amphibole and pyroxene from both the hornblendic phase (sample 59026) and the more alkaline phase (samples 59024A, D, and E) are listed in Table 2.

MOUNT MacDONALD

The Mount MacDonald locality is a granitic mass lying about 10m northeast of Melrose Homestead, mapped by Bunting and Williams (1979) as hornblende–quartz monzonite (Agh). Samples 59064 and 59065 are seriate–irregular biotite–hornblende–quartz monzonite with sodic oligoclase and variably perthitic microcline. Accessories include fluorite, opaques, titanite, and apatite.

MOUNT BLACKBURN

The Mount Blackburn locality is a large area of low granitic outcrops mainly west of the Melrose–Wonganoo road, 35 to 40 km north of Melrose Station on SIR SAMUEL. As mapped by Bunting and Williams (1979), the area of granitic outcrop is almost continuous for 26 km to the northwest. The mass is heterogeneous and contains sheets of syenite, quartz syenite, and biotite adamellite (similar to that at Mount Boreas) cutting less distinctive biotite granite and granite gneiss.

One of the most strongly alkaline bodies inspected lies in a northward-trending band, near the eastern side of the mass. Samples 59035A, B, and C are quartz syenite with bright-green aegirine-augite (Table 2) and blue to light-violet blue amphibole, much like the assemblage at McAuliffe Well. However, here the feldspar texture is much different; the feldspar is not much coarser than medium grain and the two-alkali feldspars form discrete grains, not markedly perthitic. This rather seriate texture is more similar to the textures at the Woorana and Red Hill localities than to the mineralogically similar McAuliffe locality. Sphene and apatite are present but not abundant.

WOORANA WELL

The Woorana Well locality is about 2 km northeast of Woorana Well, north of the road past Kens Bore, and about 11 km north-northeast of Yandal Homestead (see Libby and de Laeter, 1981). It was shown by Bunting and Williams (1979) as a series of north-northwesterly trending, alternating bands (steep sheets) of Ags (syenite) and Agb (medium to coarse granite). The granitic outcrop is near the north end of effectively continuous outcrops from the Mount Blackburn locality for about 26 km to the southeast. The granitic mass may continue across an area of no outcrop (extensions to Lake Maitland) to the Red Hill locality, 35 km to the north, defining a heterogeneous, richly alkali-bearing batholith 65 km or more long by 20 km wide.

The main sampling locality is about 0.5 km north of the road, in the middle of the mapped banded complex (Bunting and Williams, 1979). The samples here are all texturally similar. The feldspar in particular is seriate, coarser grains being perthitic and finer grains being discrete microcline and albite. All samples have bright-green clinopyroxene which appears largely to be sodian ferrosalite to sodian ferroaugite (Table 2). A few samples have accessory alkali amphibole. The abundance of mafic minerals ranges from little more than 1% to

an estimated local maximum of 35% in sample 59046C. Quartz in most samples is sparse, probably under 5%, but ranges in some samples up to 15% or 20%. Sphene and apatite are locally abundant, apparently in a reciprocal relationship. Sample 59041A, about 2 km southwest of the main sampled locality, is more calcic. While similar in microscopic texture (seriate, irregular), megascopically the rock is more strongly foliated and the mafic mineral assemblage is dominated by hornblende, the subordinate clinopyroxene is pale green, and the plagioclase is sodic oligoclase. As at much of the main locality, the rock is essentially quartz free and, in igneous terms, is thus perhaps a slightly alkaline hornblende monzonite.

As discussed by Bunting and Williams (1979), the Woorana locality also has subalkaline granitic rocks. Samples 59043A and B are richer in quartz than the alkaline rocks, and contain biotite (now largely chloritized) as the sole mafic phase. An abundance of sphene, and especially metamict grains (probably allanite), suggests affinities with the Mount Boreas adamellite. The texture of these samples is seriate but here the coarser grains are discrete microcline and plagioclase. Plagioclase was not determined, but zoning and small Michel-Lévy extinction angles suggest oligoclase.

The ubiquitous seriate texture in rocks of various compositions, as well as gneissic structure at this locality suggests cataclastic deformation either late in emplacement or after emplacement. The rocks are quite free of the obvious igneous texture at McAuliffe Well. The texture is descriptively trans-solvus, with coarser feldspar being perthitic to mesoperthitic, while finer grains are discrete microcline and albite. However, with *partial metamorphism a possible process for unmixing the feldspars*, this term might be inappropriate.

RED HILL

Red Hill is 10 km west-southwest of Wonganoo Homestead on SIR SAMUEL. Sampling was centred on two areas; the first is a group of hills about 3 km southeast of Red Hill proper, the second centred about Red Hill itself. The granitic mass (of which the alkaline rocks are a part) may extend under alluvial cover to the Woorana Well and Mount Blackburn localities to the south.

The more alkalic rocks at the Red Hill area are too diverse to be easily summarized, but the majority of sampled specimens have pale-green clinopyroxene and plagioclase in the range An_5 to An_{15}. Quartz is generally 15% to 20% of the rock, somewhat lower on average than in normal granite. The pyroxene is a sodian ferrosalite to sodian ferroaugite, slightly poorer (*in analysed samples*) *in* Na_2O *than at some other* localities, but still more sodic than most pyroxenes in the diopside–hedenbergite series listed by Deer and others (1978). The texture is seriate and generally coarser and more uniform than at Woorana Well.

In igneous terms, the average sampled rock at Red Hill is a pyroxene–quartz monzonite to pyroxene monzogranite, but in places, as at locality 59056,

samples are more alkaline, ranging to quartz syenite and containing bright-green pyroxene and hypersolvus alkali feldspar. At the other extreme, sample 59050 is a Boreas-type biotite granite. More unusual rocks include 59057A, a microcline-dominant hornblende–quartz monzonite with minor amounts of biotite, titanite, and metamict allanite. In sample 59057B very coarse pale-green clinopyroxene (and felted amphibole after clinopyroxene) encloses rounded plagioclase (An_{10}) and quartz in a texture resembling the cumulus–intercumulus relationships of layered-mafic rocks. However, here this texture may represent remelting. Sample 59057C is a quartz-free gneissic rock with small-scale heterogeneity wherein plagioclase and sphene are in layers associated with hornblende and biotite, while microcline and apatite are associated with light-green clinopyroxene.

The suite was sampled for alkaline rock, thus the average composition in the Red Hill area is probably closer to conventional granite than indicated by these samples. The variety of textures and rock types, together with extensive outcrop, suggest that the Red Hill area, perhaps together with the Mount Blackburn area, would be a productive subject for detailed study.

WILUNA AND NABBERU 1:250 000 SHEETS

Syenite from the Teague Ring Structure has been described by Bunting and others (1982). Within the ring structure is a porphyritic clinopyroxene–microcline–albite syenite with mostly discrete feldspars, ophitic microcline megacrysts, and zoned, euhedral, bright-green clinopyroxene. Titanite is a prominent accessory. Some pyroxene grains in sample 46514 have cores of a pale, dusky-blue amphibole. Despite the discrete nature of groundmass feldspars, microcline megacrysts are strongly perthitic. In some samples the groundmass is intergrown, approaching aplitic or granophyric texture.

Immediately southwest of the Teague Ring Structure is a large area of hornblende–quartz monzonite to quartz syenite, commonly with pale, partly altered clinopyroxene. Plagioclase is albite, but epidote in some samples suggests downgrading in some cases. Titanite is prominent.

No clearly alkaline felsic rocks have been reported from WILUNA despite its location between the richly alkaline SIR SAMUEL and the Lake Teague syenites on NABBERU. However, two samples (50060 and 50061) are quartz syenite, respectively 15 km south and 25 km southeast of the Teague Ring Structure. The dominant mafic mineral in 50060 is hornblende, but there is some colourless, partly altered clinopyroxene. The mafic minerals in sample 50061 have been weathered but the whiskery habit of the amphibole indicates that it is secondary and the overall grain outline suggests that the original mafic mineral was probably pyroxene. In both cases the plagioclase is albite (near oligoclase in the case of 50060). Sample 50060 (and perhaps 50061) is part of the mass of similar rocks adjacent to the Teague Ring Structure on NABBERU.

89

MAJOR ELEMENTS

New whole-rock major-element analyses have been performed on rocks collected in the course of the present study, as well as on samples collected earlier during regional mapping by the Geological Survey. Samples from Gilgarna Rock were contributed by D. F. Blight. In all cases the reported new analyses were performed by the Western Australian Government Chemical Laboratories. Most elements were determined by X-ray fluorescence, but Fe-oxides, MgO, SO_3, Na_2O, H_2O+, H_2O-, and CO_2 were determined chemically. Further analyses were drawn from the published literature, mainly from explanatory notes accompanying 1:250 000 geological sheets (SIR SAMUEL, LAVERTON, LEONORA, DUKETON, MINIGWAL) and by Roddick and others (1976). Only analyses of plutonic rocks were used, which resulted in very few analyses of basic and truly intermediate rocks.

For purposes of study, the rocks have been classed in three principal categories: Mount Boreas type, correlated with the Mount Boreas adamellite in the northern part of LAVERTON (Gower, 1976); the alkaline suite (Libby, 1978); and other, undifferentiated granitoids. In some contexts, hornblende-bearing monzogranite (adamellite) and tonalite are considered separately from the other granitoids, which makes five working categories. The Boreas rocks are considered as a separate group because of the wealth of analytical data available for them, their generally compact plots on variation diagrams, and their field association with the alkaline suite. Furthermore, there is some evidence that both may be late in the Yilgarn tectonic cycle, the Boreas unit perhaps being somewhat younger than the alkaline suite (Stuckless and others, 1981). Similarity and association suggest that an hypothesis of genetic association between the Boreas and alkaline suites should be tested.

New analytical data are shown in Table 3. Samples are identified by GSWA sample number. Details on each locality can be found in Table 4.

The three classes of rock are well differentiated on a plot of alkalinity (agpaitic) index against the Thornton–Tuttle (1960) differentiation index (Fig. 3A). The agpaitic index (Sorenson, 1974) is the molecular ratio $Na_2O + K_2O : Al_2O_3$. A ratio over 1 represents an alkali to alumina ratio in excess of that required to form alkali feldspar. It is a measure of alkalinity with respect to alumina. The differentiation index is the sum of normative quartz, alkali feldspars and feldspathoids. It is a measure of the degree to which the rock has attained the goal of evolution to 'petrogeny's residua system' (Thornton and Tuttle, 1960).

There are two distinct trends in Figure 3A, the 'other granites' have a low alkalinity index at low degrees of differentiation, becoming higher with increasing differentiation. The alkaline rocks, on the other hand, maintain a high alkalinity index at all values of differentiation index. There is even a suggestion of a negative slope for the alkaline rocks. The rocks of Boreas type cluster at high values of differentiation

index and also tend to have a flat curve, but lower than the alkaline rocks. The hornblende-bearing rocks have a near-constant alkalinity index, similar to the Boreas suite. On the other hand, the limited data on tonalite fit the trend of common granite. Of particular interest is the apparent gap between the two main trends, which suggest that the two main series have distinct histories rather than being parts of a continuum. Several samples collected as possible alkaline rocks lie closer to the trend of the Boreas and hornblende-bearing rocks than to the alkaline rocks. These samples are identified on Figure 3B.

The two most anomalous samples on Figure 3B are from Red Lake, a locality having dubious affinity with the alkaline suite and having some sign of metasomatic modification; sample 59029A is a hornblende granodiorite and, although bearing green clinopyroxene, 59029F is dominated by oligoclase near An_{11} and is nearly devoid of K-feldspar. The other four, less anomalous, samples are from Red Hill (59049 and 59051) and WIDGIEMOOLTHA (5687 and 6589). All four have some characteristic suggesting alkaline affinity and their anomalous position is unexplained. None of the rocks identified as strongly alkaline (on the basis of petrographic characteristics) plot in an anomalous or transitional position.

Two other outlying samples are on an extension of the main trend of the alkaline rocks. Samples 59011C (Twelve Mile Well) and 59046C (Woorana Well) are strongly mafic, consequently with high differentiation indices. Sample 59011C is from the margin of a mafic to ultramafic enclave in otherwise felsic alkaline rock, and may be a product of reaction. Sample 59046C is a relatively mafic phase of the rather heterogeneous set of alkaline rocks at the Woorana locality. The most mafic alkaline rocks are the most alkaline.

As might be expected, total alkaline oxides are more abundant in the alkaline suite than in the other granites of the area; the two suites plot in distinct areas when K_2O is plotted against Na_2O (Fig. 3C). However, the two suites overlap widely when individual alkalis are plotted. This again suggests that the two suites differ in origin.

The Boreas group is more closely associated with the 'other granites' than with the alkaline granites in the $K_2O–Na_2O$ plot (unlike its opposite behaviour in the relative plots, below); though at the K_2O-rich end of the distribution Boreas samples cluster with several rebel alkaline samples.

The low Al_2O_3 content of the Boreas samples allows this suite to have a higher agpaitic index than 'other granites' although it has no more than average alkalis. Boreas rocks average about 14.5% Al_2O_3 as against about 15.2% for the other classes.

The alkalinity of the mafic minerals, and the general paucity of quartz, suggest that the alkaline rocks should have both high alkali to alumina and alkali to silica ratios with respect to more usual granitic rocks. Figures 3D and 3E demonstrate that this is indeed so; weight percent $(Na_2O + K_2O)$ is plotted against Al_2O_3

in Figure 3D, and against SiO_2 in Figure 3E. The alkaline rocks not only tend to have a higher alkali to alumina ratio than the granitic rocks, but the amount of alkali increases with increasing alumina, whereas alkalis decrease in the 'other granitic' rocks. Again, the Boreas rocks occupy an intermediate position with a positive slope, suggesting affinity with the alkaline suite. The alkaline suite trend is again opposite to the trend of other granites in the plot of alkali against silica (Fig. 3E). Plotting individual alkali oxides against SiO_2

and Al_2O_3 (Figs 3F and 3G) results in broad areas of overlap between all three rock classes, but shows a tendency for prominence of alkalis in the alkaline suite in all plots.

TRACE ELEMENTS

Trace-element analyses generated in the course of the current work are listed in Table 5. Analyses from a variety of other granitoids, including several alkaline

TABLE 3. MAJOR ELEMENTS — NEW ANALYSES

	5687	6520	6522A	6589	56481	56482	59011A	59011C	59011D	59011D2	59011E	59012A	59022D	59022E
SiO_2 (%)	64.40	70.00	66.60	62.20	64.72	62.86	66.40	57.60	65.10	63.80	66.50	69.50	65.20	61.70
Al_2O_3	16.60	15.90	17.60	17.20	17.1	16.38	13.80	8.00	16.40	17.20	17.40	16.10	15.10	17.00
TiO_2	0.41	0.17	0.22	0.34	0.16	0.28	0.43	0.40	0.53	0.48	0.29	0.11	0.33	0.60
Fe_2O_3	1.90	1.10	1.40	1.80	1.26	1.51	1.40	2.00	1.30	1.20	0.60	0.90	2.10	3.40
FeO	0.86	0.32	0.38	1.30	0.23	0.58	1.22	2.23	0.79	0.57	0.33	0.22	0.93	1.08
MgO	0.72	0.11	0.56	1.47	0.47	0.78	1.61	8.46	1.06	0.85	0.44	0.16	0.56	0.84
CaO	2.21	0.17	0.28	4.24	2.13	2.95	3.33	13.72	2.41	2.63	0.78	0.84	2.64	2.09
Na_2O	5.05	6.31	8.52	6.86	8.09	8.15	5.46	3.45	6.18	5.60	5.37	5.93	5.36	5.58
K_2O	5.59	4.25	3.25	3.39	3.54	3.47	4.42	2.50	4.98	6.42	7.16	4.59	5.49	5.93
H_2O+	0.74	0.81	0.71	0.68	0.34	0.38	0.34	0.23	0.37	0.28	0.31	0.25	0.36	0.32
H_2O-	0.19	0.15	0.13	0.12	0.15	0.15	0.16	0.10	0.22	0.18	0.07	0.03	0.11	0.24
MnO	0.15	0.05	0.04	0.18	0.03	0.06	0.17	0.18	0.14	0.16	0.07	0.04	0.17	0.29
P_2O_5	0.05	0.01	0.02	0.08	0.10	0.17	0.04	0.07	0.03	0.02	0.01	0.01	0.05	0.06
CO_2	0.36	0.47	0.43	0.40	1.07	1.47	0.34	0.16	0.20	0.20	0.16	0.10	0.70	0.12
Total	99.20	99.80	100.10	100.30	99.38	99.18	99.10	99.10	99.70	99.60	99.50	98.80	99.10	99.30

	59024D	59026	59028A	59029A	59029F	59033	59035A	59044C	59045A	59045B	59045C	59046A	59046B	59046C
SiO_2 (%)	67.40	67.10	62.70	62.30	63.60	73.20	69.50	62.20	66.80	63.80	70.90	64.10	63.40	58.50
Al_2O_3	16.50	16.70	17.30	15.60	15.80	14.50	15.50	15.80	13.40	16.00	15.40	15.40	16.50	10.20
TiO_2	0.20	0.21	0.42	0.52	0.37	0.15	0.23	0.76	0.08	0.48	0.12	0.03	0.50	0.11
Fe_2O_3	1.40	1.80	1.80	1.80	1.90	0.60	1.50	1.80	1.50	1.50	0.50	1.50	1.60	2.80
FeO	0.29	0.35	1.24	2.55	1.57	0.29	0.33	1.34	1.39	1.31	0.20	1.14	1.03	2.91
MgO	0.55	0.70	1.38	2.99	1.75	0.23	0.38	1.27	1.60	1.06	0.25	1.66	0.96	4.83
CaO	0.70	1.21	3.26	4.90	5.87	1.11	0.71	3.92	3.49	3.11	0.87	3.82	2.99	10.60
Na_2O	6.95	6.58	7.26	4.93	6.95	4.30	5.93	4.89	4.18	5.02	5.40	4.89	5.50	3.54
K_2O	4.30	4.12	3.08	2.78	0.85	4.28	5.24	6.60	5.63	6.64	5.29	6.35	6.49	4.59
H_2O+	0.32	0.36	0.43	0.67	0.28	0.51	0.21	0.37	0.45	0.30	0.20	0.30	0.23	0.29
H_2O-	0.13	0.10	0.19	0.12	0.10	0.07	0.04	0.15	0.22	0.14	0.11	0.10	0.14	0.16
MnO	0.13	0.10	0.04	0.23	0.10	0.03	0.13	0.47	0.30	0.18	0.07	0.37	0.19	1.19
P_2O_5	0.03	0.06	0.17	0.07	0.20	0.01	0.02	0.09	0.10	0.11	0.01	0.09	0.06	0.19
CO_2	0.00	0.14	0.04	0.08	0.10	0.44	0.28	0.16	0.18	0.32	0.00	0.12	0.16	0.06
Total	98.90	99.50	99.30	99.50	99.40	99.70	100.00	99.80	99.30	100.00	99.30	99.90	99.80	100.00

	59047	59049A	59049B	59049C	59050	59051	59052	59054A	59056	59061	59062	59064	66283
SiO_2 (%)	70.80	71.40	70.70	70.40	70.60	71.20	70.10	70.70	64.60	62.00	67.30	67.30	61.30
Al_2O_3	13.00	13.90	13.90	13.80	14.70	15.20	13.80	14.40	16.10	15.80	14.20	16.70	16.30
TiO_2	0.70	0.40	0.23	0.52	0.31	0.18	0.27	0.26	0.37	0.64	0.34	0.34	0.76
Fe_2O_3	1.10	0.90	0.80	1.40	1.00	0.40	0.90	1.20	1.40	2.20	1.40	1.50	3.60
FeO	0.80	0.32	0.57	0.69	0.69	0.29	0.57	0.60	0.65	1.08	1.03	0.73	1.48
MgO	0.79	0.43	0.42	0.62	0.46	0.34	0.49	0.34	0.79	1.32	1.10	0.54	1.11
CaO	2.41	1.33	1.66	1.99	1.17	1.79	1.86	1.23	1.79	3.28	2.95	1.56	3.02
Na_2O	3.84	3.36	3.54	3.56	3.90	5.20	4.33	4.90	5.75	4.09	5.13	5.45	5.97
K_2O	5.82	6.62	6.34	5.81	5.09	3.69	5.27	3.63	5.67	8.16	4.85	4.67	5.36
H_2O+	0.22	0.29	0.24	0.31	0.47	0.28	0.29	0.42	0.29	0.23	0.33	0.34	0.58
H_2O-	0.08	0.14	0.07	0.08	0.07	0.07	0.06	0.06	0.14	0.07	0.09	0.06	0.08
MnO	0.13	0.19	0.11	0.17	0.01	0.07	0.13	0.06	0.19	0.50	0.32	0.03	0.15
P_2O_5	0.06	0.06	0.03	0.08	0.09	0.03	0.04	0.01	0.06	0.05	0.09	0.11	0.10
CO_2	0.16	0.09	0.47	0.10	0.24	0.16	0.49	0.33	0.31	0.13	0.19	0.17	0.37
Total	99.90	99.40	99.10	99.50	98.80	98.90	98.60	98.10	98.10	99.60	99.30	99.50	100.20

TABLE 4. LOCATIONS OF REFERENCED SAMPLES AND ELEMENTAL ANALYSES PRESENTED

Sample	Lat.	Long.	Map sheet	Major	Trace	REE
2346	30°20′	122°25′	KURNALPI			
5674	31°19′	122°45′	WIDGIEMOOLTHA			
5679	31°39′	122°08′	WIDGIEMOOLTHA			
5687	31°21′	122°31′	WIDGIEMOOLTHA	X	X	X
6520	31°07′	121°48′	WIDGIEMOOLTHA	X	X	X
6522 A	31°07′	121°49′	WIDGIEMOOLTHA	X	X	X
6522 B	31°07′	121°49′	WIDGIEMOOLTHA			
6589	31°00′	122°15′	WIDGIEMOOLTHA	X	X	X
6893	30°55′	122°33′	KURNALPI			
6894	30°58′	122°36′	KURNALPI			
8886	29°17′	121°27′	MENZIES			
9437	30°09′	122°25′	KURNALPI			
11099	30°57′	122°38′	KURNALPI			
11922	30°11′	122°30′	KURNALPI			
24818	29°55′	122°04′	EDJUDINA			
24821	29°56′	122°03′	EDJUDINA			
24823	29°57′	122°03′	EDJUDINA			
24825	29°57′	122°03′	EDJUDINA			
24828	29°57′	122°03′	EDJUDINA			
24829	29°56′	122°03′	EDJUDINA			
24831	29°42′	121°57′	EDJUDINA			
26689	29°33′	121°43′	EDJUDINA			
26690	29°29′	121°55′	EDJUDINA			
28736	32°53′	121°09′	LAKE JOHNSTON			
29802	32°53′	121°07′	LAKE JOHNSTON			
29803	32°53′	121°07′	LAKE JOHNSTON			
29804	32°53′	121°07′	LAKE JOHNSTON			
29805	32°53′	121°07′	LAKE JOHNSTON			
29806	32°53′	121°07′	LAKE JOHNSTON			
29807	32°53′	121°07′	LAKE JOHNSTON			
29808	32°53′	121°07′	LAKE JOHNSTON			
29810	32°53′	121°07′	LAKE JOHNSTON			
29811	32°53′	121°08′	LAKE JOHNSTON			
29812	32°53′	121°08′	LAKE JOHNSTON			
29813	32°53′	121°09′	LAKE JOHNSTON			
29815	32°53′	121°09′	LAKE JOHNSTON			
29817	32°53′	121°09′	LAKE JOHNSTON			
29818	32°53′	121°09′	LAKE JOHNSTON	(a)		
29819	32°53′	121°09′	LAKE JOHNSTON			
29820	32°53′	121°08′	LAKE JOHNSTON			
29821	32°53′	121°09′	LAKE JOHNSTON	(a)		
29822	32°53′	121°09′	LAKE JOHNSTON			
29823	32°53′	121°09′	LAKE JOHNSTON			
29824	32°53′	121°09′	LAKE JOHNSTON			
29825	32°53′	121°09′	LAKE JOHNSTON			
29826	32°53′	121°09′	LAKE JOHNSTON			
29827	32°53′	121°09′	LAKE JOHNSTON			
29828	32°53′	121°08′	LAKE JOHNSTON			
29830	32°53′	121°08′	LAKE JOHNSTON			
29831	32°53′	121°08′	LAKE JOHNSTON	(a)		
29832	32°53′	121°11′	LAKE JOHNSTON			
29833	32°53′	121°11′	LAKE JOHNSTON			
29834	32°53′	121°11′	LAKE JOHNSTON			
29835	32°53′	121°11′	LAKE JOHNSTON			
29836	32°53′	121°11′	LAKE JOHNSTON			
29837	32°53′	121°10′	LAKE JOHNSTON			
29839	32°53′	121°10′	LAKE JOHNSTON			
29840	32°53′	121°10′	LAKE JOHNSTON			
29841	32°53′	121°09′	LAKE JOHNSTON			
29843	32°53′	121°09′	LAKE JOHNSTON			
29844	32°53′	121°09′	LAKE JOHNSTON			
29845	32°53′	121°09′	LAKE JOHNSTON			
29846	32°53′	121°09′	LAKE JOHNSTON			
29847	32°53′	121°09′	LAKE JOHNSTON			
29848	32°53′	121°09′	LAKE JOHNSTON			
29849	32°53′	121°09′	LAKE JOHNSTON			
29850	32°53′	121°09′	LAKE JOHNSTON			
29851	32°53′	121°08′	LAKE JOHNSTON			

TABLE 4. (continued)

Sample	Lat.	Long.	Map sheet	Major	Trace	REE
29852	32°53′	121°08′	LAKE JOHNSTON			
29853	32°53′	121°08′	LAKE JOHNSTON			
29855	32°53′	121°07′	LAKE JOHNSTON			
29857	32°53′	121°07′	LAKE JOHNSTON			
29858	32°53′	121°07′	LAKE JOHNSTON			
29859	32°53′	121°09′	LAKE JOHNSTON			
29860	32°53′	121°09′	LAKE JOHNSTON			
29861	32°53′	121°08′	LAKE JOHNSTON			
29862	32°53′	121°08′	LAKE JOHNSTON			
29863	32°53′	121°10′	LAKE JOHNSTON			
29864	32°53′	121°09′	LAKE JOHNSTON			
29865	32°53′	121°09′	LAKE JOHNSTON			
29866	32°53′	121°09′	LAKE JOHNSTON			
29869	32°53′	121°06′	LAKE JOHNSTON			
29960	28°22′	121°57′	LAVERTON			
38674 A	28°35′	122°32′	LAVERTON			
39803	28°37′	121°21′	LEONORA			
40555 A	28°46′	121°26′	LEONORA			
40555 B	28°46′	121°26′	LEONORA			
40591 A	27°51′	121°53′	DUKETON			
40592 B	27°51′	121°53′	DUKETON			
40598 A	27°28′	121°12′	SIR SAMUEL	X		
40802	31°19′	121°35′	WIDGIEMOOLTHA			
40810	31°59′	122°24′	WIDGIEMOOLTHA			
40813	31°39′	122°09′	WIDGIEMOOLTHA			
41436	32°08′	121°58′	NORSEMAN			
41452	31°10′	122°38′	WIDGIEMOOLTHA			
46301	25°50′	120°55′	NABBERU			
46302	25°50′	120°55′	NABBERU			
46303	25°50′	120°55′	NABBERU			
46304	25°58′	125°04′	NABBERU			
46305	25°58′	125°04′	NABBERU			
46514	25°50′	120°55′	NABBERU			
46521	25°57′	120°47′	NABBERU			
46522	25°58′	120°45′	NABBERU			
46523	25°58′	120°45′	NABBERU			
50060	26°04′	120°54′	WILUNA			
50061	26°09′	120°07′	WILUNA			
56481	30°20′	122°25′	KURNALPI	X	X	X
56482	30°20′	122°25′	KURNALPI	X	X	X
56483	27°10′	121°15′	SIR SAMUEL			
59009 A	29°55′	122°04′	EDJUDINA			
59009 C	29°55′	122°04′	EDJUDINA			
59009 D	29°55′	122°04′	EDJUDINA			
59010 B	29°55′	122°04′	EDJUDINA			
59011 A	29°56′	122°03′	EDJUDINA	X	X	
59011 B	29°56′	122°03′	EDJUDINA			
59011 C	29°56′	122°03′	EDJUDINA	X	X	
59011 D	29°56′	122°03′	EDJUDINA	X	X	
59011 D2	29°56′	122°03′	EDJUDINA	X	X	
59011 E	29°56′	122°03′	EDJUDINA	X	X	
59011 G	29°56′	122°03′	EDJUDINA	X	X	
59011 H	29°56′	122°03′	EDJUDINA			
59012 A	29°55′	122°04′	EDJUDINA	X	X	
59012 B	29°55′	122°04′	EDJUDINA			
59013 A	29°55′	122°04′	EDJUDINA			
59013 C	29°55′	122°04′	EDJUDINA			
59014 B	29°55′	122°04′	EDJUDINA			
59020 D	29°55′	122°04′	EDJUDINA			
59022 A	29°45′	121°55′	EDJUDINA			
59022 B	29°45′	121°55′	EDJUDINA			
59022 C	29°45′	121°55′	EDJUDINA	X	X	
59022 D	29°43′	121°58′	EDJUDINA			
59022 E	29°45′	121°55′	EDJUDINA	X	X	
59022 F	29°45′	121°55′	EDJUDINA			
59022 G1	29°45′	121°55′	EDJUDINA			
59023 A	29°45′	121°58′	EDJUDINA			

TABLE 4. (continued)

Sample	Lat.	Long.	Map sheet	Major	Trace	REE
59024 A	29°29′	121°55′	EDJUDINA			
59024 C	29°29′	121°55′	EDJUDINA			
59024 D	29°29′	121°55′	EDJUDINA	X	X	X
59024 E	29°29′	121°55′	EDJUDINA			
59024 G	29°29′	121°55′	EDJUDINA			
59025 I	29°57′	122°04′	EDJUDINA			
59025 K	29°57′	122°04′	EDJUDINA			
59025 L2	29°57′	122°04′	EDJUDINA			
59026	29°29′	121°55′	EDJUDINA	X	X	
59027 A	29°33′	121°42′	EDJUDINA			
59027 B	29°33′	121°42′	EDJUDINA			
59028 A	29°33′	121°42′	EDJUDINA	X	X	
59028 E	29°33′	121°42′	EDJUDINA			
59029 A	29°59′	121°55′	EDJUDINA	X	X	
59030 D	29°57′	122°04′	EDJUDINA			
59033	29°56′	122°03′	EDJUDINA	X	X	X
59035 A	27°37′	121°21′	SIR SAMUEL	X	X	
59035 B	27°37′	121°20′	SIR SAMUEL			
59035 C	27°37′	121°20′	SIR SAMUEL			
59036	27°37′	121°20′	SIR SAMUEL			
59037	27°37′	121°20′	SIR SAMUEL			
59038 B	27°37′	121°20′	SIR SAMUEL			
59038 C	27°37′	121°20′	SIR SAMUEL			
59038 D	27°37′	121°20′	SIR SAMUEL			
59039	27°37′	121°20′	SIR SAMUEL			
59040	27°37′	121°19′	SIR SAMUEL			
59041 A	27°29′	121°11′	SIR SAMUEL			
59042 A	27°28′	121°12′	SIR SAMUEL			
59042 D	27°28′	121°12′	SIR SAMUEL			
59043 A	27°29′	121°12′	SIR SAMUEL			
59043 B	27°29′	121°12′	SIR SAMUEL			
59044 A	27°29′	121°12′	SIR SAMUEL			
59044 C	27°29′	121°12′	SIR SAMUEL	X	X	
59045 A	27°29′	121°12′	SIR SAMUEL	X	X	X
59045 B	27°28′	121°12′	SIR SAMUEL	X	X	
59045 C	27°28′	121°12′	SIR SAMUEL	X	X	
59046 A	27°28′	121°13′	SIR SAMUEL	X	X	X
59046 B	27°28′	121°13′	SIR SAMUEL	X	X	
59046 C	27°28′	121°13′	SIR SAMUEL	X	X	
59047	27°28′	121°13′	SIR SAMUEL	X	X	
59048	27°29′	121°12′	SIR SAMUEL			
59049 A	27°11′	121°15′	SIR SAMUEL	X	X	X
59049 B	27°11′	121°15′	SIR SAMUEL	X	X	
59049 C	27°11′	121°15′	SIR SAMUEL	X	X	
59050	27°11′	121°15′	SIR SAMUEL	X	X	
59051	27°11′	121°15′	SIR SAMUEL	X	X	
59052	27°11′	121°15′	SIR SAMUEL	X	X	
59054 A	27°11′	121°15′	SIR SAMUEL	X	X	
59056	27°11′	121°14′	SIR SAMUEL	X	X	
59057 A	27°10′	121°14′	SIR SAMUEL			
59057 B	27°10′	121°14′	SIR SAMUEL			
59057 C	27°10′	121°14′	SIR SAMUEL			
59058 C	27°10′	121°14′	SIR SAMUEL			
59061	27°11′	121°14′	SIR SAMUEL	X	X	
59062	27°11′	121°14′	SIR SAMUEL	X	X	
59064	27°52′	121°22′	SIR SAMUEL	X	X	
59065	27°52′	121°22′	SIR SAMUEL			
66283	31°39′	122°09′	WIDGIEMOOLTHA	X	X	

(a) Analyses in Lewis and Gower, 1978

rocks, were drawn from explanatory notes on SIR SAMUEL (Bunting and Williams, 1979). Localities for all samples are included in the locality list, Table 4. Both groups were analysed at the Government Chemical Laboratories by X-ray fluorescence and chemical methods (F, Li). In addition to the elements reported in Table 5, Be, S, Ta, and U were analysed but were invariably at, or little above, detection limits. Results for these analyses are available from the GSWA, on request.

TABLE 5. TRACE ELEMENTS

	59011A	59011C	59011D	59011D2	59011G	59011E	59012A	59022A	59022E	59024D	59026	59028A
Ba (ppm)	1 100	650	700	1 000	450	1 200	800	1 200	3 400	1 300	1 400	1 400
Ce	110	80	70	60	110	20	40	140	230	20	80	90
F	270	250	250	240	1 500	140	50	1 100	960	300	430	280
Ga	18	10	18	18	14	18	20	20	20	18	18	14
La	80	30	40	20	20	0	20	90	140	0	50	60
Li	15	20	5	3	2	1	1	15	9	18	18	4
Nb	12	2	6	10	22	6	8	12	6	2	0	6
Rb	100	30	100	120	80	180	80	190	200	100	120	60
Sr	500	600	650	1 100	650	460	600	600	1 200	600	1 400	900
Th	10	0	0	0	0	0	10	15	15	5	10	1
Y	18	12	9	3	15	9	18	35	60	6	15	18
Zr	80	40	60	40	80	40	160	200	440	120	180	160

	59029A	59029F	59033	59035A	59044C	59045A	59045B	59045C	59046A	59046B	59046C	59047
Ba (ppm)	1 500	250	750	350	1 700	1 100	1 300	750	850	1 500	600	800
Ce	100	100	20	60	190	120	280	50	60	280	220	160
F	1 100	250	210	180	600	300	290	130	1 400	340	1 100	280
Ga	18	18	20	24	18	18	20	20	22	20	16	18
La	50	60	20	20	90	50	120	30	40	140	120	90
Li	43	43	20	9	27	17	19	1	20	20	50	16
Nb	8	8	0	24	50	4	22	4	0	24	4	32
Rb	50	10	170	200	220	170	220	160	190	190	150	180
Sr	850	000	230	70	850	650	700	550	600	650	550	380
Th	5	5	20	15	0	0	10	0	0	10	10	10
Y	12	15	9	12	27	6	24	3	6	24	9	15
Zr	140	80	100	80	200	20	40	20	40	260	80	40

	59049A	59049B	59049C	59050	59051	59052	59054A	59056	59062	59064	59061
Ba (ppm)	1 400	1 000	1 100	1 300	600	900	800	1 400	1 300	1 800	1 700
Ce	160	90	190	180	40	130	320	120	200	150	260
F	320	170	210	470	110	180	480	250	360	920	550
Ga	16	20	18	18	18	20	18	22	18	18	20
La	80	40	80	120	0	60	190	60	80	90	130
Li	4	8	8	20	5	4	16	8	14	28	14
Nb	22	6	32	2	10	14	2	26	12	2	22
Rb	220	210	190	200	110	110	120	150	120	170	240
Sr	550	600	550	300	650	500	500	550	650	1 300	550
Th	10	0	15	55	15	10	95	0	10	10	10
Y	45	9	27	12	15	12	24	15	15	15	24
Zr	40	20	20	260	40	20	280	40	80	180	320

For the purpose of studying the trace elements, the rocks were considered to constitute six groups based on field identification. The first is the Boreas adamellite and correlatives; the second a small group of hornblende-bearing quartz monzonite to monzogranite (adamellite), the Agh of Bunting and Williams (1979); the third consists of the otherwise undifferentiated granite and granitic gneiss of the area; the fourth is the very small group, tonalitic gneiss; the fifth is alkaline rock; and the sixth is a group of basalt samples from the Anaconda Mine (Hallberg, 1985). The alkaline rock is drawn both from the current study and from Bunting and Williams (1979). The order of the grouping was chosen to make a reasonably orderly plot, it is not independent of trace element abundance.

Figures 4A to 4G compare average element abundance with the various rock groups. Fluorine in Figure 4A decreases regularly, except for the tonalite, in the sequence from Boreas-type through the Agh-type

hornblende-bearing rocks, the granites, and the tonalite to the alkaline rocks. The richness of F in the Boreas-type rocks is consistent with conspicuous visible fluorite in the type area of the Mount Boreas adamellite on LAVERTON and DUKETON (Gower, 1976; Bunting and Chin, 1979). The Li pattern is generally parallel to the F pattern. Figure 4C studies the distribution of Th by rock type. Again there is a general decrease from the Boreas-type rocks to the alkaline rocks, the exception being the hornblende-bearing Agh samples. Zirconium (Fig. 4D) decreases steadily from Boreas-type to alkaline rocks, while Ti (Fig. 4E) increases steadily. Figure 4F is a plot of the K_2O:Rb ratio which increases regularly, apart from tonalite, from the Boreas rocks to basalt. Figure 4G is a plot of the Zr:Ti ratio, which decreases regularly from the Boreas suite to basalt.

Figure 4H is a plot of Rb against Sr. The alkaline rocks have substantially the greatest range of Sr values. Rubidium values are more distinctive; the alkaline
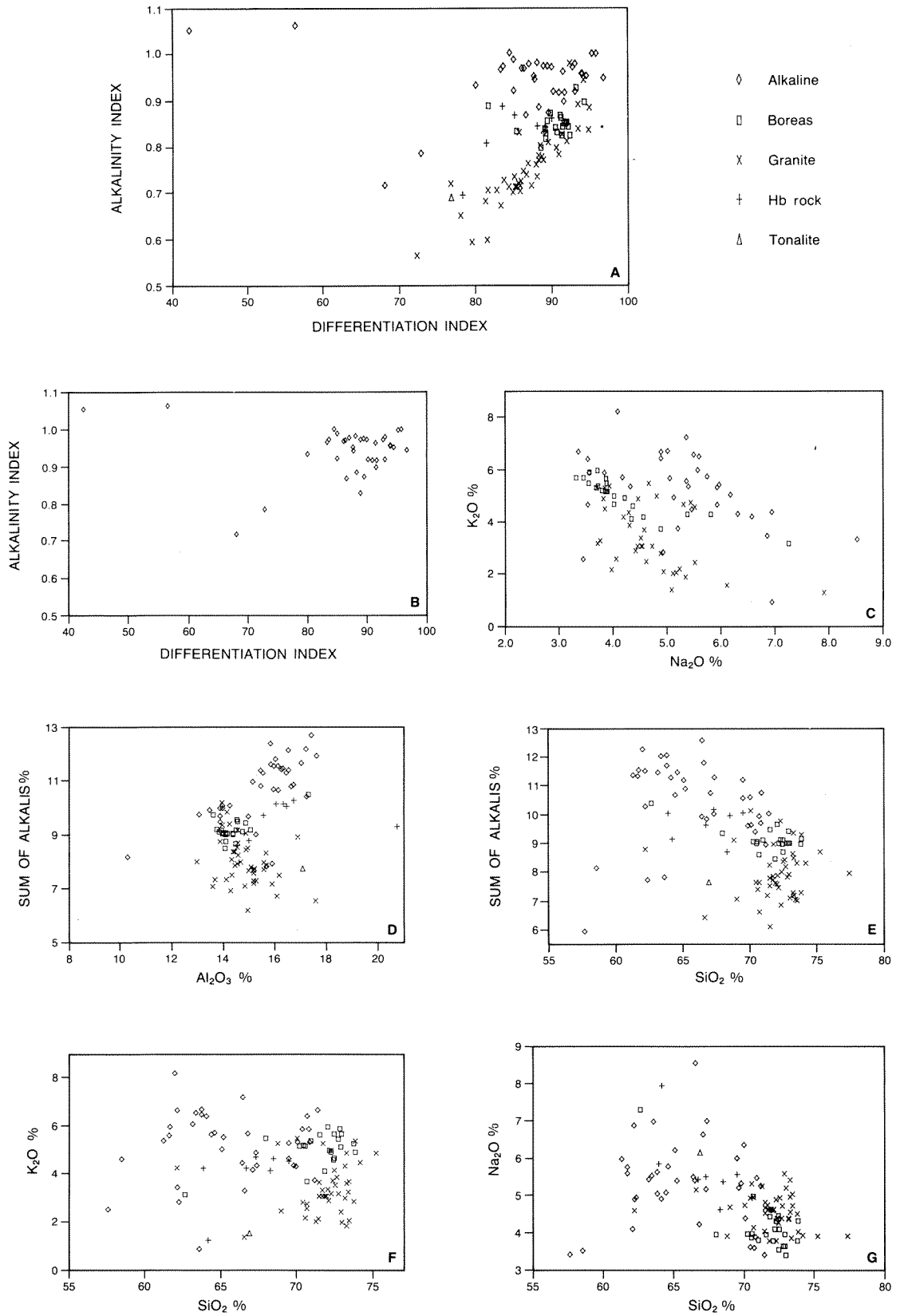
Figure 3. Major-element chemistry, a comparison of alkaline with subalkaline rocks of the Eastern Goldfields Province.
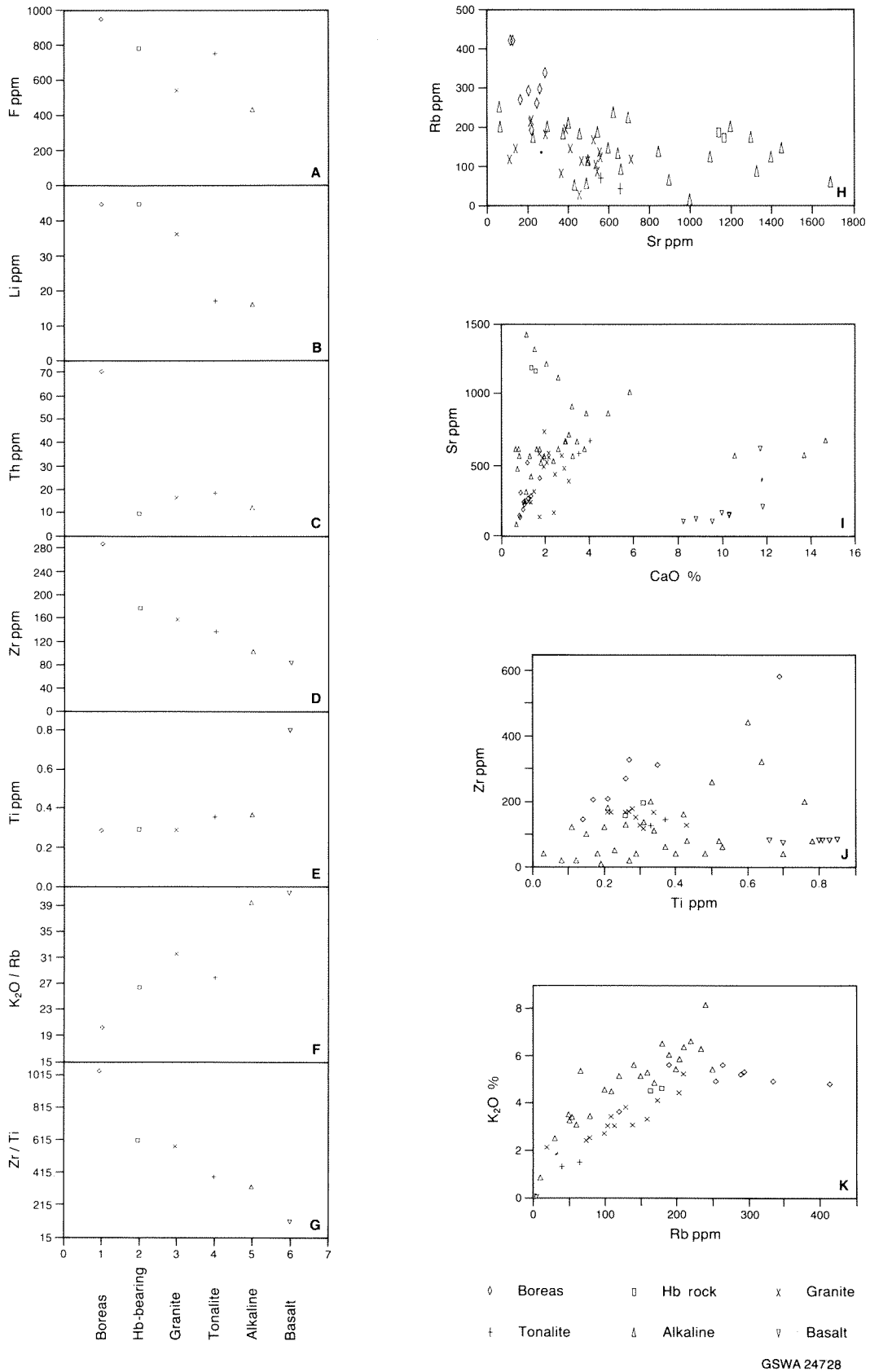
GSWA 24727

Figure 4. Trace-element chemistry, a comparison of alkaline with subalkaline rocks of the Eastern Goldfields Province.

97

rocks are richer in Rb than the tonalite, about the same as the average 'granite', and lower than the hornblende-bearing rocks or the Boreas group. The extreme values are noteworthy; the alkaline rocks on average are rich in Sr, poor in Rb, as opposed to the Boreas group with the opposite enrichment. The alkaline rocks in Figure 4I tend to have high values of combined CaO and Sr although they are greatly scattered. The plot of Zr against Ti in Figure 4J shows a similar tendency, the Boreas rocks plotting as a compact group on the Zr-rich, Ti-poor side of the more dispersed field of the alkaline rocks. Again, the other lithological types occupy a compact field in a mean position.

In all of the diagrams of Figure 4, the elements commonly taken as indices of strong or repeated fractionation of a magma are concentrated in the Boreas-type rocks, have intermediate values in the granite samples, and are least abundant in the alkaline suite. In some measures, the alkaline rocks seem not greatly evolved from the basalts. As might be expected due to low sample numbers, values from the tonalite and the hornblende-bearing rocks are more variable, but suggest that the hornblende-bearing rocks are more evolved than the granite samples. The tonalite seems less evolved than the alkaline rocks but, as might be expected, more evolved than the 'other granite'. The rock types are placed in a sequence for comparison of the state of evolution of the Boreas and alkaline suites with more usual rock types; not to imply that they form a cogenetic series.

RARE-EARTH ELEMENTS

All rare-earth elements (except Pm, Tb, and Tm) were determined by the Government Chemical Laboratories using the inductively coupled plasma spectrometer (ICP) after concentration by chemical means. The results for twelve samples collected from the alkaline suite in the Eastern Goldfields are listed in Table 6. Chondritic normalized values are plotted in Figure 5; normalization is according to the composite values of 12 chondrites by Wakita and Zellmar (unpublished), quoted by Henderson (1984, p. 10).

The normalized rare-earth patterns in Figure 5 are very similar, differing more in abundance of elements than in distribution pattern. The most exceptional

sample is 6520 in which the heavy rare earths (HREE) are strongly enriched over those from other samples.
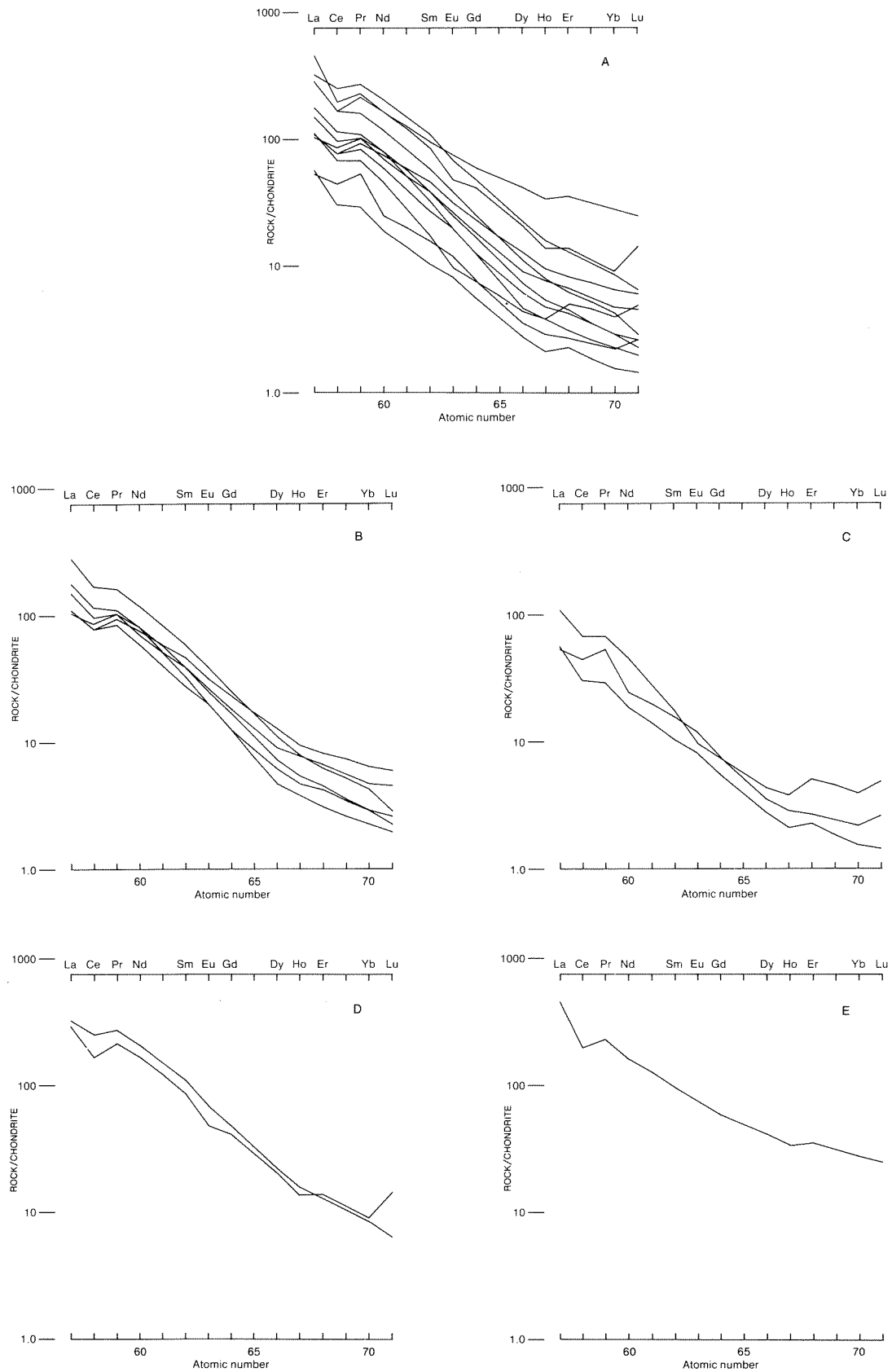
All analyses are plotted together on Figure 5A. General REE characteristics of the suite shown here are moderately strong enrichment in light rare-earth elements (LREE) — La ranging from about 50 to about 400 times chondritic values. The substantially lower enrichment of HREE ranges from near 1 to 10. The form of the curves is relatively featureless though there is some flattening of the curves toward the heavy rare earths, especially in the less enriched samples. The most notable general feature of the curves is the lack of any substantial Eu anomaly. Only samples 59046A (Red Hill) and 59049A (Woorana Well) show a trace of a negative Eu anomaly. There is a suggestion of a small but persistent negative Ce anomaly.

Although differences between samples are slight, four groups can perhaps be distinguished on rare-earth patterns. Group 2 (Fig. 5B) has a strongly enriched pattern with only weak flattening in the HREE range. The group includes samples 5687, 6522A, and 6589 from Widgiemooltha; 59045A from Woorana; and samples 56481 and 56482 from Gilgarna Rock. Group 1, which has the lowest overall enrichment in REE and somewhat greater flattening of HREE than other groups, is plotted on Figure 5C and includes samples 59024D from McAuliffe Well, 59033 from Twelve Mile Well, and 59046 from Woorana Well. The third group, plotted on Figure 5D (the most enriched with the least flattening of HREE for the first three groups), is represented by samples 66283 from WIDG-IEMOOLTHA and 59049A from Red Hill. The fourth group, shown by the single sample 6520 near Mount Martin on WIDGIEMOOLTHA, is plotted on Figure 5E, and among other samples on Figure 5A, and is much more enriched in HREE.

Petrographic and geographic differences seem not to correlate with the various groups which, with the exception of the sample classed as group four, are distinguished primarily on overall REE enrichment. Thus, variation in overall enrichment in this suite is probably best attributed to local variations within each locality, perhaps local concentration of REE-rich minerals. Indeed, there is a positive correlation of REE enrichment with TiO_2 in Figure 5E, suggesting that the rare earths reside in titanite and that enrichment in

TABLE 6. RARE EARTH ELEMENTS — NEW ANALYSES

Sample	5687	6520	6522A	6589	66283	59024D	59033	59045A	59046A	59049A	56481	56482
La (ppm)	96.3	154.00	51.6	36.7	109.1	18.2	19.6	62.3	37.7	98.9	38.5	35.3
Ce	154.00	185.00	88.7	71.9	233.0	42.0	28.1	104.0	62.0	154.0	72.2	79.8
Pr	19.8	27.8	12.8	11.3	33.0	6.62	3.67	13.7	8.25	26.1	10.2	12.6
Nd	75.4	105.0	45.1	48.0	132.0	16.2	12.4	51.5	30.3	109.0	38.5	52.5
Sm	11.7	19.1	7.66	9.09	21.5	3.18	2.11	6.48	3.44	17.3	5.49	7.72
Eu	2.91	5.51	1.98	2.33	4.95	0.9	0.61	1.46	0.72	3.51	1.49	1.82
Gd	6.67	15.6	4.83	6.2	12.6	2.01	1.5	3.31	2.01	11.0	3.26	4.44
Dy	3.38	12.7	2.78	3.87	6.76	1.33	0.85	1.44	1.11	6.35	1.91	2.25
Ho	0.62	2.73	0.60	0.75	1.26	0.31	0.17	0.30	0.23	1.09	0.38	0.43
Er	1.27	7.19	1.38	1.67	2.60	1.04	0.46	0.63	0.55	2.83	0.87	0.92
Yb	0.96	6.20	1.07	1.46	1.89	0.89	0.35	0.51	0.50	2.01	0.65	0.65
Lu	0.10	0.85	0.16	0.21	0.22	0.17	0.05	0.07	0.09	0.49	0.08	0.09

Figure 5. Chondrite-normalized trace-element distributions in the alkaline rocks.

GSWA 24729

99

titanite carries with it an overall enrichment in REE. The correlation does not extend to sample 6520, thus providing further evidence that its rare-earth suite has a different history than that of the other alkaline rocks.

It seems reasonable to attribute the smooth curve of normalized rare earths, strong LREE enrichment, and moderate flattening of the HREE pattern, to residual garnet in the source domain (Henderson, 1984a), especially considering the absence of an Eu anomaly in most samples. The lack of an Eu anomaly seems to eliminate residual plagioclase from either an anatectic or crystal-settling environment in the development of the rock. Derivation from an eclogitic source, or at least a source leaving residual eclogite, is suggested by residual garnet without feldspar. However, garnet peridotite is also a possible source.

MINERALS

Pyroxene and amphibole grains at several localities were analysed by microprobe at the CSIRO laboratories, Floreat Park, Western Australia, during 1980. Analyses were by energy-dispersive techniques on the MAC electron-beam microanalyser. One repesentative analysis from each sample scanned is listed in Table 2, other analyses are available on request from the GSWA (Libby, 1988).

Pyroxenes cluster strongly into two groups, one being aegirine-augite, the other a sodian ferrosalite to sodian augite, collectively referred to as ferrosalite. There is a distinct gap in the compositions of the two groups of pyroxenes in FeO* (total Fe as FeO), MgO, CaO, and Na_2O. For example, Na_2O in the aegirine-rich group lies between 7% and 9%, but between 1% and 3% in the aegirine-poor group.

The ferrosalite contains approximately 15% FeO*, 10% MgO, 20% CaO, 2% Na_2O, and 1% Al_2O_3. TiO_2 is a minor constituent or is absent. The mineral is notable for its high content of Na_2O relative to most salite, and low content of Al_2O_3 and TiO_2. The ferrosalite is light to medium green to rarely deep green in colour, and in some cases it may have a noticeably larger optic axial angle than diopside. Pyroxene of this group was analysed from Twelve Mile Well, Twin Peaks, Hamdorf Bore, Woorana Well, and Red Hill. Apart from those with aegirine-augite, most of the other localities considered as alkaline have pyroxene corresponding optically to that analysed as sodian ferrosalite. At a few localities the pyroxene is pale green and is presumed to be more diopsidic.

The aegirine-augite contains approximately 21% FeO*, 5% MgO, 10% CaO, 8% Na_2O, and only 0.5% to 0.65% Al_2O_3. The mineral has optical properties typical of aegirine-augite; small extinction angle, large optic axial angle, length-fast elongation, and deep-green colour. The mineral was positively identified, either optically or chemically, only at the analysed localities (McAuliffe Well and Mount Blackburn), at the Fitzgerald Peaks (Lewis and Gower, 1978), and at Gilgarna Rocks. However, much of the pyroxene at Woorana Well and at the localities on WIDGIEMOOLTHA has

the characteristic deep-green colour, rather large extinction angles and, in some cases, length-fast elongation of aegirine-augite.

Amphibole from parts of the McAuliffe Well body is clearly alkaline, varying from richterite to magnesio-riebeckite. However, at locality 59026 it is hornblendic, despite the association with coarse igneous clinopyroxene and the zoned, euhedral, alkali feldspar seen at the more alkaline localities. The hornblende may be explained by proximity to an ultramafic xenolith; however, other parts of the McAuliffe body also have amphibole for which there is no optical reason to suppose to be alkaline. It seems probable that the body is zoned, varying in alkalinity.

Riebeckite, identified optically, is the characteristic amphibole at Gilgarna Rocks and at locality 6522A on WIDGIEMOOLTHA. A dusky blue-grey amphibole, probably richterite or arfvedsonite, is the principal mafic mineral in sample 6522B, accompanied by sodic clinopyroxene. Sodic amphiboles are also present in certain samples at Mount Blackburn and in the Woorana Well area.

The most characteristic feldspar is subhedral grains of sharply zoned hypersolvus alkali feldspar sitting in a finer seriate matrix of quartz and alkali mafic minerals. The strong zoning appears to be between K_2O and Na_2O in most cases. These feldspars are described further in the section on petrography. Apatite is prominent in some alkaline samples, reflecting the moderately high average P_2O_5 content of 0.22%, compared with 0.10% for the 'other granite', and 0.08% average for the Boreas group. Titanite (sphene) is characteristic of both the alkaline and Boreas suites. The titanite of both suites tends to be mottled orange in colour and have patches of low birefringence.

Because of the unusual properties of titanite in the alkaline and the Boreas suites, several grains were analysed in the course of analysis of pyriboles; however, the distinctive properties are probably due to elements present below the detection limits of the probe. The analyses are listed in Table 7.

GEOCHRONOLOGY

Dating of the alkaline and associated rocks (to 1981) has been summarized by Libby and de Laeter (1981). Two mildly alkaline masses were dated by Rb–Sr whole-rock techniques at 2520 ± 113 Ma (I.R. = 0.7014) at Woorana Well, and 2489 ± 82 Ma (I.R. = 0.7012) at Twelve Mile Well. The Mount Boreas adamellite had earlier been similarly dated by Roddick at 2480 Ma (Bunting and Chin, 1979), which suggests it is slightly younger than the alkaline suite. Subsequent dating by Stuckless and others (1981), by Pb–Pb methods, separated the Boreas and alkaline suites further, with a date of 2370 ± 100 Ma for the former and 2760 ± 210 Ma for the latter. The relative ages expressed in these dates are consistent with field observations of Bunting (Stuckless and others, 1981).

TABLE 7. REPRESENTATIVE MICROPROBE ANALYSES — TITANITE

Sample	59029F	59042A	59043B	59044C	59045A	59058C	59064
TiO_2 (%)	36.44	35.55	32.99	36.35	36.64	35.92	33.83
Al_2O_3	0.87	(a)	3.17	1.10	1.29	1.88	2.84
Cr_2O_3	0.19	(a)	(a)	0.31	0.23	0.22	(a)
FeO	2.29	2.98	2.46	2.58	2.14	2.1	3.13
NiO	(a)	(a)	(a)	0.36	(a)	(a)	(a)
MnO	(a)	(a)	(a)	0.24	(a)	(a)	(a)
CaO	28.06	28.45	29.07	28.82	28.76	28.88	19.43
K_2O	(a)	(a)	(a)	(a)	(a)	0.29	1.21
Total	97.52	98.46	97.81	100.16	99.57	100.59	94.96

(a) Below limit of detection.

The date of the alkaline rocks measured by the Pb–Pb method differs uncomfortably from that measured by Rb–Sr, even though the ranges of uncertainty for the two methods overlap slightly between 2550 and 2571 Ma. However, all measures of age indicate that the Boreas suite is younger than the alkaline suite. This result is consistent with the geochemical evidence that the Boreas suite is more evolved than the alkaline suite.

If it is accepted that the date of emplacement of the alkaline rocks lies within the range of overlap in the uncertainties of the two techniques (2550 to 2570 Ma), then the alkaline rocks are slightly younger than the 2565 to 2650 Ma dates of Roddick and others (1976), and Cooper and others (1978), on synkinematic granitoids between the Keith–Kilkenny and Ida lineaments (Stuckless and others, 1981). This places the alkaline suite after the synkinematic suite, but before late, evolved Boreas granites.

Further Rb–Sr dating of rocks with alkaline affinity at the Fitzgerald Peaks has produced an age of 2360 ± 96 Ma, very close to the Pb–Pb date on the Boreas suite (de Laeter and Lewis, 1978). Furthermore, the initial $^{87}Sr/^{86}Sr$ ratio of 0.70436 is much greater than that of the alkaline rocks at Woorana and Twelve Mile Wells. The Fitzgerald Peaks body is heterogeneous. The isochron is made up of data from biotite and hornblende adamellite as well as from the alkaline rocks, with no indication on the isochron of mixed data. It seems that the various rock types have equilibrated together. Remobilization of the alkaline rocks either by Boreas-type magmas, or in the course of generation of Boreas-type magma, is suggested by the later date and higher initial $^{87}Sr/^{86}Sr$ ratio than alkaline rocks elsewhere in the province; as well as by the apparently intimate involvement of alkaline rocks with possible Boreas equivalents.

The Sr-development line at the Fitzgerald Peaks (Libby and de Laeter, 1981, figure 3) projects to the mantle development curve at a younger date than the Woorana and Twelve Mile Well samples, as might be expected of an evolved or 'partially evolved' rock.

Preliminary Sm–Nd model (T_{CHUR}) dates (I. R. Fletcher, written communication) from Woorana Well (samples 59046A, 59046B, and 59047) are respectively 2500 ± 40 Ma, 2550 ± 40 Ma, and 2510 ± 60 Ma, but are sensitive to the assumed original reservoir composition. Similar dating on the Mount Boreas body (samples 40591A and 40592A, near Granites Bore, DUKETON) gives model dates of 2600 ± 30 Ma and 2630 ± 30 Ma. If the assumptions of the model can be accepted, then the data are consistent with Rb–Sr dating and are within the extreme error limits of the Pb–Pb dating of the alkaline suite. Together with the Rb–Sr results, they imply virtually no crustal residence time for the alkaline magma before emplacement to its present position. Accepted as presented, the Sm–Nd data eliminate the alkaline suite as a precursor to the Boreas suite, but would accept as precursors the Windarra granite or the regional synkinematic granites of Roddick and others (1976), or Cooper and others (1978).

The recent dating of single zircon grains from granites in the central and southern Eastern Goldfields (Hill and Compston, 1986) has produced ancient dates on relict grains of 2900 to 3200 Ma in the southern part of the Eastern Goldfields, and emplacement dates of 2650 to 2690 Ma for large bodies of granite near Norseman. The Norseman rocks are perhaps equivalent to the regional synkinematic granites farther north. Alkali-rich granite at Mungari is dated at 2610 Ma. Further work is required to show whether the Mungari locality belongs to the alkaline or to the subalkaline suite, but with more than 73% SiO_2 (Oversby, 1975) giving 30% normative quartz and 0.65% normative corundum, the rocks of this locality look to be firmly subalkaline.

Thus the dating suggests a plutonic history in which ancient crust existed, at least in the southern part of the province, as long ago as 2900 to 3200 Ma. Through this crust, major granitic bodies were emplaced between 2650 and 2690 Ma. Near the end of this period of widespread orogenesis, plutonic activity became more restricted during the emplacement of subalkaline granitic rock (Mungari) at about 2610 Ma. Perhaps after partial stabilization of this part of the craton, alkaline rock was effectively injected directly from the mantle at about 2550 Ma. The final identified major plutonic activity seems to have been the remobilization of regional granite to form the Mount Boreas adamellite and equivalent bodies, emplaced at 2370 to 2480 Ma, together with emplacement of Norseman quartz reefs (Turek, 1966).

101

Other dated alkaline rocks in the Eastern Goldfields are difficult to relate to the Archaean alkaline suite. The Mount Weld carbonatite has been dated by K–Ar techniques at 2064 Ma, and by Rb–Sr as 2020 Ma (Willett and others, 1986). The alkaline rocks at the Teague Ring Structure are petrographically similar to the Archaean alkaline rocks, but have been dated by Bunting and others (1982) as Proterozoic. However, the isochron is seriously disturbed; not only have the rocks been affected by weathering but they show abundant evidence of late high-energy disturbance. Tentative isochrons were placed at 1630 and 1260 Ma with very high initial $^{87}Sr/^{86}Sr$ ratios. Other dating techniques (e.g. zircon) may establish a correlation with the Archaean rocks.

DISCUSSION

DISCRETE SUITE

The alkaline suite, though only weakly alkaline, seems to be sharply distinct from the more normal subalkaline granitic rocks of the Eastern Goldfields. Compositional gaps between the suites exist in various plots of the chemistry (e.g. Fig. 3A). Furthermore, chemical trends between the groups seem distinct; again on Figure 3A the alkalinity index of the alkaline suite is either independent of differentiation index, or decreases slowly with differentiation, while the alkalinity of the more normal granitoids increases strongly with differentiation index.

Most of those alkaline rocks which have been dated are further distinguished from the subalkaline rocks by their low initial $^{87}Sr/^{86}Sr$ ratio. The exception is the dated locality at the Fitzgerald Peaks (de Laeter and Lewis, 1978) where the initial ratio of the suite is high, 0.7044. However, here the date at 2360 Ma (de Laeter and Lewis, 1978) corresponds more closely with the Boreas suite at 2370 Ma (Stuckless and others, 1981) than with other alkaline rocks at about 2500 Ma (Libby and de Laeter, 1981) or 2760 Ma (Stuckless and others, 1981). The intimate involvement of the two suites at this locality, and the dating, suggest resetting of the initial $^{87}Sr/^{86}Sr$ ratio upon remobilization and re-emplacement of the alkaline rocks.

The alkaline suite seems to have been developed in response to a tectonic situation which developed in a restricted area. It is restricted not only to the Eastern Goldfields, but perhaps more specifically to the more tectonically active portions of the province (Hallberg, 1985).

The alkaline rocks probably evolved from the mantle or mantle-like rocks, at a later date than calc-alkaline granitic rocks of the area, perhaps from a more alkaline source, or with a metamsomatic stage in their history.

METASOMATISM

Some features of the alkaline suite argue for, and others against, a metasomatic origin. The vague, seriate textures of most samples are consistent with metamorphism *in-situ*. The alkalinity of the suite, while weak, is unusual and difficult to explain by differentiation from conventional deep-seated mafic material. The constant alkalinity index, together with varying differentiation index, may be an artifact of the manner in which the alkaline rocks are recognized. But the compositional gap between the two suites suggests that this is a real genetic difference between the alkaline and subalkaline rocks. The flat trend suggests lack of systematic magmatic evolution. Also, the general scatter in X–Y plots of various chemical variables is more consistent with variable addition of elements than with an orderly line of liquid descent. However, some of this scatter may be due to the mixing of analyses from samples at widely separated localities.

The Ce anomaly in the chondrite-normalized rare-earth plots is similar to that of carbonatites, and suggests that a fenitic origin of the alkaline rocks should be considered. However, other trace and rare-earth data would require that the fenitized material be a primitive rock, say a gabbro. Gabbro is not characteristically associated with the syenites at the surface (but note the association of the syenite at McAuliffe Well with a sequence of mafic volcanics). Thus, if the syenite is derived from mafic rock, at most localities this association would have to be at depth and the syenites would require a later stage of injection to their present level.

IGNEOUS EMPLACEMENT

A few igneous features are opposed to a purely metasomatic origin for the syenites. Some localities (e.g. McAuliffe Well) have euhedral alkali feldspar with euhedral oscillatory zoning which is difficult to explain as a product of metamorphism. Likewise, the pipe-like body with xenoliths and associated alkali dykes at Hamdorf Bore is more easily explained as an igneous feature.

MAFIC INCLUSIONS

Many of the units have mafic enclaves or schlieren, presumably after such enclaves. Both Gower and Bunting (1976) and Lewis and Gower (1978) have graphically described mafic enclaves at the Fitzgerald Peaks, attributing them tentatively to the breakup of dykes observed in the enclosing granitoids. However, the mafic materials may well be of deeper origin. A sample (29804) described by Lewis and Gower is a strongly layered andesine–hornblende–clinopyroxene granofels of granulitic texture in which the hornblende is deep olive green and the pyroxene is green. Most of the plagioclase in the leucocratic layers has been altered to fine sericite, but, where fresh, it can be identified as andesine (about An_{45}) at least as calcic as the plagioclase in the body of the xenolith. Thus, if the leucocratic layers are syenite, which has been injected into the rock, they have reached equilibrium with the enclave. Another possibility is that the enclave is a relic of a deep-seated, layered mafic source rock. However, there is no evidence of eclogitic texture or of relic garnet, or garnet-like masses which rare-earth data at other localities would seem to require in the immediate source

area. It is also to be noted that this is an atypical syenite locality complicated by a high $^{87}Sr/^{86}Sr$ ratio and lithological heterogeneity, presumably associated with mixing of rock types. The locality also lacks rare-earth data. In any case, mafic schlieren and xenoliths are common as well at other alkaline localities. Examples are the ultramafic biotite–clinopyroxene xenolith which was found at locality 59026 at McAuliffe Well, and the xenoliths, rafts, and relatively mafic schlieren at Twelve Mile Well. Although the McAuliffe body is emplaced in mafic rock, the Twelve Mile Well locality is far from mapped mafic rock. Thus, if the xenoliths at this locality have been involved in the origin of the rock it would need to have been at depth.

OTHER CONSIDERATIONS

Further constraints on a general petrogenesis for the suite include the low $^{87}Sr/^{86}Sr$ ratios which would seem to preclude anatexis after any substantial residence of material with intermediate composition. That is, if magmatic, then direct derivation from mafic rock (or very quick evolution) is favoured over multiple separate stages of crustal evolution. Likewise, lack of Eu anomalies would seem to eliminate from consideration any evolution, either crystal fractionation or partial melting, in the upper crust where plagioclase might be assumed to be a residual product. This latter point is of special significance for these low-Ca rocks.

SUMMARY

Rather mildly alkaline rocks are sparsely, but rather evenly, distributed throughout the length of the Eastern Goldfields Province. They occur especially in its tectonically more active parts and are sharply confined to the province. Some of this alkaline activity is Proterozoic (the Mount Weld carbonatite), but most seems to be late Archaean, though there is possible disagreement among techniques on exact dates. The alkalinity of the suite is expressed by the following: pyroxene compositions which range from slightly sodic ferrosalite to aegirine-augite; a lower quartz content than is normal in granitic rocks; and hypersolvus alkaline feldspar. All analysed samples are quartz normative, but some have an alkalinity index greater than one and have normative acmite.

The origin of the alkaline rocks is still obscure, but they have geochemical signatures of little-evolved rocks; most indices of evolution range between those of the tonalites and of the basic rocks of the area. Rare-earth geochemistry indicates that if the alkaline rocks are the product either of conventional anatexis or of differentiation by crystal settling, then it took place at depth and probably involved eclogite (or perhaps garnet pyroxenite) as a restite. Alternatively, the alkaline rocks may be of metasomatic origin; however, trace-element geochemistry suggests that the parent of the fenitized rock would be quite basic. A pure fenitic explanation lacks general appeal, because some localities display igneous features in the alkaline materials.

A possible (compromise) origin is through metasomatism, at either moderate depth (fenitization) or profound depth (lower crustal or upper mantle metasomatism), with near-complete melting in the former case or partial melting in the latter case, preceding final emplacement by igneous processes. In the former process, depletion of primary Ca is difficult without separating plagioclase, thus the latter process is preferred.

FURTHER WORK

A complete understanding of the alkaline rocks requires more work. There is a special need for detailed field mapping, which might be particularly productive at Twelve Mile Well, at McAuliffe Well, and in the batholith between Mount Blackburn and Red Hill. At Twelve Mile Well, field relationships with included mafic rafts are important. The Mount Blackburn–Red Hill batholith is a large body with complex lithology, fine exposures, and substantial and varied alkaline rocks. The McAuliffe Well area combines some of the most alkaline rock in the belt with a large area of good exposure.

Dating is needed on the aegirine-augite bearing rocks at McAuliffe Well and Mount Blackburn to establish whether these strongly alkaline bodies may be chronologically more closely related to the Proterozoic Mount Weld carbonatite than to the Archaean alkaline suite. Zircon dating on the less alkaline rocks should resolve apparent conflicts between current Rb–Sr, Sm–Nd, and lead dating.

REFERENCES

BONIN, B., 1986, Ring complex granites and anorogenic magmatism: North Oxford Academic Press, London.

BUNTING, J. A., 1980, Kingston, Western Australia: Western Australia Geological Survey 1:250 000 Geological Series Explanatory Notes.

BUNTING, J. A., BRAKEL, A. T. and COMMANDER, D. P., 1982, Nabberu, Western Australia: Western Australia Geological Survey 1:250 000 Geological Series Explanatory Notes.

BUNTING, J. A., and CHIN, R. J., 1979, Duketon, Western Australia: Western Australia Geological Survey 1:250 000 Geological Series Explanatory Notes.

BUNTING, J. A., and WILLIAMS, S. J., 1979, Sir Samuel, Western Australia: Western Australia Geological Survey 1:250 000 Geological Series Explanatory Notes.

COOPER, J. A., NESBITT, R. W., PLATT, J. P. and MORTIMER, G., 1978, Crustal development in the Agnew region, Western Australia, as shown by Rb/Sr isotopic and geochemical studies: Precambrian Research, v. 7, p. 31–59.

DEER, W. A., HOWIE, R. A. and ZUSSMAN, J., 1978, Rock-forming minerals, v. 2A, single-chain silicates: Longman, London.

de LAETER, J. R. and LEWIS, J. D., 1978, The age of the syenitic rocks of the Fitzgerald Peaks, near Norseman: Western Australia Geological Survey Annual Report for 1977.

ELIAS, M. and BUNTING, J. A., 1982, Wiluna, Western Australia: Western Australia Geological Survey 1:250 000 Geological Series Explanatory Notes.

GOWER, C. F., 1976, Laverton, Western Australia: Western Australia Geological Survey 1:250 000 Geological Series Explanatory Notes.

GOWER, C. F. and BUNTING, J. A., 1976, Lake Johnston, Western Australia: Western Australia Geological Survey 1:250 000 Geological Series Explanatory Notes.

HALLBERG, J. A., 1985, Geology and mineral deposits of the Leonora-Laverton area, Northeastern Yilgarn Block, Western Australia: Hesperian Press, Perth, Western Australia.

HENDERSON, P., 1984, Rare Earth Element Geochemistry: Elsevier, Amsterdam.

HENDERSON, P., 1984a, General geochemical properties and abundances of the rare earth elements *in* Rare Earth Element Geochemistry *edited by* P. HENDERSON: Elsevier, Amsterdam.

HILL, R. I. and COMPSTON, W., 1986, Age of granite emplacement, southeastern Yilgarn Block, Western Australia: Australian National University Research School of Earth Sciences, Annual Report for 1986.

HONMAN, C. S., 1917, The geology of the North Coolgardie Goldfield, Part 1: The Yerilla District: Western Australia Geological Survey, Bulletin 73, p. 36.

JAQUES, A. L., CREASOR, R. A., FERGUSON, J. and SMITH, C. B., 1985, A review of the alkaline rocks of Australia: The Geological Society of South Africa, Transactions, v. 88, p. 311–334.

JAQUES, A. L., LEWIS, J. D. and SMITH, C. B., 1986, The kimberlites and lamproites of Western Australia: Western Australia Geological Survey, Bulletin 132.

JUTSON, J. T., 1915, Yerilla: Western Australia Geological Survey progress report for 1914, p. 20.

LEWIS, J. D. and GOWER, C. F., 1978, Syenitic rocks of the Fitzgerald Peaks, near Norseman, *in* Contributions to the geology of the Eastern Goldfields Province of the Yilgarn Block: Western Australia Geological Survey Report 9.

LIBBY, W. G., 1978, The felsic alkaline rocks, *in* Contributions to the geology of the Eastern Goldfields Province of the Yilgarn Block, by W. G. Libby, J. D. Lewis and C. F. Gower: Western Australia Geological Survey Report 9.

LIBBY, W. G., 1988, Analyses of alkaline rocks and minerals from the Eastern Goldfields Province: Western Australia Geological Survey, Petrology Report 1486 (unpublished).

LIBBY, W. G. and de LAETER, J. R., 1981, Rb-Sr geochronology of alkaline granitic rocks in the Eastern Goldfields Province: Geological Survey of Western Australia, Annual Report for 1980, p. 98–103.

LIBBY, W. G. and LIPPLE, S. L., 1978, A monzonitic pluton near Lake Shaster: Geological Survey of Western Australia, Annual Report for 1977, p. 60–63.

MUTSCHLER, F. E., GRIFFIN, M. E., SCOTT STEVENS, D. and SHANNON, S. S., Jr., 1985, Precious metal deposits related to alkaline rocks in the North America Cordillera – an interpretive review: Geological Society of South Africa, Transactions, v. 88, p. 355–377.

OVERSBY, V. M., 1975, Lead isotopic systematics and ages of Archaean acid intrusives in the Kalgoorlie–Norseman area, Western Australia: Geochimica et Cosmochimica Acta, v. 39, p. 1107–1125.

RODDICK, J. C., COMPSTON, W. and DURNEY, D. W., 1976, The radiometric age of the Mount Keith Granodiorite, a maximum age estimate for an Archaean greenstone sequence in the Yilgarn: Precambrian Research, v. 3, p. 55–78.

SOFOULIS, J., 1963, Boorabbin, Western Australia: Western Australia Geological Survey, 1:250 000 Geological Series Explanatory Notes.

SOFOULIS, J. and BOCK, W., 1962, Progress report on the regional survey of the Widgiemooltha sheet area, SH51-14, International Series: Western Australia Geological Survey, Annual Progress Report for 1961.

SORENSON, H., 1974, Alkali syenites, feldspathoidal syenites and related lavas, *in* The Alkaline Rocks *edited by* H. SORENSON: John Wiley and Sons, London.

STRECKEISEN, A. L., 1973, Classification and nomenclature of plutonic rocks, recommendations: Neues Jahrbuch fur Mineralogie, Monatshefte 1973, p. 149–164.

STUCKLESS, J. S., BUNTING, J. A. and NKOMO, I. T., 1981, U-Th-Pb systematics of some granitoids from the northeastern Yilgarn Block, Western Australia and implications for uranium source: Journal Geological Society Australia, v. 28, p. 365–375.

THOM, R., LIPPLE, S. L. and SANDERS, C. C., 1977, Ravensthorpe, Western Australia: Western Australia Geological Survey 1:250 000 Geological Series Explanatory Notes.

THORNTON, C. P. and TUTTLE, O. F., 1960, Chemistry of igneous rocks I. Differentiation Index: American Journal Science, v. 258, p. 664–684.

TUREK, A., 1966, Rubidium–strontium isotopic studies in the Kalgoorlie–Norseman area, Western Australia: Australian National University, Ph. D. thesis, (unpublished).

van de GRAAFF, W., and BUNTING, J. A., 1975, Neale, Western Australia: Western Australia Geological Survey 1:250 000 Geological Series Explanatory Notes.

WILLETT, G. C., DUNCAN, R. K. and RANKIN, R. A., 1986, Geology and economic evaluation of the Mt. Weld carbonatite, Laverton, Western Australia: Fourth International Kimberlite Conference, Perth 1986, Extended abstracts.

WILLIAMS, I. R., GOWER, C. F. and THOM, R., 1976, Edjudina, Western Australia: Western Australia Geological Survey 1:250 000 Geological Series Explanatory Notes.

HYDROGEOLOGY OF THE GILLINGARRA BOREHOLE LINE, PERTH BASIN

by J. S. Moncrieff

ABSTRACT

The Gillingarra Line consists of twenty bores drilled at eight sites on an east–west line across the Perth Basin between Lancelin and Mogumber, about 100 km north of Perth. The bores were drilled between August 1981 and August 1986 to a maximum depth of 1201 m and with an aggregate depth of 10 868 m, to investigate the geology and hydrogeology of the central Dandaragan Trough.

The drilling intersected a complex sequence consisting of block-faulted, largely non-marine, Early Jurassic to Early Cretaceous sedimentary rocks which are unconformably overlain by gently folded, marine and non-marine, Early to Late Cretaceous sedimentary rocks, and flat-lying, marine and non-marine, Late Tertiary–Quaternary sediments beneath the Swan Coastal Plain.

The Leederville Formation beneath the Swan Coastal Plain, the Leederville and Parmelia Formations (which are in hydraulic continuity) beneath the Dandaragan Plateau, and the Yarragadee Formation form major aquifer systems of interbedded sandstone, siltstone, and shale that range in thickness from about one hundred to nearly three thousand metres. The Late Tertiary–Quaternary sediments are composed of sand and limestone, and form a 30 m-thick, unconfined aquifer system beneath the Swan Coastal Plain. The aquifer systems are separated by discontinuous confining units of siltstone and shale.

Groundwater salinity is generally less than 1000 mg/L total dissolved solids, but in the Leederville and Parmelia Formations aquifer system the salinity ranges up to 1850 mg/L, the higher salinity groundwater occurring near the Darling Fault.

Large potable groundwater resources are present in this area, principally beneath the Swan Coastal Plain and the western part of the Dandaragan Plateau.

KEYWORDS: Perth Basin; hydrogeology; geology; groundwater; stratigraphy

INTRODUCTION

The Gillingarra Line consists of twenty bores drilled at eight sites (designated GL1 to GL8) on an east–west line across the Perth Basin between Mogumber and Lancelin, 100 km north of Perth (Fig. 1).

The drilling was undertaken by the Geological Survey of Western Australia (GSWA) as part of an assessment of the deep groundwater resources of the Perth Basin and was jointly funded by the Commonwealth and State Governments under the National Water Resources Assessment Program. The nearest lines of similar deep bores are the Moora Line (Briese, 1979a), 40 km to the north, and the Gingin Brook Line (Sanders, 1967), 35 km to the south. A network of deep monitoring bores (Artesian Monitoring Network), drilled for the Water Authority of Western Australia, extends southwards from the Gingin Brook Line and a number of deep bores drilled for private water supplies are located in the area.

The shallow groundwater resources of the Lancelin–Guilderton area have been described by Moncrieff and Tuckson (1989), and of the Lancelin–Cervantes area by Kern (1989).

About half of the area is cleared for agriculture, mainly grazing. The remaining native bushland includes the Moore River National Park on the eastern part of the Swan Coastal Plain, south of the Moore River.

Water supplies for all the towns in the area are obtained from groundwater which is also used for farm water supplies, and increasingly for irrigation. Abstraction in the Gingin Groundwater Area (Fig. 1) is licensed by the Water Authority.

PHYSIOGRAPHY AND CLIMATE

The area can be divided into five physiographic regions (Fig. 2): the Darling Plateau, the Yarra Yarra Region, the Dandaragan Plateau, the Arrowsmith Region, and the Swan Coastal Plain (Playford and others, 1976).

The Darling Plateau is a laterite-capped plateau formed over Precambrian crystalline rocks immediately east of the Perth Basin. It is bounded to the west by the Darling Scarp. The fault-line scarp of the Darling Fault, near Mogumber, is over 100 m high and is about 2.5 km east of the subsurface position of the fault.

The Yarra Yarra Region lies at the foot of the Darling Scarp between the Darling and Dandaragan Plateaus. It is characterized by poor drainage and numerous lakes and swamps, and in the Mogumber area has an elevation of 170–190 m above sea level.

The Dandaragan Plateau is an undulating sand and laterite covered plateau with an elevation of 140–260 m. Its western boundary in the south is the Gingin

Scarp, a former shoreline, which rises 60–160 m from the Swan Coastal Plain, and in the north is the Dandaragan Scarp, an erosion scarp, which rises 50–100 m from the Arrowsmith Region. There is little runoff from the plateau because of the permeable surface cover. The Moore River has eroded a steep-sided valley, up to 40 m deep, into the plateau surface.

The Arrowsmith Region is similar to the Dandaragan Plateau but is more dissected. It occurs between the Gingin and Dandaragan Scarps.

The Swan Coastal Plain lies between the Gingin Scarp and the coast and is about 38 km wide in the vicinity of the Gillingarra Line. It may be subdivided into three main units; the Pinjarra Plain, the Bassendean

Dunes, and the Coastal Belt. The Pinjarra Plain is a flat area of between 80 m and 90 m elevation at the base of the Gingin Scarp west of Gingin. The Bassendean Dunes are a belt of low dunes with interdunal lakes and seasonal swamps which occur on the eastern part of the coastal plain. The unit reaches a maximum elevation of 95–120 m in the east. The Coastal Belt consists of the Spearwood Dunes to the east, which are rounded dunes and reach a maximum elevation of about 145 m south of GL2, and the Quindalup Dunes along the coast, which are steep sided and reach an elevation of about 80 m.

The area has a Mediterranean climate. The average annual rainfall decreases from 626 mm at Lancelin to 559 mm at Mogumber (Commonwealth Bureau of
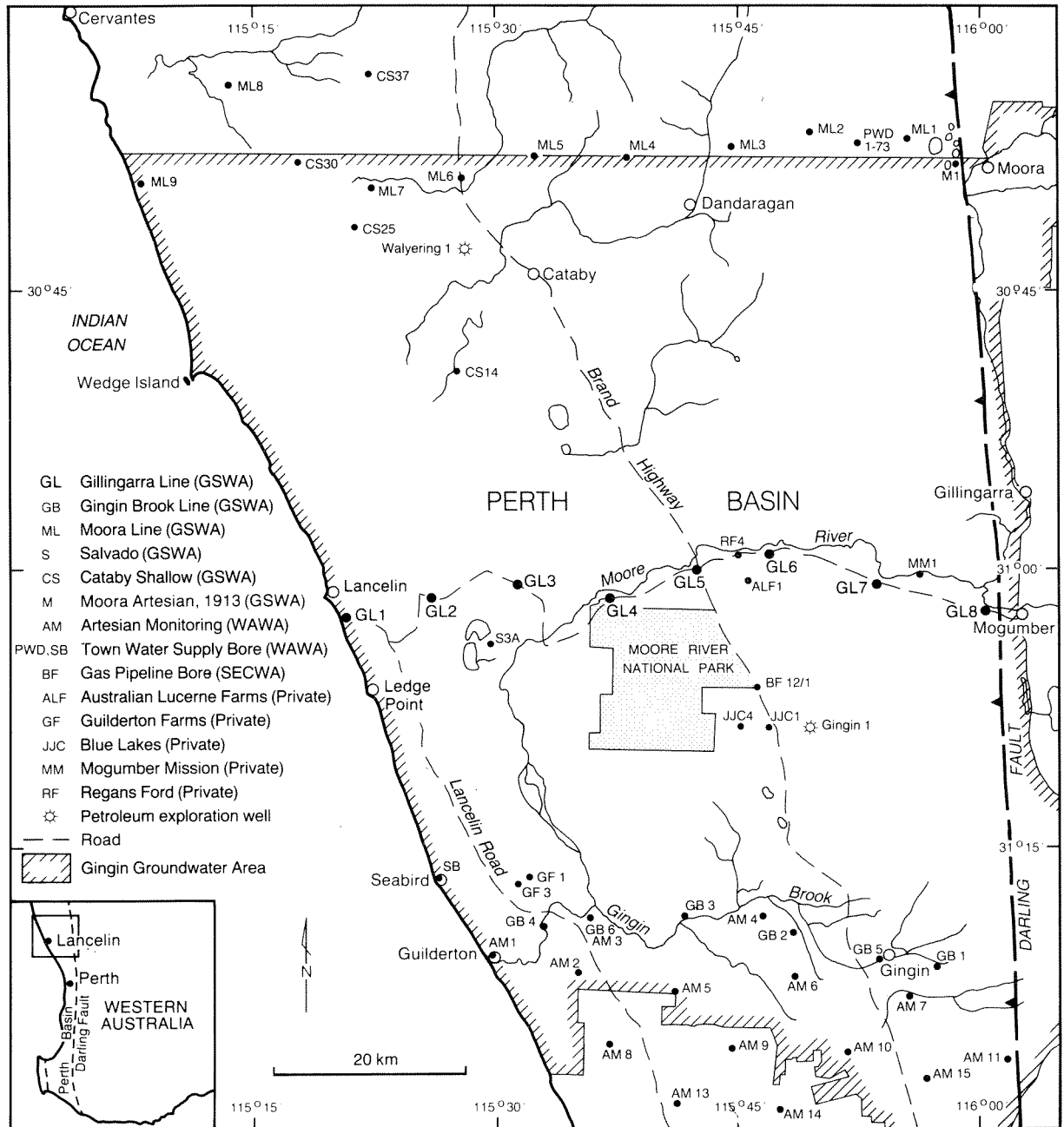

Figure 1. Location map

106

Meteorology) and 90% of this falls between April and October. The mean annual evaporation ranges from about 1950 mm at the coast to about 2150 mm at the Darling Scarp. Evaporation exceeds rainfall except during the months of June to August.

INVESTIGATION PROGRAM

Drilling of the Gillingarra Line was undertaken in two stages; from August 1981 to February 1982, and from September 1985 to August 1986. The bores were drilled to a maximum depth of 1201 m (GL7A) and the aggregate depth drilled was 10 868 m.

The bores were all drilled by the Mines Department Drilling Branch using a Midway-Skytop rig employing the mudflush rotary technique, except for the water-supply bore GL1W, which was drilled by the Royal Australian Engineers using the airflush rotary technique. A summary of drilling and bore information is given in Table 1 and a detailed account of the bore construction and sampling techniques is contained in Moncrieff (1989) and Moncrieff and Smith (1989).

Cuttings were collected over three-metre depth intervals for lithological logging and are stored at the GSWA Core Library. A suite of wire-line geophysical logs was run at the completion of each stage of drilling (Moncrieff, 1989; Moncrieff and Smith, 1989).
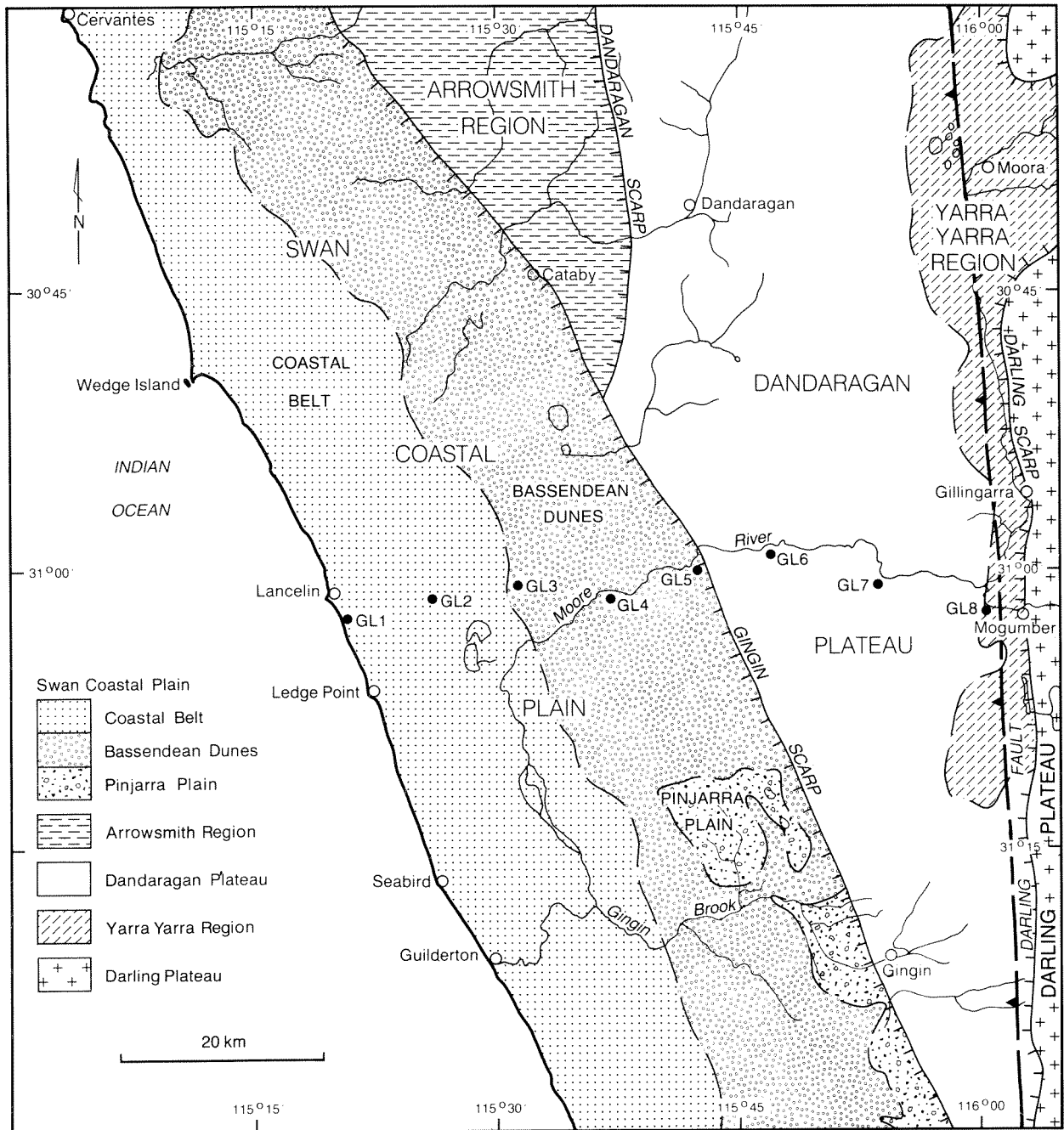

Figure 2. Physiography

GSWA 24766

107

TABLE 1. SUMMARY OF BORE DATA

Bore	Interval	AMG Zone 50		Construction		Total depth (m bns)	Elevation (m AHD)		Perforated interval (m bns)	Form-ation	Potentiometric head (m AHD)	Salinity TDS (mg/L)	Airlift yield (m3/d)	Status
		Easting	Northing	Commenced	Completed		Natural surface	Top of casing						
1A	1	348000	6564250	05.03.86	10.04.86	1 002	4.29	4.98	200.5–206.5	Kll	19.84(b)	910	150	Observation
	2							–	291–297	Juy	18.88(b)	740	245	Abandoned
	3							5.17	953–959	Juy	19.77(b)	990	104	Observation
1B				15.04.86	22.04.86	121	4.32	4.94	102–108	Kll	18.16(b)	550	29	Observation
1W				15.09.81	25.09.81	27	4.43	4.69	21–27	Cz	0.28	740	(a)	Observation
2A		350300	6566300	29.04.86	30.06.86	195	130.42	131.02	125.5–140.5	Cz	14.9	–	(a)	Observation
2B	1			20.05.86	24.06.86	1 004	130.11	130.50	273–279	Kll	29.06	770	27	Observation
	2							–	589–595	Kll	32.90	710	229	Abandoned
	3							131.07	939–945	Juy	35.61	960	18	Observation
3A	1	358700	6567800	08.07.86	04.08.86	1 007	59.13	59.32	477–483	Kll	34.29	630	48	Observation
	2							–	680–686	Klg	51.67	870	104	Abandoned
	3							59.93	980–986	Juy	48.67	1 130	104	Observation
3B				06.08.86	12.08.86	306.5	59.12	59.88	239–251	Kll	34.70	680	84	Observation
3W				17.09.85	02.10.85	140	59.40	59.95	42.5–48.5	Cz	49.86	380	151	Observation
4A	1	368150	6566600	06.10.81	05.11.81	1 200	77.34	77.72	759–765	Juy	62.42	855	364	Observation
	2							77.83	1 076–1 082	Juy	62.34	792	63	Observation
4B				06.11.81	10.11.81	88	–	–	–	–	–	–	–	Abandoned
4C				12.11.81	25.11.81	450	77.34	78.20	408–414	Kll	63.03	631	365	Observation
4W				29.09.81	01.10.81	95	77.07	77.47	84–90	Kll	67.17	1 050	1 170	Observation
5A	1	376750	6569250	28.08.81	18.09.81	1 200	85.23	85.69	726–732	Juy	66.51	642	365	Observation
	2							85.75	1 092–1 098	Juy	66.62	899	245	Observation
5B	1			18.09.81	25.09.81	350	85.14	85.79	93–99	Kll	70.55	793	84	Observation
	2							85.89	318–324	Juy	66.63	794	245	Observation
5W				21.08.81	26.08.81	60	85.29	85.55	52–58.4	Kll	80.91	849	890	Observation
6A	1	383700	6571200	04.12.81	16.02.82	974	128.38	128.76	574–580	Juy	68.35	864	49	Observation
	2							128.84	949–955	Juy	68.21	683	272	Observation
6W				01.12.81	03.12.81	114	127.56	127.87	100–106	JKp	110.81	551	229	Observation
7A	1	394350	6568600	08.10.81	10.12.81(c)	1 201	145.01	145.21	226–232	Kll	119.00	1 310	48	Observation
	2							–	693–699	JKp	113.70	530	272	Abandoned
	3			09.12.85	24.02.86(c)			146.00	1 026–1 032	JKp	89.56	1 210	125	Observation
7W				09.12.81	10.12.81	61	145.19	145.39	54–60	Kuo	143.83	760	27	Observation
8A	1	405000	6566000	25.09.85	03.12.85	1 169	171.66	171.86	224–233	Kll	161.14	1 850	245	Observation
	2							–	495–501	Juy	154.13	5 180	3.2	Abandoned
	3							172.66	757–763	Jlo	156.49	8 660	27	Observation
8W				04.09.85	13.09.85	103	171.52	171.97	97–103	Kud	161.74	1 720	579	Observation

Cz	Superficial formations	Klg	Gage Formation	(a)	Not developed
Kuo	Osborne Formation	JKp	Parmelia Formation	(b)	Flowing bore
Kud	Dandaragan Sandstone	Juy	Yarragadee Formation	(c)	Conductor pipe drilled during 1981, bore completed during 1986
Kll	Leederville Formation	Jlo	Cockleshell Gully Formation		
Kls	South Perth Shale				

later date after geothermal gradients had been re-established. Between eighteen and forty sidewall cores were recovered, for palynological examination, from each site.

The bores were completed with steel casing and a cement grout, and additional bores were constructed to enable three, four, or five aquifer intervals to be sampled and tested at each site (Table 1). Between one and three intervals were perforated or screened in each bore, but a maximum of two intervals per bore were retained for monitoring; the other was isolated by compressible packers and abandoned in the bores where three intervals were perforated. In the bores with two monitoring intervals, water levels are measured inside an internal pipe for the deep interval and inside the casing annulus for the shallow interval. The two intervals are separated by compressible packers inserted in the annulus below the upper interval. Gate valves are fitted to control artesian flows from GL1A1, GL1A3 and GL1B.

Each interval was developed by airlifting and surging to obtain a clear, uncontaminated water sample for analysis by the Chemistry Centre. Filtered, acidified samples were later taken from GL1A1, GL1A3 and GL1B and analysed for iron content. Artesian flows from these three intervals contained a small amount of gas consisting mainly of nitrogen and 5–14% hydrocarbons.

Potentiometric heads for each interval were recorded after the water levels had recovered following airlifting. Water levels from all observation intervals were also measured at monthly intervals after their completion until July 1987, except between August 1982 and October 1985.

To allow comparisons with potentiometric heads from other intervals, the measured heads for the high-salinity intervals (GL8A2 and GL8A3) have been adjusted from the values shown in Table 1 to compensate for the density distribution resulting from salinity variations with depth in the bore, according to the method of Luscyzynski (1961). For comparisons in a vertical direction (Fig. 10, see Hydrogeology section), measured heads have been converted to environmental heads. The measured head in GL8A2 was adjusted by +1 m and the measured head in GL8A3 by +2 m.

GEOLOGY

SETTING

The Gillingarra Line bores were drilled in the central part of the Dandaragan Trough, a structural subdivision of the Perth Basin that is bounded to the east by the Darling Fault and to the west by the Beagle Fault and associated faults (Fig. 3). In this part of the basin the Phanerozoic section is about 13 km thick in the east, and 7 km thick near the coast (Playford and others, 1976). It consists of Palaeozoic and Mesozoic deposits under a thin Cainozoic cover. Rifting and sagging along the continental margin, associated with the separation of southwestern Australia from the rest of Gondwana

during the Neocomian (Playford and others, 1976), has resulted in an intensely block-faulted, pre-breakup sequence. This is overlain by comparatively unde-formed, middle Neocomian and younger rocks deposited during the tectonically quiet period following breakup. Cretaceous and younger deposits of the Perth Basin onlap Precambrian crystalline rocks of the Yilgarn Craton by possibly as much as 1 km.

STRATIGRAPHY

Sedimentary rocks intersected in the Gillingarra Line bores range in age from Jurassic to Quaternary. The age of the units has been established by palynological work reported by Backhouse (unpublished reports listed in Moncrieff, 1989). The stratigraphic sequence is given in Table 2.

Cockleshell Gully Formation

The upper 490 m of the Cockleshell Gully Formation was intersected in GL8A in a fault block at the eastern edge of the Dandaragan Trough, between the Muchea (Skilbeck and Lennox, 1984) and Darling Faults (Fig. 4). The formation is overlain by the Cadda Formation; a weathered zone at the top of the Cockleshell Gully Formation suggests an unconformable or disconformable relationship.

The formation consists of interbedded shale, claystone, siltstone, and sandstone, together with minor amounts of coal and conglomerate. The shale, claystone, and siltstone are medium to dark grey and are often laminated. The sandstone is light grey, consists of very fine-grained to fine-gravel sized, poorly sorted, very angular to subrounded quartz, and is often clayey. Minor amounts of grey and light yellow-brown, medium- to coarse-grained and very well rounded quartz also occur. Accessory minerals include feldspar, pyrite, garnet, mica, and opaque heavy minerals. A weathered section about 45 m thick at the top of the formation is indicated by reddish brown colouration.

Palynological assemblages from sidewall cores have been assigned to the *Dictyophyllidites harrisii* miospore Assemblage Subzone or the lower *Dictyotosporites complex* miospore Zone of Early to Middle Jurassic (Toarcian to Aalenian) age and indicate a non-marine environment of deposition. Based on lithology and age the sequence is assigned to the Cattamarra Member.

Cadda Formation

The Cadda Formation was also intersected only in GL8A, where it is 96 m thick. It is overlain with apparent conformity by the Yarragadee Formation.

The formation consists of weakly to moderately consolidated, light-grey to black sandstone, claystone, and shale, together with minor amounts of siltstone and conglomerate. The sandstone is weakly consolidated and consists of very fine to very coarse, moderately to very well-sorted, sub-rounded to rounded quartz, and traces of mica, garnet, feldspar, and opaque heavy minerals.

109

Palynological assemblages recovered from sidewall cores are assigned to the *D. complex* miospore Zone and the *Dissiliodinium caddaensis* microplankton Zone. They indicate a Middle Jurassic (Bajocian) age and deposition in a lagoonal or semi-marine environment.

Yarragadee Formation

The Yarragadee Formation (Backhouse, 1984) was intersected at all sites except GL7. The maximum thickness penetrated during drilling was 902 m in GL5A. It is conformably overlain by the Parmelia Formation in GL6A, but elsewhere the top of the formation has been eroded and it is unconformably overlain by the Warnbro Group.

The formation is mainly weakly consolidated, light-grey sandstone together with minor amounts of conglomerate, shale, siltstone, and claystone, and rare thin coal horizons and filaments of black carbonaceous material. The lower part of the formation, intersected in GL8A, contains about 50% siltstone and shale interbeds.

The sandstone consists of very fine to very coarse-grained, very poorly to well-sorted, angular to rounded quartz, and is often kaolinitic, particularly in the west. It contains accessory feldspar, mica, pyrite, garnet, and dark-coloured heavy minerals. Some beds near the base of the formation in GL8A contain up to 5% garnet, and a weathered zone, about 3 m thick, may be present at
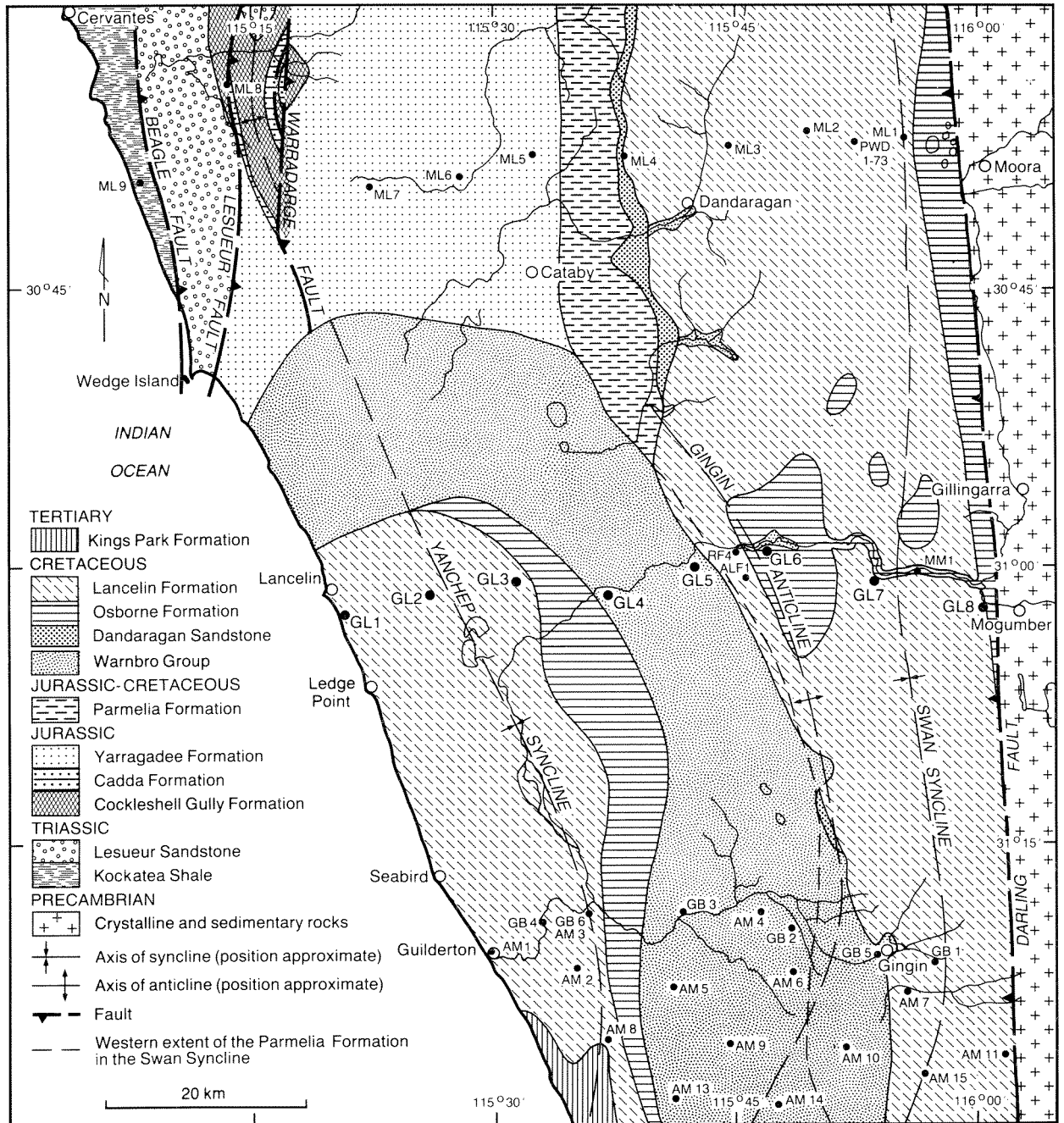

Figure 3. Early Tertiary and Mesozoic geology

TABLE 2. STRATIGRAPHIC SEQUENCE

Age	Stratigraphic unit	Maximum thickness intersected (m)	Lithology	Aquifer potential
QUATERNARY–TERTIARY	Superficial formations and surficial deposits	142 (GL2)	Sand, limestone	Major aquifer
	_____UNCONFORMITY_____			
CRETACEOUS Late	COOLYENA GROUP Lancelin Formation	47 (GL3)	Glauconitic siltstone, mudstone, sandstone	Confining bed
	Poison Hill Greensand Member	10 (ALF1)	Glauconitic clayey sandstone	Minor aquifer
	Gingin Chalk Member	18 (GL1)	Chalk, mudstone	Confining bed
	Molecap Greensand Member	25 (GL7)	Glauconitic silty sandstone	Minor aquifer
	_____DISCONFORMITY_____			
Early-Late	Osborne Formation	108 (MM1)	Glauconitic shale, siltstone, sandstone	Confining bed
Early	Dandaragan Sandstone	18 (GL8)	Feldspathic sandstone, gravel	Minor aquifer
	_____UNCONFORMITY_____			
	WARNBRO GROUP Leederville Formation	649 (GL2)	Sandstone, siltstone, shale	Major aquifer
	South Perth Shale	88 (GL3)	Shale, siltstone	Confining bed
	Gage Formation	88 (GL4)	Sandstone, siltstone, shale	Minor aquifer
	_____UNCONFORMITY_____			
JURASSIC Late	Parmelia Formation	829 (GL7)	Sandstone, siltstone, shale	Major aquifer
	Otorowiri Member	82 (GL6)	Shale, siltstone	Confining bed
	Yarragadee Formation	(a) 902 (GL5)	Sandstone, gravel, minor shale	Major aquifer
Middle	Cadda Formation	96 (GL8)	Shale, siltstone, sandstone	Minor aquifer
Early	Cockleshell Gully Formation (Cattamarra Member)	(a) 490 (GL8)	Shale, siltstone, sandstone	Minor aquifer

(a) Not fully penetrated

the top of the formation in the same bore. Thin bedding and laminations were observed in fine sandstone in several sidewall cores, and fine cross-bedding in one.

Sidewall cores recovered from the Yarragadee Formation, particularly at the western end of the line, either contained sparse palynological assemblages or were barren. The assemblages range from the _D. complex_ Zone up to the _Aequitriradites acusus_ miospore Zone and indicate that the formation is a non-marine, predominantly fluvial deposit, of Middle to Late Jurassic (Late Bajocian to Kimmeridgian) age.

Parmelia Formation

The Parmelia Formation (Backhouse, 1984) was intersected in GL6A, GL7A, and in the nearby Australian Lucerne Farms bore ALF1 (Fig. 1). A maximum thickness of 829 m was penetrated in GL7A which bottomed in the formation. The base was penetrated in GL6A where the formation is 439 m thick, and in Gingin 1 where it is 168 m thick. The formation is unconformably overlain by the Leederville Formation.

The Parmelia Formation consists of interbedded, weakly to well consolidated sandstone, siltstone, shale, and claystone, together with minor amounts of conglomerate. The sandstone is light-greenish-grey to grey, variably silty and clayey, and commonly feldspathic or kaolinitic. It contains grains of very fine to very coarse, poorly to very well sorted, angular to rounded quartz. The siltstone, shale, and claystone are light to dark-brownish-grey and grey. The rocks are slightly micaceous and contain traces of pyrite, dark-coloured heavy minerals, and glauconite. Laminations and bedding, up to 8 mm thick, were observed in sidewall cores.

The formation includes two mainly siltstone and shale members — the Otorowiri Member at the base, and the Carnac Member (Backhouse, 1984). The Carnac Member is not recognized in the Gillingarra Line bores, but 82 m of Otorowiri Member were penetrated in GL6A. The section above the Otorowiri Member in GL6A and in ALF1 contains only about 20% sandstone, but the formation thickens and becomes more sandy eastwards into the Swan Syncline where, in GL7A, probable Otorowiri Member is overlain by a section which is about 50% sandstone.

Palynological assemblages from the formation are assigned to the _Biretisporites eneabbaensis_ miospore Zone, and indicate a Late Jurassic to Early Cretaceous age (Tithonian to Berriasian), and deposition in a non-marine, mainly fluvial environment. Deposition of
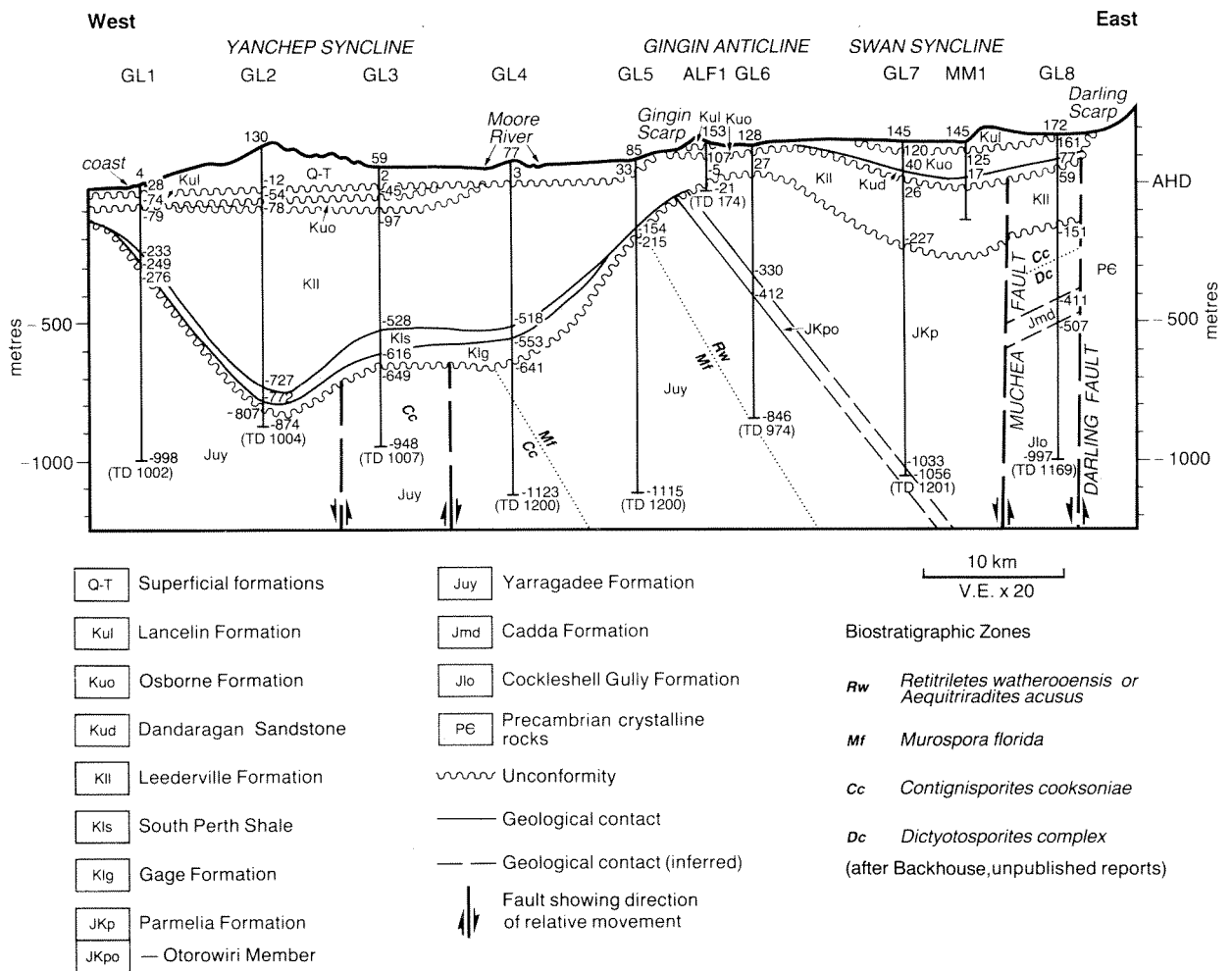
West   East

YANCHEP SYNCLINE   GINGIN ANTICLINE   SWAN SYNCLINE

GL1   GL2   GL3   GL4   GL5   ALF1 GL6   GL7   MM1   GL8

Legend:

Q-T	Superficial formations
Kul	Lancelin Formation
Kuo	Osborne Formation
Kud	Dandaragan Sandstone
Kll	Leederville Formation
Kls	South Perth Shale
Klg	Gage Formation
JKp	Parmelia Formation
JKpo	— Otorowiri Member
Juy	Yarragadee Formation
Jmd	Cadda Formation
Jlo	Cockleshell Gully Formation
PƐ	Precambrian crystalline rocks

vvvvv Unconformity

——— Geological contact

— — Geological contact (inferred)

Fault showing direction of relative movement

10 km   V.E. x 20

Biostratigraphic Zones

Rw   Retitriletes watherooensis or Aequitriradites acusus

Mf   Murospora florida

Cc   Contignisporites cooksoniae

Dc   Dictyotosporites complex

(after Backhouse, unpublished reports)

GSWA 24768

Figure 4. Geological cross section

the Otorowiri Member was predominantly in a restricted marine (lagoonal) or lacustrine environment. Reworked Permian and Early Jurassic palynomorphs were recovered from the Parmelia Formation, particularly from the Otorowiri Member.

Warnbro Group

The Warnbro Group was intersected in all bores, and unconformably overlies the Yarragadee or Parmelia Formations. The thickest section of 729 m was penetrated in GL2B in the axis of the Yanchep Syncline.

The group consists of the Gage Formation, the South Perth Shale, and the Leederville Formation. The Gage Formation and the South Perth Shale occur only in the Yanchep Syncline (Fig. 4).

The Warnbro Group section is characterized by reworked Permian, Triassic, and Jurassic palynomorphs which increase in abundance towards the west. This indicates rapid erosion of the pre-existing strata during deposition of the Warnbro Group, and a possible major source of sediment from the northwest on the Beagle Ridge where Triassic and Permian deposits subcrop beneath the superficial formations*.

Gage Formation: The deposits immediately above the Yarragadee Formation in GL1A, GL2B, GL3A, GL4A, and GL5A are assigned to the Gage Formation (Davidson and Moncrieff, 1989) based on their stratigraphic position and age. The formation attains a maximum thickness of 88 m in GL4A. It is conformably overlain by the South Perth Shale with a sharp contact in GL1A and GL3A, and a gradational contact in GL2B and GL4A; and by the Leederville Formation in GL5A with a sharp contact.

The Gage Formation consists of about 50% light-grey sandstone which is interbedded and interlaminated with about 50% siltstone and shale. The sandstone consists of fine to very coarse, poorly to well-sorted and angular to subrounded quartz, with traces of feldspar, pyrite, and garnet. The siltstone and shale are very light-grey to grey and contain traces of mica.

Palynological assemblages from the formation are assigned to the *Gagiella mutabilis* microplankton Zone and to the *Balmeiopsis limbata* miospore Zone. They

*Superficial formations are Pliocene to Holocene sediments which underlie the Swan Coastal Plain in the Perth Basin; despite their variability in lithologies these formations form a single aquifer system (Allen, 1976).

112

indicate an Early Cretaceous age (Valanginian) and deposition in a mainly lagoonal or shallow, restricted-marine environment.

South Perth Shale: The South Perth Shale was intersected in GL1A, GL2B, GL3A, and GL4A. It attains a maximum thickness of 88 m in GL3A, but thins or is absent above structurally high parts of the unconformity at the base of the Warnbro Group along the crest of the Gingin Anticline and west of GL1 (Fig. 4). It is conformably overlain by the Leederville Formation with a sharp contact in GL1A and GL3A, and a gradational contact in GL2B and GL4A.

The South Perth Shale consists predominantly of medium-greyish-brown to black, moderately to well-consolidated shale with some siltstone. The rocks are slightly micaceous and commonly contain minor amounts of pyrite.

Palynological assemblages from the formation are assigned to the *G. mutabilis* to *Phoberocysta lowryi* microplankton Zones and the *Balmeiopsis limbata* miospore Zone. They indicate an Early Cretaceous age (Valanginian to Hauterivian) and deposition in a mainly shallow-marine environment or lagoonal environment.

Leederville Formation: The Leederville Formation was intersected in all Gillingarra Line bores, as well as in ALF1 and Mogumber Mission bore MM1 (Fig. 1). It attains a maximum thickness of 649 m (GL2B) in the Yanchep Syncline and thins to 89 m over the Gingin Anticline in GL6A. The formation is probably discon-formably overlain by the Dandaragan Sandstone in the Swan Syncline, and is disconformably overlain by the Osborne Formation beneath the Gingin Scarp and in the western part of the Yanchep Syncline. Across the coastal plain up to the Gingin Scarp it is unconformably overlain by the superficial formations. The formation is poorly exposed in the bed of the Moore River over about a 10 km section near GL6.

The formation consists of about 50% weakly to moderately consolidated sandstone, and some conglom-erate, interbedded with weakly to well-consolidated siltstone, claystone, and shale. Individual sandstone beds may be as thick as 40 m, but are usually less than 10 m thick.

The sandstone is light-to-medium grey and rarely black, may be silty and clayey, and consists of very fine-grained to very coarse, very poorly to very well-sorted, angular to rounded quartz with variable amounts of feldspar. The siltstone, claystone, and shale are medium grey or brownish grey to black, slightly micaceous and, rarely, pyritic. Sidewall cores were commonly laminated or thinly bedded. At the western-most three sites, the top of the formation consists of up to 40 m (GL2B) of dark-greenish-grey to greenish-black, slightly clayey, sandy, glauconitic siltstone and silty sandstone. The quartz in this section is very fine to fine grained, subrounded to rounded and well sorted.

Palynological assemblages from the Leederville For-mation indicate deposition during the Early Cretaceous (Valanginian to earliest Aptian) in both marine and

non-marine (dominantly fluvial) environments. In the east, in the Swan Syncline, the whole of the Warnbro Group is almost exclusively non-marine and has been assigned to the Leederville Formation, although there is evidence that the lower part in GL7A is a time equivalent of the South Perth Shale elsewhere (Back-house, unpublished report). In the Yanchep Syncline there is a basal marine section ranging from the *G. mutabilis* to the *Aprobolocysta alata* microplankton Zones. This is overlain by a non-marine section, and at the top of the formation in the west is a shallow-marine section corresponding to the *Batioladinium jaegeri* to *Fromea monilifera* Zones. The entire sequence falls within the *B. limbata* miospore Zone. The lowermost section in the Yanchep Syncline, in GL2B, is appar-ently older than sections ascribed to the Leederville Formation elsewhere in the Perth Basin where the formation does not extend into the *G. mutabilis* Zone (Backhouse, 1988).

Sidewall cores collected from GL1A and GL2B, from immediately below the shallow-marine section, show signs of oxidation (flecks of light-brown coloura-tion). This is evidence that the formation was subject to subaerial weathering, and possibly erosion, in this part of the Perth Basin at approximately the level of the *A. alata* Zone — a biostratigraphic level marked by a significant regression in other parts of the Perth Basin (Backhouse, 1988).

Coolyena Group

The Coolyena Group, consisting of the basal Danda-ragan Sandstone, the Osborne Formation, and the Lancelin Formation, was deposited during a period of tectonic stability when there was little input of ter-rigenous material, but much reworking of pre-existing Cretaceous strata, under shallow-marine conditions. The Dandaragan Sandstone was intersected only in the Swan Syncline, but the Osborne and Lancelin Forma-tions occur in both the Swan and Yanchep Synclines.

Dandaragan Sandstone: The Dandaragan Sandstone (McWhae and others, 1958) was intersected in GL7A, GL8A, and MM1 in the Swan syncline. The maximum thickness identified from geophysical logs was 25 m in MM1, but the thickness is known to vary considerably (Low, 1965). The formation pinches out on the east flank of the Gingin Anticline and does not occur in the Yanchep Syncline. It overlies the Leederville Formation and is probably conformably overlain by the Osborne Formation. However, in outcrop in the Dandaragan area, it rests directly on the Parmelia Formation (Fig. 3). The formation has been considered an equivalent of the Leederville Formation (Playford and others, 1976) and may correlate with the shallow-marine section of the Leederville Formation that was intersected in the western three bores of the line. However, it is more likely to be a basal unit of the Coolyena Group.

The formation consists of weakly consolidated, coarse to very coarse, angular to subrounded, moder-ately sorted sandstone, feldspathic sandstone, and fine conglomerate with minor amounts of siltstone, clayst-one, and glauconite.

113

No fossils were found to establish either the environment of deposition or age of the Dandaragan Sandstone, but the lithology and texture of the deposit indicate deposition in a high-energy, possibly shallow-marine environment, and an Early Cretaceous age is interpreted from its stratigraphic position at the base of the Osborne Formation.

Osborne Formation: The Osborne Formation was intersected at GL1–3, GL6–8, ALF1, and MM1, and it attains a maximum thickness of 108 m (MM1). It thins markedly over the Gingin Anticline and at the western end of the borehole line above structurally high parts of the unconformity at the base of the Warnbro Group

(Fig. 4). It is disconformably overlain by the Lancelin Formation in the western part of the Yanchep Syncline, in the axis of the Swan Syncline, and near the crest of the Gingin Anticline. In the western part of the Swan Syncline, and adjacent to the Darling Scarp, it occurs beneath a thin cover of sand and laterite. It is exposed sporadically in the valley of the Moore River between the Gingin Scarp and Mogumber, and small lateritized outcrops occur elsewhere on the Dandaragan Plateau. Near the axis of the Yanchep Syncline it is unconformably overlain by the superficial formations.

The Osborne Formation consists of weakly to well-consolidated, dark-greenish-grey to black, glauconitic
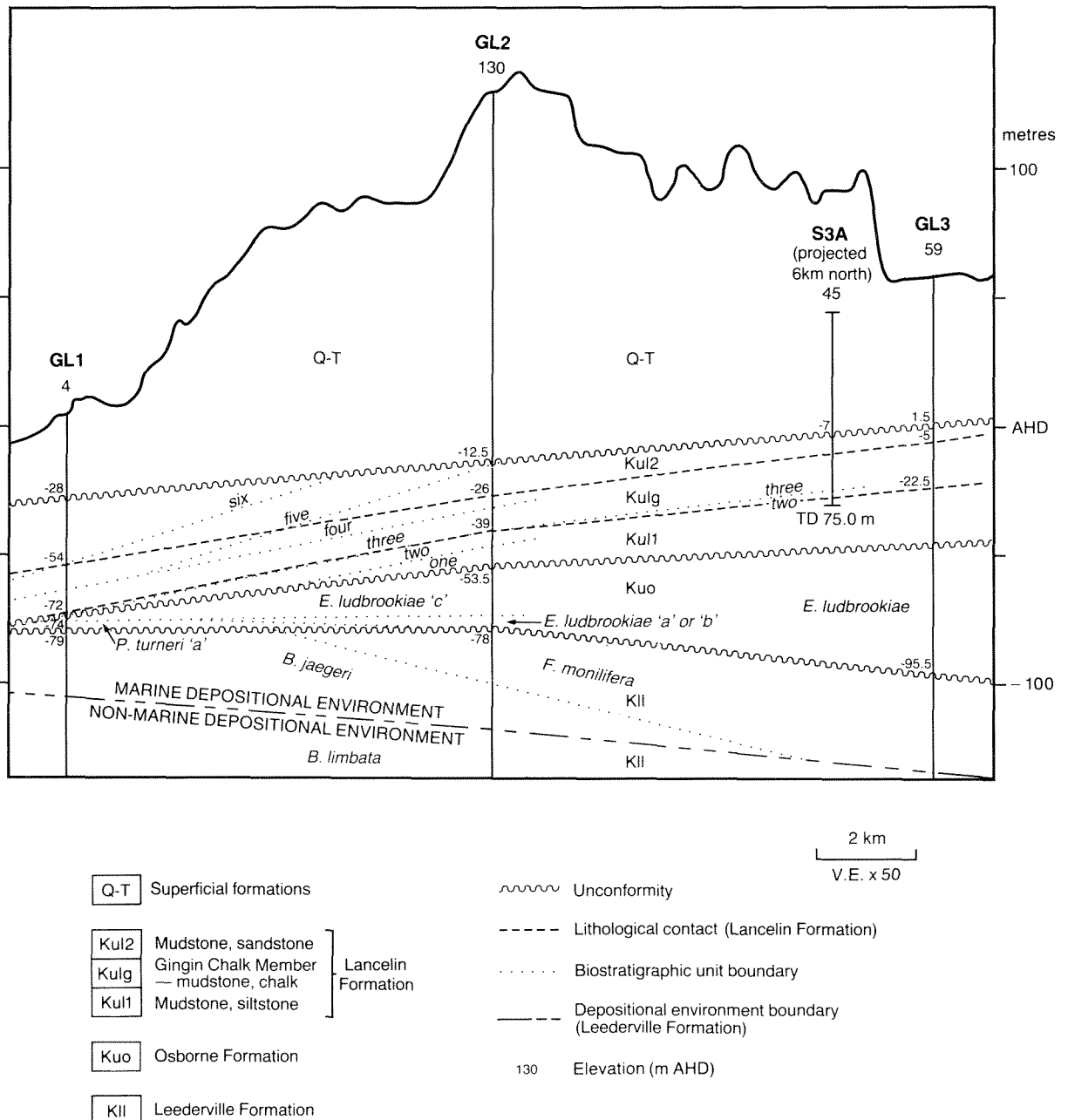
Figure 5. **Geological cross section GL1–3 showing detail in the upper Warnbro and Coolyena Groups**

114

shale, siltstone, and silty and clayey sandstone. The sandstone consists of very fine- to medium-grained, well-sorted, subangular to subrounded quartz with very fine to fine glauconite. The rocks are slightly micaceous and rarely pyritic.

Palynological assemblages from the formation range from the *Pseudoceratium turneri* or *Odontochitina operculata* microplankton Zones to the *Endoceratum ludbrookiae* 'c' microplankton Subzone and indicate deposition during the Early to Late Cretaceous (Late Aptian to Cenomanian) in a near-shore marine environment. At the western end of the line the sequence appears to be condensed and the section belonging to the lower *E. ludbrookiae* Zone is either very thin or absent (Fig. 5).

Lancelin Formation: The Lancelin Formation (Davidson and Moncrieff, 1989) occurs in the axis of the Swan Syncline, above the Gingin Anticline and in the western part of the Yanchep Syncline (Fig. 3). It was intersected at GL1–3, GL7, GL8, ALF1, and MM1, and attains a maximum thickness of 47 m in GL3A. The formation is unconformably overlain by the superficial formations in the western part of the Yanchep Syncline and it is mainly concealed by a thin sand and laterite cover in the Swan Syncline. Scattered, weathered exposures occur on the Dandaragan Plateau, mainly north from the Gillingarra Line and near Gingin.

The Lancelin Formation has three members: the Molecap Greensand Member at the base, the Gingin Chalk Member in the middle, and the Poison Hill Greensand Member at the top. The Molecap Greensand Member and the Poison Hill Greensand Member occur only in the Swan Syncline. The thickness of the units varies greatly and they pinch out laterally.

The Lancelin Formation consists of weakly to moderately consolidated, very light-grey to dark-greenish-grey, sandy mudstone, sandy siltstone, and silty sandstone. The carbonate and glauconite contents range from low to high, and fragments of the bivalve *Inoceramus* are common in some horizons. It occurs in the Yanchep Syncline in the corresponding stratigraphic position to the Molecap Greensand and the Poison Hill Greensand Members in the Swan Syncline (Fig. 5).

The Molecap Greensand Member was intersected at GL7, ALF1, and MM1, and attains a maximum thickness of 25 m in GL7A. It consists of poorly consolidated, grey to dark-greenish-grey silty sandstone which is weathered yellow to brown to a depth of as much as 25 m (GL7A). The sandstone consists of very fine to coarse, moderately to well-sorted and subangular to rounded quartz with 5–10% very fine to fine glauconite.

The Gingin Chalk Member was intersected at GL1–3, ALF1, and MM1, and the maximum thickness penetrated was 18 m (GL1A). It consists of weakly to moderately consolidated, very light-grey to greyish-white mudstone, chalk and claystone, all of which contain a high percentage of carbonate. The section is characterized by a low glauconite content and a low natural gamma-ray response, usually with a thin, low

peak near the middle (Fig. 6). It contains minor amounts of very fine quartz, some *Inoceramus* fragments, and (rarely) pyrite in some horizons.
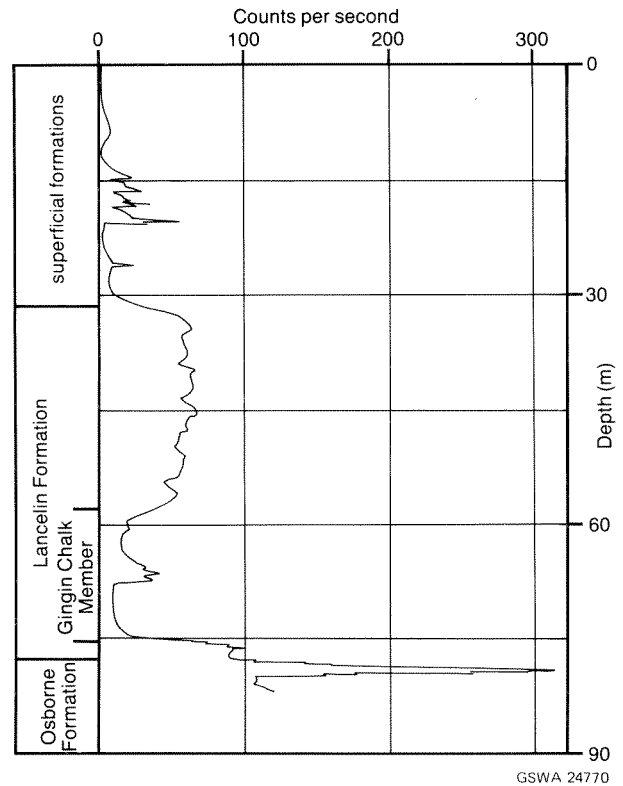

Figure 6. Lancelin Formation: natural gamma-ray log of GL1A

The Poison Hill Greensand Member was intersected at GL8, ALF1, and MM1 and attains a maximum thickness of 10 m (ALF1). The sections that were penetrated are all weathered and consist of poorly consolidated, light-reddish-brown to brown, ferruginous, clayey sandstone in which the grains are very fine to coarse, poorly sorted, and subrounded to rounded.

Palynological examinations of samples from the Yanchep Syncline indicate that the formation was deposited during the Late Cretaceous (Turonian or Late Cenomanian to Campanian) in a near-shore marine environment with some open-marine input; the Gingin Chalk Member is assigned a Santonian to earliest Campanian age. Informal biostratigraphic correlations in GL1–3, based on unpublished work by Marshall (1984), are shown in Figure 5.

Superficial formations

Sediments of Tertiary to Quaternary age occur beneath the Swan Coastal Plain and were intersected at sites GL1–5. They attain a maximum thickness of 142.5 m in GL2B, and unconformably overlie weathered Cretaceous rocks of the Leederville, Osborne, or Lancelin Formations. The units have been collectively referred to as the superficial formations; a detailed description of them is given by Moncrieff and Tuckson (1989).
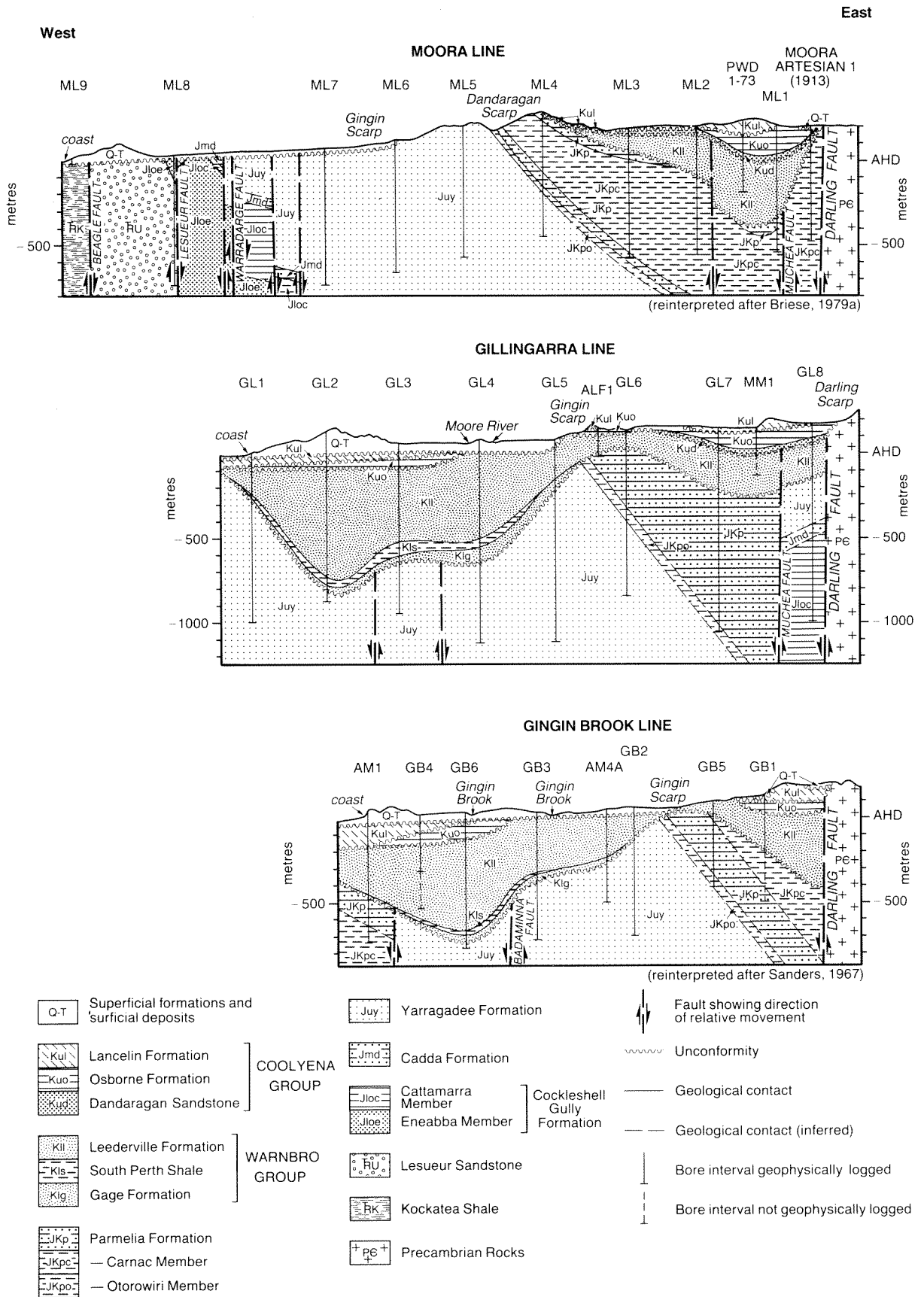
West / East

MOORA LINE

GILLINGARRA LINE

GINGIN BROOK LINE

(reinterpreted after Briese, 1979a)

(reinterpreted after Sanders, 1967)

Q-T	Superficial formations and surficial deposits
Kul	Lancelin Formation
Kuo	Osborne Formation
Kud	Dandaragan Sandstone

COOLYENA GROUP

Kll	Leederville Formation
Kls	South Perth Shale
Klg	Gage Formation

WARNBRO GROUP

JKp	Parmelia Formation
—	Carnac Member
—	Otorowiri Member

Juy	Yarragadee Formation
Jmd	Cadda Formation
Jloc	Cattamarra Member
Jloe	Eneabba Member

Cockleshell Gully Formation

℞U	Lesueur Sandstone
℞K	Kockatea Shale
PЄ	Precambrian Rocks

Fault showing direction of relative movement

Unconformity

Geological contact

Geological contact (inferred)

Bore interval geophysically logged

Bore interval not geophysically logged

GSWA 24771

Figure 7. Geological cross sections through adjacent borehole lines

116

Surficial deposits

Sand and laterite cover most of the Cretaceous rocks on the Dandaragan Plateau. Massive laterite is confined to the ridges where it may have a sand veneer. The surface sand elsewhere is mainly less than 5 m thick.

The sand on the Dandaragan Plateau is generally very light grey to light yellow, very fine to coarse grained, poorly to moderately sorted, and subangular to rounded.

The laterite is believed to be of early Tertiary to Quaternary age (Playford and others, 1976). The sand may be a residual deposit associated with the lateritization. It has been reworked and forms low dunes in the Yarra Yarra Region.

STRUCTURE

The geological structure inferred from the drilling on the Gillingarra Line is shown in Figure 4.

The Dandaragan Trough is bounded to the east by the Darling Fault which, near Mogumber, dips to the west at 50–60° and has a throw of about 10 km (Playford and others, 1976). Easterly dipping Early Neocomian and older rocks, which occur beneath a major intra-Neocomian unconformity in the trough, are affected by extensive normal faulting which apparently does not greatly affect later deposits, although small growth faults may extend further up the sequence than is indicated in Figure 4.

Folding of the rocks was probably caused by movement along growth faults in the style suggested by Cope (1972). The growth faults are associated with unequal compaction and subsidence over basement fault blocks. This style of folding in the middle Neocomian and younger strata has resulted in marked thickening of the sedimentary sequence in synclinal troughs, and thinning along the crests of anticlines.

The Warnbro Group is draped over the block-faulted pre-Neocomian strata and thins markedly over the Gingin Anticline. The Gingin Anticline (Playford and others, 1976) continues southwards in the Warnbro and Coolyena Groups as the Pinjar Anticline (Allen, 1979). The Warnbro and Coolyena Groups are thickest in the Swan and Yanchep Synclines, and the Gage Formation occurs in the structurally lowest depressions. In the Yanchep Syncline the thickest sections of the two groups are offset; this indicates a shift in the depocentre.

The superficial formations beneath the Swan Coastal Plain are flat-lying and rest on a gentle westward-sloping unconformity at the top of the Cretaceous.

GEOLOGICAL REINTERPRETATION OF ADJACENT BOREHOLE LINES

Moora Line

Briese (1979a) assigned the thick siltstone sequence (Fig. 7) occurring below the unconformity at the base of the Leederville Formation to the Otorowiri Siltstone Member of the Yarragadee Formation. This sequence is now assigned to the Carnac and Otorowiri Members of the Parmelia Formation (Backhouse, 1984). The Carnac Member section in Moora Line 1–4 (ML1–4) is not recognized in the Gillingarra Line where a thick, more sandy facies occurs above the Otorowiri Member. Thin carbonate-bearing beds occur in several sections of the Carnac Member in Moora Artesian 1 (Fig. 1), but have not been identified elsewhere.

A fault affecting the Parmelia Formation and the Warnbro Group has been placed in the position of the hydraulic discontinuity shown on Plate 1 of Briese (1979b). This has been inserted to account for the large decrease in the thickness of the Coolyena Group west of the fault, and the large difference in hydraulic head in the Leederville Formation between PWD 1-73 and ML2 (Fig. 8). The Muchea Fault is believed to pass east of ML1.

The sequence from 19 m to 52 m in the Moora Artesian bore has been assigned to the Osborne Formation. West of ML2 the Osborne Formation pinches out against the Dandaragan Sandstone. The Dandaragan Sandstone occurs at shallow depth between ML2 and the vicinity of ML4, where it is exposed discontinuously along the Dandaragan Scarp. The Lancelin Formation lies beneath a thin, discontinuous cover of surficial deposits between ML1 and the vicinity of ML4.

The geological structure between the Warradarge and Lesueur Faults has been modified based on information obtained from exploratory drilling for coal in the area.

Gingin Brook Line

Since the drilling of the Gingin Brook Line (Sanders, 1967), changes to the stratigraphic nomenclature, and the drilling of AM1 and AM4, have resulted in a substantial modification of the original interpretation (Fig. 7). The inferred structure is now similar to the Gillingarra Line, and a direct correlation of strata can be made between the two lines.

Evidence from Ginginup 1 (Ingram and Cockbain, 1979), 6.7 km northwest of GB1, shows that the Osborne Formation is not continuous between the two lines, but pinches out against the Gingin Anticline so that the Molecap Greensand directly overlies the Leederville Formation in that bore. The Osborne Formation is also absent at the western end of the line; in AM1, Lancelin Formation directly overlies Leederville Formation (Backhouse, unpublished report). The Dandaragan Sandstone appears to be absent in the eastern part of the Gingin Brook Line (GB1), although it is exposed along the Gingin Scarp about 10 km northwest from GB5 (Biggs, 1976).

HYDROGEOLOGY

AQUIFER SYSTEMS

There are four main aquifer systems. These are the superficial formations, the Leederville Formation beneath the Swan Coastal Plain, the Leederville and
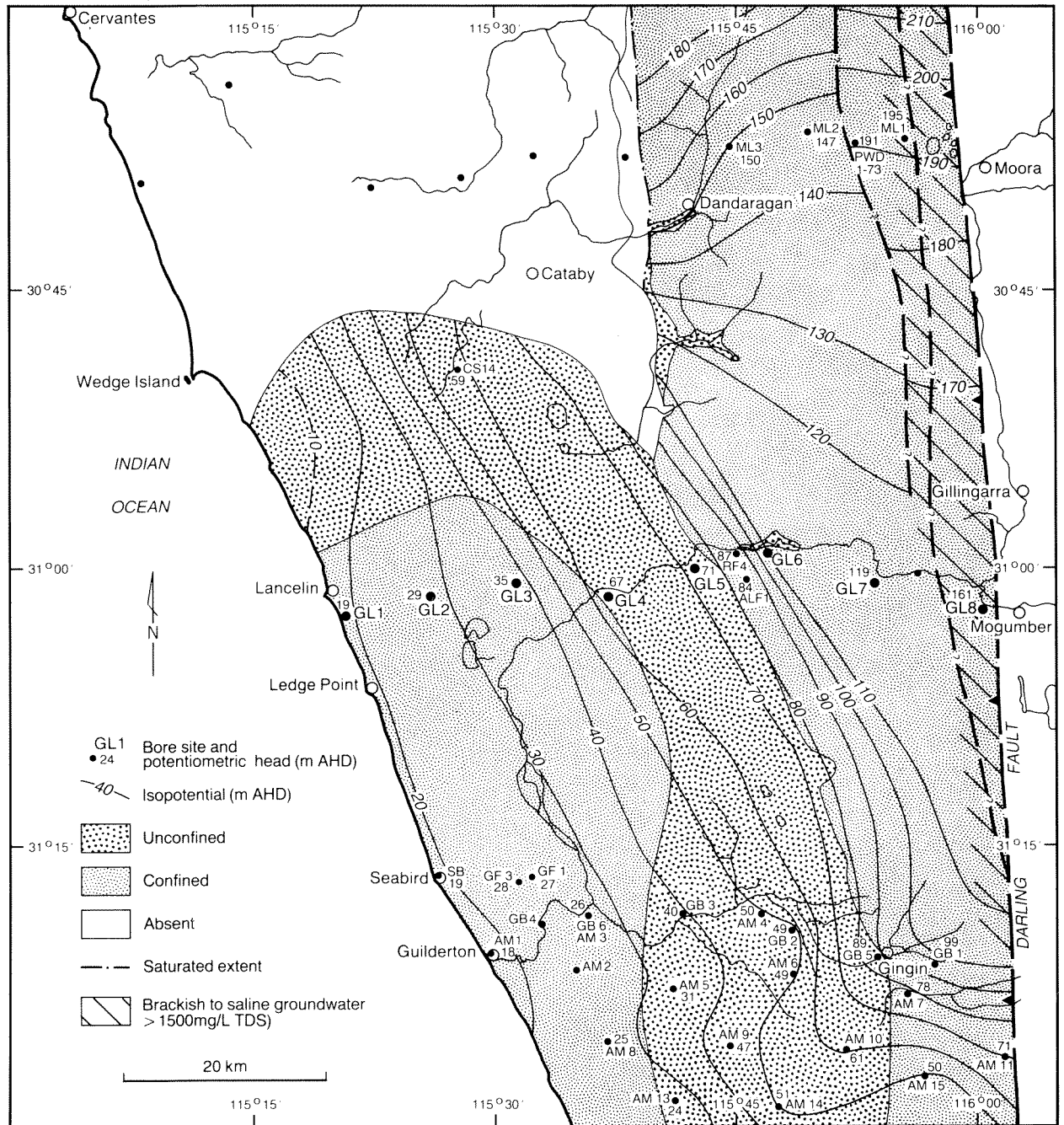
Parmelia Formations beneath the Dandaragan Plateau, and the Yarragadee Formation which occurs beneath the whole region. The main aquifer systems are locally interconnected where (because of geological structure) the separating confining units are absent. The Leederville Formation is in hydraulic continuity with the interconnected Leederville and Parmelia Formations across the top of the Gingin Anticline.

In the fault block between the Darling and Muchea Faults, groundwater in the Yarragadee, the Cadda, and the Cockleshell Gully Formations is saline (Fig. 9), and seems to be hydraulically distinct from both the overlying Leederville Formation and the Parmelia Formation to the west of the Muchea Fault. This groundwater appears to be in a flow system isolated from the main systems.

Perched groundwater, identifiable on electric logs (e.g. ALF1), occurs above some of the thicker shale beds in the Leederville Formation beneath the western part of the Dandaragan Plateau.

Supplies of up to $60 \text{ m}^3/\text{d}$ of fresh to brackish groundwater are obtained locally from the Lancelin Formation (Molecap Greensand or Poison Hill Greensand Members) beneath the eastern part of the Dandaragan Plateau. The groundwater is isolated from the

GSWA 24773
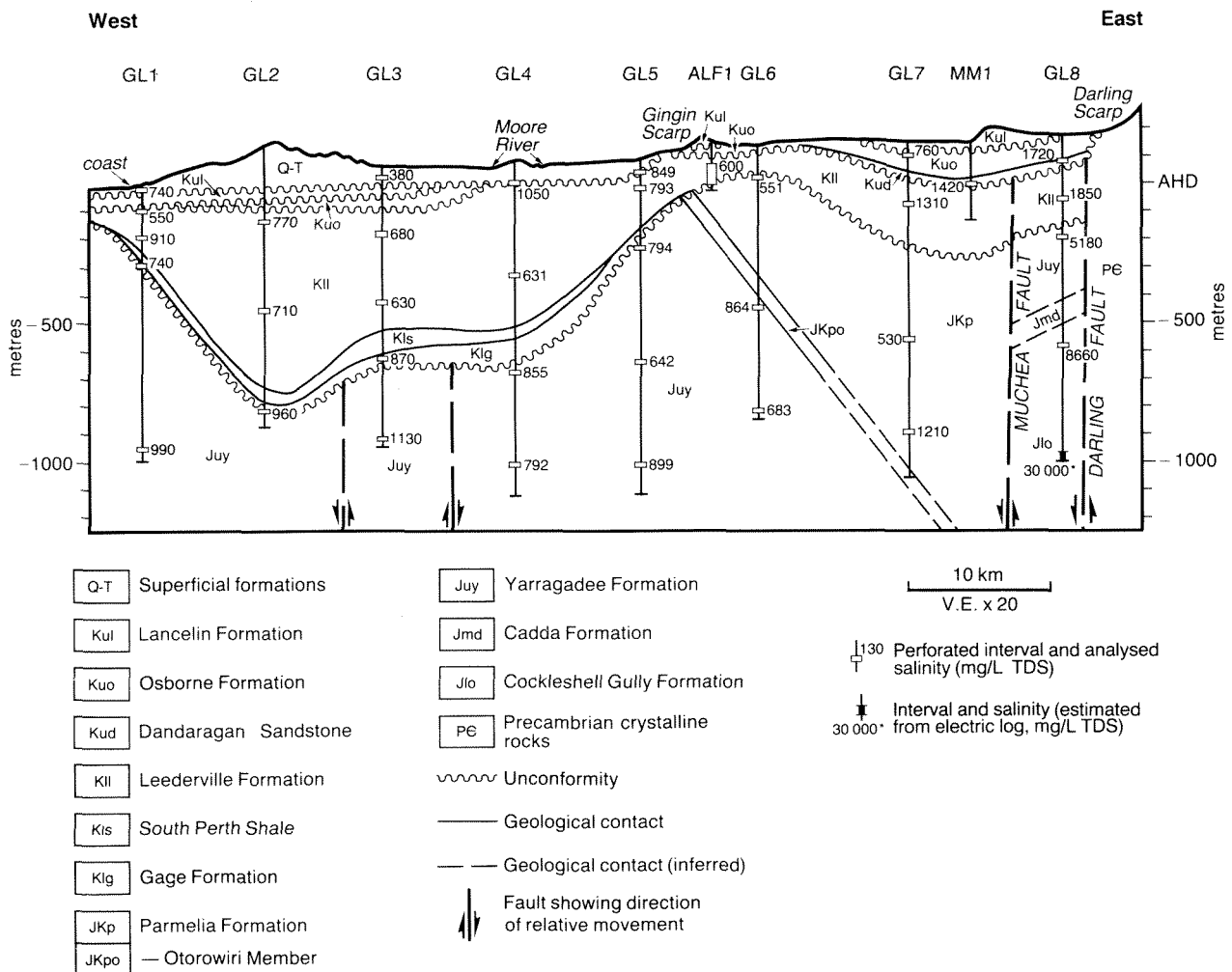
Figure 8. Leederville Formation regional isopotentials

118

GL1   GL2   GL3   GL4   GL5 ALF1 GL6   GL7 MM1 GL8

Moore River — Gingin Scarp — Darling Scarp — coast

Values shown in section: 740, 550, 910, 740, Q-T, 770, Kuo, 680, 380, 1050, 849, 793, 794, 600, 551, 760, Kuo, 1720, Kul, 1420, 1310, 1850, 5180, Juy, PЄ, KII, 710, 630, 631, Kls, 870, Klg, 855, 642, Juy, 864, JKpo, JKp, 530, 8660, 960, 1130, 792, 899, 683, 1210, Jlo, 30 000*, 990, Juy, Juy, MUCHEA FAULT, DARLING FAULT, Jmd

AHD, 500 metres, 1000, −500, −1000, metres

Q-T — Superficial formations	Juy — Yarragadee Formation
Kul — Lancelin Formation	Jmd — Cadda Formation
Kuo — Osborne Formation	Jlo — Cockleshell Gully Formation
Kud — Dandaragan Sandstone	PЄ — Precambrian crystalline rocks
KII — Leederville Formation	∿∿∿ Unconformity
Kls — South Perth Shale	——— Geological contact
Klg — Gage Formation	— — Geological contact (inferred)
JKp — Parmelia Formation	Fault showing direction of relative movement
JKpo — — Otorowiri Member	

10 km   V.E. x 20

130 — Perforated interval and analysed salinity (mg/L TDS)

30 000* — Interval and salinity (estimated from electric log, mg/L TDS)

GSWA 24774

Figure 9. Groundwater salinity

underlying Leederville and Parmelia Formations flow system by the Osborne Formation. Some leakage of groundwater through the Osborne Formation is indicated by the low salinity and high head in the formation in GL7W (760 mg/L TDS, 144 m AHD) when compared to that in the underlying Leederville Formation in GL7A1 (1310 mg/L TDS, 119 m AHD).

Groundwater also occurs in surface sand overlying the Coolyena Group elsewhere on the Dandaragan Plateau; in the Yarra Yarra Region, where the sand is thick, supplies of up to 15 m³/d of fresh groundwater (<500 mg/L TDS) have been obtained.

Groundwater flow in the east of the area is southward, and in the west and central part of the area it is westward. The potentiometric head distribution is shown in section along the Gillingarra Line in Figure 10. There are substantial head differences across many of the confining units.
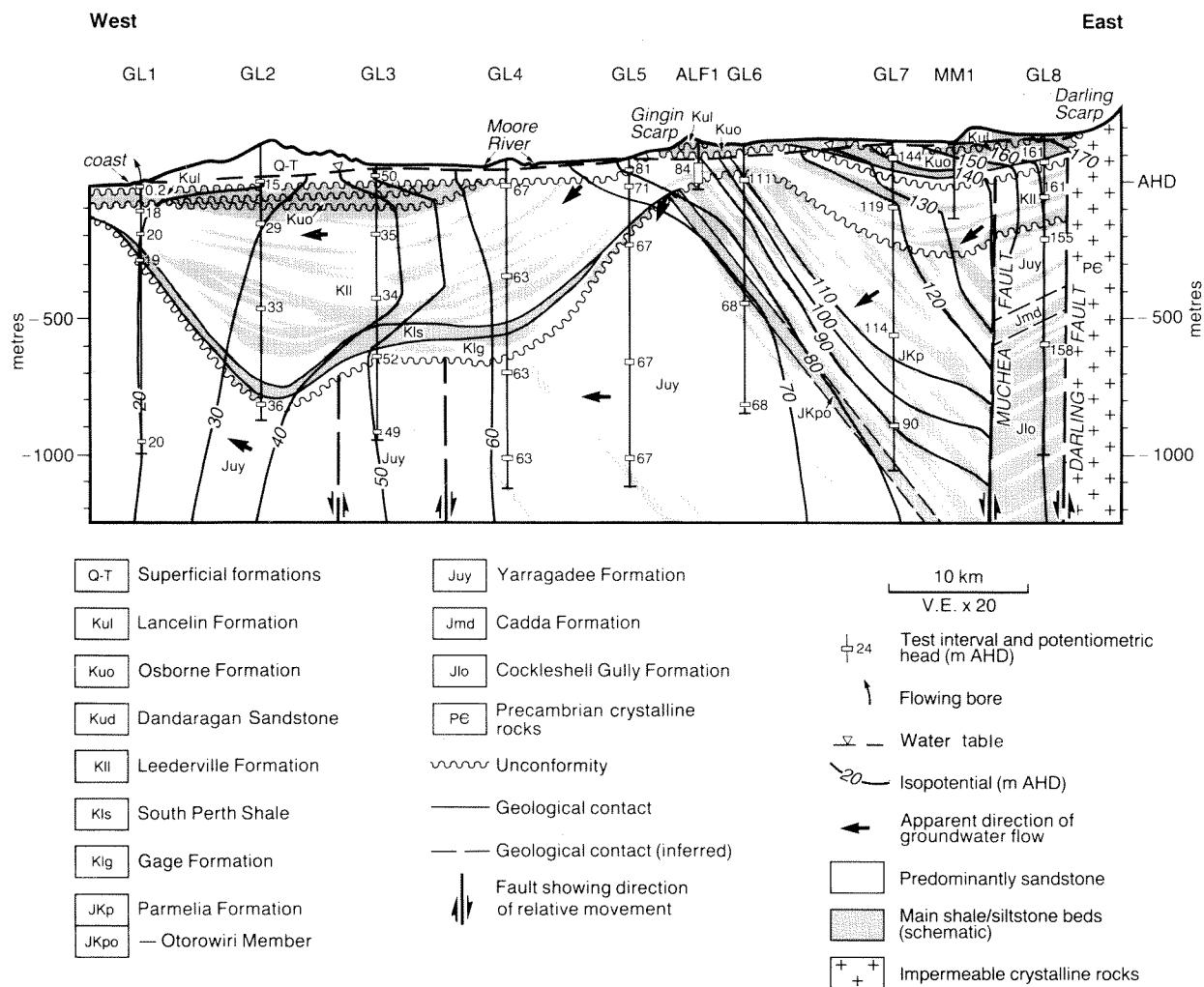
Superficial formations

A detailed account of the hydrogeology of the superficial formations is given by Moncrieff and Tuckson (1989).

The superficial formations form an inhomogeneous, anisotropic, mainly unconfined aquifer system which has a saturated thickness of 20–60 m. The aquifer system is underlain by low permeability rocks of the Coolyena Group west of GL4, and permeable rocks of the Leederville Formation to the east, up to the Gingin Scarp. Recharge is by direct infiltration of rainfall and, to a lesser extent, from streams which dissipate on the Swan Coastal Plain from the Dandaragan Plateau. Groundwater flows southward and westward from the Regans Ford Area (Moncrieff and Tuckson, 1989), where the water-table elevation is above 50 m AHD, to discharge to Gingin Brook and the Indian Ocean over a saltwater interface. There is also downward leakage of groundwater into the Leederville Formation adjacent to the Gingin Scarp.

Throughflow from the Regans Ford Area is about 16 x 10⁶ m³/year (Moncrieff and Tuckson, 1987).

The salinity of groundwater in the superficial formations is generally less than 750 mg/L TDS, except near the Moore River where the groundwater is locally brackish (1500–4000 mg/L TDS).

Figure 10. Isopotentials and apparent groundwater flow directions

Groundwater from the superficial formations is mainly used for stock and domestic purposes, including the Lancelin Town Water Supply, and also for irrigation.

Leederville Formation

The Leederville Formation is a multilayered aquifer system which extends beneath the Swan Coastal Plain. The section of the formation east of ALF1 forms part of the Leederville and Parmelia Formations aquifer system and is discussed in the next section.

The aquifer system attains a maximum thickness of about 650 m (GL2B), but is generally much thinner. It is about half sandstone, but individual sandstone beds are commonly less than 10 m thick and many contain a proportion of clay. It is overlain west of GL4 by low permeability strata of the Coolyena Group, but where these are absent, between GL4 and GL5, and north of the Gillingarra Line, there is hydraulic connection with the superficial formations (Fig. 10). The Leederville Formation is separated from the underlying Yarragadee Formation by discontinuous shale and siltstone beds of the South Perth Shale. A significant head difference between the Leederville and Yarragadee aquifer systems occurs only in GL3A where a thick shale and siltstone sequence is present at the base of the formation and in the South Perth Shale.

The main recharge to the Leederville Formation occurs from the superficial formations, and from the Leederville and Parmelia Formations by groundwater flow across the Gingin Anticline. Minor recharge is presumed to occur along the crest of the Gingin Anticline by leakage from the thin Coolyena Group section.

Regional isopotential contours (Fig. 8) and the hydrogeological cross section (Fig. 10) indicate that groundwater flow is westward towards the coast. The hydraulic gradient is steep along the Gingin Anticline where the aquifer thins. There is also a steepening of the hydraulic gradient between GL3 and GL4. This may be the result of a reduction in aquifer thickness due either to a thicker siltstone and shale section in the South Perth Shale, or a reduction of permeability along a fault. The potentiometric surface is 20 m above AHD

along the coast, which indicates that fresh water extends for some distance offshore. Bores in low-lying areas along the coast flow.

The salinity of groundwater in the Leederville Formation is generally 500–1000 mg/L TDS (Fig. 9). The lowest salinity is 550 mg/L TDS in GL1B and implies a source of groundwater recharge from the superficial formations to the northeast. The comparatively high salinity in GL4W (1050 mg/L TDS) is attributed to seepage of brackish water from the superficial formations where they have been recharged from the Moore River.

Groundwater from the Leederville Formation commonly contains a high concentration of iron; a value of 18 mg/L was obtained from GL2B2 (Table 3).

Groundwater is extracted from the Leederville Formation for the Gingin and Seabird town water supplies and for irrigation to support intensive agricultural projects. Licensed abstraction from the aquifer system in the Gingin Groundwater Area north of Gingin Brook was about 10×10^6 m^3/yr in December 1988 (Water Authority).

Leederville and Parmelia Formations

The Leederville Formation, Dandaragan Sandstone, and the sandy facies of the Parmelia Formation form a multilayered aquifer system, here termed the Leederville and Parmelia Formations aquifer system, which extends eastwards from ALF1 beneath the Dandaragan Plateau. The Parmelia Formation forms an important part of the aquifer system only in the vicinity of GL7 where it has a significant proportion of sandstone (Fig. 10). This may also occur at the eastern end of the Gingin Brook Line. In the Moora Line, the Carnac Member is thick and there is very little sandstone in hydraulic connection with the Leederville Formation.

The aquifer system is confined by the Coolyena Group, except along parts of the valleys of the Moore River and other drainages, as far north as Dandaragan where the Coolyena Group has been removed by erosion (Fig. 8). It is underlain by low permeability rocks of the Otorowiri Member of the Parmelia Formation. Because the Otorowiri Member comes close to the surface near ALF1, and the overlying Parmelia Formation is more shaly than to the east, the westward flow of groundwater is restricted and results in an increased hydraulic gradient over the Gingin Anticline.

Recharge is by direct infiltration of rainfall where the Coolyena Group is thin or absent. The main recharge area is about 100 km north from the Gillingarra Line (Commander, 1981), but some recharge also occurs along the Gingin Anticline. Groundwater flows southward from the main recharge area, and south of the Gillingarra Line it is deflected to the west (Fig. 8). A downward head potential of 24 m over 470 m depth occurs between GL7A2 and GL7A3 (Fig. 10). This may indicate that there is leakage through the Otorowiri Member to the Yarragadee Formation, at least in this

vicinity. Groundwater outflow is mainly by flow across the Gingin Anticline into the Leederville Formation aquifer system.

A section of Leederville Formation at the eastern edge of the basin, against the Darling Fault, is hydraulically separated from the rest of the aquifer system, probably by faulting (Fig. 8). Hydraulic heads in this section are higher than to the west.

Brackish groundwater in the east is progressively diluted by fresher water towards the west (Fig. 9). The higher salinity in the east is due to local recharge north of the Gillingarra Line from saline drainage in the Yarra Yarra Region (Briese, 1979a). Fresher groundwater, with a salinity of about 550 mg/L TDS, occurs in GL6W and GL7A2 probably as a result of local recharge near the crest of the Gingin Anticline by leakage from the thin Coolyena Group section. The low salinity in GL7A2 may indicate that this part of the aquifer system has a higher hydraulic conductivity than other parts.

The aquifer system contains a large, undeveloped resource of fresh to brackish groundwater.

Yarragadee Formation

The Yarragadee Formation aquifer system is confined either by the South Perth Shale, or by the Otorowiri Member of the Parmelia Formation, except beneath the Gingin Scarp where it is overlain directly by the Leederville Formation. Sandstone beds in the Gage Formation are locally in hydraulic connection with the Yarragadee Formation. The aquifer system may also be compartmentalized by north–south trending faults. The section between the Darling and Muchea Faults is hydraulically separate from the main part of the aquifer system. The Yarragadee Formation is about 90% sandstone, although many of the sandstones tend to be somewhat clayey.

Recharge occurs by downward leakage in areas where the confining South Perth Shale and Otorowiri Member of the Parmelia Formation are thin or absent and where a downward head potential exists (GL5). Recharge also occurs directly from rainfall 50 km north of the Gillingarra Line where the Yarragadee Formation is exposed. The main recharge area extends from about 25 km north of the Gillingarra Line and is centered about 50–90 km north (Briese, 1979b). Groundwater movement is mainly southward from the main recharge area and westward beneath the Swan Coastal Plain (Fig. 11). Vertical hydraulic gradients within the Yarragadee Formation are low (Fig. 10).

The groundwater salinity is generally less than 1000 mg/L TDS and ranged from 642 mg/L TDS (GL5A1) to 1130 mg/L TDS (GL3A3) in the Gillingarra Line bores (Fig. 9). The formation is inferred to contain groundwater of less than 1000 mg/L TDS to a depth of 1500 m (-1406 m AHD) in Walyering 1 (Nowak, 1978), and groundwater of similar quality to a depth of 2743 m (-2536 m AHD) in Gingin 1 (Johnson, 1965). There is a slight increase in salinity westwards from GL5 to the coast, and fresh water probably extends offshore.

TABLE 3. CHEMICAL ANALYSES

Bore interval	Sample number (a)	pH	Colour (A.P.H.A. units)	EC (mS/m 25°C)	TDS	T.Hard.	T.Alk.	Ca	Mg	Na	K	CO₃ (mg/L)	HCO₃	Cl	SO₄	NO₃	SiO₂	B	F	Fe
1A1	60687	8.3	<5	177	910	138	127	24	19	266	28	2	151	417	55	<1	21	0.1	0.1	0.32(b)
1A2	60688	8.3	5	141	740	136	161	28	16	222	16	2	192	293	47	<1	21	0.1	0.1	–
1A3	60689	8.3	5	192	990	114	152	21	15	315	19	2	181	456	48	<1	21	0.21	0.2	0.05(b)
1B	60690	8.5	5	107	550	156	103	33	18	138	19	4	118	246	23	2	12	0.11	0.2	1.5 (b)
1W	60686	7.6	<5	141	740	306	217	83	24	161	6	<2	265	287	33	1	16	0.08	0.2	–
2B1	60695	7.9	15	156	770	252	83	55	28	187	10	<2	101	393	32	<1	12	0.05	0.1	9.5
2B2	60696	8.4	5	137	710	111	142	18	16	222	11	2	169	294	48	<1	18	0.08	0.2	18
2B3	60697	8.2	<5	189	960	202	109	25	34	251	45	<2	133	458	59	2	17	0.05	0.2	2
3A1	12495	7.6	<5	119	630	119	52	13	21	169	13	<2	63	307	31	<1	43	0.07	0.4	–
3A2	12496	8.4	5	171	870	90	110	13	14	270	36	2	130	409	53	<1	11	0.07	0.2	–
3A3	12497	8.3	<5	220	1 130	243	117	30	41	293	48	2	139	552	71	<1	21	0.07	0.1	–
3B	12498	8.1	<5	130	680	196	121	49	18	171	7	<2	148	310	20	<1	29	0.07	0.1	–
3W	60700	8.5	10	71.1	380	168	156	51	10	75	3	5	180	120	7	1	18	0.05	0.1	–
4A1	70480	8.0	20	160	855	150	122	23	23	249	27	<2	149	377	62	1	18	0.08	<0.1	–
4A2	70479	7.6	<10	147	792	120	108	16	19	235	22	<2	132	347	60	<1	27	0.08	<0.1	–
4C	72811	7.6	59	112	631	110	93	16	17	177	11	<2	113	273	34	<1	46	0.08	0.2	–
4W	72812	7.8	17	190	1 050	280	184	69	27	272	9	<2	224	484	35	<1	40	0.06	<0.1	–
5A1	71077	8.1	6	116	642	84	128	19	9	200	15	<2	156	248	50	<1	23	0.07	0.2	–
5A2	71076	8.0	10	166	899	150	117	19	26	264	31	<2	143	398	68	<1	21	0.08	0.2	–
5B1	71079	6.8	20	151	793	170	25	17	32	219	15	<2	30	420	37	<1	38	0.10	0.2	–
5B2	71078	7.8	11	144	794	130	110	29	14	233	16	<2	134	338	56	<1	41	0.08	0.2	–
5W	71080	7.0	6	163	849	180	15	13	35	235	13	<2	18	461	44	<1	39	0.08	0.3	–
6A1	72834	8.5	10	162	864	66	144	20	4	300	10	3	170	391	34	<1	17	<0.05	<0.1	–
6A2	72833	7.6	10	122	683	36	165	11	2	245	4	<2	201	267	23	<1	30	<0.05	0.1	–
6W	72814	7.4	96	98.2	551	110	57	16	17	148	11	<2	70	250	28	<1	46	0.11	0.2	–
7A1	60684	6.9	<5	258	1 310	260	22	25	48	373	30	<2	27	738	67	<1	14	0.07	0.1	–
7A2	60683	8.3	5	90.5	530	89	172	19	10	157	12	3	204	157	43	<1	29	0.06	0.1	–
7A3	60682	8.3	<5	227	1 210	203	150	40	25	359	20	3	177	546	107	<1	20	0.07	0.1	–
7W	60679	6.4	<5	145	760	79	48	7	15	242	12	<2	58	378	40	<1	39	0.06	0.1	–
8A1	60675	7.1	5	352	1 850	258	70	21	50	595	19	<2	85	983	120	1	23	0.22	0.1	–
8A2	60676	7.6	5	904	5 180	599	116	34	125	1 720	59	<2	142	2 780	385	<1	1	0.31	0.1	–
8A3	60677	6.9	<5	1 460	8 660	2 500	41	313	419	2 250	97	<2	50	4 950	595	<1	15	0.42	0.1	–
8W	60678	6.5	5	316	1 720	265	30	32	45	522	22	<2	37	905	128	<1	44	0.18	0.2	–

(a) Airlift samples taken at completion
(b) Acidified, filtered sample taken from flowing bore

EC Electrical conductivity
TDS Total dissolved solids by calculation

T.Hard Total hardness (as CaCO₃)
T.Alk. Total alkalinity (as CaCO₃)

The dissolved iron concentration was 0.05 mg/L in a sample from GL1A3 and was 2 mg/L in a sample from GL2B3.

The Yarragadee Formation contains a very large groundwater resource which is undeveloped in this area.

HYDROCHEMISTRY

Chemical analyses of groundwater samples from the Gillingarra Line are presented in Table 3. The concentration of the major ions, when expressed as a percentage of the total milliequivalents per litre on a trilinear diagram, lie within the sodium and the chloride fields (Fig. 12). The percentage concentrations of Ca^{++} and HCO_3^- in groundwater from the superficial formations (GL1W and GL3W) is comparatively high, as is the percentage concentration of HCO_3^- in GL7A2. Samples from near the top of the Leederville Formation in GL1–4 (GL1B, GL2B1, GL3B, GL4W) contain slightly higher Ca^{++}: $(Na^+ + K^+)$ ratios than those deeper in the aquifer system. This ratio may therefore decrease with distance from recharge sources in the limestone of the superficial formations.

The Cl^- to total anions ratio increases with increasing salinity.
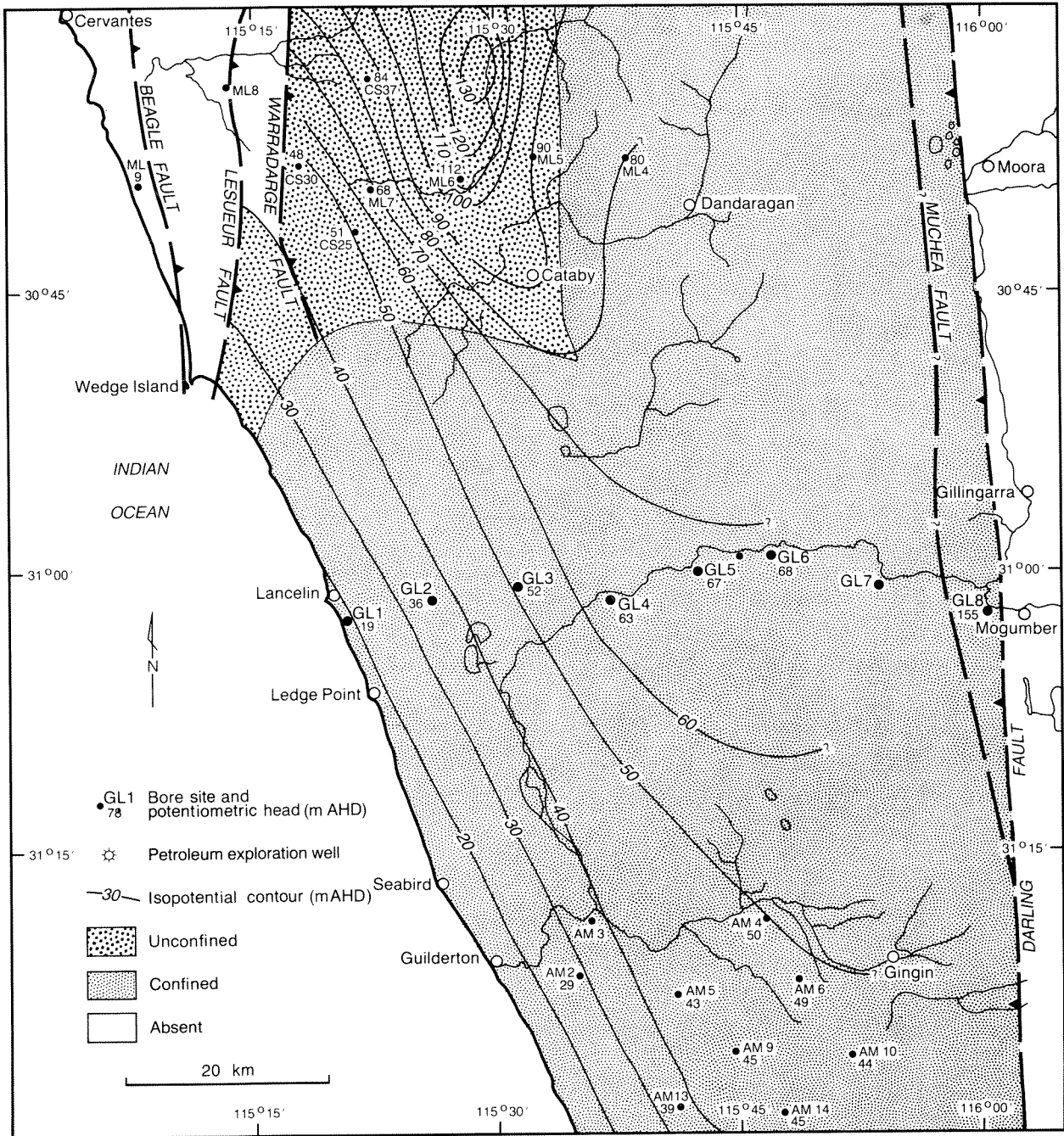
GSWA 24775

Figure 11. Yarragadee Formation regional isopotentials

123

A cross section showing isotherms and based on temperature logs and bottom-hole temperatures measured during wire-line logging is given in Figure 13. Temperatures ranged from about 20°C at the water table in GL4A, to 56°C at the bottom of GL6A.

The geothermal gradients ranged from about 2.1°C per 100 m in the sandy Yarragadee Formation, to 4.8°C per 100 m in the more shaly sections of the Parmelia Formation (GL6A). The average gradient in the area is about 2.5°C per 100 m.

CONCLUSIONS

Drilling of the Gillingarra Line of bores has provided new information on the deep aquifer systems of the Perth Basin between Mogumber and Lancelin. It has enabled revision of the geological structure and stratigraphy of adjacent borehole lines in which there were major inconsistencies, and provides a link between the exploratory drilling in the northern and central parts of the Perth Basin.

A narrow fault block containing the Early and Middle Jurassic Cockleshell Gully and Cadda Formations, and a thin sequence of Yarragadee Formation, underlying the Leederville Formation, was intersected adjacent to the Darling Fault. To the west these rocks are in fault contact with the Jurassic–Cretaceous Parmelia Formation. An exceptionally thick, sandy sequence of the Parmelia Formation occurs in GL7A, but these strata become more shaly towards the axis of the Gingin Anticline.

The Gage Formation was identified in the structurally lowest depressions in the intra-Neocomian unconformity. The South Perth Shale extends into the western part of the area from the south, but was not recognized east of the Gingin Anticline. The Leederville Formation thins markedly over the Gingin Anticline which demonstrates that this was a palaeo-high during the Early Cretaceous. The Osborne Formation thins and is truncated by the Lancelin Formation above the Gingin Anticline, and towards the coast in the Yanchep Syncline.
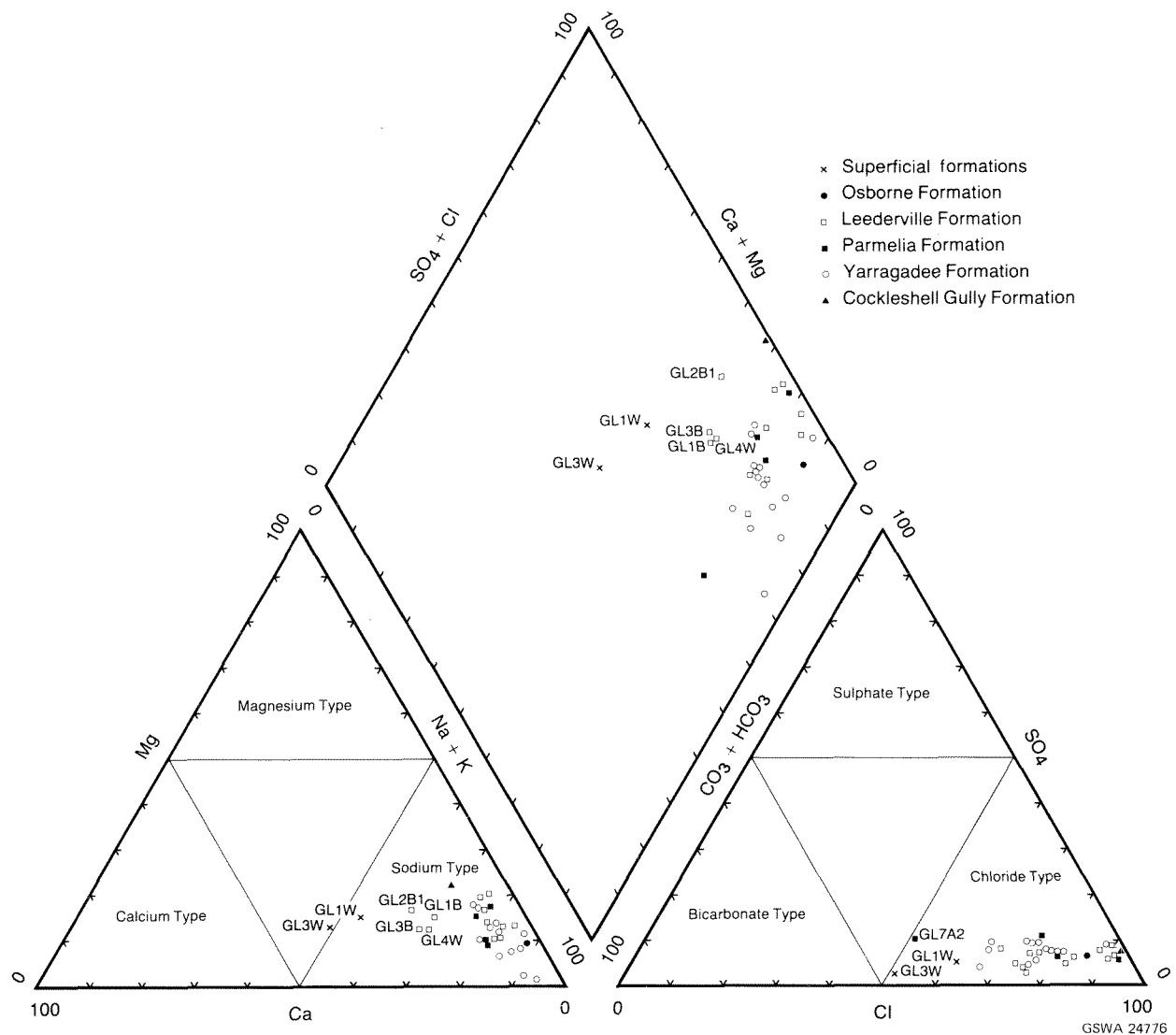

Figure 12. Trilinear plot of chemical analyses

124

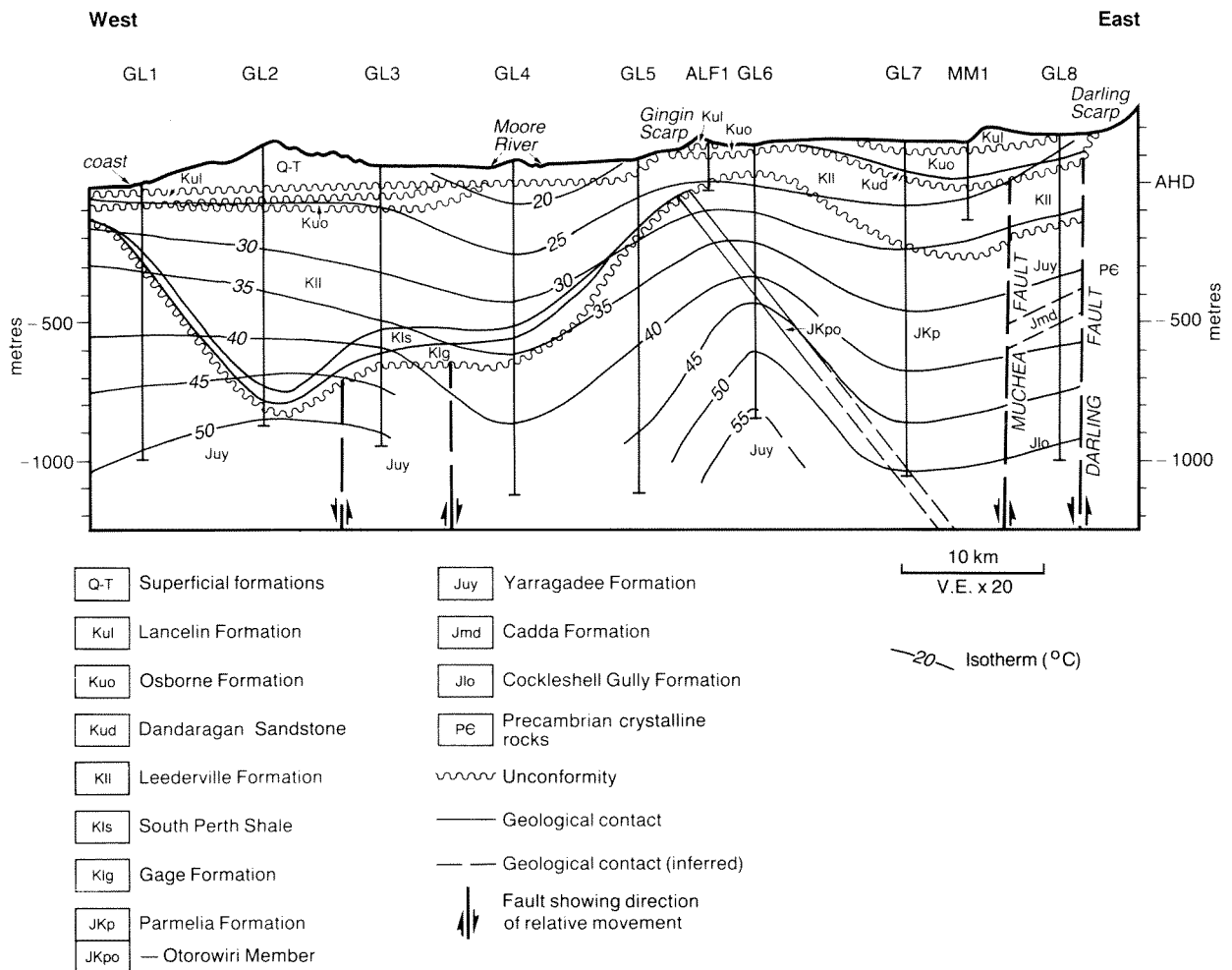**Figure 13. Isotherms**

Legend:

Q-T	Superficial formations
Kul	Lancelin Formation
Kuo	Osborne Formation
Kud	Dandaragan Sandstone
Kll	Leederville Formation
Kls	South Perth Shale
Klg	Gage Formation
JKp	Parmelia Formation
JKpo	— Otorowiri Member
Juy	Yarragadee Formation
Jmd	Cadda Formation
Jlo	Cockleshell Gully Formation
Pε	Precambrian crystalline rocks

∿∿∿ Unconformity
—— Geological contact
— — Geological contact (inferred)
⇊ Fault showing direction of relative movement

10 km   V.E. x 20

∽20∽ Isotherm (°C)

GSWA 24777

Four main strata-controlled aquifer systems occur: the superficial formations, the Leederville Formation beneath the Swan Coastal Plain, the Leederville and Parmelia Formations beneath the Dandaragan Plateau, and the Yarragadee Formation beneath the whole region. They are largely separated by confining units of shale and siltstone.

The aquifer systems all contain groundwater with a salinity of less than 1000 mg/L TDS. The Leederville and Parmelia Formations, however, also contain marginal to brackish groundwater adjacent to the Darling Fault. This appears mainly to be derived from downward leakage of saline surface water along the fault zone farther north.

Large resources of fresh to marginal groundwater are indicated in this part of the Perth Basin. Groundwater is being drawn from the superficial formations and Leederville Formation, but the resources in the Leederville and Parmelia Formations, and the very large resources in the Yarragadee Formation, are virtually undeveloped.

REFERENCES

ALLEN, A. D., 1976, Outline of the hydrogeology of the superficial formations of the Swan Coastal Plain: Western Australia Geological Survey, Annual Report 1975, p. 31–42.

ALLEN, A. D., 1979, An outline of the confined groundwater resources in the vicinity of Perth, Western Australia: Western Australia Geological Survey, Annual Report 1978, p. 30–40.

BACKHOUSE, J., 1984, Revised Late Jurassic and Early Cretaceous stratigraphy in the Perth Basin: Western Australia Geological Survey, Report 12, Professional Papers, p. 1–6.

BACKHOUSE, J., 1988, Late Jurassic and Early Cretaceous palynology of the Perth Basin, Western Australia: Western Australia Geological Survey, Bulletin 135.

BIGGS, E. R., 1976, Urban Geology of the Gingin Sheet: Western Australia Geological Survey, 1:50 000 Urban Geology Series Map and Notes.

BRIESE, E. H., 1979a, The geology and hydrogeology of the Moora borehole line: Western Australia Geological Survey, Annual Report 1978, p. 16–22.

BRIESE, E. H., 1979b, The geology and hydrogeology of the Moora borehole line and adjacent area, Perth Basin: Western Australia Geological Survey, Record 1979/12.

125

COCKBAIN, A. E. and PLAYFORD, P. E., 1973, Stratigraphic nomenclature of Cretaceous rocks in the Perth Basin: Western Australia Geological Survey, Annual Report 1972, p. 26–31.

COMMANDER, D. P., 1981, The hydrogeology of the Eneabba area Western Australia: University Western Australia Geology M.Sc. thesis (unpublished).

COPE, R. N., 1972, Tectonic style in the southern Perth Basin: Western Australia Geological Survey, Annual Report 1971, p. 46–50.

DAVIDSON, W. A. and MONCRIEFF, J. S., 1989, Revised Cretaceous stratigraphic nomenclature in the central Perth Basin, Western Australia: Western Australia Geological Survey, Record 1989/14.

INGRAM, B. S. and COCKBAIN, A. E., 1979, The stratigraphy of Ginginup No. 1 central Perth Basin: Western Australia Geological Survey, Annual Report 1978, p. 49–50.

JOHNSON, N. E. A., 1965, Gingin No. 1 well completion report: West Australian Petroleum Pty Ltd, Petroleum Search Subsidy Acts Report (unpublished).

KERN, A. M., 1989, Hydrogeology of the superficial formations between Cervantes and Lancelin, Perth Basin: Western Australia Geological Survey, Hydrogeology Report, 1988/22 (unpublished).

LOW, G. H., 1965, Drilling of Upper Cretaceous glauconite deposits at Dandaragan, Gingin, and Bullsbrook: Western Australia Geological Survey, Record 1965/6.

LUSCYZYNSKI, N. J., 1961, Head and flow of ground water of variable density: Journal Geophysical Research, v. 66, no. 12, p. 4247–4256.

MARSHALL, N. J., 1984, Late Cretaceous dinoflagellates from the Perth Basin, Western Australia: University Western Australia Ph.D. thesis (unpublished).

McWHAE, J. R. H., PLAYFORD, P. E., LINDNER, A. W., GLENISTER, B. F. and BALME, B. E., 1958, The stratigraphy of Western Australia: Geological Society Australia Journal, v. 4, pt. 2.

MONCRIEFF, J. S., 1989, Hydrogeology of the Gillingarra borehole line, Perth Basin: Western Australia Geological Survey, Hydrogeology Report 1988/31 (unpublished).

MONCRIEFF, J. S. and SMITH, R. A., 1989, Gillingarra Line Bore Completion Reports: Western Australia Geological Survey, Hydrogeology Report 1989/28 (unpublished).

MONCRIEFF, J. S. and TUCKSON, M., 1987, The geology and hydrogeology of the superficial formations between Lancelin and Guilderton, Perth Basin (Salvado Project): Western Australia Geological Survey, Hydrogeology Report 2750 (unpublished).

MONCRIEFF, J. S. and TUCKSON, M., 1989, Hydrogeology of the superficial formations between Lancelin and Guilderton, Perth Basin: Western Australia Geological Survey, Report 25, Professional Papers, p. 39–57.

NOWAK, I. R., 1978, Walyering No. 1 water salinities: Western Australia Geological Survey, Geophysics File Report 1/78 (unpublished).

PLAYFORD, P. E., COCKBAIN, A. E. and LOW, G. H., 1976, The geology of the Perth Basin: Western Australia Geological Survey, Bulletin 124.

PLAYFORD, P. E. and LOW, G. H., 1976, Definitions of some new and revised rock units in the Perth Basin: Western Australia Geological Survey, Annual Report 1971, p. 44–46.

SANDERS, C. C., 1967, Exploratory drilling for underground water, Gingin Brook area, Perth Basin: Western Australia Geological Survey, Annual Report 1966, p. 27–33.

SKILBECK, C.G. and LENNOX, M.J., (eds), 1984, The Seismic Atlas of Australia and New Zealand: Earth Resources Foundation, University of Sydney.

THRUST SHEETS ON THE SOUTHERN FORELAND OF THE CAPRICORN OROGEN, ROBINSON RANGE, WESTERN AUSTRALIA

by John S. Myers

ABSTRACT

The Yilgarn Craton extends further north than previously thought and is overlain by thrust sheets transported southward from the Capricorn Orogen. Rocks previously mapped as Proterozoic siliceous metasedimentary rocks are found to be derived from early Archaean granite, intensely deformed in major thrust zones. They are overlain by an exotic thrust sheet of deformed metagabbroic and ultramafic rocks previously mapped as a diverse assemblage of Archaean greenstones and Proterozoic metavolcanic and siliceous metasedimentary rocks. These rocks are here interpreted as either the lower part of an ophiolite sequence, or crustal underplate obducted onto the Yilgarn Craton. They are overlain by thrust sheets of early Proterozoic metasedimentary rocks of the Nabberu Basin.

KEYWORDS: Capricorn Orogen; Yilgarn Craton; thrust faults.

The southern boundary of the Gascoyne Complex of the Capricorn Orogen with the Yilgarn Craton was formerly considered to be marked by a series of *en echelon* vertical shear zones (Gee, 1979; Elias and Williams, 1980; Williams, 1986) (Fig. 1). To the north of these shear zones, Archaean structures were thought to be overprinted by, or transposed into, early Proterozoic tectonic and metamorphic fabrics. Recent remapping of this region does not support this interpretation.

The shear zones formerly taken as the northwestern boundary of the Yilgarn Craton occur within the craton (Fig. 1). Some shear zones formed during a late Archaean episode of tectonic and magmatic activity at about 2.7 Ga, and some were active during the early Proterozoic Capricorn Orogeny. Muhling (1986) gives a detailed account of the structure and petrology of some of these shear zones. She distinguishes two groups of early Proterozoic east-northeast and east-southeasterly trending shear and mylonite zones: an early group associated with dolerite dyke emplacement at a deep crustal level with temperature of $700 \pm 70°C$ and pressure of 800 ± 150 MPa, and a younger group which formed at a higher crustal level at a temperature of $<550°C$ and pressure of <500 MPa. Gascoyne granites were emplaced about 1.8–1.6 Ga, between these two episodes of shear zone formation.

The gneisses on both sides of these shear zones (Fig. 1) are similar in composition and structure and are part of the early Archaean Narryer Gneiss Complex (3.7–3.3 Ga) which was intensely deformed and metamorphosed about 2.7 Ga (Myers, 1988). They do not show widespread tectonic and metamorphic modification related to the Capricorn Orogen and are considered to be part of the Yilgarn Craton which therefore extends much further north than previously recognized (Fig. 1).

The southern margin of the Capricorn Orogen in the vicinity of Trillbar and the Robinson Range (Fig. 2A) is marked by three major thrusts which transported rocks southward from the orogen onto the Yilgarn Craton. The lowest thrust sheet (A on Fig. 2A) consists of Dugel Gneiss partly converted to mylonite and quartz–muscovite schist. Mylonite and schist form thick
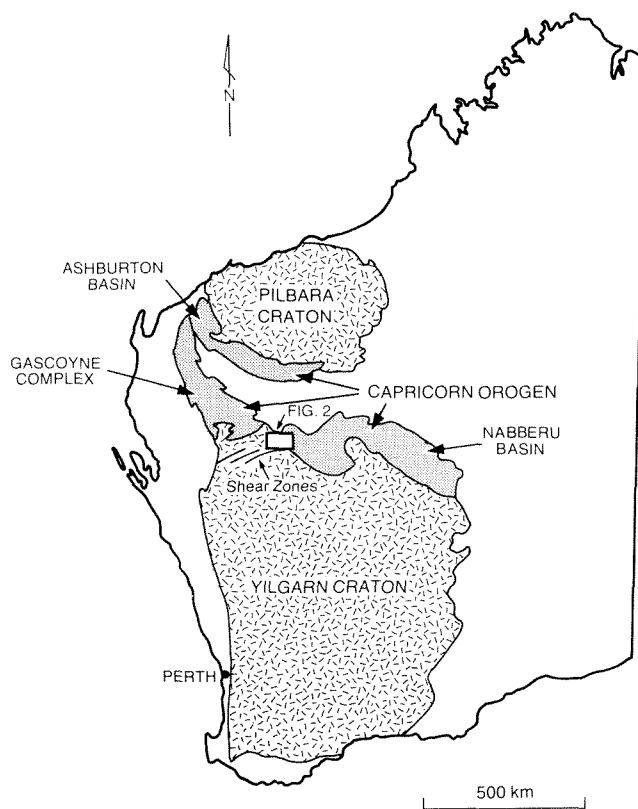
Figure 1. Location of the Capricorn Orogen between the Pilbara and Yilgarn Cratons and location of the region described in Figure 2. Shear zones in the northwest Yilgarn Craton were formerly considered to mark the boundary between the craton and the Gascoyne Complex.
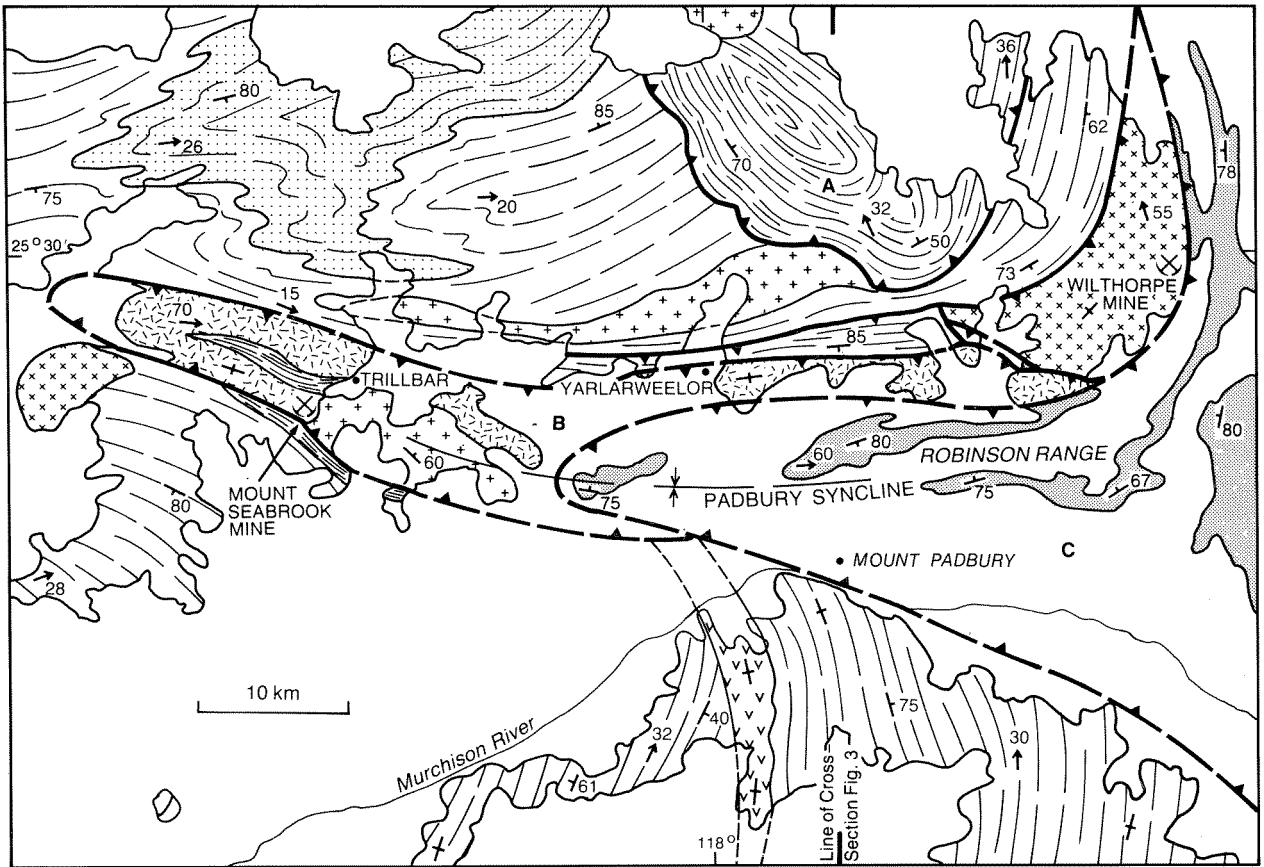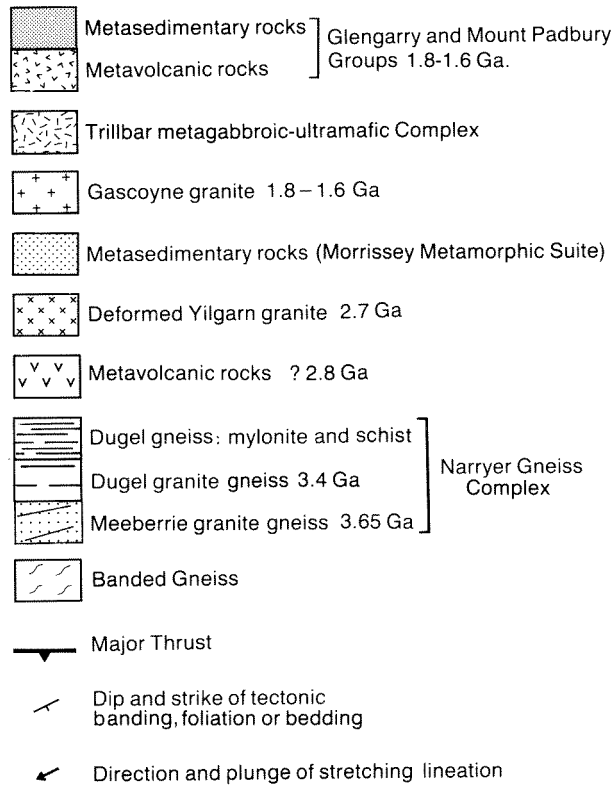
127

Figure 2A. Simplified new geological map showing the main geological units and major thrust sheets A, B, and C on the southern foreland of the Capricorn Orogen, located on Figure 1.

Reference for Figures 2A, 2B and 3.

Metasedimentary rocks	Glengarry and Mount Padbury
Metavolcanic rocks	Groups 1.8-1.6 Ga.

Trillbar metagabbroic-ultramafic Complex

Gascoyne granite 1.8 – 1.6 Ga

Metasedimentary rocks (Morrissey Metamorphic Suite)

Deformed Yilgarn granite 2.7 Ga

Metavolcanic rocks ? 2.8 Ga

Dugel gneiss: mylonite and schist	
Dugel granite gneiss 3.4 Ga	Narryer Gneiss Complex
Meeberrie granite gneiss 3.65 Ga	

Banded Gneiss

Major Thrust

Dip and strike of tectonic banding, foliation or bedding

Direction and plunge of stretching lineation
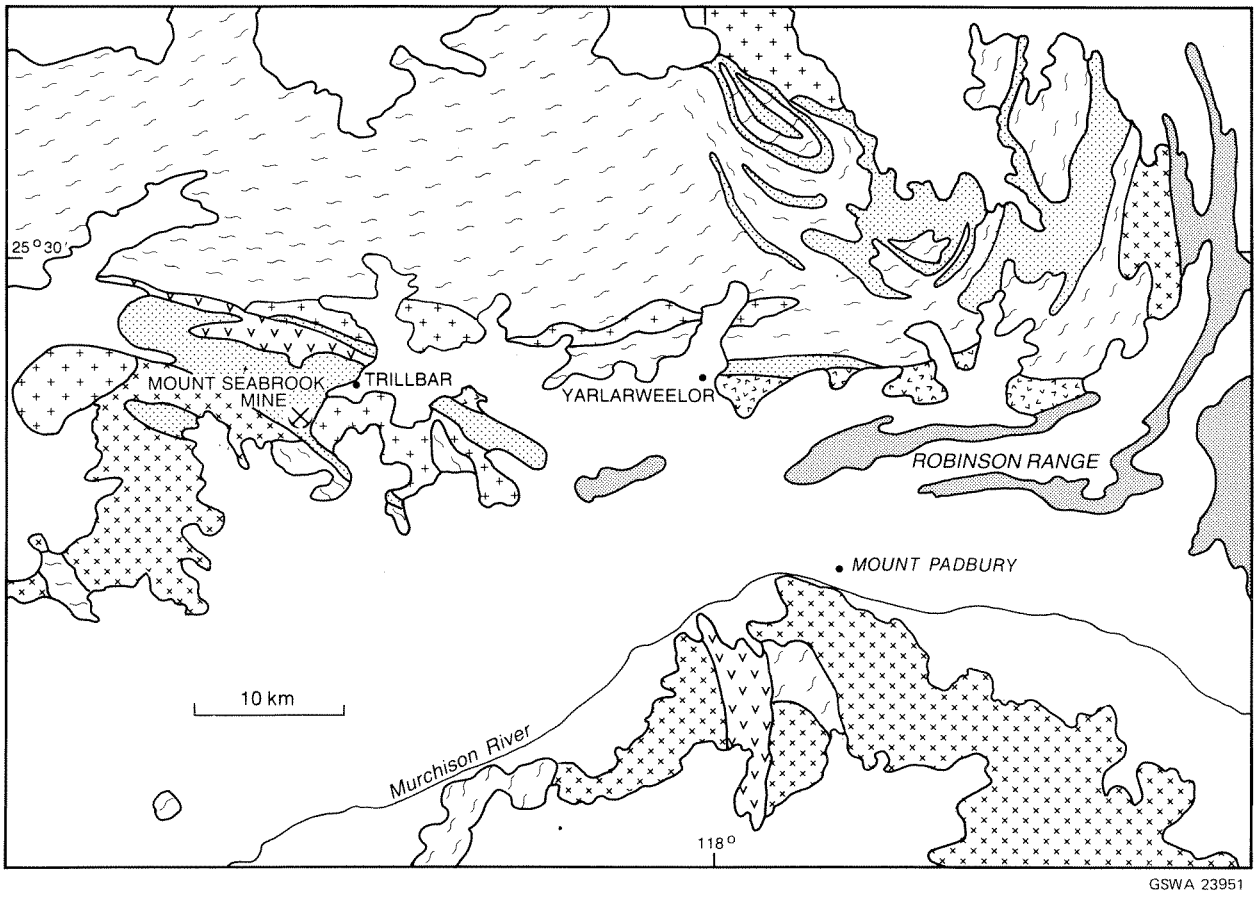
GSWA 23951

128

Figure 2B. Outline of the geological units previously mapped by Elias and Williams (1980) from the 1:250 000 geological map sheet.
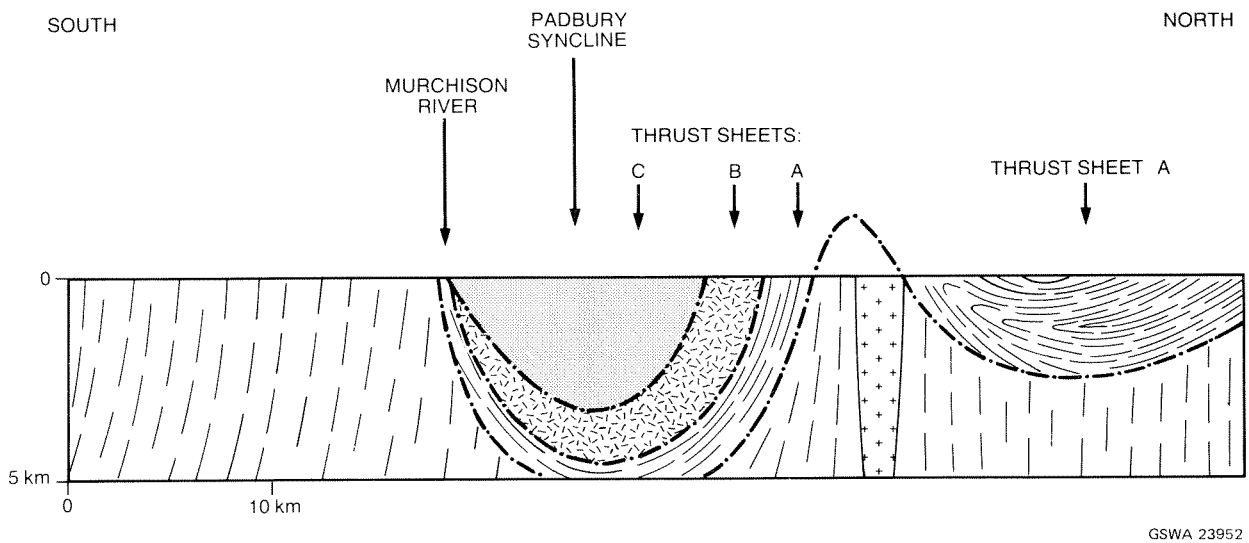

Figure 3. Generalized north–south section across the Trillbar Complex and adjacent thrust sheets in the Padbury Syncline. Ornament as on Figure 2A except: dot-dash lines represent thrust planes.

subparallel zones within and at the base of the thrust sheet and, together with intervening layers of Dugel Gneiss preserving Archaean banding, are folded into recumbent structures. Thrust sheet A cuts across Gascoyne granite (Figs 2A, 3) that gives a whole-rock Rb–Sr isochron of about 1750 ± 70 Ma (de Laeter, pers. comm., 1987) and in the north is cut by Gascoyne granite that gives a whole-rock Rb–Sr isochron at about 1600 ± 50 Ma (Williams and others, 1978).

Thrust sheet A is overlain by a more extensive thrust sequence which can be divided into two main components: a lower thrust sheet (B, Figs 2A, 3) of metagabbroic and ultramafic rocks (here called the Trillbar Complex), and an upper composite thrust sheet (C, Figs 2A, 3) of early Proterozoic metasedimentary rocks. Dugel Gneiss immediately below the Trillbar Complex is intensely mylonitized (Fig. 3). There is a gradual increase in ductile deformation upwards towards the base of the complex over tens of metres in which the banding of the Dugel Gneiss is transposed into a new tectonic banding parallel to the contact with the Trillbar Complex. Within a few metres below the Trillbar Complex the Dugel Gneiss is converted to mylonite with upward decrease in grain size. The internal structure of the Trillbar Complex has not been mapped in detail but it appears to be an imbricate sequence of mafic and ultramafic schists, metagabbro, and metaperidotite. Little-deformed and undeformed metagabbro and serpentinized peridotite occur *en echelon*, in lenses which grade into the schists and indicate the former nature of the schists.

The Trillbar Complex is overlain by composite thrust sheet C (Figs 2A, 3) comprising early Proterozoic metasedimentary rocks (1.8–1.6 Ga) of the Glengarry and Padbury Groups of the Nabberu Basin (Elias and Williams, 1980; Williams, 1986). The metasedimentary rocks are mainly derived from shale, sandstone, and banded iron-formation, which are folded and possess pronounced cleavage. The structure of these rocks is not known in detail, but previous mapping (Elias and Williams, 1980) indicates that there are major breaks within the stratigraphy which could be interpreted as thrusts.

Parts of the Trillbar Complex were previously mapped as a diverse assemblage of Archaean greenstones, early Proterozoic metabasalt equated with the Narracoota Volcanics of the Glengarry Group (recently described by Hynes and Gee, 1986), and siliceous metasedimentary rocks of the Morrissey Metamorphic Suite (Elias and Williams, 1980; Willians, 1986) (Fig. 2B). However, in contrast to previous mapping, no sedimentary or volcanic structures were identified during the present investigation, and the only primary structures observed were igneous textures in metagabbro and metaperidotite. Rocks previously mapped as siliceous metasedimentary rocks were found to consist of either intensely deformed Dugel Gneiss reduced to quartz–muscovite schist and mylonite, or weathered and bleached schistose ultramafic rocks.

The talc deposit mined at Mount Seabrook (Fig. 2A), and interpreted by Lipple (1975) as a metamorphosed dolomite, may be an integral part of the Trillbar metagabbroic and ultramafic complex. The gold deposit mined at Wilthorpe (Fig. 2A) occurs in an intensely deformed thrust sheet of late Archaean granite which contains schistose greenstone remnants.

Stretching lineations and shear criteria within the mylonites and schists indicate southward transport of the thrust sheets. The upper thrust sheets were subsequently folded into a major syncline called the Padbury Syncline by Elias and Williams (1980). The occurrence of major thrusts on the southern foreland of the Capricorn Orogen accords with the recognition of major northward-directed thrusts along the northern margin of the orogen (Tyler, 1986; Tyler and others, in press) and the interpretation of the Capricorn Orogen as a consequence of collision between the Yilgarn and Pilbara Cratons between 2.0–1.7 Ga. The Trillbar Complex could represent the lower part of an ophiolite sequence or crustal underplate obducted along a major thrust onto the Yilgarn Craton.

REFERENCES

ELIAS, M., and WILLIAMS, S.J., 1980, Robinson Range, Western Australia: Western Australia Geological Survey, 1:250 000 Geological Series Explanatory Notes.

GEE, R.D., 1979, Structure and tectonic style of the Western Australian Shield: Tectonophysics, v. 58, p. 327–369.

HYNES, A., and GEE, R.D., 1986, Geological setting and petrochemistry of the Narracoota Volcanics, Capricorn Orogen, Western Australia: Precambrian Research, v. 31, p. 107–132.

LIPPLE, S.L., 1975, The Mount Seabrook talc deposit: Western Australia Geological Survey, Annual Report 1974, p. 65–67.

MUHLING, J.R., 1986, Tectonothermal history of the Mukalo Creek area, southern Gascoyne Province, Western Australia: crustal evolution of Archaean gneisses reworked during Proterozoic orogenesis: University of Western Australia, Ph.D. thesis, (unpublished).

MYERS, J.S., 1988, Early Archaean Narryer Gneiss Complex, Yilgarn Craton, Western Australia: Precambrian Research, 38, 297–307.

TYLER, I.M., 1986, The metamorphic and tectonic development of the southeastern margin of the Pilbara Craton, Western Australia. Evidence from the Sylvania Inlier: Geological Society of Australia, 8th Geological Convention, Adelaide, Abstract v. 15, p. 105.

TYLER, I.M., and THORNE, A.M., in press, Capricorn Orogen, structural evolution of the northern margin, *in* Geology and mineral resources of Western Australia: Western Australia Geological Survey, Memoir 3.

WILLIAMS, S.J., 1986, Geology of the Gascoyne Province, Western Australia: Western Australia Geological Survey Report 15, 85 p.

WILLIAMS, S.J., ELIAS, M., and de LAETER, J.R., 1978, Geochronology and evolution of the eastern Gascoyne Province and the adjacent Yilgarn Block: Western Australia Geological Survey Annual Report 1977, p. 50–56.